AN INVESTIGATION INTO THE FEASIBILITY OF INCORPORATING DIDANOSINE INTO INNOVATIVE SOLID LIPID NANOCARRIERS

A Thesis Submitted to Rhodes University in
Fulfilment of the Requirements for the Degree of

DOCTOR OF PHILOSOPHY (PHARMACY)

by

Kasongo Wa Kasongo

February 2010

Faculty of Pharmacy
Rhodes University
Grahamstown
South Africa

ABSTRACT

The research undertaken in these studies aimed to investigate the feasibility of developing and manufacturing innovative solid lipid carriers, such as solid lipid nanoparticles (SLN) and/or nanostructured lipid carriers (NLC) using a hot high pressure homogenization method, for didanosine (DDI). In addition, studies using *in vitro* differential protein adsorption were undertaken to establish whether the SLN and/or NLC have the potential to deliver DDI to the central nervous system (CNS). Prior to initiating pre-formulation, formulation development and optimization studies of DDI-loaded SLN and/or NLC, it was necessary to develop and validate an analytical method for the *in vitro* quantitation and analysis of DDI. An accurate, precise and sensitive RP-HPLC method with UV detection set at 248 nm was developed, optimized and validated for the quantitative *in vitro* analysis of DDI in formulations.

Pre-formulation studies were designed to evaluate the thermal stability of DDI and to select and characterize lipid excipients that may be used for the manufacture of the nanocarriers. It was established that DDI is thermostable at temperatures not exceeding 163°C and therefore a hot high pressure homogenization technique could be used to manufacture DDI-loaded SLN and/or NLC. Lipid screening studies revealed that DDI is poorly soluble in both solid and liquid lipids. A combination of Precirol® ATO 5 and Transcutol® HP was found to have the best solubilizing-potential for DDI of all lipids investigated. The inclusion of Transcutol® HP into Precirol® ATO 5 changed the polymorphic form of the solid lipid from the stable β-modification to a material that exhibited the co-existence between α- and β-polymorphic forms. The relatively high solubility of DDI in Transcutol® HP compared to Precirol® ATO 5 was an indication that a solid lipid matrix prepared from a binary mixture of Precirol® ATO 5 and Transcutol® HP was likely to have a higher loading capacity and encapsulation efficiency for DDI than a matrix consisting of Precirol® ATO 5 alone. Furthermore, the

potential for the solid lipid matrix to exist in the α- and/or β-modifications when Transcutol® HP was added to Precirol® ATO 5 suggested that expulsion of DDI from a solid lipid matrix during prolonged storage periods was likely to be minimal. Therefore it was considered logical to investigate the feasibility of incorporating DDI into NLC and not in SLN. However, due to the limited solubility of DDI in lipids, formulation development of DDI-loaded NLC commenced using small quantities of DDI.

Formulation development and optimization studies of DDI-loaded NLC were initially aimed at selecting a surfactant system that was capable of stabilizing NLC in an aqueous environment. Solutol® HS alone or a ternary mixture consisting of Solutol® HS, Tween® 80 and Lutrol® F68 was found to stabilize the nanoparticles in terms of particle size and the polydispersity index. The use of the ternary mixture as the surfactant system was preferred to using Solutol® HS alone as Lutrol® F68 and especially Tween® 80 have been successfully used to target the delivery of API to the brain. Aqueous DDI-free and DDI-loaded NLC containing increasing amounts of DDI were manufactured using hot high pressure homogenization at 800 bar for three cycles. The NLC formulations were characterized in terms of particle size, polydispersity index, zeta potential, and polymorphism, degree of crystallinity, encapsulation efficiency (EE), shape and surface morphology.

The mean particle size for all formulations was below 250 nm with narrow polydispersity indices, indicating that narrow particle size distribution had been achieved. The d99% values for all formulations tested, were generated using laser diffractometry, and were below 400 nm, with span values ranging from 0.84 - 1.19 also suggesting that a narrow particle size distribution had been achieved. The zeta potential values measured in double distilled water with the conductivity adjusted to 50 μS/cm ranged from -18.4 to -11.4 mV. In addition, all the formulations showed a decrease in the degree of crystallinity as compared to the bulk

lipid material and WAXS shows that the formulations existed in a single β-modification form. Furthermore DDI that had been incorporated into the NLC appeared to be molecularly dispersed in the lipid matrices. These parameters remained unaffected for most formulations following storage for two months at 25°C. In addition these formulations contained a mixture of spherical and non-spherical particles irrespective of the amount of DDI that was added during the manufacture of the formulations.

These studies showed that it was feasible to develop and incorporate small amounts of DDI into NLC. However in order to use these delivery systems for oral administration of DDI to paediatric patients, strategies to improve the amount of DDI that could be loaded into the particles and to achieve high encapsulation efficiencies had to be developed. The limited solubility of DDI in lipid media was identified as a major factor that affected the loading capacity and encapsulation efficiency of DDI in the NLC. Therefore, a novel strategy aimed at increasing the saturation solubility of DDI in the lipid by attempting to increase the dissolution velocity of the drug in the lipid using a particle size reduction approach, was designed and investigated. DDI was dispersed in Transcutol® HP and the particle size of DDI in the liquid lipid medium was reduced gradually using hot high pressure homogenization and the product obtained from these studies was used to manufacture DDI-loaded NLC using a cold high pressure homogenization procedure. Although the encapsulation efficiency and drug loading following use of this approach was relatively high, the particles were large and showed a tendency to grow in size leading to the formation of microparticles after storage for two months at 25°C. In addition, the degree of crystallinity of the nanoparticles increased rapidly over the same storage period which led to expulsion of DDI nanoparticles for the NLC, despite the DDI loading in NLC being unaffected. It was clearly evident that this new approach of manufacturing solid lipid nanocarriers could be used as a platform not only for

enhancing the loading capacity of DDI in solid lipid nanocarriers but also for other hydrophilic drugs.

Differential protein adsorption patterns of DDI-loaded NLC were generated *in vitro* using two-dimensional polyacrylamide gel electrophoresis (2-D PAGE) in order to establish the potential for these systems to deliver DDI to the CNS. NLC formulations containing small amounts of DDI were used as these formulations showed a better stability profile than the formulation with a higher encapsulation efficiency and drug loading capacity. Furthermore, the encapsulation efficiency and drug loading of DDI were considered sufficient for use in 2-D PAGE studies. Data obtained from 2-D PAGE analysis reveal that DDI-loaded NLC preferentially adsorb proteins *in vitro* that are responsible for specific brain targeting *in vivo.* More importantly, these studies reveal that in addition to Tween® 80 that has already been shown to have the potential to target CDDS to the brain, Solutol® HS15 has the potential to achieve a similar objective. Consequently, DDI-loaded NLC have the potential to deliver DDI to the brain and these results may be used as a platform for conducting *in vivo* studies to establish whether DDI can cross the blood brain barrier and enter the CNS when administered in NLC which may in turn lead to a major breakthrough in the management of HIV/AIDS and Aids Dementia Complex (ADC).

ACKNOWLEDGEMENTS

First and foremost, I thank the Almighty God for His presence in my life and for providing me with protection, strength and resolve to succeed throughout my studies. It is only through His grace, mercy and willingness that I was able to carry out and complete this work in a timely manner.

I would like to express my sincere gratitude to the following people and organizations:

My parents, Kabange and Kasongo Mukalay for giving me a life that I have come to love and cherish, for their prayers, encouragement, love, support and financial assistance not only throughout the duration of my academic career, but also throughout my entire life. I am forever grateful to my parents for the values, teachings and beliefs that they instilled in me as well as for the sacrifices and decisions that they made to support my education.

My supervisor, Professor R.B. Walker for giving me the opportunity to be part of his research group and for his support, patience, guidance and assistance throughout the course of my studies and during the preparation of this thesis and also for providing me with laboratory facilities and financial assistance. I am grateful to Professor R.B. Walker for having gone through my manuscript during its preparation in a timely manner. In addition, many thanks to Professor R.B. Walker for giving me the opportunity to attend the 14th International Pharmaceutical Technology Symposium that was held in Antalya, Turkey in 2008 and for facilitating and allowing me to carry out some of my research work at the Freie Universität Berlin, Germany, in collaboration with Professor Dr. Rainer H. Müller.

The Head and Dean, Professor R.B. Walker and the staff of the Faculty of Pharmacy, Rhodes University for use of the facilities in the Faculty and for their support and friendship during my time as a postgraduate student in the Faculty.

Professor Dr. Rainer H. Müller for giving me the opportunity to carry out some of my work in his research group at the Freie Universität Berlin, Berlin, Germany, for a six-month period that started on 1 May 2009. I am eternally indebted to Professor Dr. Rainer H. Müller for providing me with bench space and allowing me to use research facilities in his laboratory and also for guidance and sharing his expertise, experience, theoretical and practical knowledge in the design and characterization of innovative solid lipid nanocarriers.

Dr. Jana Pardeike, Dr. Cornelia M. Keck and Ms. Ranjita Shegokar for their insightful suggestions during my studies in Berlin. Special thanks to Dr. Jana Pardeike and Ms. Ranjita Shegokar for their practical assistance during the production of my formulations. In addition, special thanks to Dr. Jana Pardeike for her assistance in the interpretation of some of the data that were obtained from my studies in Germany.

Mr. Mirko Jansch for his guidance, assistance and sharing his experience and expertise during my studies of the *in vitro* differential protein adsorption, in addition to his technical assistance in the manipulation and presentation of data obtained from these studies. I am also grateful to Mr. Mirko Jansch for the time he spent going through Chapter 6 of this dissertation.

Ms. Corinna Schmidt, Ms. Inge Volz, Ms. Gabriela Karsubke and Mr. Alfred Protz for their valuable technical assistance during my research work at Freie Universität Berlin, and Mr. Tichaona Samkange, Mr. Leon Pardon, Mr. Collin Nontyi, Ms Linda Emslie, Mr. Dave Morley, Ms. Vuyelwa T. Menze, Ms. Shirley Pinchuck and Mr. Marvin Randall for their technical assistance during my studies at Rhodes University. Special thanks to Ms. Carol Leff for proofreading this manuscript in a timely manner.

My immediate and extended family members for their encouragement, love, support and understanding throughout my years as a student. Special thanks to my uncle Mungala and my late grandparents for having played a major role in my upbringing, my sisters, Jolie and Kabila, my brother, Junior, my uncle André for their encouragement, support, patience and understanding during my many days of absence from home.

Ms. Adrienne C. Müller, who has always been there for me through thick and thin and a special source of inspiration throughout my academic life in South Africa, for her unfailing love, support, encouragement and understanding, in addition to always showing interest in my research work. Many thanks Adie!

My colleagues, friends, past and present fellow postgraduate students in the Biopharmaceutical Research Group (BRG), in the Faculty of Pharmacy and Rhodes University at large who have been a source of support and sometimes just laughter that kept me going throughout my research experience: Dr. Ralph Tettey-Amlalo, Mr. Daniel Munene, Mr. Abdinassir Osman, Mr. Sandile Khamanga, Ms. Faith Chaibva, Ms. Wai Ling Au, Ms.

Henusha Jhundoo, Mr. Loti King'ori, Ms. Natisha Dukhi, Ms. Tinotenda Sachickonye, Mrs. Claris Magadza, Ms. Fateemah Fauzee, Ms. Natalie Parfitt, Mrs. Margaret Molefi, Ms. Antonia Afolayan, Ms. Tariro Mpofu, Mr. Evison Kapangaziwiri and Mr. Nyasha Chigwamba, Dr. Rosa Klein, Ms Candice Webber, Mr. Lukhanyiso Vumazonke, students in Celeste House and Drostdy Hall and other members of Celeste House and Drostdy Hall leadership committees. Special thanks to Ms. Faith Chaibva and Ms. Henusha Jhundoo for their practical assistance in one way or another during my research and the preparation of this manuscript and to Ms. Henusha Jhundoo for kindly volunteering to proofread this dissertation. I thank all my friends that I have not mentioned here for having played a positive role during my academic life in Grahamstown, in one way or another.

My colleagues and friends at the Freie Universität Berlin and in Berlin at large who made my stay in Berlin a memorable experience: Mr. Mirko Jansch, Ms. Juliane Wattky, Ms. Senem Acar, Mr. Thore Kübart, Mr. Jaime Salazar, Mr. Daniel Peters, Mr. Ansgar Brinkmann, Mr. Szymon Kobierski, Mr. Benjamin Wessinger, Mr. Loaye Al Shaal, Mr. Gunnar Seewald, Dr. Heni Rachmawati, Mr. Yücel Baspinar, Mr. Marc Muchow, Dr. Aiman Hommoss, Ms. Andjelka Kovacevic and Ms. Pornthida Riangjanapatee.

Aspen Pharmacare (Port Elizabeth, Eastern Cape, South Africa) for their kind donation of didanosine. Gattefossé SAS (Saint-Priest Cedex, France) for their kind donation of lipidic excipients. Special thanks to Gattefossé's representatives in South Africa and Germany, Ms. Nathalie Jelonek and Dr. Joachim Quadflieg for responding to my emails requesting for samples and sending me the requested samples in a timely manner.

The Andrew Mellon Foundation, the Deutscher Akademischer Austausch Dienst (DAAD) and the Joint Research Committee of Rhodes University for financial assistance during my studies.

STUDY OBJECTIVES

There are two major obstacles to the successful and/or adequate management of the Human Immunodeficiency Virus (HIV), in paediatric patients using an antiretroviral agent (ARV) such as didanosine (DDI). The first obstacle is the susceptibility of DDI to hydrolytic degradation in the acidic environment of the stomach which in turn leads to a reduction in bioavailability and *in vivo* activity of DDI when administered orally. The second drawback is the inability of DDI to cross the blood brain barrier and maintain a sufficiently high therapeutic concentration in the central nervous system. Consequently, the virus multiplies and accumulates unabatedly in the structures of the CNS leading to the emergence of HIV/AIDS-related complications such as AIDS dementia complex (ADC), which can impact on the quality of life of a patient negatively. Innovative solid lipid carriers such as solid lipid nanoparticles (SLN) and nanostructured lipid carriers (NLC) have the potential to prevent chemical degradation of active pharmaceutical ingredients (API) to deliver drugs to the CNS.

The objectives of this research were:

1. To acquire data relating to the physicochemical properties of DDI that would aid the development of quality formulations using empirical studies and the literature.
2. To develop, optimize and validate a simple, sensitive, precise, accurate and linear RP-HPLC method suitable for the quantitative analysis of DDI for use during formulation development and optimization studies of DDI-loaded SLN and/or NLC.
3. To establish the thermal stability of DDI, select and characterize lipidic excipients for the manufacture of nanoparticulate delivery systems.
4. To design and investigate the feasibility of manufacturing DDI-containing SLN and/or NLC.
5. To identify and apply approaches to enhance the loading capacity and encapsulation efficiency of DDI in SLN and/or NLC.
6. To establish the potential for DDI-containing SLN and/or NLC to cross the blood brain barrier using differential protein adsorption studies.

TABLE OF CONTENTS

LIST OF FIGURES

LIST OF TABLES

LIST OF ACRONYMS

%RSD	Percentage relative standard deviation
^{13}C-NMR	Carbon magnetic resonance
^{1}H-NMR	Proton magnetic resonance
2-D PAGE	Two-dimensional polyacrylamide gel electrophoresis
ACV	Acyclovir
ADC	AIDS Dementia Complex
AIDS	Acquired Immunodeficiency Syndrome
API	Active pharmaceutical ingredient
Apo A-I	Apolipoprotien A-I
Apo A-IV	Apolipoprotein A-IV
Apo C-I	Apolipoprotein C-I
Apo C-II	Apolipoprotein C-II
Apo E	Apolipoprotein E
ARV	Antiretroviral
AUC_{0-24}	Area under the curve, up to 24 hours
AZT	Zidovudine
BBB	Blood brain barrier
BMS	Bristol-Myers Squibb Company
BSA	Body surface area
C.I.	Confidence interval
CA	Carrier Ampholytes
CDDS	Colloidal drug delivery systems
CHAPS	Cholamido propyldimethyl hydroxypropansulphate
C_{max}	Maximum plasma concentration
CNS	Central nervous system
CSF	Cerebro-spinal fluid
DDADP	2′,3′-dideoxyadenosine-5′-monophosphate
DDAMP	2′,3′-dideoxyadenosine-5′-monophosphate
DDATP	2′,3′-dideoxyadenosine-5′-triphosphate
DDI	Didanosine
DDIMP	2′,3′-Dideoxyinosine-5-monophosphate
d-DMSO	Deuterated dimethyl sulfoxide

DLS	Dynamic light scattering
DSC	Differential scanning calorimetry
DTE	Dithioerythritol
EE	Encapsulation efficiency
EPO	Erythropoetin (EPO)
FDA	Food and Drug Administration
FSH	Follicle stimulating hormone (FSH)
GIT	Gastrointestinal tract
GRAS	Generally regarded as safe
HIV	Human Immunodeficiency Virus
HLB	Hydrophilic lipophilic balance
HPH	High pressure homogenization
HPLC	High performance liquid chromatography
IEF	Isoelectric focusing
Ig A	Immunoglobulin A
Ig G	Immunoglobulin G
IPG	Immobilized pH gradient
IR	Infrared
IS	Internal standard
IV	Intravenous
K_a	Acid dissociation Constant
KBr	Potassium bromide
KH_2PO_4	Potassium dihydrogen phosphate
L.L.	Lower limit
LC	Loading capacity
LD	Laser diffractometry
LDA	Laser Doppler anemometry
LDC	Lipid-drug conjugate
LDL	Low density lipoprotein
LOD	Limit of detection
Log $P_{o/w}$	Octanol/water Partition Coefficient
LOQ	Limit of quantitation
MeOH	Methanol
MP	Melting maximum or point

MPS	Mononuclear phagocytic system
MS	Mass spectrum
MSF-HAART	Médecins Sans Frontières Highly Active Anti-Retroviral Therapy
MW	Molecular weight
NC	Nanocapsules
NE	Nanoemulsions
NLC	Nanostructured lipid carriers
O/F/W	Oil-in-fat-in-water
PCS	Photon correlation spectroscopy
PEG	Polyethylene glycol
PEO	Polyethylene oxide
PEPFAR	Presidents' Emergency Plan for AIDS Relief
pI	Isoelectric point
PI	Polydispersity index
PIDS	Polarization intensity differential scattering
PN	Polymeric nanoparticles
PS	Particle size
PSD	Particle size distribution
RH	Relative humidity
RI	Recrystallization index
RP-HPLC	Reversed phase-HPLC
RT	Reverse transcriptase
SAA	Surface active agents
SD	Standard deviation
SDS	Sodium dodecyl sulphate
SDS-PAGE	Sodium dodecyl sulphate polyacrylamide gel electrophoresis
SEM	Scanning electron microscopy
SI	Syncytium-inducing
SLN	Solid lipid nanoparticles
SLS	Static light scattering
SOP	Standard operating procedures
$t_{1/2}$	Plasma elimination half-life
TEM	Transmission electron microscopy
TEMED	Tetramethylenediamine

TGA	Thermogravimetric analysis
TRIS	Tris(hydroxymethyl) aminomethan
Tris-HCl	TRis-(hydroxymethyl) aminomethan hydrochloride
U.L.	Upper limit
UNICEF	United Nations Children's Fund
USA	United States of America
UV	Ultraviolet
WAXS	Wide-angle X-ray scattering
WHO	World Health Organization
WME	Width of the melting events
Z-ave	Mean particle size
ZP	Zeta potential

CHAPTER 1

INTRODUCTION

1.1 BACKGROUND

A technical consultation report [1] compiled by the United Nations Children's Fund (UNICEF) and the World Health Organization (WHO) estimates that 13% of the people infected with the Human Immunodeficiency Virus (HIV) in 2003 were children, of which 90% lived in sub-Saharan Africa. Furthermore, the report suggested that 500 000 children were in need of antiretroviral (ARV) therapy worldwide [1]. Despite a number of global initiatives, such as the Presidents' Emergency Plan for AIDS Relief (PEPFAR) and the Médecins Sans Frontières Highly Active Anti-Retroviral Therapy (MSF-HAART) projects that make clear commitments to securing equitable access to ARV treatment in resource-poor settings for infants and children, the reality is that the treatment of children with HIV has not yet been a high priority in most practice settings [1].

The lack of availability of ARV medicines in appropriate formulations for paediatric use is one of four obstacles that were identified as a major hindrance to accessing ARV treatment for children, particularly in developing countries [1]. Most of the currently available paediatric ARV formulations require children to take frequent doses of unpalatable syrups and/or solutions, many of which need strict adherence to cold chain maintenance and storage. In addition, many of these products have a limited shelf-life or a poor stability profile after opening, since harsh climatic conditions prevail in many developing countries [1].

In reality, the few children that are on ARV treatment in developing countries are reliant on the use of adult formulations to achieve appropriate therapy. The use of adult formulations requires manipulation of the dosage form by breaking or crushing by parents or care-givers which may lead to dangerous under or over-dosing if the providers are not supported and guided accordingly [1]. This practice is likely to lead to drug resistance, the consequence of which is an impaired quality of life for the patient and a barrier in the fight against HIV/AIDS in paediatric patients. It is therefore imperative that research into the development of new drug delivery systems for the oral administration of ARV agents to paediatric patients is

conducted as a matter of urgency. Consequently, the UNICEF/WHO technical consultation report [1] recommends that more research be directed towards the development of novel oral liquid formulations for ARV drugs that have suitable taste-masking and stability profiles at room temperature. Furthermore, the dosage forms should have a shelf-life that is appropriate for products that are exposed to elevated temperatures and humidities that prevail in sub-Saharan Africa. Such formulations would be more appropriate for use in these resource-poor settings than conventional paediatric delivery systems.

This research seeks to investigate potential innovative formulations that could be used as drug carriers for the oral administration of didanosine (DDI) to paediatric patients. DDI was selected for these studies as the drug has been approved by the United States Food and Drug Administration (FDA) for the treatment of adult and paediatric patients (older than six (6) months of age) that present with advanced HIV infection and are intolerant to zidovudine (AZT) therapy or have demonstrated significant clinical or immunologic deterioration whilst using AZT [2, 3]. Furthermore, there are many challenges associated with the use of DDI formulations following oral administration to adult and paediatric patients, and these challenges are discussed in detail in the next few paragraphs of this dissertation.

DDI is susceptible to hydrolytic degradation in the acidic environment of the stomach, the consequence of which is a reduction in bioavailability and *in vivo* activity of the compound when administered orally [3-5]. It has been shown that DDI has a t_{90} of less than 2 min in solutions of pH 3 at 37°C [3, 6]. In order to improve the acid stability and bioavailability of DDI, the compound is usually formulated as buffered chewable or dispersible tablets in addition to buffered or non-buffered paediatric powders for reconstitution as an oral solution [3-5, 7]. The non-buffered paediatric powders are usually mixed with antacids following reconstitution, prior to oral administration of the mixture to patients [8]. However, the oral bioavailability of DDI is highly variable and may range between 21-54% in adults and 13-29% in children with HIV infection [9, 10] when DDI is administered concomitantly with a buffer or an antacid [3].

An added complication is that buffered DDI powders for oral solution can only be stored up to four (4) hours at room temperature (20-22°C) following reconstitution [3]. Conversely non-buffered DDI paediatric powders for oral solution are stable for 30 days under refrigerated conditions (2-8°C) following reconstitution with water and mixed with an

appropriate antacid as directed [3, 8]. This poses a major challenge in developing countries, particularly those in which harsh climatic conditions prevail, where patients seldom have access to suitable cold chain technologies to promote in-use stability. Consequently, the success of ARV therapy with DDI alone or in combination with other ARV agents in paediatric patients in developing countries can be severely compromised.

Furthermore, DDI buffered formulations are unpalatable [5, 7] and the presence of buffers and/or antacids in these formulations has been reported to cause diarrhoea, nausea, vomiting [5, 7] or abdominal discomfort [7, 10, 11]. The presentation of side-effects in addition to pancreatitis and peripheral neuropathy that can be directly attributed to DDI [10, 11] may impact negatively on the quality of life of patients. Therefore, the adherence of patients to chronic DDI therapy may be negatively affected further hindering the management of HIV/AIDS in children. In addition, the presence of buffers and/or antacids in DDI-containing formulations has been shown to significantly decrease the oral absorption of certain active pharmaceutical ingredients (API) [5, 12], which may be administered concomitantly with DDI. The oral bioavailability of these API is significantly affected by changes in gastric pH, chelation with cations of buffers and/or antacids [5, 12].

An acidic pH is necessary for the adequate absorption of drugs such as ketoconazole and indinavir when administered orally [5, 12], whereas the bioavailability of ciprofloxacin is decreased by chelation with buffers and/or antacids following oral dosing [5, 12]. Indinavir is a protease inhibitor that is usually administered in combination with DDI for the management of HIV whereas ketoconazole and ciprofloxacin are routinely co-administered with DDI for the treatment of opportunistic infection [12]. It is possible that the co-administration of DDI buffered formulations with ketoconazole, indinavir and/or ciprofloxacin may lead to drug interactions. Although these drug interactions may be managed by adjusting the relative times of dosing of each product [12], such adjustments may complicate treatment regimens and would compromise adherence to therapy by patients, further increasing the possibility of therapeutic failure [12].

In order to overcome the challenges associated with the use of buffered DDI formulations, Bristol-Myers Squibb Company (BMS) developed an encapsulated enteric-coated bead formulation of DDI that is commercially available as Videx® EC [13]. This product is a small capsule containing coated beadlets that was approved by the FDA in 2000 [14, 15] and is

currently marketed in the United States of America (USA) and Europe [12], but is yet to be approved in developing countries. Damle *et al.,* [5] reported that Videx® EC was bioequivalent to buffered DDI tablets (Videx® tablets) in terms of extent of exposure (AUC), but not in terms of rate of absorption (C_{max}) in both healthy volunteers and HIV-infected patients [5].

In a separate study, Damle *et al.,* [12] also showed that co-administration of Videx® EC with indinavir, ketoconzole and ciprofloxacin had no significant influence on the oral absorption of these API. Consequently, the authors concluded that Videx® EC appears to be a better dosage form for the administration of DDI as it eliminates the concomitant use of buffers and/or antacids to ensure bioavailability [12]. However, the manufacturers of Videx® EC recommend that the capsules be swallowed whole [13], which implies that paediatric patients must continue to use paediatric formulations of DDI that contain buffers or those that require reconstitution followed by mixing with antacids [8, 16].

Another obstacle to the successful and/or adequate management of HIV/AIDS in both adult and paediatric patients using currently available ARV formulations is the emergence of HIV/AIDS-related complications, such as AIDS dementia complex (ADC) [17, 18]. ADC is a debilitating syndrome characterized by the progressive degeneration of specific cognitive and psychomotor functions [17, 18]. The initial phase of ADC is characterized by deterioration in the memory, attention and concentration of a patient, which is followed by the late onset of spasticity, paraparesis, mutism and psychosis [19]. In addition, mental slowness, reduced rate of speech and changes in speaking volume are features of the late stages of ADC [20-22]. Clearly, the syndrome also impacts negatively on the quality of life of HIV/AIDS patients and it has been estimated that HIV/AIDS patients have a one in four chance of eventually developing ADC [23].

The main cause of ADC is the migration, followed by replication and accumulation of the HIV in the central nervous system (CNS). The HIV actively invades the CNS and the microglial cells in the brain have been shown to be the most important reservoirs of the virus [24]. The currently used dideoxynucleosides, such as DDI are apparently inefficient at crossing the blood brain barrier (BBB) to maintain sufficiently high therapeutic concentrations in the affected brain structures [17]. Consequently, the HIV is able to multiply and accumulate in the CNS unabatedly, leading to the onset of ADC. It is therefore inevitable that the adequate management of HIV infection and inhibition of viral replication within the

CNS structures will require the use of drug delivery systems with the ability to deliver anti-retroviral agents to the CNS by circumventing and/or crossing the BBB.

Innovative solid lipid carriers, such as solid lipid nanoparticles (SLN) [25-29] and nanostructured lipid carriers (NLC) [30-33] are potentially useful drug delivery systems. SLN and NLC are alternate colloidal drug carrier systems to polymeric nanoparticles [27, 29] and consist of a matrix of lipid, which is solid at room and body temperatures and have a mean particle size of between 50-1000 nm [26, 29, 34]. The primary difference between SLN and NLC is that the latter are prepared by mixing solid lipid materials with liquid lipids rather than using highly purified lipids with a relatively similar molecular structure as those used in the formulation of SLN [30, 34]. Consequently, NLC matrices consist of a less ordered lipid matrix with imperfections which may lead to an increase in the drug loading capacity (LC) of the nano-particles with the ability to prevent drug expulsion during prolonged storage [30-34].

A number of methods for the manufacture of SLN and NLC have been reported [29, 34]. Regardless of the method of manufacture, the basic principle in the preparation of SLN and NLC is that at a certain point during the manufacturing process, a solid lipid or solid lipid/liquid lipid blend needs to be melted and re-dispersed in an aqueous medium as lipid droplets of submicron size [29, 34]. This process can be accomplished by use of mechanical or thermodynamic methods in order to allow for the formation of SLN or NLC [29, 34]. It is therefore critical that the drug to be encapsulated partitions into molten lipid droplets in order to achieve suitable drug encapsulation efficiency (EE) and loading capacity (LC) in the SLN and NLC [29]. Hydrophobic drugs are readily incorporated into SLN and NLC as these molecules partition relatively easily into lipids or lipid blends that are used to prepare SLN and NLC. The incorporation of hydrophilic compounds into SLN or NLC is a challenge and the EE and LC for these compounds is likely to be limited. Low EE and LC values are adequate for highly potent hydrophilic molecules such as protein and/or hormones including follicle stimulating hormone (FSH) and erythropoetin (EPO) [34, 35]. However, low EE and LC values are unsuitable for hydrophilic drugs that require the administration of high doses in order to achieve effective therapeutic concentrations [34, 35]. Therefore, there is need for the identification of process and/or formulation approaches that would permit more efficient incorporation of hydrophilic drugs such as DDI into SLN or NLC to achieve suitable EE and LC.

Various process and formulation strategies have been devised to incorporate hydrophilic drugs into SLN. In terms of manufacturing techniques, cold high-pressure homogenization has been suggested as a suitable production method to produce SLN and/or NLC designed to incorporate hydrophilic compounds [29]. This technique has been shown to minimize the partitioning of hydrophilic molecules from a lipid phase into an aqueous phase of a dispersion during the homogenization process [29]. Recently, You *et al.,* [36] used this process to produce SLN loaded with vinorelbine bitartrate, a hydrophilic drug with EE and LC as high as 80% and 6.6%, respectively. The EE and LC varied, depending on the concentration of surfactant used.

Another approach that has been used to enhance the EE of hydrophilic molecules in SLN involved the addition of organic counter ions in order to form ionic pairs with charged drug molecules [37]. Gasco *et al.*, [37] used decyl phosphate or hexadecyl phosphate to increase the LC of salt forms of doxorubicin and idarubicin in SLN prepared using stearic acid as the solid lipid [37]. The authors reported a significant increase in partitioning of the drugs into the lipid [37]. This method of charge neutralization may not be applicable to enhance the incorporation of hydrophilic drug molecules that are neutral.

A more recent strategy that has been used to enhance the EE and LC of hydrophilic compounds in SLN involves the preparation of novel solid lipid carriers known as lipid-drug conjugate (LDC) nanoparticles [34, 35]. This technology transforms hydrophilic drug molecules into hydrophobic LDC bulk materials by use of a covalent linkage such as for example an ester linkage or by salt formation using a fatty acid, such as stearic or oleic acid [34, 35]. Following formation of the bulk LDC material, it is added to an aqueous surfactant solution and is then transformed into LDC nanoparticles using cold high-pressure homogenization [34, 35]. Olbrich *et al.,* [35] encapsulated the hydrophilic drug, dimenazenediaceturate into SLN using this approach and the LC was approximately 33%. The main drawback of this technology is that a drug must have functional groups capable of interacting with the carboxylic functional groups of the specific fatty acid used. In addition, an evaluation of the stability, safety and efficacy of drug derivatives is essential prior to the implementation and widespread use of this approach of incorporation of API into LDC.

The first objective of this research was to investigate the feasibility of incorporating DDI in SLN and/or NLC, in addition to identifying and applying process and/or formulation

approaches that would enhance the incorporation of DDI into SLN and/or NLC with adequate EE and LC. It was anticipated that the successful incorporation of DDI in SLN and/or NLC with efficient EE and LC could lead to the use of these innovative drug delivery systems as carriers for the oral administration of DDI to paediatric patients. Consequently, the administration of buffered DDI formulations to paediatric patients would be avoided thereby eliminating a major source of pharmacokinetic interactions with co-administered drugs and potentially improving adherence to chronic therapy by paediatric patients in addition to improving their quality of life.

The second purpose of this research was to investigate the feasibility of using the concept of *in vitro* differential protein adsorption to determine the potential for DDI-loaded SLN and/or NLC to target the brain. The assumption here is that successful targeting of DDI-loaded SLN and/or NLC to the brain would be a breakthrough in facilitating the delivery of DDI and possibly other ARV agents to the CNS. This could potentially lead to the management of HIV in the CNS, thereby alleviating certain AIDS-related complications, such as ADC in both adult and paediatric patients and consequently improving their quality of life.

Prior to initiating formulation development studies of DDI-loaded SLN and NLC, it was essential to obtain preliminary data on the physicochemical properties of DDI. Consequently, a literature survey was conducted to acquire data relating to the physicochemical properties of DDI that would aid the development of quality formulations. In addition, information pertinent to the stability, synthesis, clinical pharmacology and pharmacokinetics of DDI was collected so as to elucidate the appropriate characteristics of DDI.

1.2 DESCRIPTION OF DIDANOSINE

Didanosine (DDI) (Figure 1.1.) is 9-(2,3-dideoxy-β-D-*glycero*-pentofuranosyl)-1-9-dihydro-6-purin-6-one [38] or inosine, 2′,3′-dideoxy [3] or dideoxyinosine [39] or 2′,3′-dideoxyinosine [2, 3, 8, 13, 38-42].

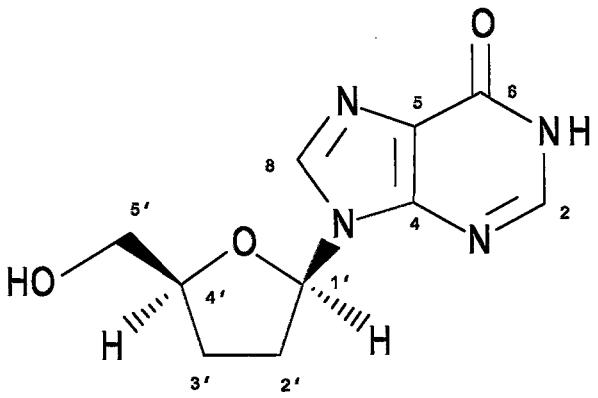

Figure 1.1. Chemical structure of DDI ($C_{10}H_{12}N_4O_3$, MW = 236.23)

DDI occurs as a white [3, 8, 13, 38, 39, 41] or almost white [38] crystalline powder [3, 8, 13, 38, 39] that contains not less than 98.5 percent and not more than 101.0 percent of $C_{10}H_{12}N_4O_3$, calculated with reference to a hydrous reference standard substance [38].

1.3 SYNTHESIS OF DIDANOSINE

The synthesis of DDI is depicted in Figure 1.2. DDI is synthesised from 2′-deoxyinosine by a Barton-type deoxygenation reaction [3]. Initially 2′-deoxyinosine (I) is converted to 5′-O-benzoyl-2′-deoxyinosine (II) through selective benzoylation of the 5′ hydroxyl group of 2′-deoxyinosine. Benzoylation is achieved by dropwise addition of a pyridine solution of benzoyl chloride to 2′-deoxyinosine suspended in pyridine solution [3]. The treatment of 5′-O-benzoyl-2′-deoxyinosine with a portion of 1-1′-thiocarbonyldiimidazole leads to the formation of 5′-O-benzoyl-2'-deoxyinosine (III). Deoxygenation of 5′-O-benzoyl-2'-deoxyinosine (III) at the 3′ position gives rise to 5′-O-benzoyl-2′,3′-dideoxyinosine (IV) [3]. The treatment of 5′-O-benzoyl-2′,3′-dideoxyinosine with anhydrous methanol saturated with anhydrous ammonia at 0°C leads to the formation of DDI (V) [3]. DDI may also be prepared by enzymatic deamination of 2′, 3′-dideoxyadenosine at room temperature using adenosine deaminase, followed by recrystallization from methanol [3].

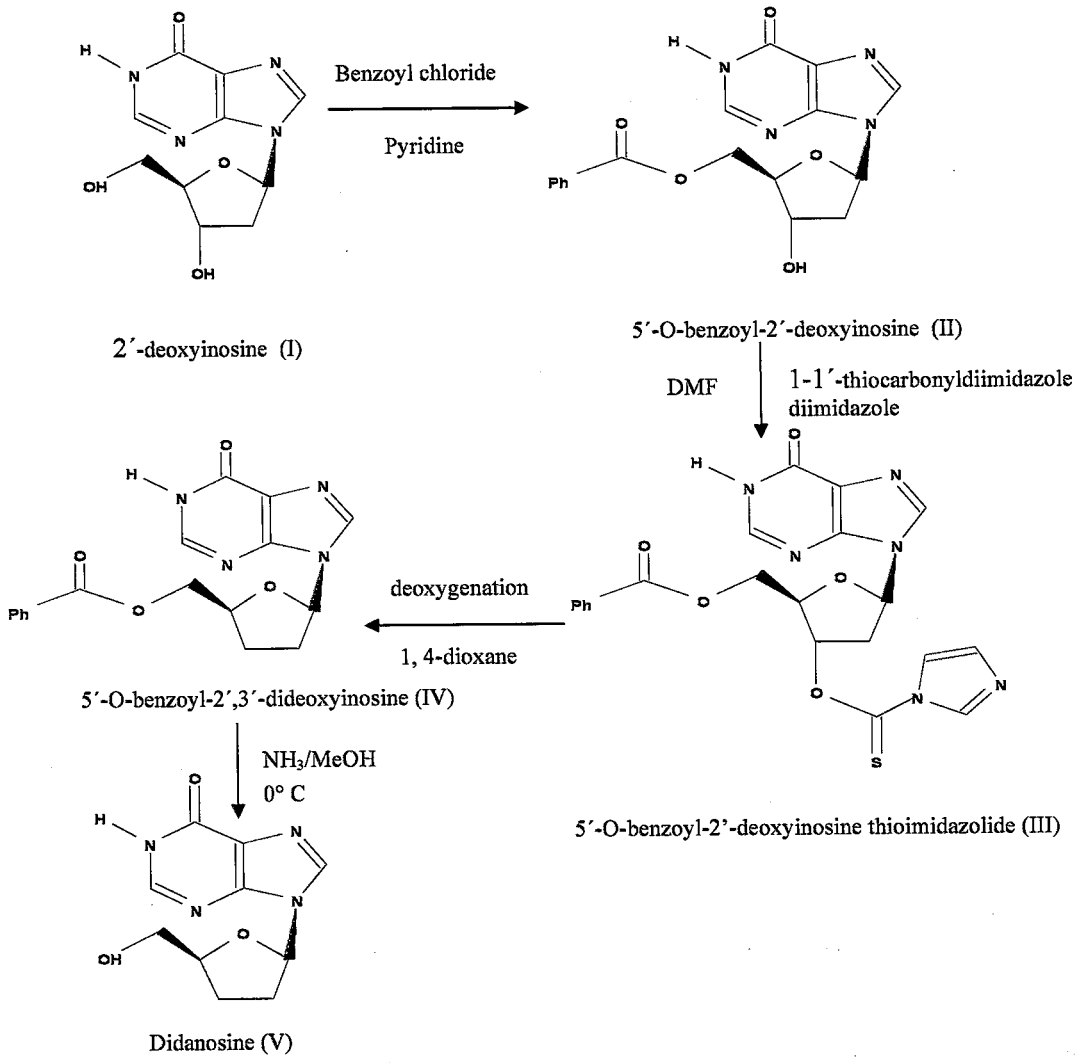

Figure 1.2. The synthesis of DDI from 2′-deoxyinosine [3].

1.4 PHYSICOCHEMICAL PROPERTIES OF DIDANOSINE

1.4.1 Solubility

Anderson *et al.,* [6] and Sanchez-Lafuente *et al.,*[43] generated aqueous pH-solubility profiles of DDI at 25°C and 22°C, respectively. Both sets of authors reported that the solubility of DDI in water is pH-dependent. A summary of the aqueous solubility of DDI at 25°C as a function of pH reported by Anderson *et al.,* is summarised in Table 1.1 [6]. Sanchez-Lafuente *et al.,*[43] showed that the aqueous solubility of DDI is 20.29 mg/ml at 22°C at a pH of 6 [3, 41].

Table 1.1. Aqueous solubility of DDI at 25°C as a function of pH [6]

pH	Solubility (mg/ml)
6.21	27.3
8.06	31.1
8.60	38.2
9.06	67.6
9.64	188
9.71	224
10.01	429
10.08	460

The solubility of DDI in different organic solvents at 23°C is summarized in Table 1.2 [3, 41].

Table 1.2. Solubility of DDI in different organic solvents at 23°C [3, 41]

Solvent	Solubility (mg/ml)
Acetone	<1
Acetonitrile	<1
t-Butanol	<1
Chloroform	<1
Dimethyl acetamide	45
Dimethyl sulfoxide	200
Ethanol	1
Ethyl acetate	<1
Hexane	<1
Methanol	6
Methylene chloride	<1
Polyethylene glycol 300	<1
1-Propanol	<1
2-Propanol	<1
Propylene glycol	8

1.4.2 Dissociation constant

The acid dissociation constant (K_a) is a measure of the ability of an acid to lose a proton in solution and thus determines the strength of an acid [44]. The K_a is usually expressed as negative logarithm or the pK_a [44]. Most drugs are either weak acids or weak bases that ionize in solution at specific pH values. Weakly acidic drugs ionize as the pH of a solution increases and conversely weak bases ionize with decreasing pH [45]. It should be noted that pK_a values alone do not allow for the specific designation of whether a drug behaves as an acid or a base in solution [44] but rather describes the pH at which equimolar concentrations of unionized (neutral) and ionized forms of a molecule co-exist [45].

DDI is an amphoteric compound that has a weakly acidic hydrogen atom on the hypoxanthine moiety and a number of basic nitrogen atoms (Figure 1.1) [44]. The apparent *pKa* of DDI in

water, uncorrected for activity coefficients by titrating a 0.01M DDI solution with a standard 0.1M NaOH solution at ambient temperature is 9.12 ± 0.02 [6]. It has been reported that the basic pKa values of nucleoside analogues such as DDI are ≤ 4 and their acidic pKa values are approximately 9 [46]. Therefore the pKa of DDI as determined and reported by Anderson *et al.*, represents the acidic properties of DDI. However, there is dearth of information indicating the exact *pKa* of DDI that represents the basic properties of the molecule.

An unionized form of a pharmacological compound is likely to interact with lipid materials more readily than a drug in the ionized form [45]. It has been suggested that maintaining a pH range of between pH 6-7 in solution keeps amphoteric nucleoside analogues such as DDI in their unionized forms [46]. Consequently, the EE and LC of DDI in SLN and/or NLC may be enhanced by formulating these products at a pH of 6 or 7.

1.4.3 Partition coefficient

The log $P_{o/w}$ value is defined as the logarithm of the partitioning ratio of a substance between octanol and water and is commonly used to characterize the lipophilic nature of pharmacological compounds, quantitatively [46-48]. The octanol/water partition coefficient (log $P_{o/w}$) of DDI reported to be 0.068 ± 0.005 has been experimentally determined [46]. The log $P_{o/w}$ value of DDI was measured by the traditional shake-flask method using 1-octanol and 0.05 M phosphate buffer pH 7.0 as the organic and aqueous phases, respectively [46]. The log $P_{o/w}$ of DDI has also been reported to be 1.24 [39].

Hydrophobicity may be described as a molecular parameter which can be used to describe the distribution equilibrium of a drug molecule between water and immiscible lipid-like organic solvents or other solubilising media such as, for example, biological membranes [47, 49, 50]. The published log $P_{o/w}$ values for DDI suggest that DDI will not partition readily into a lipid phase during the manufacture of DDI-loaded SLN and NLC and would therefore result in low EE and LC of SLN and/or NLC. Therefore formulation and/or process approaches to enhance EE and LC of SLN and/or NLC for DDI would have to be investigated as an integral part of formulation optimization studies.

1.4.4 Melting range

DDI has a melting range of approximately 160.0-163.0°C. At these temperatures DDI melts with decomposition [39, 41, 51]. However, studies conducted by Sanchez-Lafuente *et al.*, [43] revealed that DDI melts at 196.8°C with an onset temperature of 189.2°C. Nevertheless, the melting point of DDI used in these studies was investigated using differential scanning calorimetry (DSC) (Chapter 4, Section 4.3.1.2). Data obtained from these preliminary studies revealed that DDI melts at 187.3°C with an onset temperature of 184.1°C. SLN and NLC are usually formulated at temperatures of between 60-80°C depending on the type of a solid lipid used as a matrix. Therefore, it is possible to formulate and manufacture DDI-loaded SLN and/or NLC at these temperatures since DDI would not melt and/or decompose during the manufacturing process. However, additional studies using thermogravimetric analysis (TGA) have to be conducted to determine the thermo-stability of DDI prior to exposing the drug to high temperatures.

1.4.5 Optical rotation

The specific optical rotation of a 10 mg/ml aqueous solution of DDI is -26.3° [3, 41] when determined at 589 nm using a Model 241-MC Perkin-Elmer polarimeter and a 1 dm cell at ambient temperature (25°C) [3].

1.4.6 Hygroscopicity

DDI was found to absorb 1.5% w/w moisture when exposed to an environment of 87% relative humidity (RH) at room temperature (25°C) for 8 weeks [3] indicating that DDI is slightly hygroscopic. Data concerning the prevalence of polymorphs, hydrates and/or solvates of DDI have not yet been reported.

1.4.7 Ultraviolet absorption spectrum

The ultraviolet (UV) absorption spectrum of DDI generated in water using a Model-8450A Hewlett-Packard Spectrophotometer and 1 cm Quartz cell is shown in Figure 1.3 [3]. The data reveal that DDI has a wavelength of maximum absorption (λ_{max}) of 248 nm with a molar

absorptivity of 12350 $M^{-1}cm^{-1}$ [3]. Therefore, a wavelength of 248 nm was used for *in vitro* analyses of DDI during formulation development and optimization studies.

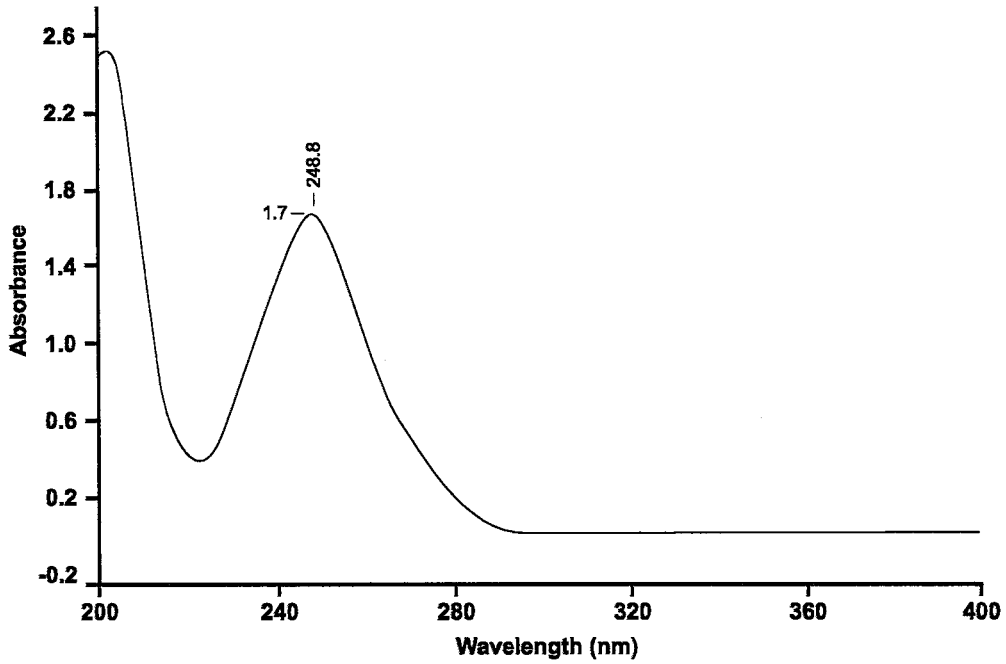

Figure 1.3. Ultraviolet (UV) visible absorption spectrum of DDI in water

1.4.8 Circular dichroism

The circular dichroism absorption spectrum of DDI generated using a Model J-600 Jasco spectropolarimeter with the scanning range and speed set at between 180-300 nm and 100 nm/min respectively and a sensitivity of 20 mdeg is shown in Figure 1.4 [3]. The data reveal that DDI produces a band at 203 nm, reportedly corresponding to the $n \rightarrow \delta^*$ transition of the terminal hydroxyl group [3] (Figure 1.1, Section 1.2). This functional group is reported to be directly adjacent to one of the two optical centres in the tetrahydrofurfuryl alcohol (oxolan-2-methanol) portion of the DDI molecule and is responsible for the circular dichroism exhibited by DDI. The molar ellipticity for DDI at 203 nm is 16583 $deg.cm^2.decimol^{-1}$ [3].

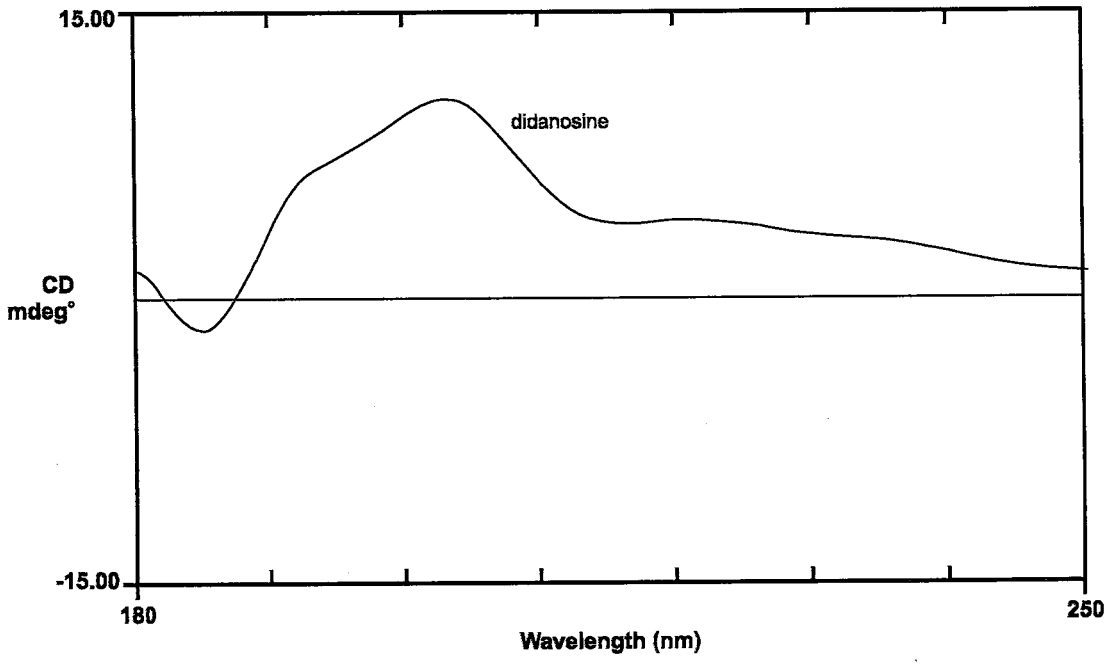

Figure 1.4. Circular dichroism absorption spectrum of DDI

1.4.9 Differential scanning calorimetry

The DSC thermogram of DDI recorded using a Perkin-Elmer DSC-7 is depicted in Figure 1.5 [3]. DDI was hermetically sealed in an aluminium pan and heated under a nitrogen purge with the temperature scanning range and heating rate set at between 40-250°C and 10°C/min, respectively [3]. It is clear that DDI melts at a peak onset of 176°C, at which temperature it also decomposes [3]. Sanchez-Lafuente *et al.,* [43] generated a DSC thermogram of DDI using an automatic thermal analyzer with the temperature scanning range and heating rate set at between 30-400°C and 10°C/min, respectively. The DSC thermogram of DDI reported by Sanchez-Lafuente *et al.,* [43] reveals an endothermic peak for DDI at 196.8°C with an onset temperature of 189.2°C [43]. In addition, the DSC thermogram reported by Sanchez-Lafuente *et al.,* [43] shows an extra endothermic peak at 277.15°C with an onset temperature of 259.23°C [43].

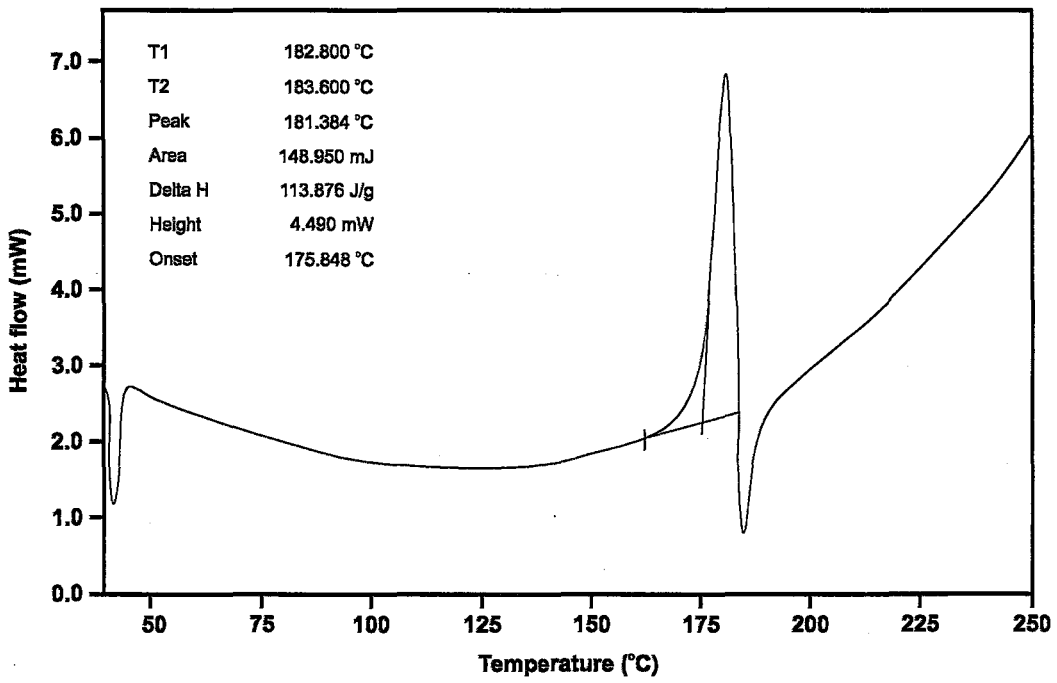

Figure 1.5. Differential scanning calorimetry (DSC) thermogram of DDI (adapted from [3])

1.4.10 X-ray powder diffraction

The X-ray powder diffraction pattern of DDI generated using a 114.6 mm diameter Debye-Scherrer powder camera with a copper target X-ray tube and a nickel filter of pore size 1.54505 Å [3, 3] during which DDI was irradiated at 25 Kv/40 mA, is shown in Figure 1.6 [3]. The interplaner distance, D (Å) in addition to the relative intensity, I (I_o) data for DDI are summarized in Table 1.6 [3].

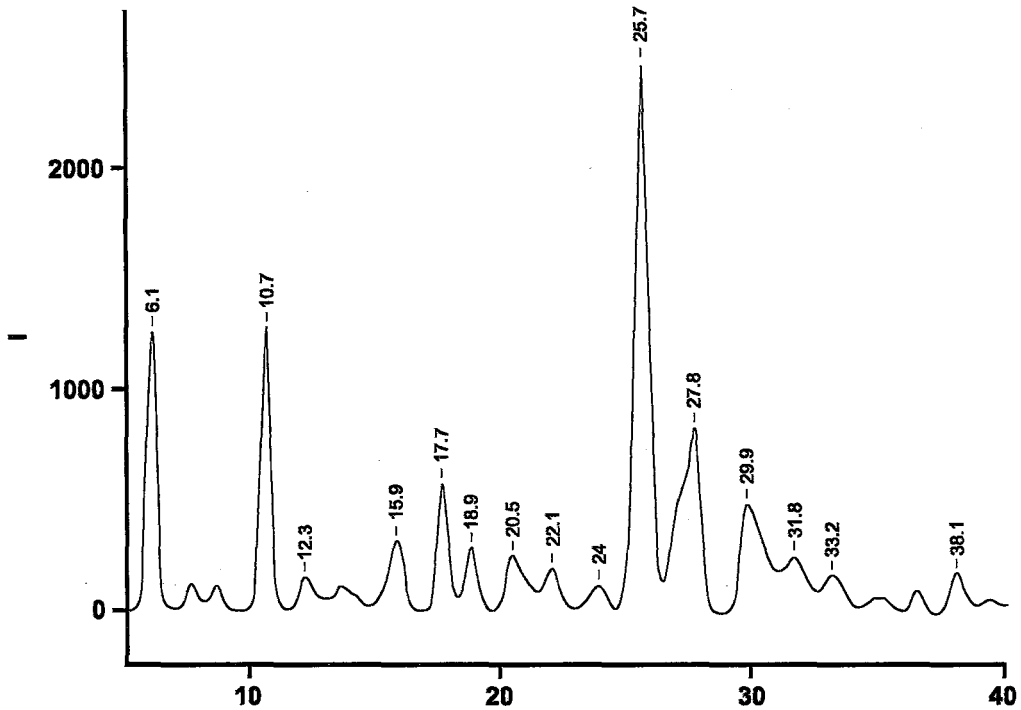

Figure 1.6. X-ray powder diffraction pattern of DDI (adapted from [3])

Table 1.3. Data showing the interplaner distance, D (Å) and relative intensity, I (I_o) of DDI

D (Å)	I (I_o)	D (Å)	I (I_o)
14.62	60	4.80	30
8.20	70	4.41	20
7.21	10	3.50	100
6.43	10	3.32	60
6.02	10	3.02	20
5.55	20	2.96	20
5.18	30	2.37	10

1.4.11 Infrared absorption spectrum

The infrared (IR) absorption spectrum of DDI determined using a Model FTS-45 Bio-Rad Digilab IR spectrometer with resolution set at 4 cm^{-1} is depicted in Figure 1.7 [3]. DDI was diluted in potassium bromide (KBr) and compressed to form a clear pellet [3]. The relevant band assignments of the principal peaks of the IR absorption spectrum for DDI at specific wave-numbers are summarized in Table 1.4 [3].

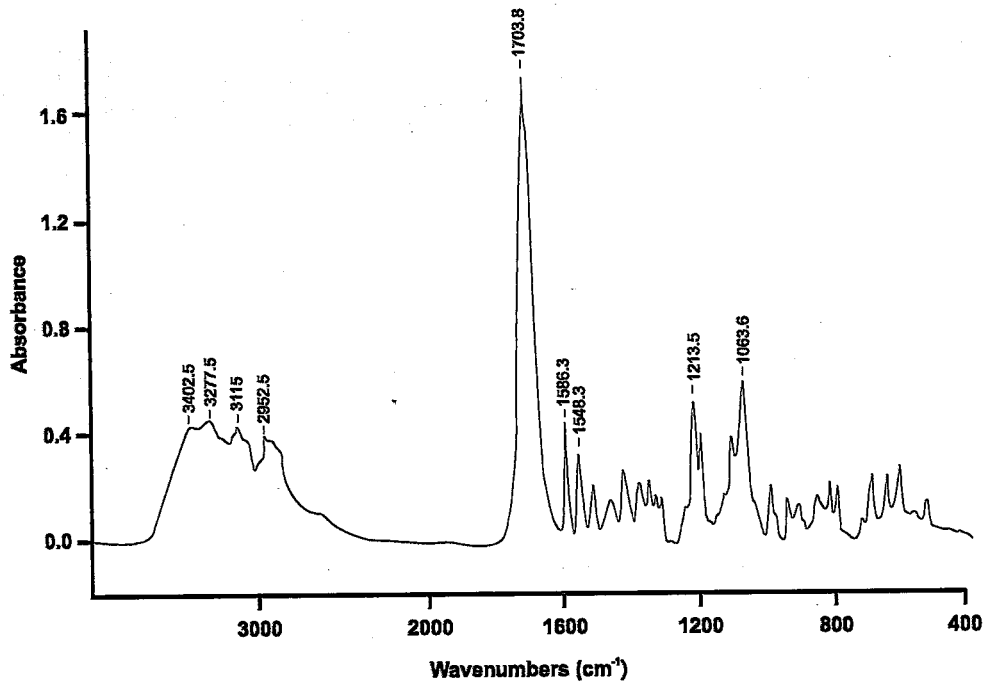

Figure 1.7. Infrared absorption spectrum of DDI (adapted from [3])

Table 1.4. Major infrared band assignments for DDI

Frequency (cm-1)	Intensity	Assignment
3100-3400	M	NH, OH stretches
2800-3000	M	CH stretches
1704	S	C=O stretch
1213	M	C-N stretch
1102	M	C-O-C asymmetric stretch
1064	M	C-O-C symmetric stretch

1.4.12 Proton magnetic resonance spectrum

The proton magnetic resonance (^{1}H-NMR) absorption spectrum of DDI generated in deuterated dimethyl sulfoxide (d-DMSO) using a Model AM-360 Bruker FTNMR spectrometer is shown in Figure 1.8 [3]. The spectrum was generated with a composite pulse broad-band using a 30° flip angle pulse with a 5 second total recycle time for 32 scans [3] and for which TMS was used as an external reference material [3]. The chemical shifts (δ) and assignments of the ^{1}H-NMR of DDI are listed in Table 1.5 [3] and are consistent with the structure of DDI shown in Figure 1.1, Section 1.2.

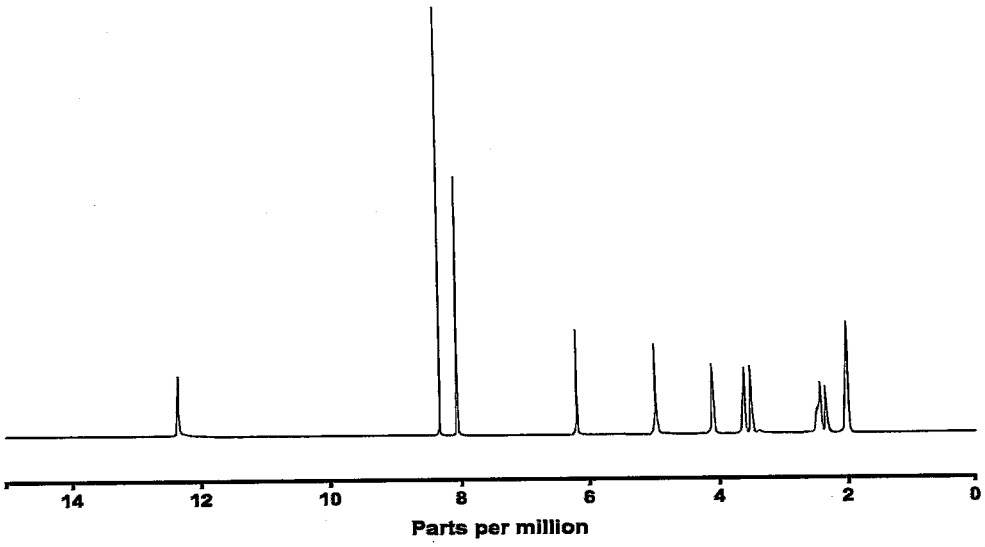

Figure 1.8. ^{1}H-NMR absorption spectrum of DDI obtained in d-DMSO (adapted from [3])

Table 1.5. ^{1}H-NMR characteristics of DDI in d-DMSO using TMS as external reference

Chemical Shift (ppm)	Multiplicity	Coupling constant	Assignment
12.36	Singlet	-	N1H
8.34	Singlet	-	C8H
8.05	Singlet	-	C2H
6.19	Doublet, Doublet	6, 7, 2, 9	C1'H
4.98	Doublet, Doublet	5, 2, 5, 2	C5'OH
4.10	Multiplet	-	C4'H
3.56	Multiplet	-	C5'H2
3.40	Singlet (broad)		H2O
2.49	-	-	DMSO-D5
2.39	Doublet, Multiplet	-	C2'H2
2.00	Doublet, Multiplet	-	C3'H2

1.4.13 Carbon magnetic resonance spectrum

The carbon magnetic resonance (^{13}C-NMR) absorption spectrum of DDI generated in d-DMSO using a Model AM-360 Bruker FT NMR spectrometer is shown in Figure 1.9 [3]. The spectrum was acquired with composite pulse broad-band using a 45° flip angle pulse with a 1 second total recycle time for 4096 scans [3] and for which TMS was used as an external reference [3]. The chemical shifts (δ) and assignments of the ^{13}C-NMR of DDI are summarized in Table 1.6 [3].

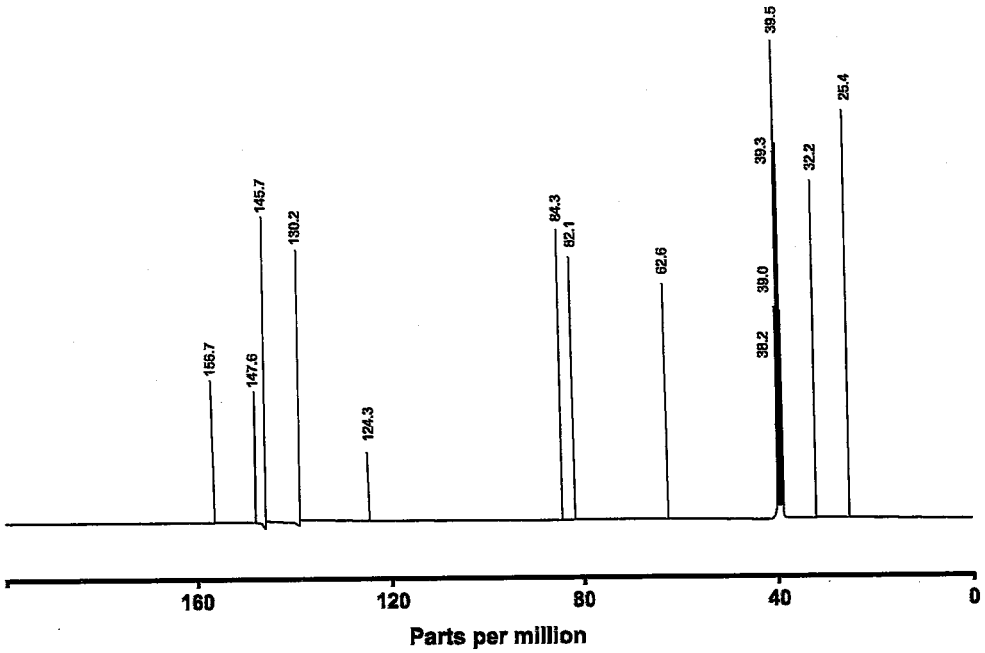

Figure 1.9. ^{13}C-NMR absorption spectrum of DDI obtained in d-DMSO (adapted from [3])

Table 1.6. ^{13}C-NMR characteristics of DDI in d-DMSO using TMS as external reference

Chemical shift (ppm)	Multiplicity	Assignment
156.7	Singlet	C6
147.6	Singlet	C4
145.7	Doublet	C2
138.3	Doublet	C8
124.3	Singlet	C5
84.5	Doublet	C1'
82.1	Doublet	C4'
62.6	Triplet	C5'
39.5	Multiplet	-
32.2	Triplet	C2'
25.4	Triplet	C3'

1.4.14 Mass spectrum

The mass spectrum (MS) of DDI is shown in Figure 1.10 and was generated using a Model-5985B Packard mass spectrometer equipped with a Model-701 Vestec thermospray interface and coupled to a Model-600MS Waters Associates high performance liquid chromatography (HPLC) instrument [3]. The MS shows that DDI has a peak base at 137 mass units which is due to the protonated hypoxanthine fragment [3]. The dimerization of the hypoxanthine in highly ionized plasma of the thermospray source is apparently responsible for the ionic fragment at 273 mass units [3]. The ionic fragments at 154 and 178 mass units are due to the ammonium and acetonitrile adducts of oxanthine, respectively [3]. The MS of DDI is indicative of extensive abduct data [3].

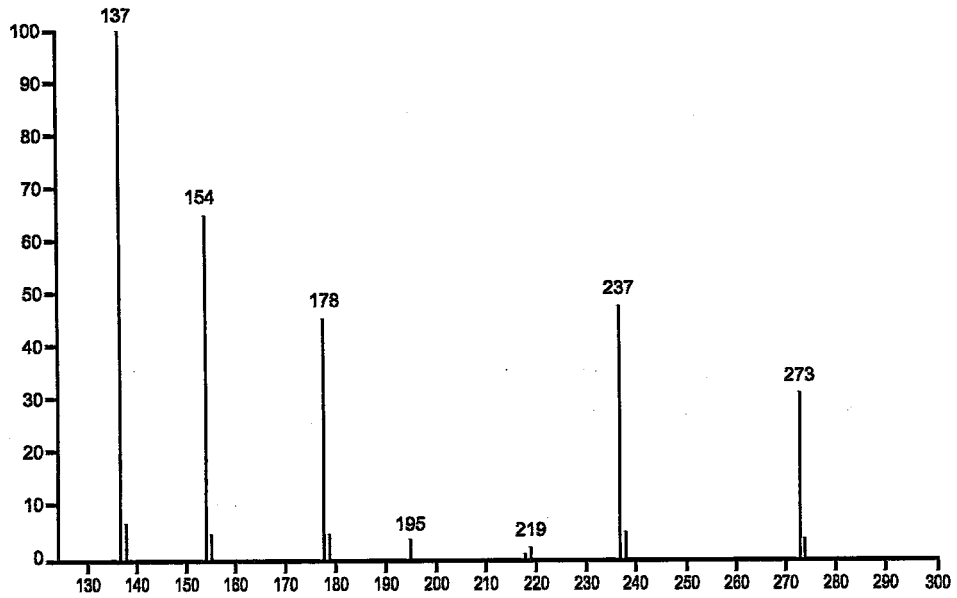

Figure 1.10. Mass spectrum of DDI (adapted from [3])

1.5 STABILITY

1.5.1 Solid state stability

In the solid state, DDI is stable at room temperature (25°C) and for at least 24 months when exposed to temperatures of 30°C [3]. In addition, DDI is stable when exposed to 25°C under high light intensity such as, for example 400 foot-candles or when stored at 87% RH [3]. The potency of DDI does not change significantly under these storage conditions and remains at > 95% following exposure at 50°C for eight (8) weeks [3]. However, DDI should be stored in a tightly closed container with the inclusion of a desiccant to prevent excessive moisture uptake [3].

1.5.2 Solution stability

The stability of DDI in aqueous solutions was monitored as a function of temperature and pH [4, 6], DDI concentration [6], ionic strength and buffer composition [4]. The degradation of DDI in dilute aqueous solutions follows pseudo first-order kinetics with a maximum stability observed in solutions of pH ranging between 12 and 13 [6]. The degradation rate constants of DDI in dilute and concentrated aqueous solutions of the API were not significantly different [6]. The degradation rate profile of DDI as a function of pH in dilute aqueous solution at 25°C is shown in Figure 1.11 [6] and reveals that the degradation of DDI is acid-catalyzed.

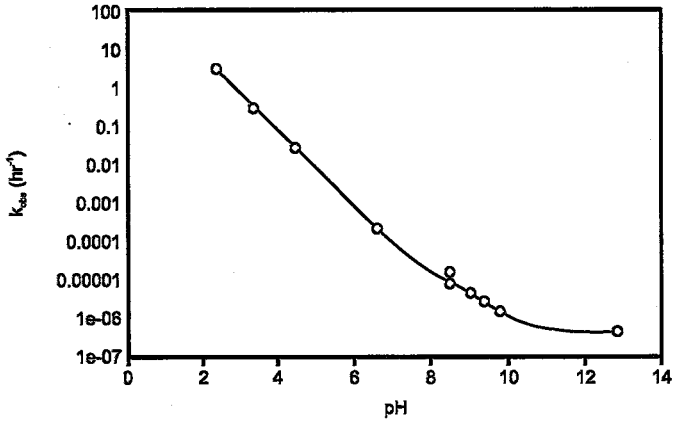

Figure 1.11. The pH-rate profile of DDI in aqueous solution at 25°C (adapted from [3])

DDI has a t_{90} at 37°C of less than 2 min at pH 3 [3, 6] and 509 days at pH 9.5 [3] indicating that the drug is highly acid labile but is relatively stable in alkaline environments [4, 6]. The

acid-catalyzed hydrolytic degradation reaction of DDI to hypoxanthine and 2′,3′-dideoxyribose is depicted in Figure 1.12. It is clearly evident that the N-glycosidic bond in DDI is susceptible to acid-catalyzed hydrolysis.

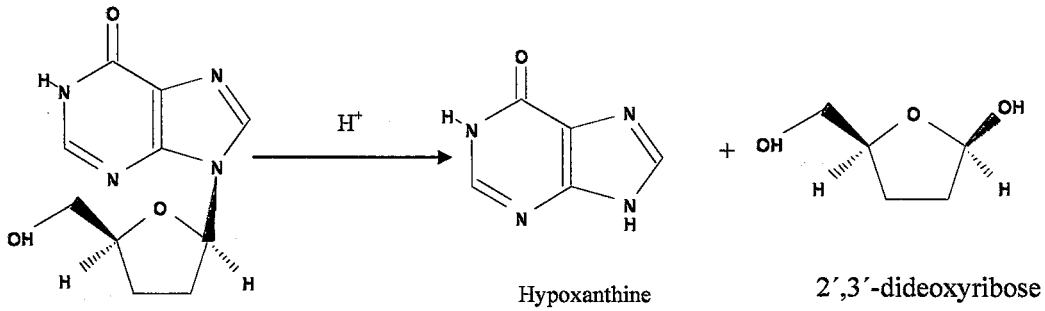

Didanosine

Figure 1.12. Hydrolytic degradation of DDI to hypoxanthine and 2′,3′-dideoxyribose

The ionic strength and buffer components *viz.*, acetate and phosphate ions have no apparent influence on the degradation rate of DDI at pH 2 (T = 25°C) and pH 6 (T = 80°C) [4]. However, the potency of DDI decreases to 40% following the addition of 3% v/v hydrogen peroxide to an aqueous solution of the API prepared in a 0.18 M phosphate buffer at pH 6.9 and allowed to stand for 6 hours at 37°C [3]. Conversely, the activity of DDI remains > 96% following exposure of an aqueous solution of DDI to high light intensity (minimum 1000 foot-candles) for eight (8) weeks in a solution of pH 9.0 at 30°C [3].

1.5.3 Dosage form stability

DDI chewable buffered tablets are stable for up to 36 months at controlled ambient temperatures of between 15-30°C [3, 8]. However, following the dispersion of DDI buffered tablets in water to form a suspension the compound is only stable for at least an hour at room temperatures of 20-22°C) [3, 8] and under lighting conditions of 0.0048-0.0059 foot-candles [3]. The expiry date of DDI buffered powder and non-buffered paediatric powder for oral solution is 24 months and 12 months respectively when these formulations are stored at temperatures between 15 and 30°C [3, 8, 16]. The buffered DDI powder for oral solution can only be stored up to four (4) hours at room temperatures of between 20 and 22°C following reconstitution [3, 8, 16]. Conversely non-buffered DDI paediatric powder for oral solution is

stable for 30 days if stored in a refrigerator at between 2-8°C following reconstitution with water and mixed with an appropriate antacid as directed [3, 8].

1.6 CLINICAL PHARMACOLOGY

1.6.1 Mechanism of action

DDI (2′,3′-dideoxyinosine) is a dideoxy synthetic analogue of the purine nucleoside, inosine that inhibits the replication of the HIV [3, 10, 40, 52-54]. DDI is a prodrug and is converted to an active moiety, namely 2′,3′-dideoxyadenosine-5′-triphosphate (DDATP) through intracellular phosphorylation [3, 10, 40, 42, 52-54]. Following passive diffusion of DDI into human lymphoid cells the drug is phosphorylated to 2′,3′-dideoxyinosine-5′-monophosphate (DDIMP) by a 5′-nucleotidase [10]. DDIMP is subsequently converted to 2′,3′-dideoxyadenosine-5′-monophosphate (DDAMP) through the activity of adenylosuccinate synthetase and lyase [10]. Phosphorylation of DDAMP by the purine nucleoside, monophosphate kinase leads to the formation of 2′,3′-dideoxyadenosine-5′-monophosphate (DDADP) [10]. DDATP is eventually formed when DDADP is phosphorylated further by the purine nucleoside, monophosphate kinase [10].

DDATP competes with a natural substrate for HIV reverse transcriptase (RT) and cellular DNA polymerase in the formation of HIV DNA [10]. The incorporation of DDATP into newly formed viral DNA results in the termination of the viral DNA chain elongation since DDATP lacks the 3′-hydroxyl functional group that is usually present in naturally occurring nucleosides [10, 42, 54]. Therefore additional nucleoside triphosphates cannot be added to the DNA chain and the synthesis of the HIV DNA is halted [10, 42, 54]. In addition, the competition of DDATP with endogenous 2′-deoxynucleoside-5′-triphosphate for binding to the active site of the HIV reverse transcriptase (RT) interferes with the synthesis of HIV DNA [54].

1.6.2 Spectrum of activity

In vitro studies have shown that DDI has a high affinity for both the HIV-1 [10, 54] and HIV-2 viruses [40, 54]. However, the inhibitory activity of DDI is greater against the HIV-1 virus [10, 55]. DDI has also been shown to have significant ARV activity against laboratory strains

and clinical isolates of HIV-1 including AZT-resistant strains present in T-lymphocytes, lymphoblastic cell lines, monocytes and human MT-cells when administered *in vitro* as mono-therapy [10, 13]. The minimum inhibitory concentration (MIC) of DDI required to reduce the replication HIV-1 by 50% (IC_{50}) ranges between 0.24-0.6 μg/ml in *in vitro* lymphoblastic cell lines and between 0.002-0.02 μg/ml in monocyte/microphage cell culture lines [10, 13].

DDI is more active in quiescent and non-dividing lymphoblastic and monocytes/macrophages cells whilst AZT and stavudine are potent in active cells [10]. Additive inhibitory activity of DDI against HIV-1 in AZT-resistant strains, various quiescent and/or dividing *in vitro* cell lines has been reported when the API is administered in combination with other ARV agents such as AZT, stavudine and delavirdine [9, 10, 56]. Co-administration of DDI with adenovir in MT-2 *in vitro* cell lines resulted in the synergistic inhibition of the HIV-1 virus [57]. However, there is dearth of information establishing a correlation between *in vitro* susceptibility of HIV to DDI and inhibition of HIV replication by DDI in humans [13]. The affinity of DDI for DNA polymerases is only restricted to the DNA polymerase gamma found in the mitochondria of the HIV virus [54].

1.6.3 Indications

DDI is indicated for the management of advanced HIV infection in adults and paediatric patients, older than 6 months, who are intolerant to AZT therapy or have demonstrated significant clinical or immunologic deterioration whilst using AZT [2, 3, 53]. DDI may be used alone or in combination with other ARV agents as an important component of triple combination HIV treatment regimens [10, 11].

1.6.4 Resistance

The most important cause of therapeutic failure in patients infected with HIV is the development of HIV-1 resistance to ARV drugs [10, 58]. A number of factors associated with rapid emergence of resistance of HIV-1 to ARV drugs have been reported and these include an advanced HIV disease state, low CD4 cell counts, high plasma viral loads, a syncytium-inducing (SI) phenotype, pre-existing drug-resistant variants and poor adherence to ARV drug regimens [10, 59]. Resistance is associated with one or more mutations in the HIV gene

of the protein that is targeted by an ARV agent [10, 59]. The resistance of HIV-1 to DDI may occur when the compound is used alone or in combination with other ARV drugs, albeit the rate and extent of emergence of resistance appear to differ significantly in each case [10].

The resistance of the HIV-1 virus to DDI in patients receiving long term *viz.*, one year DDI mono-therapy is mainly mediated through a mutation at codon 74 of the HIV-1 reverse transcriptase (HIV-RT) gene, that results in an amino acid change from leucine to valine (L74V mutation) [58, 60-67]. The L74V mutation causes a 5- to 26-fold decrease in the susceptibility of HIV-1 to DDI *in vitro* [58, 60-67]. Subsidiary resistance of the HIV-1 virus to DDI, which is observed with prolonged DDI mono-therapy is mediated via mutations at codon 65 that lead to an amino acid change from lysine to arginine (K65R mutation) and at codon 184, resulting in a change of amino acid from methionine to valine (M184V mutation) [58, 62, 68]. The K65R mutation leads to a 3- to 5-fold reduction in the *in vitro* sensitivity of the HIV-1 virus to DDI [68].

Co-administration of DDI with AZT significantly decreases the *in vitro* rate of emergence of resistance of the HIV-1 virus to DDI [58, 69, 70]. Resistance is characterized by the emergence of mutations at codons 62 (alanine to valine, A62V), 75 (valine to isoleucine, V75I), 77 (phenylalanine to leucine, F77L), 116 (phenylalanine to tyrosine, F166Y) and 151 (glutamine to methionine, Q151M) in the HIV-RT gene [13]. In addition, a 6-basepair insert between codons 69 and 70 of the HIV-RT gene has been reported in patients receiving DDI in combination with AZT [10]. A mutation at codon 181 (tyrosine to cysteine, Y181C) of the HIV-RT gene has also been observed in patients receiving DDI in combination with delavirdine [10].

1.6.5 Contra-indications

DDI formulations are contraindicated in patients with a known history of hypersensitivity to the drug or any of the components of formulations used to deliver the API [71]. In addition, DDI formulations should be avoided in patients with hepatic or renal impairment due to lack of sufficient data recommending the use of DDI in these patients [71]. The safety and efficacy of DDI in children younger than six months of age has not yet been established [71]. Buffered tablets of DDI contain phenylalanine and sodium and therefore caution should be exercised when it is administered to patients with phenylketonuria and/or those on sodium-

restricted diets [72]. Other contra-indications include risk factors for pancreatitis such as alcoholism and hyper-triglyceridaemia [72] and medicines that have the potential to cause pancreatitis should be avoided [72].

1.6.6 Drug interactions

DDI formulations containing buffers and/or antacids have the potential for interaction with pharmacological agents for which the oral absorption is affected by changes in gastric pH and/or chelation with cations of the buffer salts and/or antacids [5, 12]. An acidic pH is necessary to ensure adequate absorption of delavirdine [73], ketoconazole [74] and indinavir following oral administration [75] whereas the bioavailability of ciprofloxacin is decreased due to chelation of the drug by buffers and/or antacids [76]. Therefore, co-administration of buffered DDI formulations with delavirdine, ketoconazole, indinavir and/or ciprofloxacin may result in lower bioavailability of delavirdine, ketoconazole, indinavir and ciprofloxacin [5, 12, 73]. In addition, buffered DDI formulations should not be co-administered with formulations containing tetracycline antibiotics [3].

Co-administration of DDI with allopurinol, ganciclovir, tenofovir or disoproxil fumarate is not recommended as these drugs increase the plasma concentration of DDI while concurrent administration of DDI with methadone decreases plasma concentrations of DDI [13]. Ribavirin increases intracellular triphosphate levels of DDI *in vitro* and therefore may exacerbate clinical toxicity of DDI [8]. The risk of peripheral neuropathy and pancreatitis may be increased when DDI is co-administered with other drugs known to cause these side effects [3]. It is recommended that co-administration of DDI with pentamidine, sulphonamides and cimetitine be avoided [42].

1.6.7 Adverse effects

DDI is well tolerated by most HIV-positive patients, when administered alone or in combination with other ARV agents and the tolerability profile of DDI remains unchanged when a patient is switched from a once-daily to a twice-daily regimen of the drug [10, 53]. Clinical studies have shown that adverse effects observed during DDI therapy frequently occur in patients that present with an advanced HIV infection more so than in HIV-naïve patients [8-10]. Peripheral neuropathy and pancreatitis are the most serious dose-related

adverse reactions of DDI in both adult and paediatric patients, however these side effects are usually reversible on discontinuation of DDI therapy [3, 8, 10, 42]. Lactic acidosis and severe hepatomegaly with steatosis have been reported as rare but are potentially life-threatening side effects of DDI when the drug is administered alone or in combination with other ARV agents, especially in female patients [8-10].

Retinal and visual changes as well as optic neuritis have also been reported in adult and paediatric patients receiving DDI [8-10]. Other adverse effects that have been associated with DDI therapy include nausea, vomiting, diarrhoea and/or abdominal pain [10, 42, 53]. However these side effects have been attributed to the presence of buffers and/or antacids in the DDI formulation that is administered [10, 42, 53]. Alopecia, anaphylactoid reaction, aesthenia, chills/fever, pain, anorexia, dyspepsia, anaemia, leukopaenia, thrombocytopaenia, diabetes mellitus, hypoglycaemia, hyperglycaemia, myalgia, rhabdomyolysis, arthralgia and myopathy are some of the adverse events that have been identified following post-approval marketing authorization of DDI [8, 10, 53].

1.6.8 High risk groups

1.6.8.1 Fertility and pregnancy

Reproductive studies conducted in rats and rabbits using doses of up to 12 and 14.2 times those that are typically administered to humans showed no evidence of impaired fertility and/or foetal risk following DDI use [8]. Consequently, DDI is a category B risk factor for use in these populations as defined by the United States Food and Drug Administration (FDA) [8]. However, results from adequate and well-controlled studies of DDI use in pregnant women are not available and therefore, it is recommended that DDI therapy during pregnancy be initiated only if the potential benefit of using the compound outweighs risk [8]. Co-administration of DDI and stavudine with other ARV agents has resulted in fatal lactic acidosis in pregnant women and should therefore be avoided [8].

1.6.8.2 Lactation

Studies conducted in rats revealed that DDI and/or its metabolites are secreted in the milk following oral administration DDI [8]. There are currently no data available to show whether

DDI is secreted in human breast milk and consequently, it is strongly recommended that nursing mothers on DDI therapy not to breast-feed their children in order to avoid the potential for, not only HIV transmission but for serious adverse reactions in breast-feeding infants [8].

1.6.8.3 Paediatric use

There is lack of data available to substantiate the safety of DDI in paediatric patients whether given alone or in combination with other ARV agents. However, the effectiveness of DDI as a mono-therapeutic option or in combination with AZT was demonstrated in a randomized, double-blind controlled trial [16]. The study revealed that paediatric patients receiving DDI alone or in combination with AZT showed lower rates of HIV progression or death compared to those treated with AZT alone [16].

Pharmacokinetic studies of DDI conducted in HIV-exposed and/or infected paediatric patients from birth to 19 years of age revealed that the pharmacokinetic parameters of DDI in paediatric patients are similar to those DDI in adult patients treated with the drug [16]. However, the pharmacokinetic parameters of DDI in paediatric patients less than two weeks of age are highly variable and therefore, determination of an appropriate dose for these patients is extremely difficult [16]. Consequently DDI is only indicated for use in paediatric patients older than six (6) months of age [54].

1.6.8.4 Geriatric use

In clinical studies in which DDI was administered to patients with advanced HIV infection, a sufficient number of patients over the age of 65 years were not included to determine categorically whether geriatric patients respond differently to DDI therapy than younger patients [8]. However, the results of another clinical study revealed that 10% of patients over the age of 65 years had a higher frequency of pancreatitis compared to 5% of their younger counterparts [8]. It has also been reported that DDI is extensively excreted by the kidneys and therefore, the risk of a toxic reaction to DDI is likely to be greater in patients with impaired renal function [8]. The greater frequency of decreased hepatic, renal or cardiac function and concomitant disease drug therapy suggest that extreme caution must be observed when

treating elderly patients with DDI [8]. The pharmacokinetic parameters of DDI have not yet been established in patients older than 65 years [16].

1.7 PHARMACOKINETICS

1.7.1 Dosage

DDI formulations for oral use usually contain buffers or antacids to minimize the potential for acid-catalyzed degradation of the drug in the gastric environment following administration [3, 10, 53]. DDI is currently available as chewable and/or dispersible buffered tablets of 25, 50, 100, 150 and 200 mg strength [8, 42, 71] or as buffered powder for oral solution in single 100, 167, 250 or 375 mg doses packed in child-resistant sachets [8, 10, 42]. In addition, a non-buffered paediatric formulation containing 2 g or 4 g of DDI which must be reconstituted with water and mixed with an equal amount of an antacid, prior to administration to patients is also available [8, 10, 71]. DDI has also recently been approved for marketing in the United States of America (USA) and Europe as an encapsulated-coated bead formulation (Videx® EC) for oral administration to adult patients [13, 77]. Videx® EC capsules are available in strengths of 125 mg, 200 mg, 250 mg and 400 mg [13].

DDI may be administered to adult patients as a once or twice daily regimen but the latter approach is preferable as there is evidence to support the effectiveness of a twice daily regimen [8]. However, once daily dosing should be considered for adult patients in which a once-daily regimen is preferred [8]. The recommended daily dose for DDI in adult patients is usually based on the weight of the patient. Adult patients weighing $\geq$ 60 kg receive 200 mg twice daily or 400 mg once a day and those weighing $\leq$ 60 kg receive 125 mg twice daily or 250 mg once daily [8, 39, 53, 71]. The dose of DDI for paediatric patients is usually based on the body surface area (BSA) of the patient and the average recommended dose in these patients is 125 mg/m^2 twice-daily [8] or 200 mg/m^2/day [78] .There are no data to support a once-daily dosing regimen in children [8] and consequently paediatric patients having a BSA of 0.4, 0.5-0.7, 0.8-1.0 and 1.1-1.4, m^2 should be given 25, 50, 75 and 100 mg of DDI twice daily [78].

1.7.1.1 Administration

The oral absorption of DDI is reduced in the presence of food [3, 10] and consequently, it is recommended that oral administration should take place on an empty stomach [3, 10, 78] or at least 30 minutes before or 2 hours after meals [10, 78]. In addition, in order to ensure adequate antacid effects and prevent and/or minimize acid-catalyzed degradation of the drug in the stomach, it is recommended that each dose be administered as two tablets of appropriate strength in adults and paediatric patients over one year of age or as one tablet in children between the ages of six months and one year [8, 53, 78]. Each dispersible tablet should be dissolved in 15 ml of water or apple juice [78] or in ≥ 30 ml of water [10].

Each sachet containing buffered DDI powder for oral solution should be reconstituted with 120 ml of water [8, 10] and not with fruit juice or other acid-containing liquids [8]. Non-buffered paediatric DDI powder for oral solution should be reconstituted with 100 ml or 200 ml of purified water for 2 g or 4 g powder, respectively to form an initial solution of 20 mg/ml in the original bottle in which the product was packaged [8, 16]. One part of the 20 mg/ml solution should be mixed with one part of magnesium and/or aluminium hydroxide antacid suspension to produce a final DDI concentration of 10 mg/ml and this reconstituted suspension can be stored at 2-8°C for up to 30 days [8, 16].

1.7.2 Absorption

The oral absorption of DDI is permeability-limited and intestinal site-dependent with absorption of the drug decreasing in the distal regions of the small intestine [79]. DDI is rapidly absorbed from the gastro-intestinal tract (GIT) [39] with maximum plasma concentrations (C_{max}) being observed within 0.25-1.50 hours following oral administration of the drug [8]. The C_{max} of DDI ranges between 0.52-2.79 μg/ml after multiple oral doses of between 125-375 mg of DDI powder formulations given twice daily to HIV-infected adult patients [9, 10]. Similarly, the C_{max} values of DDI in paediatric patients infected with HIV ranged between 0.5-4.1 μmol/l after single oral doses of between 20-180 mg/m^2 [9, 10]. The mean C_{max} and area under the plasma concentration-time curve calculated up to 24 hours ($AUC_{0\text{-}24h}$) in HIV-infected patients receiving DDI once daily has been reported to be equivalent to the C_{max} and $AUC_{0\text{-}24h}$ observed in patients receiving the drug twice daily [10].

The oral absorption of DDI in both adult and paediatric patients infected with HIV is however incomplete and erratic, resulting in considerable inter-individual variation in the oral bioavailability of the drug [9, 10, 80], which is more than likely due to differences in the physiology of each individual. The oral bioavailability of DDI ranges between 21-54% in adults and 13-29% in children [9, 10] or between 30-40% in adults and 19% ± 17% in paediatric patients [54] or 42 ± 12% in adults and 25% ± 20% in paediatric patients [8] or between 20-40% in adult patients [39]. The rate and extent of absorption of DDI following oral administration decreases in the presence of food [8-10, 39, 77] and although the mechanism of this reduction is unclear, it has been suggested that an increase in acid secretion in the presence of food may lead to an enhanced acid-catalyzed degradation of DDI [10]. In addition, the presence of food in the stomach delays gastric emptying, thereby prolonging contact of DDI with the acidic contents of the stomach [10].

1.7.3 Distribution

The mean apparent volume of distribution (V_d) of DDI determined at steady state following oral administration in adults and paediatric patients with HIV infection is 1.08 ± 0.22 L/kg and 28 ± 15 L/m^2, respectively [8] or 54 L and 9-40 L/m^2 [9, 10]. DDI crosses the placenta and is usually detected in both amniotic fluid and foetal blood [39]. However, the concentrations of DDI in placental and foetal circulation are 20 to 50% lower than those found in the maternal circulation [9, 10]. The concentrations of DDI achieved in the cerebro-spinal fluid (CSF) one (1) hour following a single intravenous dose to adult patients were 20% [39, 42] or 21% [10] of those observed in plasma at the same time-point. The plasma protein binding of DDI is less than 5% [9, 10, 39] and DDI is not as widely distributed as AZT [9, 10, 39].

1.7.4 Metabolism

The metabolism of DDI in patients with HIV infection has not yet been fully studied. However available data indicate that DDI is extensively metabolized via one of two pathways [3, 10, 39]. The minor metabolic pathway of DDI is responsible for the ARV activity of DDI and involves a cascade of reactions that ultimately leads to the production of the active DDI metabolite, DDATP [3, 10, 39] as described in Section 1.6.1 of this Chapter. DDI is also metabolized to form uric acid via purine nucleotide phosphorylase that leads to the

production of hypoxanthine and this is a major metabolic pathway for DDI [3, 10, 39, 42]. Hypoxanthine can either re-enter the purine nucleotide metabolic pathway or can be metabolized further to form uric acid through the action of xanthine oxidase [3, 10].

1.7.5 Elimination

The plasma elimination half-life ($t_{1/2}$) of DDI is relatively short and ranges between 0.5-2.74 hours [10] or 0.5-4 hours [39]. However, the intracellular $t_{1/2}$ of the active moiety, DDATP, is longer than 12 hours [39] or 25 hours [10] and is further increased in patients with renal impairment [39]. The plasma clearance of DDI ranges between 600-800 ml/min in adults and 510 ml/min/m^2 in children [39]. However, the total body clearance of DDI in adults ranges between 20.1-22 L/h following a single oral dose of 300 mg [10] or 0.08 L/kg/h [39]. Approximately 40% of the total dose of DDI is eliminated unchanged drug in the urine, 50% as hypoxanthine and 4% as uric acid [9, 10].

1.8 CONCLUSIONS

There are two major obstacles to the successful and/or adequate management of HIV, especially in paediatric patients using an antiretroviral agent such as DDI. The first obstacle is the susceptibility of DDI to hydrolytic degradation in the acid environment of the stomach [4, 5, 10] which in turn leads to a reduction in bioavailability and *in vivo* activity of the orally administered compound [3-5]. In order to improve the acid stability and bioavailability of DDI, the compound has been formulated as buffered or non-buffered powder for reconstitution as an oral solution for use in paediatric patients [3-5, 7]. The non-buffered DDI powders are usually mixed with antacids following reconstitution, prior to oral administration of the drug to patients [3-5, 7, 8].

However the buffered or antacid-containing formulations are unstable at room temperature and invariably require cold room storage conditions, yet these facilities are usually out of reach of the majority of the population in developing countries. Furthermore, the DDI formulations are unpalatable [5, 7] and cause gastrointestinal disturbances [5, 7] such as diarrhoea, nausea, vomiting and/or abdominal discomfort [7, 10, 11] which are a consequence of the presence of buffers in the formulations. The side-effects, in addition to those directly attributed to DDI such as pancreatitis and peripheral neuropathy [10, 11] impact negatively

on the quality of life of patients. Therefore, adherence of patients to chronic DDI therapy may be negatively affected thereby further hindering the management of HIV/AIDS in children. In addition, the presence of buffers and/or antacids in DDI formulations has been shown to significantly decrease the oral absorption of certain co-administered drugs, such as for example indinavir, ketoconazole and ciprofloxacin [5, 12].

One of the main objectives of this research is to investigate the feasibility of using innovative SLN and/or NLC as drug delivery systems for the oral administration of DDI to paediatric patients. However it was anticipated that certain physicochemical properties of DDI such as its hydrophilic nature and low octanol/water partition coefficient would pose a challenge to the successful development of SLN and/or NLC with sufficient LC and EE for the drug. Consequently, a subsidiary aim to this research was to identify and apply process and/or formulation approaches that would enhance the LC and EE of SLN and/or NLC for DDI.

The emergence of HIV/AIDS-related complications such as ADC due to the accumulation of the virus in the central nervous system is another obstacle to the successful management of HIV/AIDS. This is further complicated by the inability of ARV agents such as DDI to cross through the BBB and maintain sufficient therapeutic concentrations in the affected brain structures. As a consequence the virus multiplies and accumulates in the CNS, unabatedly, leading to the onset of ADC which has been described as a very debilitating syndrome [17, 18].

Therefore there is a need for the formulation and development of novel drug delivery systems that have the ability to deliver anti-HIV agents to the CNS by circumventing the BBB in order to adequately manage HIV infection and inhibition of viral replication within the CNS. Consequently, the second objective of this research was to use the concept of differential protein adsorption to determine the potential for DDI-loaded SLN and/or NLC to target the brain. Data generated in these studies could be used to establish whether SLN and/or NLC could potentially deliver DDI to the CNS thereby leading to the adequate management of HIV in the CNS. Delivery of ARV drugs to the CNS would alleviate certain AIDS-related complications such as ADC in patients with HIV/AIDS and consequently, improve their quality of life.

CHAPTER 2

SOLID LIPID NANOPARTICLES AND NANOSTRUCTURED LIPID CARRIERS

2.1 BACKGROUND

Research and development into the field of colloidal drug delivery systems (CDDS) in the nanometre range has become vitally important over the years [30-32, 81-127]. This has been necessitated by a need for researchers in the pharmaceutical industry to find novel drug carrier systems that are non-toxic [25, 30, 31, 102] and capable of enhancing the solubility and hence the oral bioavailability of lipophilic compounds [128-131]. In addition, these systems should provide protection to unstable drug molecules [132-136] and control the release of specific drug candidates where appropriate [25, 27, 28, 137]. Furthermore, the need for further research in the field of CDDS in the nanosize range has been encouraged by a desire to realize drug carriers that are capable of targeting and delivering certain drugs to specific tissues and/or organs that would otherwise be inaccessible [138-141]. Various researchers have reported different CDDS in the nanometre range, such as for example, liposomes [96-98, 100, 101, 103, 105, 106, 142], nanoemulsions [86, 115, 143], nanocapsules [84, 94, 108, 110, 113, 118, 121], polymeric nanoparticles [85, 89, 95, 111, 116, 127, 137, 144] and solid lipid nanocarriers [25, 26, 28, 30-33, 145].

Nanoemulsions (NE) [86, 115, 143] were developed in the 1950's and were initially intended for use in parenteral nutrition applications [143]. However following years of further research, NE were developed for use as CDDS for the intravenous (I/V) administration of hydrophobic substances, which resulted in the commercialization of NEs-based products such as, for example Diazepam-Lipuro®, Disoprivan®, Lipotalon® and Stesolid® [27, 33, 115, 143, 146]. The main advantage of using NEs-based I/V products over other emulsion-based formulations such as micro-emulsions includes the minimization of pain at the site of injection [33]. In addition, NEs-based formulations may prevent or reduce haemolysis *in vivo* caused by use of high concentrations of surfactant in microemulsion formulations [33]. A major obstacle to the use of NE as CDDS is the potential for partitioning of a drug molecule from the oil droplets into the continuous phase that is aqueous in nature [33, 147]. This may compromise the stability of an active pharmaceutical ingredient (API) that has a limited

stability profile in an aqueous environment [33, 147]. In addition NE-based formulations do not provide controlled release profiles for an API due to lack of resistance to diffusion of that API encapsulated within an oil droplet [81, 120, 122].

Liposomes [99, 102, 103] were developed in 1965 and initially used as a model for depicting the structure of a cell membrane [106]. However, in the 1980's [27] these systems were introduced to the market, initially as a topical product e.g. Pevaryl®-Lipogel [104], and subsequently as CDDS intended for IV administration e.g. AmBiosome® [117, 119] and DaunoXome® [117, 148]. Various advantages to the use of liposomal products for topical [101] and parenteral administration [27, 98] of API have been reported. The topical Pevaryl®-Lipogel is apparently superior to conventional Pevaryl® products e.g. Pevaryl® cream, gel and lotion in terms of the biodisposition, which in turn results in a 7-9 fold increase in the amount of the API delivered to the epidermis [101]. The IV administration of an API in liposomal products such as AmBiosome® and DaunoXome® is associated with lower incidence of systemic side effects than when the same API is administered IV using conventional dosage forms. Liposomes have been used to encapsulate both hydrophilic and lipophilic molecules [27].

The major disadvantage of liposomal formulations is their limited intrinsic physicochemical stability over a prolonged storage period [98, 100, 103, 142]. In addition, liposomes undergo acid-catalyzed and/or enzymatic-induced degradation in the gastrointestinal tract (GIT) following oral administration [98, 100, 103, 142]. Consequently, there has been limited success with the development of liposomal pharmaceutical products intended for the oral administration of API [98, 100, 103, 142]. Furthermore, some of the methods used to produce liposomes require the use of organic solvents which may be undesirable when the solvent used is toxic and not completely removed from the product during the production stages [96, 98]. Other obstacles to the widespread use of liposomes that have been cited include the lack of availability of equipment for the large scale production and the relatively high cost of pharmaceutical excipients required for the manufacture of these systems [96, 98]. Further research into the field of CDDS has led to the development of nanocapsules (NC) [84, 94, 108, 110, 113, 118, 121] and polymeric nanoparticles (PN) [85, 89, 95, 111, 116, 127, 137, 144] for the incorporation of a range of API. The major advantage of NC and PN when compared to NE and liposomes is that NC and PN consist of a solid matrix which allows for possible protection of an API encapsulated in the polymeric matrix from a hostile

environment e.g. unfavorable aqueous conditions [109, 123, 126]. In such instances, the polymeric membrane may act as a physical barrier between the API that is encapsulated in the solid matrix and the hostile medium [109, 123, 126]. In addition, the solid polymeric matrix may retard the release of a drug from these carriers by hindering the free mobility of a drug through the solid matrix. Consequently, the solid characteristics of NC and PN may also allow for controlled release of an API from NC and/or PN, which may be desirable for certain drug candidates but that could not be achieved through the use of NE and/or liposomes [109, 123, 124, 126].

Despite these advantages, the potential for commercialization and widespread use of NC and PN as CDDS is limited due to a number of drawbacks that have been associated with these carriers. The main obstacle to the widespread use of NC and PN as CDDS is the toxic nature of some of the polymers used to manufacture the nanoparticles and/or the toxicity that may be imparted to the particles by the residual toxic organic solvents used during the production of the carrier systems [82, 92, 149, 150]. In addition, it is still difficult to find universal equipment for use in the production of NC and PN on a large scale or production scale which is undoubtedly a pre-requisite for the commercialisation of any drug delivery system [82, 92, 149, 150]. It is worth noting that notwithstanding these challenges there is one product based on PN *viz.*, Abdoscan® currently available commercially, albeit the only product that has made it to the market despite over 30 years of research in the field of polymeric nanotechnology [27].

Solid lipid nanoparticles (SLN) [25, 28, 151-156] were developed in the 1990's as alternative CDDS to the use of liposomes, nanoemulsions, nanocapsules and polymeric nanoparticles. SLN [27, 28, 30, 33, 140] combine the advantages of early CDDS while minimising their shortcomings [33. 62, 63, 66, 73]. Several advantages to the use of SLN have been reported and include the achievement of controlled release and an improvement in the stability and bioavailability of drugs incorporated into these systems [27, 28, 30, 33, 140]. In addition, SLN can be manufactured using physiologically acceptable and biodegradable lipid materials that have a GRAS (Generally Regarded as Safe) status while avoiding the use of organic solvents [27, 28, 30, 33, 140]. Furthermore, SLN may be used to incorporate hydrophilic and hydrophobic drugs under optimised conditions and can be manufactured on an industrial scale using high pressure homogenization [27, 28, 30, 33, 140].

There are however certain drawbacks that have been associated with the use of SLN which include particle growth, an unpredictable tendency to gel, limited drug LC and drug expulsion on prolonged storage [29, 157, 158]. Consequently, in order to overcome these challenges, a second generation of lipid nanocarriers, referred to as nanostructured lipid carriers (NLC) were developed at the turn of the 21st century [30, 159]. NLC matrices consist of a less ordered lipid matrix with imperfections which may lead to an increase in drug LC and prevent drug expulsion during prolonged storage [30-34]. This is because in contrast to SLN which are produced from highly purified lipids with similar molecular structures, NLC are manufactured using binary mixtures of solid and liquid lipids (oils) [30-34].

Various attempts have been made to incorporate different compounds into SLN and/or NLC intended for oral [160], parenteral [34] in addition to dermatological and cosmetic [33, 147] applications. A comprehensive list of drugs, miscellaneous and macrocyclic skeletons that have already been incorporated into SLN and/or NLC by various researchers has been published recently [161]. However, no attempts have been made to incorporate DDI into SLN and/or NLC. Therefore an objective of this research was to investigate the feasibility of incorporating DDI into SLN and/or NLC. It is important to realize that the review of SLN and NLC presented in this Chapter is not exhaustive but details information that was considered necessary and applicable to this project.

2.2 DESCRIPTION OF SLN AND NLC

2.2.1 Solid lipid nanoparticles

2.2.1.1 Overview

SLN consist of a solid lipid matrix that is solid at both room and body temperatures and that are prepared in a similar manner to an oil-in-water (o/w) emulsion except that the oil phase of the emulsion is replaced by a solid lipid or a blend of solid lipids [162]. Consequently, SLN may be composed of a solid lipid or a mixture of solid lipids dispersed in an aqueous phase and if necessary stabilized with a surfactant or combination of surfactants [162]. The mean particle size of SLN may range between 50-1000 nm but it is usually difficult to produce SLN of mean particle size lower than 80 nm as these small particles seldom re-crystallize during the manufacturing process [26, 163]. Cosmetic and pharmaceutical agents may be

incorporated into SLN in order to protect these substances from the surrounding environment [164, 165]. An aqueous SLN dispersion designed to incorporate a pharmaceutical agent may be used as granulating fluid in the manufacture of conventional dosage forms such as tablets or pellets [29, 33]. In addition an aqueous SLN can be transformed into a dry powder using spray-drying or lyophilisation to enhance their long-term stability and when required, may be reconstituted with water to produce a suspension [29, 33].

2.2.1.2 Drug incorporation into SLN

The incorporation of an API into SLN depends on numerous factors, including the solubility of the API in the lipid, the physicochemical properties of the API, lipids and surfactants in addition to the method used to produce the SLN [27, 162]. Consequently four (4) different models postulating how a drug may be incorporated into SLN have been described [26, 29, 162] and these are depicted in Figure 2.1.

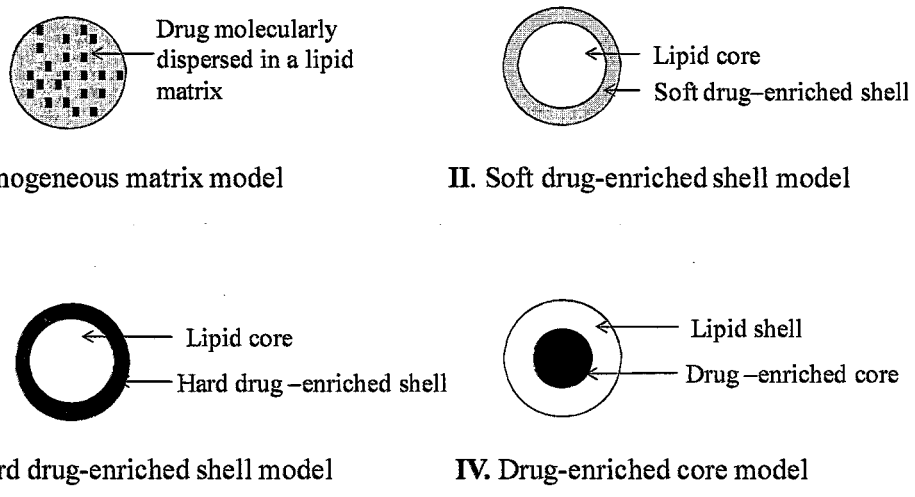

Figure 2.1. Postulated models of incorporation of drug into SLN (diagrams modified from [162])

2.2.1.2.1 Homogeneous matrix model

The homogeneous matrix or solid solution model (I) describes a situation in which an API is molecularly dispersed or is present as amorphous clusters within a solid lipid matrix [27, 162]. This model may be produced when a cold high pressure homogenization (HPH).

technique (Section 2.4.2.3) is used to produce the API-loaded SLN or when a hot HPH (Section 2.4.2.2) is used to incorporate a highly hydrophobic API into SLN [27]. In the latter situation the lipophilic drug is initially dissolved in the bulk lipid materials and then the hot HPH process is used to break down the crude drug-containing microemulsion to form SLN with a homogeneous API-containing structure [27]. Similarly the homogeneous matrix model can be produced when oil droplets that are generated following the application of the hot HPH to the crude drug-containing microemulsion are allowed to cool down and recrystallize into SLN *in situ* without the occurrence of phase separation between the lipid and the API [27]. The release of a drug from these systems is determined by the rate of diffusion of the drug within the solid lipid matrix and therefore this model of drug incorporation is associated with SLN that release an API in a controlled manner [27].

2.2.1.2.2 Soft and hard drug-enriched shell models

The soft and the hard drug-enriched shell models (II and III, respectively) describe SLN that have an inner solid lipid core which is surrounded by an outer shell enriched with API [27, 162]. These models can be achieved when SLN are also produced using a hot HPH technique but in contrast to the homogeneous matrix model, phase separation between the oil droplets and the drug occurs during cooling of the nanoemulsion [27, 162]. Initially the drug partitions from the lipid phase into the aqueous phase allowing the oil droplet to commence recrystalization to form a solid lipid core that is relatively drug-free [27, 162]. This results in a steady increase in the amount of API in the liquid oil (lipid shell) surrounding the newly formed lipid core. Subsequent recrystallization of the oily lipid shell leads to the formation of a drug-enriched solid lipid shell around the lipid core [27, 162]. The drug-enriched solid lipid shell may be soft or hard depending on the interaction between the API and the lipid used [27, 162]. A hard drug-enriched shell may be formed when the drug and the lipid have structural characteristics that enable them to fit together to form a strong, brick-like solid layer [162]. The soft and the hard drug-enriched shell models are associated with SLN formulations that show burst release of the API incorporated into the SLN [27].

2.2.1.2.3 Drug-enriched core

The drug-enriched core model (IV) describes the incorporation of a drug in SLN that involves the formation of a drug-enriched core surrounded by a shell that is relatively free of drug [27,

162]. The model can be achieved when the concentration of a drug in an SLN formulation is close to the saturation solubility of the drug in the lipid phase of the formulation [27]. This allows the drug to precipitate and form a drug-enriched core during cooling of the nanoemulsion [27]. Further cooling allows the oil droplets around the drug-enriched core to recrystallize to form a solid lipid shell that can act as a membrane to control the release of the drug from the core of the SLN [27, 33, 162]. The drug-enriched core model has been used to describe the incorporation of a drug into SLN formulations that show initial burst release followed by controlled release of API from the SLN [27, 33, 162].

2.2.2 Nanostructured lipid carriers

2.2.2.1 Overview

The disadvantages associated with the use SLN (Section 2.1. *vide infra*), especially those regarding low drug LC and drug expulsion during prolonged storage periods led the development of nanostructured lipid carriers (NLC) [31, 33]. The crystalline nature and polymorphic transition of solid lipids used in the formulation of NLC were identified as the main causes of drug expulsion [30, 31, 33, 166]. Pure solid lipids are crystalline materials which exist in a low energy and highly ordered β-polymorphic form [30, 31, 33, 166]. However, after melting during the production of SLN, the lipid recrystallizes as a high energy and less ordered α- and/or β′-polymorphic modifications [30, 31, 33, 166]. These polymorphic forms are amorphous and allow for drug incorporation and retention in the solid lipid matrix [30, 31, 33, 166]. However, during prolonged storage, the metastable α and β′ polymorphic forms revert to the stable β modification, the consequence of which is a decrease in the number of imperfections within the solid lipid matrix. This leads to subsequent expulsion of the drug from SLN into the aqueous phase of formulation, as shown in Figure 2.2 [31, 33].

In contrast to SLN, which are produced using highly purified lipids with a similar molecular structure, NLC are manufactured by controlled mixing of solid lipids with suitable liquid lipids [30, 159]. The addition of liquid oil to a solid lipid creates a less ordered crystal lattice with an increased number of imperfections which can accommodate amorphous drug clusters [30, 33]. Consequently, the LC of NLC for drug molecules is likely to be higher than that of

SLN and in addition, drug expulsion during prolonged storage is less likely to occur from NLC compared to SLN [30].

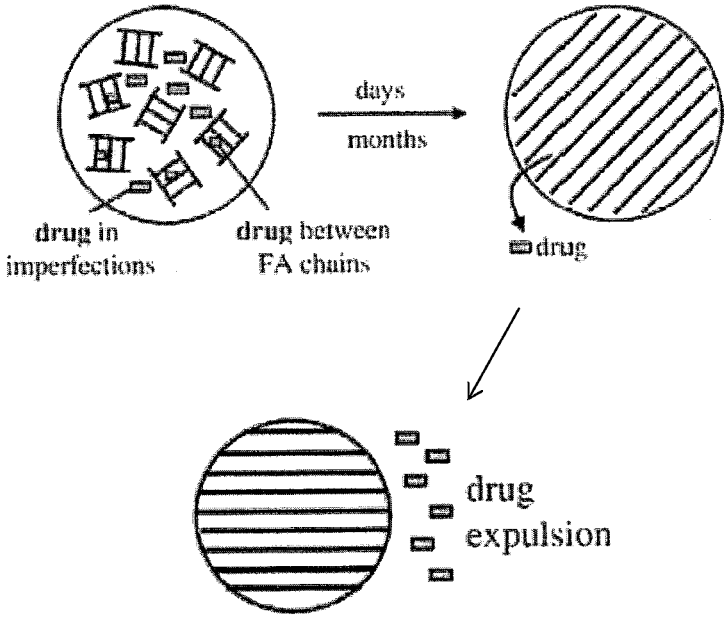

Figure 2.2. Postulated mechanism of drug expulsion from SLN aqueous dispersion on prolonged storage [31, 33].

2.2.2.2 Model of drug incorporation into NLC

Three (3) possible models have been postulated for the incorporation of drugs into NLC [30, 33] and are illustrated in Figure 2.3.

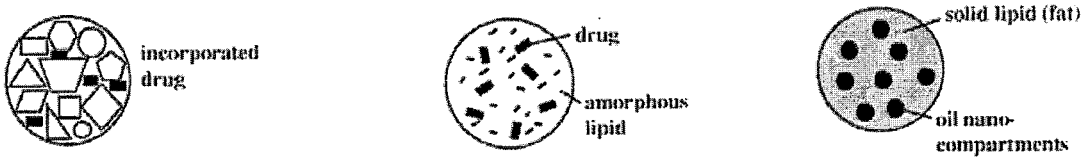

I. Imperfect crystal type ***II. Amorphous type*** ***III. Multiple type***

Figure 2.3. Postulated models of drug incorporation into NLC (diagrams modified from [30, 33])

2.2.2.2.1 Imperfect crystal type

The imperfect crystal type (I) is a model that can be achieved by blending solid and liquid lipids that are chemically dissimilar [30, 33]. Following recrystallization these blends form a highly disordered crystal lattice with many imperfections that are able to accommodate increased amounts of a drug, leading to a high LC of NLC for the drug [30, 33].

2.2.2.2.2 Amorphous type

The amorphous type (II) inclusion can be obtained by using a mixture of special lipids such as hydroxyoctacosanylhydroxy stearate and isopropyl myristate, which fail to recrystallize fully after they have been melted [30, 33]. Consequently, these lipids produce a permanent amorphous polymorphic structure (α-modification) that retain the drug that has been incorporated into the system over a long period of time and prevent or minimize expulsion of the drug from the lipid matrix [30, 33, 161].

2.2.2.2.3 Multiple type

The multiple emulsion type (III) describes a situation in which minute drug-containing oil droplets are dispersed within solid lipid nanoparticles that are themselves dispersed in water to form what is termed an "oil-in-fat-water" (O/F/W) nanoemulsion [30]. This model is based on an assumption that the solubility of a number of drugs is higher in oils than in solid lipids [161, 167]. The model can therefore be used to increase the LC of solid lipid nanoparticles for an API. This model is produced by blending a solid lipid with a liquid lipid in quantities that allow the solubility of the oil in the solid lipid to be exceeded thereby resulting in phase separation after cooling [30, 161]. Initially the two components are miscible during homogenization at relatively high temperature to form a nanoemulsion [30, 161]. However, as the nanoemulsion is allowed to cool the oil molecules begin to separate resulting in the formation of minute oil droplets within the molten lipid phase [30, 161]. Subsequent recrystallization of the lipid phase to form solid lipid nanoparticles results in the encapsulation of the drug-containing oil droplets within the solid lipid matrix [30, 161].

2.3 FORMULATION OF SLN AND NLC

Inactive pharmaceutical excipients that are used in the formulation of SLN and NLC are solid lipids (SLN), a combination of solid and liquid lipids (NLC), surfactants and water [29]. The basic principle in the preparation of SLN and NLC is that at a certain point during the process, a solid lipid or a binary mixture of solid and liquid lipids needs to be melted and re-dispersed as lipid droplets of submicron size in an aqueous medium, to produce what is referred to as "aqueous SLN or NLC dispersion" [29, 34, 160]. This process can be accomplished by either mechanical or thermodynamic means in order to allow for the formation of SLN or NLC [29, 34, 160]. One or more emulsifying agents can be added to either the lipid or aqueous phase, depending on the hydrophilic lipophilic balance (HLB) of the surfactant in order to produce a thermodynamically stable system [162]. It is recommended that excipients with a Generally Regarded as Safe (GRAS) status be used in the formulation of SLN and NLC in order to minimize the risk of acute and/or chronic toxicity during *in vivo* use, which has been associated with the administration of other CDDS such as polymeric nanoparticles [29]. Mehnert and Mäder [29] as well as Souto and Müller [161] have reported comprehensive lists of lipids and surfactants that have been used in the formulation of SLN and/or NLC by different investigators.

2.4 THE PRODUCTION OF SLN AND NLC

2.4.1 Overview

Numerous methods have been developed and used in the production of SLN and/or NLC, including high pressure homogenization [153, 161], microemulsion [151, 161, 168], solvent emulsification-evaporation [157, 161, 169, 170], solvent displacement [171-173], emulsification-diffusion [174-177] and phase inversion [161, 178] techniques. It has been suggested that the high pressure homogenization technique (HPH) is the most reliable and powerful technique for the production SLN and/or NLC [29]. This is because the technique avoids the use of toxic organic solvents and/or the need to use large quantities of water for dilution purposes as required when other techniques are used [29]. In addition, HPH is traditionally used in the production of nanoemulsions for parenteral nutrition in the pharmaceutical industry [29]. Therefore, in contrast to other techniques that are used for the production of SLN and NLC at lab-scale only the use of HPH technique may allow for lab-

scale and industrial scale production of SLN and NLC [29]. Consequently a HPH technique [153, 161] was selected as the preferred method for the production of SLN and NLC in these studies.

2.4.2 High pressure homogenization

2.4.2.1 Principle of particle size reduction

The basic principle behind the production of SLN or NLC dispersion using a high pressure homogenizer is the forceful movement of a preliminary microemulsion through a narrow gap at a velocity generally higher than 1000 Km/hr at high pressure usually ranging between 100-2000 bars [29]. This can be achieved using either a jet stream or a piston-gap high pressure homogenizer [179]. The jet stream homogenizer forces the flow of the microemulsion through either a "Z" or "Y" type cavity to achieve the desired flow pattern [179]. These flow patterns are designed to force the particles to collide with each other and with the walls of the cavity. These collisions apply a shear stress as a result of the turbulent flow in addition to other forces within the cavity and result in the breakdown of microparticles into nanoparticles [29, 179]. Jet stream homogenizers are commonly used in the production of nanocrystals [179]. The piston-gap homogenizer forces a microemulsion through a narrow piston-gap at a high velocity and pressures over a very short distance. The microemulsion is usually placed in a cylinder that has a relatively large diameter compared to the piston-gap placed immediately after the cylinder [179]. This concept can be used to explain the process by which an homogenizer allows for particle size reduction using the Bernoulli's equation (Equation 2.1).

$$K = p_s + \frac{\rho V^2}{2} \qquad \text{Equation 2.1.}$$

Where K = constant
p_s = static pressure
ρ = density
v = velocity
$\frac{\rho V^2}{2}$ = dynamic pressure

The Bernoulli equation suggests that as a fluid enters the narrow piston-gap from a relatively large diameter cylinder preceding the gap, the dynamic pressure of the fluid within the gap

increases with a concomitant decrease in its static pressure and the overall pressure within the gap remains constant [179]. Eventually, the static pressure of the dispersion medium in the gap will drop below the vapour pressure of the fluid when kept at room temperature, consequently forcing the liquid to boil and form bubbles [179]. However, as the fluid leaves the piston-gap, the static pressure increases with a simultaneous decrease in the dynamic pressure and therefore the bubbles will collapse leading to the formation of cavitations and shockwaves within the dispersion medium [179]. These cavitations and shockwaves in addition to particles colliding with each other and with the walls of the piston-gap and the shear stress due to turbulent flow, all contribute to the reduction in the size of the microparticles in the dispersion volume [179].

The power density of a piston-gap pressure homogenizer and the distribution of power density within a given dispersion volume are the main parameters that will determine the ultimate PS distribution of the particles that are formed [161, 179]. A high power density and a uniform power density distribution within a specific sample volume result in a narrow particle size distribution (PSD) [161]. The power density is the energy that a high pressure homogenizer dissipates to a given sample volume over a specific time period and is dependent on the homogenization pressure and the width of the homogenization cavity gap [161, 179]. Consequently, the power density of high pressure homogenizers with a narrow homogenization gap may reach as much as between 10^{12} - 10^{13} W/m^3 which in turn usually provides better results in terms of particle size disruption and PSD [161]. These homogenizers can be effective even when high concentrations of a lipid phase, for example up to 40% w/w are used in the formulation of solid lipid based nanocarriers [29, 161, 180]. Piston-gap high pressure homogenizers are widely used in the production of SLN and NLC. There are two categories of high pressure homogenization (HPH) technique and these are the hot and the cold HPH [26-29, 161]. Both techniques require that an API or cosmetic agent be dissolved or dispersed in a molten lipid phase prior to homogenization at high pressure. A schematic representation of a hot and cold HPH technique is depicted in Figure 2.4.

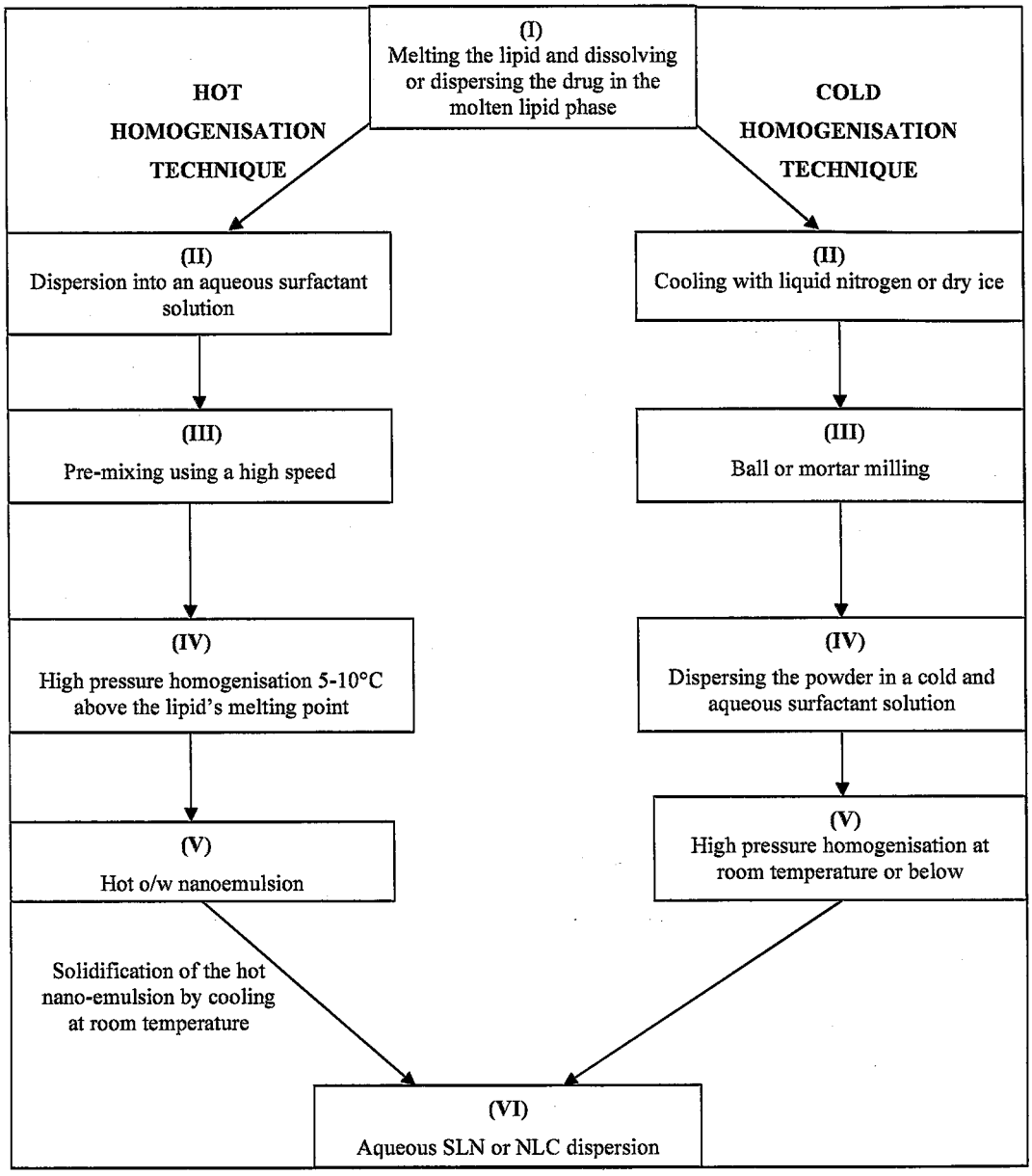

Figure 2.4. Schematic representation of hot and cold high pressure homogenization techniques for the production of SLN or NLC [29].

2.4.2.2 *Hot high pressure homogenization*

Initially an API-containing molten lipid phase (I) is dispersed in an aqueous surfactant solution (II) that has been heated to the same temperature as the lipid phase, using a high speed stirrer to form a microemulsion (III) [27, 29, 161]. The microemulsion is passed through a high pressure homogenizer (IV) to produce a nanoemulsion (V) [27, 29, 161]. The nanoemulsion is then cooled to room temperature (25°C) or below room temperature to allow for subsequent recrystallization of the lipid droplets in the nanoemulsion, to form SLN or NLC in an aqueous environment (VI) [27, 29, 161]. It is important to realize that the size of the lipid droplets in the microemulsion (IV) is vital as this may affect the quality of the final SLN or NLC produced, and ideally the smaller the microparticles, the better will be the resulting SLN or NLC dispersions [29].

The hot HPH of a microemulsion is generally carried out at approximately 5-10°C above the melting point of the lipid used in the formulation [27, 29]. The use of higher temperatures may lead to the production of SLN or NLC that are relatively small in size due to a decrease in the viscosity of the inner lipid phase [29, 181]. However, it should be kept in mind that the use of such high temperatures may accelerate temperature-induced degradation of an API and/or that of the lipid carrier [29]. The homogenization step may be repeated a number of times in order to produce SLN or NLC with a smaller PS [29]. However, the use of a number of homogenization cycles may increase the temperature of a sample by approximately 10°C when the homogenization process is performed at 500 bar [29, 182], which may accelerate API or carrier degradation. Furthermore, the use of many homogenization cycles and/or high homogenization pressures may lead to an increase in the PS of the nanoparticles due to coalescence of the particles as a result of increased kinetic energy in the system [29]. Consequently it has been suggested that the use of between 3-5 homogenization cycles at an homogenization pressure ranging between 500-1500 would provide optimal conditions for the production of high quality SLN or NLC products [29, 161].

The hot HPH is an ideal technique for the production of SLN or NLC containing hydrophobic and thermostable agents [161]. This technique may also be used to produce SLN or NLC loaded with lipophilic and/or thermolabile labile drugs if the time of exposure of the temperature-sensitive agents to a higher temperatures is short [133, 161]. However, there are a number of shortcomings that are associated with the use hot HPH. For example, it is

difficult to incorporate hydrophilic agents in SLN or NLC with sufficient LC and EE due to the partitioning of API from the lipid phase into the aqueous phase during the homogenisation process [27]. In addition, the crystallisation process of lipid droplets in the nanoemulsion (V) to form SLN or NLC can be complex due to the small PS and the presence of surfactants in the formulations and therefore the product may form and remain as supercooled melts rather than recrystallization into the desired lipid nanoparticles [29].

2.4.2.3 Cold high pressure homogenization

This technique involves the rapid cooling of an API-containing molten lipid phase (I) using dry ice or liquid nitrogen (II) to allow for the uniform distribution of an API within a lipid matrix and increase the brittleness of the lipid, which makes it easy for additional milling or size reduction [29, 161]. Following solidification the drug-containing solid lipid is milled using a ball or mortar milling (III) process, to produce lipid microparticles with sizes ranging between 50-100 μm [27, 29, 161]. The powdery lipid microparticles are then dispersed in a cold surfactant solution using a high speed stirrer to form a microsuspension (IV) [27, 29, 161]. The mircrosuspension is then allowed to pass through a high pressure homogenizer at or below room temperature (V) which results in microparticle breakdown to form an aqueous dispersion of SLN or NLC (VI) [29, 161]. The breakdown of the particles in the microemulsion to form SLN or NLC is favoured by the increased fragility of solid lipids caused by the use of low temperatures [29].

The cold HPH technique does not prevent the exposure of an API to relatively high temperatures altogether, due the fact that the drug has to be dispersed in a molten lipid prior to the rapid cooling stage [29, 161]. However, the technique shortens the time of exposure of a drug to high temperatures as high pressure homogenization is performed at room temperature. Consequently the cold HPH technique may be used for the production of SLN or NLC designed to incorporate thermolabile substances [29, 161]. In addition, the procedure can be used for the incorporation of hydrophilic drugs into SLN or NLC as the portioning of the molecules from a lipid phase to an aqueous phase during the high pressure homogenization process is apparently minimal [161]. However, it has been reported that SLN or NLC produced using the cold HPH are relatively larger in size and show a broader PSD or high polydispersity index (PI) than those produced using a hot HPH technique under similar conditions [29, 161].

2.5 CHARACTERIZATION SLN AND NLC

2.5.1 Overview

The characterization of aqueous dispersions of SLN and NLC is vital if a quality product is to be developed and manufactured [27, 29]. However, it should be kept in mind that the small size of the particles and their complex nature in terms of dynamic phenomena such as for example, hysterical kinetics and supercooling may complicate analysis [27, 29]. In addition, analytical tools that are used to analyse aqueous SLN and NLC dispersions do not permit analysis of original samples without a sample manipulation process. Such sample preparation steps may change certain physical characteristics of the particles, such as their kinetic behaviour, crystallisation patterns or lipid modifications and may therefore produce inaccurate results [29]. Therefore, care must be taken when characterizing SLN and NLC and any sample manipulation step performed prior to the analysis of SLN and NLC and/or potential influence of the sample preparation procedures on the physicochemical parameters of SLN and/or NLC must be well-documented [29].

Several important parameters that may have a direct impact on the quality of SLN and NLC, including stability and drug release kinetics must also be investigated [27, 29]. Therefore, the methods used to characterize SLN and NLC should not only be sensitive to parameters such as PS and zeta potential (ZP) which are usually regarded as the key to identification of the performance characteristics of SLN and NLC but the data obtained from such studies should also be accurate [29]. The characterization of SLN and NLC should not only be limited to the measurement of PS and ZP but other parameters, such as the degree of crystallinity and lipid modification as well as the possibility for co-existence with other colloidal carriers must also be taken into consideration and established [27, 29].
Different sophisticated techniques have been used to generate information pertaining to the inner and outer structure and the general behaviour of SLN and NLC [27, 29]. In these studies, SLN and NLC were characterized at every stage of the formulation development and optimization process in terms of size and PI, ZP, degree of crystallinity and polymorphism, in addition to surface morphology. Furthermore, the particles were analyzed in terms of their EE and LC for DDI.

2.5.2 Particle size and polydispersity index

2.5.2.1 Overview

SLN and NLC are by definition colloidal particles having a PS in the submicron range [26, 27]. Therefore all well formulated SLN and NLC dispersions should exhibit low polydispersity indices or a narrow PSD within the nanorange [183]. Particles of > 1 μm size and their time-dependent increase in number may be an indicator of the physical instability of such systems [183]. Therefore, the measurement of PS and the PI of SLN and NLC dispersions is vital to ensure the production of a stable product of suitable quality. Photon correlation spectroscopy (PCS) is a powerful technique suitable for the routine measurement of PS of SLN and/or NLC dispersions [27, 29, 183]. However, a major draw-back of PCS is that particles with sizes > 3 μm cannot be detected [27, 29]. Therefore, although PCS may be an excellent technique for the characterization of nanoparticles it is unable to detect larger microparticles that might be present in dispersions formed during formulation development and optimization studies. It is therefore recommended that PCS be used simultaneously with a complementary analytical tool such as for example, laser diffraction (LD) in order to measure the size of nanoparticles and particles larger than 3 μm [27, 29, 183].

It is essential to realize that PCS and LD do not measure the size of SLN or NLC directly, but rather detect the light scattering effects of the particles in a dispersion medium, which are then used *in situ* to calculate the PS and PSD [27, 29]. The PS is measured in this manner using PCS and LD under the assumption that SLN and/or NLC are spherical [27, 29] for reasons given in Sections 2.5.2.2 and 2.5.2.3, *vide infra*. However, there are instances in which anisometric SLN or NLC may be produced [166, 171, 184] and as a consequence PS data obtained using PCS and LC only could be misleading [27, 29]. Therefore, in addition to PCS and LD other analytical tools such as for example, light microscopy, scanning electron microscopy and/or transmission electron microscopy may be useful to fully elucidate PS and shape of SLN or NLC [27, 29].

2.5.2.2 Photon correlation spectroscopy

Photon correlation spectroscopy (PCS) or dynamic light scattering (DLS) is the most commonly used analytical tool designed to measure the mean PS (z-average) of the bulk

population of particles in an aqueous dispersion. PCS measures the fluctuation of intensity of scattered light caused by Brownian movement of particles within a dispersion sample [27, 29]. In general, PCS consists of a laser beam source, a temperature controlled sample cell holder, a light detector and a photomultiplier [185]. Initially, the sample is illuminated with the laser beam and moving particles within the sample scatter the light which is detected by the detector. The random movements of the particles allow the scattered light to fluctuate and the intensity of the fluctuation is measured by the photomultiplier at a given scattering angle and is relayed to a correlator to calculate the autocorrelation function, $G(\tau)$, which decays exponentially. The microprocessor of a PCS uses the $G(\tau)$ to calculate the diffusion coefficient (D) of the particles within the dispersion medium which in turn is used to determine information about the size of the particles using the Stokes-Einstein equation (Equation 2.2)

$$D = \frac{kT}{3\pi\eta d} \qquad \text{Equation 2.2}$$

Where
D = Diffusion coefficient
k = Boltzmann's constant
T = Absolute temperature
η = Viscosity of the dispersion medium
d = Diameter of a spherical particles

The Stokes-Einstein equation relates the diffusion coefficient of a spherical particle to the diameter of the particle and consequently, PS data would be more meaningful when SLN and/or NLC are spherical [186]. It is also essential to realize that the mean PS of non-spherical particles will more than likely be larger than that of spherical particles when measured with PCS using a similar sample volume since the former exhibits a smaller diffusion coefficient than the latter [186]. In addition, the diffusion speed of small particles is higher than that of relatively large particles and consequently the intensity of fluctuation of the scattered light is high which lead to a more rapid exponential decay of $G(\tau)$ than that observed for larger particles [186]. The scattering intensity and the experimental noise determine the lower limit of PS measurement using PCS, whilst the upper measurement limit is determined by the sedimentation rate of particles [186].

PCS is also useful for determining the PI of a colloidal system as a measure of the width of PSD [187]. The decay of $G(\tau)$ is usually a single exponential when the colloidal dispersion has a monodispersed PSD and is polyexponential when the formulation has a polydispersed

size distribution [185]. In other words, the PI measures the deviation from a single exponential decay of $G(\tau)$, and usually ranges between 0-1 with a PI value of between 0.03-0.06 reflecting a monodispersed colloidal system [188]. A colloidal dispersion is considered to have a narrow PSD when the PI value is between 0.10-0.20 whereas a PI value of between 0.25-0.50 is indicative of a formulation with a wide PSD [188]. Formulations that exhibit PI values higher than 0.50 are considered to have a broad PSD with a shape that is apparently unknown [188].

2.5.2.3 Laser diffractometry

Laser diffractometry (LD) or static light scattering (SLS) is used to measure the size of nanoparticles and microparticles as the technique generally covers a broad size ranging between 0.04-2000 μm [189, 190]. LD determines the size of particles based on the detection of light diffracted or scattered from the surface of particles at an angle that lies within the specifications of the equipment. A typical laser diffractometer consists of a source of laser light operating at a specific wavelength, a lens system that forms an optical arrangement that broadens the laser beam to ensure the complete illumination of a sample measuring cell [186]. Immediately following the sample measuring cell is a Fourrier transform lens system that collates the light scattered by the particles, irrespective of location of these particles in the sample measuring cell and focuses the collated light onto a detector [186]. The detector then relays the data to a computer that uses the information to calculate the PS using the Fraunhofer or the Mie theory, depending on the optical properties of the particles and/or dispersion medium [189].

The data are then presented as volume distribution diameters of d50%, d90%, d95%, and d99% [187]. The d99% indicates that 99% of the particles in the dispersion medium are below a given size or volume distribution [187]. On one hand, the Fraunhofer theory is usually used to determine the size of particles that have PS larger than 3 μm only and does not require the particles or dispersion medium to have certain optical properties [189]. On the other hand, the application of the Mie theory allows size measurement to be extended to particles of less than 4 μm, albeit the real and imaginary refractive indices of the particles as well as the refractive index of dispersion medium have to be known and taken into account [189]. In addition, when using the Mie theory, the particles must be spherical in order to obtain reliable data [189].

The intensity of scattered light is dependent on the scattering angle which in turn is inversely proportional to the radius of a particle [27, 29, 183]. In other words, small particles scatter light at a relatively large angle resulting in the detection of the more intense scattered light and the opposite is true for larger particles [27, 29]. Early versions of LD equipment were designed to allow particles to scatter light up to an angle of 14° and as a consequence, the use of these systems was limited to the determination of the size of particles above the micrometer range as light scattered by nanoparticles at relatively large angles is likely to be outside the detection range. However, the sensitivity of new versions of LD systems has been improved by the development and application of polarization intensity differential scattering (PIDS) technology [189-192]. The PIDS technology complements the detection system of an LD by allowing the detection of light scattered at an angle of up to between 60-146° [192] and consequently the range of PS measurement of LD when used in combination with PIDS technology as a complementary tool is between 0.04-2000 μm [189, 190].

2.5.3 Zeta potential and electrophoretic mobility

The ZP of particles in a disperse system is a key parameter that can be used to predict and control the physical stability of colloidal dispersions during long term storage [27, 29, 183, 187]. By definition the ZP is the electric potential at the hydrodynamic plane of shear which is an imaginary surface separating a thin layer of liquid constituted of counter-ions, bound to a moving charged surface [183]. The ZP is not only dependent on the charge of a particle but also on the dispersion medium in which the particles are suspended and can therefore be affected by small changes in the pH or ionic strength of the medium. The ZP of an aqueous colloidal dispersion can be measured by determining the eletrophoretic mobility of a particle using Laser Doppler Anemometry (LDA), and then applying the Helmholtz-Smoluchowsky equation (Equation 2.3) to the data [193].

$$v = \frac{\varepsilon\xi}{\eta} \qquad \text{Equation 2.3}$$

Where v = Electrophoretic mobility
ε = Dielectric constant (permittivity of the environment)
ξ = Zeta potential
η = Viscosity of the dispersion medium

The determination of the ZP of particles in distilled water or water with low conductivity is usually the key to understanding the dispersion and aggregation processes within colloidal systems [183, 187]. Particles within a colloidal dispersion interact according to the magnitude of the ZP of the system and the greater the ZP the more stable the dispersion is likely to be, due to the fact that charged particles within such dispersions will repel each other thereby overcoming the natural tendency of such particles to aggregate [183]. An aqueous colloidal dispersion is said to be physically stable if the ZP value is less than -30 mV or more than +30 mV [183, 187] depending on the type of ionic surfactant used in the system. Importantly this rule applies only to colloidal systems that are stabilized by electrostatic interactions alone [27, 29, 183, 187]. In aqueous colloidal disperse systems, in which combination of electrostatic and steric stabilizers are used, the presence of steric stabilizers decreases the ZP due to a shift in the shear plane of a particle [12, 14, 24].

2.5.4 Imaging analysis

The major drawback of PCS and/or LD as tools for the characterization of the PS of SLN and NLC is that these techniques fail to provide information about the topographical profile of the particles [29]. Imaging analysis using microscopic techniques not only provides details about the PS of the disperse phase but also generates information relating to the shape and surface morphology of the SLN and/or NLC. Microscopic tools such as for example light microscopy, scanning electron microscopy (SEM) and transmission electron microscopy (TEM) are used to measure the size of SLN and NLC and/or to determine their shape and surface morphology [29].

2.5.4.1 Light microscopy

The use of light microscopy to visualize nanoparticles is restricted by the limit of detection, which is approximately 200 nm. When polarized light is used nanoparticles with sizes ranging between 200-300 nm may be easily observed, although their PS cannot be accurately measured [186]. The resolution of a light microscope is a function of the wavelength of the light used over the numerical aperture of the objective of the microscope [186]. However, light microscopy may be accurately used to determine the size of microparticles and is generally a useful tool to visualize the presence of microparticles and/or aggregation of nanoparticles during formulation development and optimization studies of SLN and/or NLC

[186]. In addition, when polarized light is used, light microscopy can be used to detect the presence of lipophilic drug nanocrystals that have not been incorporated into SLN and/or NLC [186].

2.5.4.2 Scanning electron microscopy

SEM may be used to determine the size, shape and surface morphology of SLN and NLC. SEM allows for visualisation of SLN and NLC under dehydrated conditions since pre-treatment of the samples involves a drying process and imaging is performed under high-vacuum conditions [194]. Initially, an aqueous SLN or NLC sample is deposited on a graphite strip and allowed to dry at room temperature or in an oven with the temperature set between 25-30°C to avoid the melting of the nanoparticles. Following drying the sample is coated with a conductive metal, such as gold and then viewed under an electron beam to produce a three dimensional (3-D) image. It should be realized that the pre-treatment of the aqueous SLN or NLC sample prior to SEM analysis and/or the visualization of the particles under high-vacuum conditions and at accelerated voltage may shrink the nanoparticles and could potentially modify the shape and surface morphology of the particles [194].

2.5.4.3 Transmission electron microscopy

TEM is a useful tool that can be used to elucidate the size, shape and surface morphology of colloidal particles [195]. TEM in contrast to SEM generates two dimensional (2D) images and generally has a higher resolution than SEM and gives a good indication of the PI of a colloidal dispersion [195]. There are different techniques used to prepare samples prior to TEM analysis, including staining, freeze-fracturing and the use of cryo-electron microscopy. The technique to use is dependent on the data a researcher wishes to generate. A simple staining sample preparation technique may be sufficient to obtain information concerning the size, shape and surface morphology of aqueous or lyophilized SLN and/or NLC. A sample is initially deposited on a copper grid coated with a carbon film and if in an aqueous form, it is allowed to dry for about 30 seconds at room temperature. The sample is then stained with a dye such as for example phosphotungstic acid. The stain is allowed to dry at room temperature for another 30 seconds prior to visualisation of the sample using TEM [195].

2.5.5 Crystallographic and polymorphic analysis

The crystalline structure and polymorphic form of a lipid particle are essential parameters that must be extensively investigated when formulating SLN and NLC technologies [27]. Crystallographic analysis is critical since a strong correlation between crystallinity and polymorphism, and drug incorporation and release kinetics of API exists [27, 29]. Differential scanning (DSC) and wide-angle X-ray scattering (WAXS) as a complementary analytical tool may be used to characterize the crystalline structure and modification of bulk lipids, API and their eutectic mixtures in addition to the physical state and energetic properties of SLN and/or NLC particles [29]. DSC and WAXS can also be used to confirm the solid state of SLN and NLC and the absence of supercooled melts during formulation development and optimization studies [29, 163, 196, 197].

2.5.5.1 Differential scanning calorimetry

DSC is used to elucidate changes in the degree of crystallinity and/or polymorphic nature of substances e.g. lipid matrices and API based on the fact that different lipid modifications of the same substance possess different thermal events such as for example melting points [29]. The basic operating principle of DSC is the measurement of the difference in the amount of heat generated or lost between a sample and reference pan as a function of temperature [198]. Generally, a DSC profile of a compound may reveal information pertinent to the melting, vaporization, crystallization, condensation and/or glass transition state of that specific compound [199-201]. Melting and vaporization are endothermic events whereas crystallization and condensation are considered exothermic events [199, 200]. Thermal events can be used qualitatively to elucidate the purity, crystalline and polymorphic modification of substances such as bulk lipids, SLN and NLC [202].

There are two types of DSC systems that have been reported *viz.*, power compensated or heat flux DSC [198, 201]. The main difference between the two systems is that the heat flow to the sample and reference pans is derived from separate furnaces in the power compensated DSC, whereas a single furnace provides the heat to both pans in the heat flux DSC [198, 201]. Consequently, the power compensated DSC measures the differential heat flow to the sample and reference pans from the two heat sources and measures the power required to keep both pans at the same temperature [198, 201]. In contrast, the heat flux DSC measures

the differential temperature between the sample and reference pans that receive heat from the same source [198, 201]. The melting enthalpy values obtained from DSC analysis of aqueous SLN or NLC can be used to calculate the recrystallization index (RI) of the formulations as a measure of the percentage of the lipid matrix that has recrystallized during storage period of the nanoparticles [203]. The RI of aqueous SLN or NLC may be calculated using Equation 2.4. [203].

$$RI\ (\%) = \frac{\Delta H_{\text{aqueous SLN or NLC}}}{\Delta H_{\text{bulk lipid}} \times \text{Lipid conc.}} \times 100 \qquad \text{Equation 2.4}$$

Where:

RI = Recrystallization index
ΔH = Molar melting enthalpy

2.5.5.2 Wide-angle X-ray scattering

WAXS is widely used to evaluate the lamellar arrangement of lipid molecules, polymorphism and degree of crystallinity of fatty acid chains in triacylglycerides [196, 202, 204-206]. The use of WAXS to assess the polymorphic and crystalline nature of lipids is based on the principle that WAXS measures the length of long and short spacings between alkyl side chains within a triacylglyceride lipid layer. These appear as one or more reflections in the wide angle region of a WAXS spectrum [29]. WAXS allows the differentiation between crystalline and amorphous substances, as the WAXS profile of the former would display many reflection bands whereas that of the latter gives a WAXS profile with a relatively straight baseline [186]. Consequently, WAXS can be used in conjunction with DSC to fully elucidate the crystallinity and polymorphic nature of lipids, SLN or NLC [202]. WAXS may also be used to ascertain whether or not an API that has been incorporated into SLN or NLC exists in a crystalline, amorphous or molecular state [133, 204].

2.5.6 Drug loading capacity and encapsulation efficiency

An essential parameter that must be evaluated to determine the suitability of an innovative drug carrier system is the assessment of drug LC for the specific drug to be incorporated into the system in addition to the maintenance of long-term drug incorporation [27, 34]. Furthermore, such novel drug delivery systems should enhance the chemical stability of drug molecules that are to be encapsulated by protecting them from degradation [34]. In addition, such carrier systems should have a high entrapment or EE as well as long-term retention of the encapsulated agents [34]. Both EE and LC are important parameters of SLN and NLC as they may influence drug release characteristics and must therefore form an integral part of the formulation development process [112]. The LC of SLN and/or NLC is usually expressed as a percentage of the amount of drug entrapped in the lipid matrix relative to the total lipid phase used *viz.*, lipid matrix and the drug [12]. Invariably LC depends on the solubility of a drug in the molten lipid, miscibility of a drug melt in a lipid melt, chemical and physical structure of solid lipid matrix and the polymorphic form of the lipid material used [27]. LC can be calculated using Equation 2.5.

$$LC = \frac{\text{(Total amount of drug)} - \text{(Free amount drug)}}{\text{Total amount of lipid phase}} \times 100 \qquad \text{Equation 2.5.}$$

The EE can be calculated using Equation 2.6 by determination of the ratio of the amount of API encapsulated into the SLN and/or NLC relative to the initial amount of drug added to the formulation at the commencement of the manufacturing process [36, 112].

$$EE = \frac{\text{(Total amount of drug)} - \text{(Free amount drug)}}{\text{Total amount of drug}} \times 100 \qquad \text{Equation 2.6}$$

The LC and EE of an API, per unit weight of SLN and/or NLC in an aqueous dispersion can be evaluated using a validated analytical tool such as for example, UV spectrophotometry or HPLC following separation of free API drug from the nanoparticles.

2.6 CONCLUSIONS

Colloidal drug delivery systems (CDDS) in the nanoscale, such as nanoemulsions, liposomes, nanocapsules, polymeric nanoparticles and solid lipid nanocariers have been developed over

the years in order to achieve different objectives in the delivery of active pharmaceutical principles (API) to humans. The CDDS have both advantages and drawbacks and therefore novel carriers have been developed in an attempt to find solutions to the disadvantages associated with existing CDDS formulations. Innovative solid lipid carriers such as solid lipid nanoparticles (SLN) and nanostructured lipid carriers (NLC) consist of lipid matrices that are prepared using physiologically well-tolerated lipids, such as triglycerides. The lipid nanoparticles which have a mean PS ranging between 50-1000 nm are suspended in an aqueous medium and stabilized by one or more surface active agents.

SLN and NLC exhibit advantages over other CDDS such as polymeric nanoparticles and fat emulsions, including their high tolerability *in vivo* [39], excellent oral bioavailability and the possibility of site specific targeted delivery. In addition, the solid nature of SLN and NLC may allow for the protection of API against chemical and/or photo degradation. Drug release from such systems may be controlled and/or extended over a long period of time. Extended drug release from SLN or NLC may occur due to the slower degradation velocity *in vivo* of these particles when compared to that observed for traditional CDDS [35]. SLN and NLC have the potential for delivery of an API through the oral [42], topical [33, 40], parenteral, dermal [40], ocular [43], pulmonary [44] and rectal [45] routes of administration.

The incorporation of an API into SLN or NLC may depend on factors such as the solubility of the API in the lipid, the physicochemical properties of the API, lipids and surfactants, as well as the production method used to manufacture the nanoparticles. There are four (4) different models postulating how a drug may be incorporated into SLN, including the homogeneous matrix, the soft and hard-enriched shell and the drug-enriched lipid core models. However, there are three (3) possible models that have been postulated for the incorporation of drugs into NLC, including the imperfect crystal, amorphous and multiple emulsion types. Methods for the production of SLN or NLC include the high pressure homogenization technique that has the possibility of use for the large scale production of SLN and NLC.

Different techniques are used to fully elucidate SLN and/or NLC. The PS and PI of the nanoparticles can be measured using photon correlation spectroscopy (PCS) and laser diffractometry (LD) as a complementary analytical tool. Laser Doppler Anemometry (LDA) is used to assess the ZP of SLN and NLC which is a parameter that can be used to predict and

control the physical stability of aqueous dispersions of the nanoparticles on long term storage. The presence of microparticles and/or aggregations of nanoparticles in SLN and NLC aqueous dispersions can be monitored rapidly during formulation development and optimization studies using polarized light microscopy.

PCS and LD only provide information on the PS of SLN and NLC, but fail to produce data relating to the topographical profile of the particles under investigation. However, scanning (SEM) and transmission electron microscopy (TEM) may be used to generate information on the PS, shape and surface morphology of SLN and NLC. The crystalline nature and polymorphic modifications of SLN and NLC can be investigated using a combination of DSC and WAXS techniques. HPLC can be used to determine the LC and EE of SLN and NLC for API.

The feasibility of incorporating DDI in SLN and/or NLC was achieved using hot and/or cold high pressure homogenization techniques. The aforementioned techniques were used to characterize the nanoparticles produced in these studies in terms of PS and PI, ZP, shape and surface morphology, crystalline structure and polymorphic modification, drug LC and EE of SLN and/or NLC for DDI.

CHAPTER 3

THE DEVELOPMENT AND VALIDATION OF A REVERSED PHASE–HPLC (RP-HPLC) METHOD FOR THE *IN VITRO* ANALYSIS OF DIDANOSINE

3.1 BACKGROUND

Prior to initiating formulation development and optimization studies of DDI-loaded SLN and NLC it was necessary to develop and validate an analytical method for the *in vitro* quantitation and analysis of DDI as API in formulations. RP-HPLC is a commonly used, powerful and reliable analytical tool that can be applied to the *in vitro* analysis of active pharmaceutical ingredients (API) in formulations that are of a complex nature *viz.*, lipid-based formulations [207, 208]. RP-HPLC will not only provide a separation and generate quantitative data but also has the ability to eliminate almost all potential interference that may be associated with the analysis of these formulations [207, 208]. Therefore, a RP-HPLC with ultraviolet (UV) detection was selected for the development of a potential method for the analysis of DDI.

The intended purpose of the RP-HPLC method to be developed and validated was to analyze DDI samples collected from experiments designed to investigate the LC and EE of DDI in SLN and NLC. The RP-HPLC method was developed in accordance with standard operating procedures (SOP) set in our laboratory. According to the criteria set in our laboratory, the retention times of the analytes of interest are considered acceptable when the first peak of interest, which can be either an internal standard (IS) or an API elutes at a retention time of approximately four (4) minutes after the solvent front with the second peak eluting two to four (2-4) minutes later, thereby resulting in a maximum run time of between 10 and 15 minutes. This time criterion is meant to ensure that potential interference of the solvent front and/or other unwanted peaks with the peak(s) of interest are avoided or eliminated and to ensure that sample analysis is fairly rapid.

The majority of RP-HPLC methods that have been described and reported for DDI deal with quantitative analysis of the API alone or in combination with other antiretroviral agents (ARVs) in plasma or other biological fluids [3, 209-213]. Furthermore there appears to be a

limited number of validated RP-HPLC methods for the quantitative determination of DDI in pharmaceutical formulations. In fact there are no compendial RP-HPLC methods for the analysis of DDI in dosage forms in the United State Pharmacopeia (USP) [214] or in the British Pharmacopeia (BP) [215]. In addition, a current online literature search revealed only a few RP-HPLC methods for the quantitative determination of DDI as a bulk pharmaceutical or in pharmaceutical formulations [3, 6, 216-218]. Therefore the objective of these studies was to develop, optimize and validate a simple, sensitive, precise, accurate and linear RP-HPLC method suitable for the quantitative analysis of DDI during formulation development and optimization studies of DDI-loaded SLN and/or NLC.

3.2 METHOD DEVELOPMENT

The method development phase was designed to facilitate the selection of a suitable analytical column, wavelength of detection and choice of internal standard (IS). In addition, the intention of these studies was to select and optimize a suitable mobile phase composition to facilitate adequate separation between DDI and an IS and to achieve acceptable retention times (Section 3.1) for both the IS and DDI. Therefore, the influence of manipulating the mobile phase composition on the retention time of the IS and DDI were also investigated during the method optimization phase.

3.2.1 Chemicals and reagents

All chemicals were at least of analytical reagent grade. Didanosine (DDI) and acyclovir (ACV) were kindly supplied by Aspen Pharmacare (Port Elizabeth, Eastern Cape, South Africa). HPLC-grade methanol (MeOH) with a UV cutoff of 215 nm was purchased from Romil Ltd. (Waterbeach, Cambridge, UK). Potassium dihydrogen phosphate was purchased from Associated Chemical Enterprises (Southdale, Gauteng, South Africa). Sodium hydroxide pellets were purchased from Merck® Chemicals (Midrand, Gauteng, South Africa). HPLC-grade water was prepared using a Milli-RO® 15 water purification system (Millipore Co., Bedford, MA, USA) that consisted of a Super-C® carbon cartridge, two Ion-X® ion-exchange cartridges and an Organex-Q® cartridge. The water was filtered through a 0.22 μm Millipak® 40 stack filter (Millipore Co., Bedford, MA, USA) prior to use. HPLC-water was also prepared using a Milli Q Plus (Millipore Co, Schwalbach, Germany).

3.2.2 Instrumentation

Formulation development and optimization studies of DDI-loaded SLN and NLC were conducted in South Africa and in Germany. Therefore, two modular HLPC-UV chromatographic systems, *viz.*, HPLC-UV System A (South Africa) and HPLC-UV System B (Germany) were used in these studies. HPLC-UV System A was used for the development and validation of the analytical method and later for the characterization of DDI content in formulations developed during studies conducted in South Africa. HPLC-UV System B was used for a mini-revalidation of the analytical method prior to using the system for quantitative purposes, during studies conducted in Germany.

3.2.2.1 HPLC-UV System A

The modular HPLC-UV system consisted of an Isochrom LC dual piston solvent delivery module (Spectra-Physics, San Jose, CA, USA), a Model 712 WISP™ Autosampler (Millipore® Waters Associates, Milford, MA, USA) and a linear UV-100 detector (Spectrachrom, NV, USA) set at λ = 248 nm. Data acquisition was performed using an SP-4600 Integrator (Spectra-Physics, San Jose, CA, USA) and the separation was achieved at 22°C on a Beckman® 60 Å C_8 4-µm (4.0 i.d. x 150 mm) column (Beckman Instruments, Inc., San Ramon, CA, USA) at a flow rate of 1.0 ml/min.

3.2.2.2 HPLC-UV System B

The modular HPLC-UV system consisted of a Model 220 Kroma dual piston solvent delivery module (Kroma Systems, Berlin, Germany), a Model T360 Kroma Auto-sampler (Kroma Systems, Berlin, Germany) and a Model 430 Kroma linear UV detector (Kroma Systems, Berlin, Germany) set at λ = 248 nm. Data acquisition was performed using Kroma System 2000 v. 1.70 data acquisition and processing software (Kroma Systems, Berlin, Germany) coupled to the modular HPLC-UV system. The separation was also achieved at 22°C on a Beckman® 60 Å C_8 4-µm (4.0 i.d. x 150 mm) column (Beckman Instruments, Inc., San Ramon, CA, USA) at a flow rate of 1.0 ml/min.

3.2.3 Detection

A linear ultraviolet (UV) detector was used for the detection of DDI. The wavelength of maximum absorption (λ_{max}) of DDI is 248 nm [3, 218]. This wavelength was therefore used for the detection of DDI during formulation development and optimization studies.

3.2.4 Analytical column

The quantitative analysis of DDI in pharmaceutical formulations using RP-HPLC has been achieved using n-octylsilane (C_8) [218] or n-octadecylsilane (C_{18}) [3, 6, 43, 217] based stationary phases. DDI is a hydrophilic molecule with a low octanol/water coefficient (Section 1.4.3) and therefore a RP-HPLC column with low hydrophobicity was considered appropriate for use in order to achieve a retention time for both ACV and DDI of more than four (4) minutes. Consequently, a Beckman® 60 Å, 4 μm (4.0 i.d. x 150 mm) analytical column packed with dimethyl octylsilyl (C_8) bonded amorphous silica was selected for the development of an analytical method for the determination of DDI during formulation development and optimization studies.

3.2.5 Internal standard

An internal standard (IS) was required in these studies in order to improve the accuracy and precision of the method by compensating for varying injection volumes and day-to-day instrumental changes [219, 220]. The major criterion used when selecting an internal standard is that the physicochemical and analytical properties of the compound should be similar to those of the analyte of interest [221]. The chemical structure and analytical properties of the antiviral, acyclovir (ACV) are similar to those of DDI, therefore ACV was selected and used as the IS for this analytical method.

3.2.6 Preparation of stock solutions and calibration standards

Standard stock solutions of DDI (500 μg/ml) and ACV (200 μg/ml) were prepared by accurately weighing approximately 50 and 20 mg of DDI and ACV, respectively, using a Model AG-135 Mettler Toledo top-loading analytical balance (Mettler Instruments, Zurich, Switzerland) into 100 ml A-grade volumetric flasks, and dissolving in 20 ml HPLC-grade water. The stock solutions were sonicated for five (5) minutes in a Model 8845-30 ultrasonic

bath (Cole-Parmer Instrument Comp. Chicago, IL, USA) in order to ensure complete dissolution of DDI and ACV, after which samples were made up to volume with HPLC-grade water. Following preparation all stock solutions were stored in a refrigerator at 4°C and used within a maximum period of one week based on stability study data generated as described in Section 3.3.4.1 *vide infra*. Calibration standards for DDI were prepared by serial dilution of the standard stock solution on the day of analysis, to produce solutions containing 2.5, 5, 10, 50, 100, 150 and 200 µg/ml of DDI. A concentration of 35 µg/ml of ACV was added to all standards and test samples prior to analysis.

3.2.7 Preparation of phosphate buffer

Phosphate buffers of 2.5, 10, 25, and 50 mM strength were prepared by accurately weighing 0.3477, 1.3906, 3.3765 and 6.9530 g of potassium dihydrogen phosphate (KH_2PO_4) into a 1L A-grade volumetric flask and making up to volume with HPLC grade water, respectively. The pH of the buffer was adjusted with 1.0 M sodium hydroxide (NaOH) solution to the relevant pH for analysis. The NaOH solution was prepared by dissolving exactly 4.0 g of sodium hydroxide pellets in a 100 ml A-grade volumetric flask using 20 ml of HPLC-grade water. The solution was allowed to cool down and the flask was made up to volume with the water. All weighing was performed on a Model AG-135 Mettler five (5) place Toledo top-loading analytical balance (Mettler Instruments, Zurich, Switzerland).

3.2.8 Mobile phase selection

Suitable retention times (Section 3.1. *vide infra*) and the separation between ACV and DDI were achieved through the manipulation of the molarity and pH of the buffer, in addition to the concentration of MeOH used in the mobile phase. MeOH was selected as the organic modifier since the solvent is less toxic and more economical than other organic modifiers such as, for example, acetonitrile [222]. Various mobile phases of different composition consisting of a binary mixture of phosphate buffer and MeOH were investigated in order to optimize the retention time and hence the separation of ACV relative to DDI.

The eluting strength of a mobile phase does not only depend on the selection of an organic modifier and/or the concentration of the modifier but also on the strength of a particular buffer that is used in that mobile phase [222]. Buffers assist with controlling the pH of a

mobile phase, which may be necessary for achieving the retention and/or separation of ionic compounds [222]. Phosphate buffers are known to provide a buffering capacity over a wide pH range in addition to producing more stable analytical conditions than other buffers such as for example, acetate buffers [223]. A KH_2PO_4 buffer was selected for use as it has a pKa of 7.21 and a buffering capacity in the range between pH 6.2 and 8.2 [224].

3.2.8.1 Preparation of mobile phase

Mobile phase was prepared by adding specific volumes of HPLC-grade MeOH and the KH_2PO_4 buffer of a specific strength and pH prepared as described in Section 3.2.7 *vide infra*, to a glass Duran® Schott solvent bottle (Schott Duran GmbH, Hattenbergstrasse, Germany). The pH of the buffer was measured and adjusted prior to the addition of any MeOH. The mobile phase was allowed to equilibrate to room temperature and then filtered through a 0.45 µm Millipore® HVLP filter (Millipore, Bedford, MA, USA) and degassed under vacuum with the aid of a Model A-2S Eyela Aspirator (Rikakikai Co., Ltd, Tokyo, Japan) prior to use. The mobile phase was freshly prepared on a daily basis and was not recycled during analysis.

3.2.8.2 Effect of buffer molarity

An increase in the strength of a buffer used to prepare a mobile phase generally decreases the retention time of basic compounds when analysis is conducted using RP-HPLC [222, 225, 226]. The influence of buffer molarity on the retention time of ACV and DDI is shown in Figure 3.1.

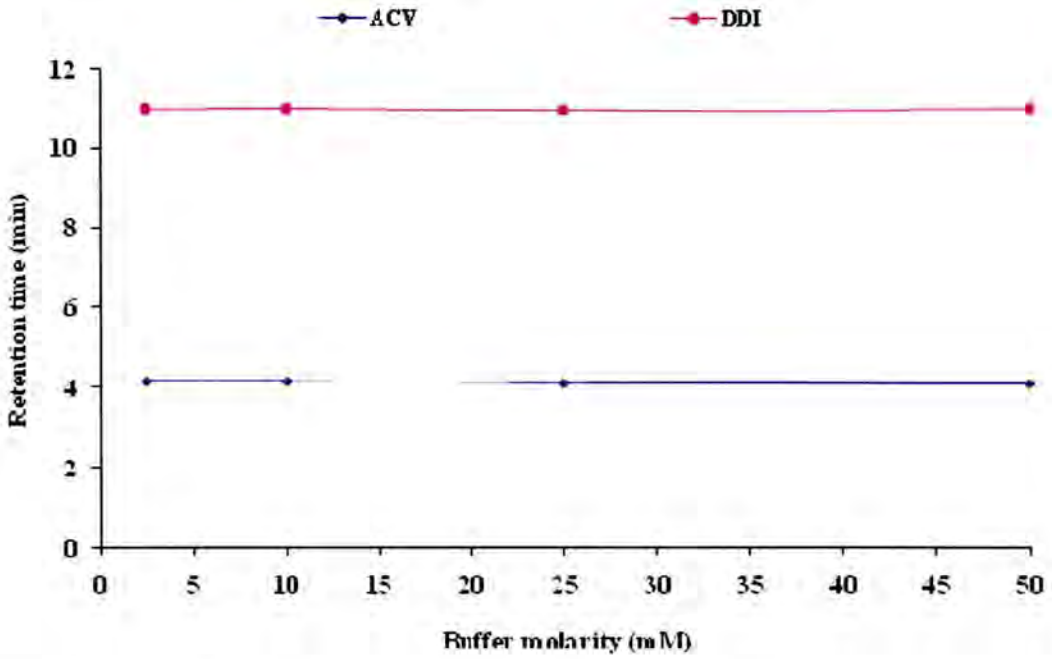

Figure 3.1. Effect of buffer molarity on the retention time of ACV and DDI

It is clearly evident that a change in the molarity of the buffer does not have an impact on the retention time of ACV or DDI since both drugs are predominantly weakly acidic, albeit both ACV [227] and DDI [44] are reported to be amphoteric. In addition, the column used in these studies was end-capped which means that the silanol functionality of the stationary phase was not in a state of ionization. Consequently, increasing the cationic strength of the mobile phase would not affect the interaction between the stationary phase and the basic functional groups of either ACV or DDI. When used in high concentrations, buffers may precipitate and increase the back pressure of an analytical column, thereby reducing the lifespan of that column. In such instances it is advisable to select and use buffers of low concentration. However adjusting the pH of buffers of low strength was not easy as the pH measurements were constantly unstable. Consequently, in order to provide for a balance between preserving the integrity of the column and to achieve stable analytical conditions, a buffer of 25 mM mollarity was selected for use in optimsation studies.

3.2.8.3 Effect of buffer pH

The influence the pH of the KH_2PO_4 buffer used in the mobile phase on the retention times of ACV and DDI was investigated in the pH range between pH 5.0-7.0 and the data are depicted

in Figure 3.2. In general, the retention time of a weakly acidic compound decreases with an increase in the pH of a mobile phase and conversely increases for weakly basic drugs [222]. The manufacturers of the column used in these studies recommend that the pH of a mobile phase to be used with the column should be between $2.0 \geq pH \leq 7.2$. However, DDI is unstable under acidic conditions and as a consequence the influence of pH on the retention times of ACV and DDI was investigated in the pH range shown Figure 3.2.

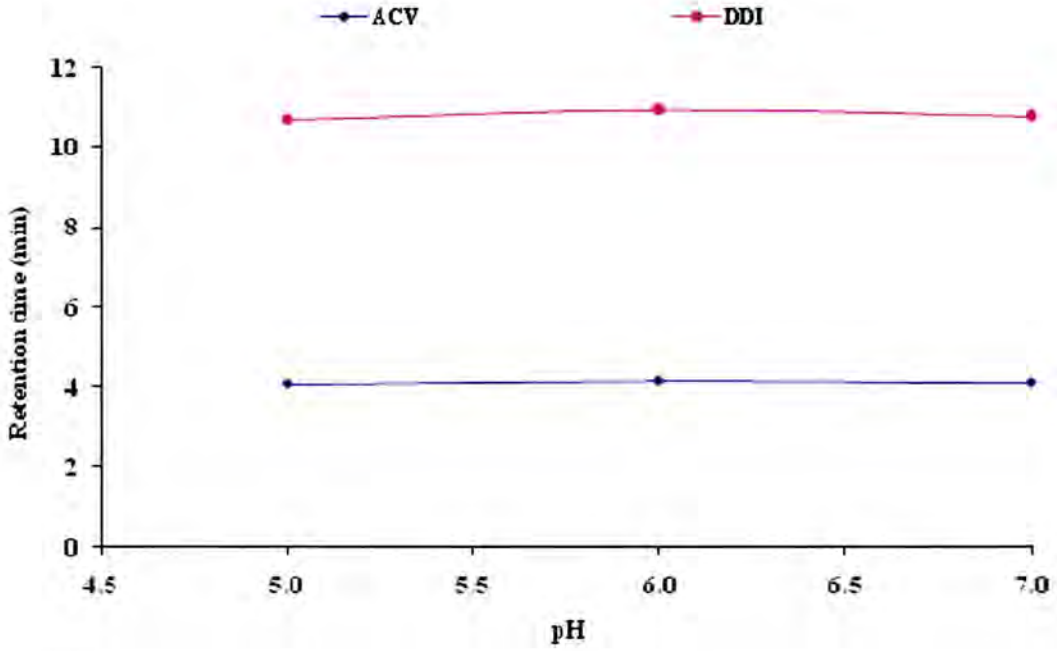

Figure 3.2. Effect of buffer pH on the retention time of ACV and DDI

It is clearly evident that the modification of the pH of the buffer used to prepare the mobile phase within the pH range studied does not affect the retention time of ACV and DDI to any great extent. The pKa values of ACV and DDI, which represent the acidic properties of the compounds are 9.35 [227] and 9.01 [44] respectively and although the molecules are amphoteric, it is possible that they remain predominantly in the neutral form over the pH range evaluated. In order to preserve the integrity and lifespan of the column and at the same time ensure that DDI remains stable during the period of analysis, a buffer of pH 6.0 was selected for use in optimization studies.

3.2.8.4 *Effect of methanol concentration*

The effects of increasing the concentration of MeOH on the retention time of ACV and DDI is shown in Figure 3.3.

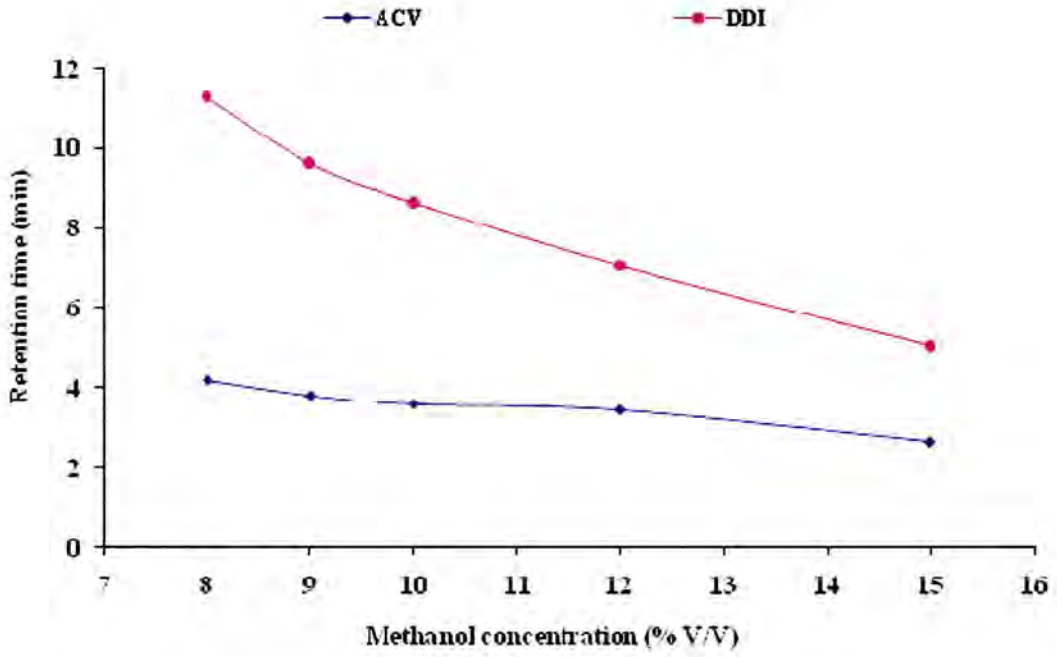

Figure 3.3. Effect of methanol concentration on the retention times of ACV and DDI

The retention times of substances in RP-HPLC may be manipulated by adjusting the solvent strength of a mobile phase, which in turn is dependent on the choice of organic modifier and the concentration of that solvent in the mobile phase used for analysis [228]. The data in Figure 3.3 reveal that an increase in the MeOH content of the mobile phase composition leads to shorter retention times for ACV and DDI. The decrease in retention times for ACV and DDI with an increase in the MeOH content is due to enhanced solute-solvent interactions and diminished solute-stationary phase interactions during the separation. A binary mixture consisting of 8% v/v MeOH and 92% KH_2PO_4 buffer (pH 6.0) resulted in retention times for both ACV and DDI that met the criteria as set in our laboratory (Section 3.1 *vide infra*) and that composition was used for future studies.

3.2.8.5 Optimal mobile phase composition

The mobile phase composition selected for the quantitative *in vitro* analysis of DDI in test formulations consisted of a binary mixture of MeOH and 25 mM KH_2PO_4 buffer (pH 6.0) in a ratio of 8:92. This composition of mobile phase produced well-resolved peaks with retention times of 4.20 min. and 11.32 min for ACV and DDI, respectively. A typical chromatogram of a separation achieved using this mobile phase is depicted in Figure 3.4.

3.2.9 Chromatographic conditions

The final and optimized RP-HPLC chromatographic conditions selected for the analysis of DDI are summarized in Table 3.1.

Table 3.1. Optimized RP-HPLC conditions for the *in vitro* analysis of DDI in test formulations

Column	Beckman® C8 125 mm x 3.3 mm i.d., 4 µm
Mobile phase	Methanol : 25 mM KH2PO4, pH 7.0 (8:92)
Flow rate	1.0 ml/min
Retention times	4.20 min (ACV) and 11.32 min (DDI)
Column pressure	1200 psi
Column temperature	Ambient (22°)
Injection volume	10 µl
Wavelength	248 nm
Sensitivity	0.005 AUFS
Integrator speed	0.25 mm/min
Recorder input	10 mV

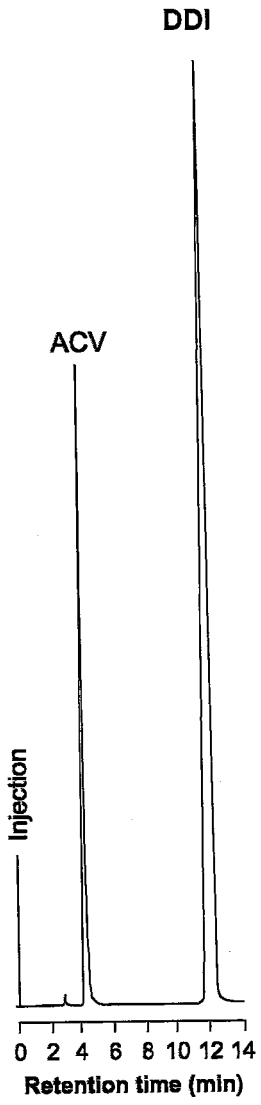

Figure 3.4. Typical chromatogram of the separation of ACV (Rt = 4.20 min) and DDI (Rt = 11.32 min)

3.3 METHOD VALIDATION

The optimized method developed in these studies was validated in order to provide documented evidence that the test method performs appropriately for the purposes for which it was intended [214, 229, 230]. The objective (Section 3.1. *vide infra*) of the RP-HPLC method allows for the classification of this method as a Level I [231] analytical method. Consequently, the RP-HPLC method was validated in terms of linearity and range, precision, accuracy, limits of quantitation (LOQ) and detection (LOD) and sample stability as required for a Level I assay methods [230, 232].

3.3.1 Linearity and range

The linearity [214, 229, 232, 233] of the method was evaluated over the concentration range 0.25-200 µg/ml. Calibration standards (Section 3.2.6. *vide infra*) spiked with ACV were injected (n = 6) onto the chromatographic system (Section 3.2.2.1) using the conditions described in Section 3.2.9. The peak height ratio of DDI response to ACV response were calculated and used to construct a calibration curve to establish whether there was linearity of response in relation to concentration. Least squares linear regression analysis of the peak height ratio versus concentration data was used to test the linearity of the method and the data generated are depicted in Figure 3.5. The calibration curve was found to be linear with an R^2 value of 0.9999, a slope of 0.0097 and a y-intercept of 0.0108, yielding an equation of the calibration line of $y = 0.0097 + 0.0108$. Consequently the RP-HPLC method was found to be linear over the concentration range of DDI used in these studies.

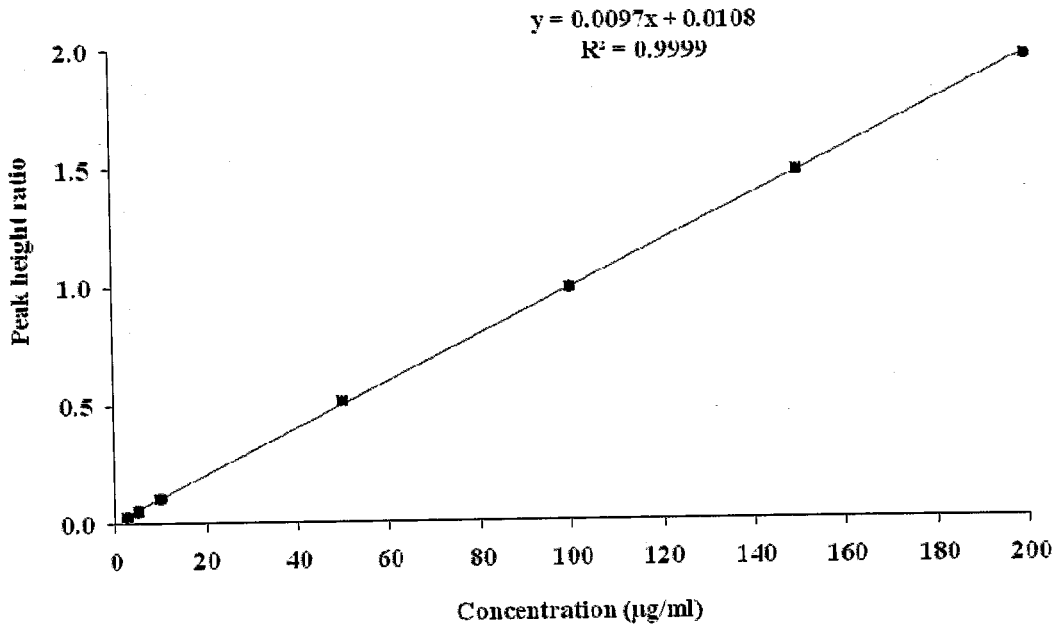

Figure 3.5. Calibration curve for DDI following least squares linear regression analysis of peak height ratios of DDI and ACV versus concentration.

3.3.2 Precision

The precision [214, 229, 232-234] of the method was evaluated at two different levels, namely repeatability [214, 234] and intermediate precision [214, 232, 234] and precision was expressed as percent relative standard deviation (% RSD) of a series of measurements. The acceptance criteria for both the repeatability and intermediate precision was set at less than or equal to 5% RSD at each concentration investigated.

3.3.2.1 Repeatability

The repeatability of the method was assessed by calculating the % RSD of peak height ratios following repeated measurements (n = 6) of three calibration standard concentrations containing 2.5, 100 and 200 µg/ml of DDI, respectively, on a single day. The repeatability data are summarized in Table 3.2. The results reveal that in all cases the % RSD values were less than 5%, indicating that the RP-HPLC analytical method is precise when used as intended (Section 3.1 *vide infra*).

Table 3.2. Repeatability data for RP-HPLC analysis of DDI (n = 6)

Conc. (µg/ml)	MPHR*	SD	% RSD
2.50	0.0429	0.000856	1.99
100.0	1.51	0.00766	0.508
200.0	3.34	0.0429	1.25

* Mean peak height ratio of DDI/ACV

3.3.2.2 Intermediate precision

The intermediate precision of the method was evaluated daily over a three day-period using similar calibration standard concentrations to those used in the repeatability studies (Section 3.3.2.1) The intermediate precision data expressed as % RSD of repeated measurements (n = 6) of the peak height ratios of DDI to ACV are summarized in Table 3.3. In all cases the % RSD values were once again less than 5%, indicating that the analytical method is precise when used for the intended purpose (Section 3.1. *vide infra*).

Table 3.3. Intermediate precision data for RP-HPLC analysis of DDI (n = 6)

Day	Conc. (µg/ml)	MPHR*	SD	% RSD
1	2.50	0.0429	0.000856	1.99
	100.0	1.51	0.00766	0.508
	200.0	3.34	0.0429	1.25
2	2.50	0.0275	0.000268	3.40
	100.0	1.05	0.00753	0.150
	200.0	2.03	0.00850	0.235
3	2.50	0.0337	0.000823	2.44
	100.0	0.908	0.00932	1.02
	200.0	1.83	0.0173	0.948

* Mean peak height ratio of DDI/ACV

3.3.3 Accuracy

The accuracy [232, 234] of the RP-HPLC method was determined by replicate analysis of samples containing known amounts of DDI. Three (n=3) samples representing low (7.5 µg/ml), medium (75 µg/ml) and high (175 µg/ml) concentrations prepared in mobile phase were injected in replicates of six (n=6). The accuracy was reported as % recovery, % RSD and % Bias. A summary of the data generated in accuracy studies is listed in Table 3.4.

Table 3.4. Accuracy data for RP-HPLC analysis of DDI (n = 6)

Theortical conc. (µg/ml)	Actual conc. (µg/ml)	SD	% RSD	% Bias	% Recovery
7.500	7.130	0.1527	2.143	4.91	95.07
75.50	74.67	0.9408	1.260	0.435	99.56
175.0	173.7	2.228	1.283	0.762	99.24

The acceptance criteria for accuracy were that the mean % recovery and % RSD should be 100 ± 5% and less than 5% respectively, at each concentration level. The largest value generated for % bias was 4.91%, which indicates that no value deviated by more than 5% of the stated value. In addition, the resultant % RSD values were all less than 5%, indicating that the analytical method is accurate and suitable for use (Section 3.1 *vide infra*).

3.3.4 Limits of quantitation and detection

The limit of quantitation (LOQ) [229, 235] of the method was determined by evaluating the lowest concentration of DDI that resulted in a precision not exceeding 5% [235]. The limit of detection (LOD) [229, 235] was by convention taken as 30% of the LOQ value. Low concentration samples of DDI were evaluated as potential LOQ values using the method described by Paino *et al.,* [235] and the data are summarized in Table 3.5.

Table 3.5. LOQ data for the analysis of DDI (n = 6)

Conc. (µg/ml)	MPHR*	SD	% RSD
5.00	0.0364	0.000542	1.49
4.50	0.0319	0.000252	0.790
4.00	0.0293	0.000165	0.563
3.00	0.0226	0.0000912	0.404
2.50	0.0271	0.000713	2.63

* Mean peak height ratio of DDI/ACV

All concentrations investigated resulted in a % RSD of less than 5%. However, under the chromatographic conditions established in Section 3.2.9, the method could not integrate peak heights obtained following the injection of a solution of DDI of concentrations lower than 2.5 µg/ml. Therefore based on these data, the LOQ for the method was selected as 2.50 µg/ml and by convention, the LOD value was taken as 0.75 µg/ml, which, when injected into the HPLC resulted in a detectable but not quantifiable peak.

3.3.5 Sample stability

DDI is susceptible to and undergoes acid-catalyzed and/or induced degradation when stored in aqueous solutions of acidic pH (Section 1.5.2). As a consequence, a stability study of DDI in aqueous solution was performed in order to determine a suitable storage period for the calibration and stock solutions in addition to test samples. The stability of DDI was evaluated in HPLC grade water and in phosphate buffer of pH 7.4 to mimic the preparation of the standard stock solutions (stability stock solutions) and samples prepared in phosphate buffer (in-process sample stability) respectively. Stability data generated in these studies were analyzed using a statistical test method developed by Timm *et al.*, [236].

According to Timm *et al.*, [236] a lower limit (L.L.) and an upper limit (U.L.) of a confidence interval (C.I.) may be calculated using a measured percentage response difference (D) between stored and freshly prepared samples for replicate analyses (n = 5) and the true percentage change in response lies within that limit with 90% certainty [236]. A change of response during storage may be considered statistically relevant if the values for both the L.L. and U.L. of the C.I. are either < -10 or > 10. The possible outcomes that could be generated when stability data are analyzed using this method are depicted in Figure 3.6.

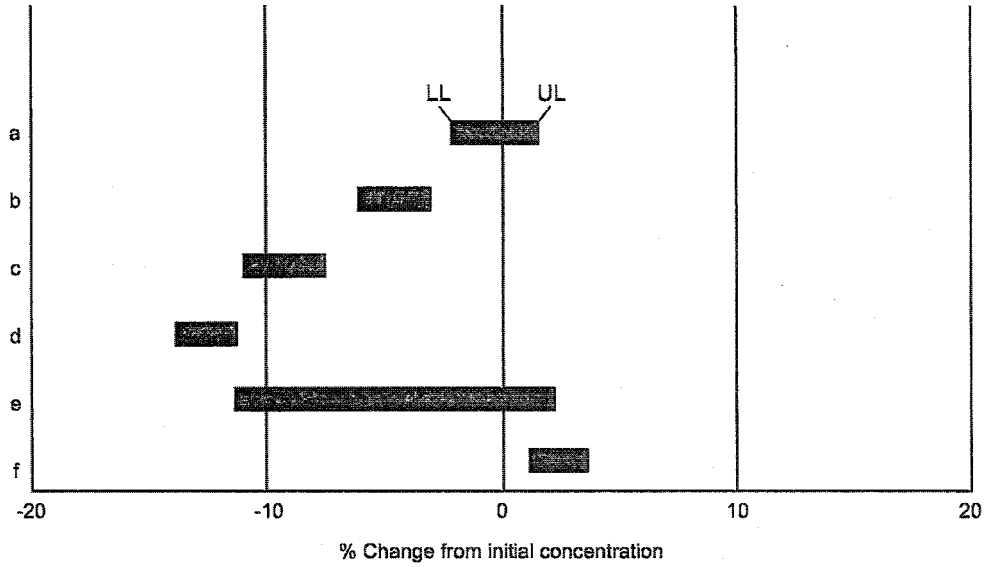

The bars above the axis depict the ranges of the 90% CI for the % change between stored and freshly prepared samples.

a) change of response, not significant and not relevant
b) decrease of response, significant, but not relevant
c) decrease of response, significant and possibly relevant
d) decrease of response, significant and relevant
e) decrease of response, not significant, but possibly relevant
f) increase of response, significant

Figure 3.6. Interpretation of stability data, as described by Timm *et al.*, [236].

3.3.5.1 Stability in stock solutions

The stability of DDI in stock solutions prepared in HPLC grade water was evaluated following storage for one week at 4°C. The stability studies were conducted at two concentration levels of DDI with a concentration of 2.5 μg/ml (n = 5) and 200 μg/ml (n = 5), representing the lower and upper concentrations of the calibration range, respectively. Fresh samples at each concentration were prepared from a freshly made stock solution of DDI on each day of analysis and analysed together with the five (5) stored samples. Both freshly made and stored samples were spiked with 35 μl of a freshly prepared ACV stock solution prior to analysis, and for each sample analyzed, the peak height ratio of DDI to ACV was

used as the response. The resultant data generated are depicted in Figure 3.7 and reveal that the change of response for DDI at 2.5 μg/ml and 200μg/ml stored at 4°C for a week was neither significant nor relevant. Consequently, stock solutions of DDI were prepared in HPLC-grade water, stored at 4°C and used within a period of one week, after which fresh solutions were made.

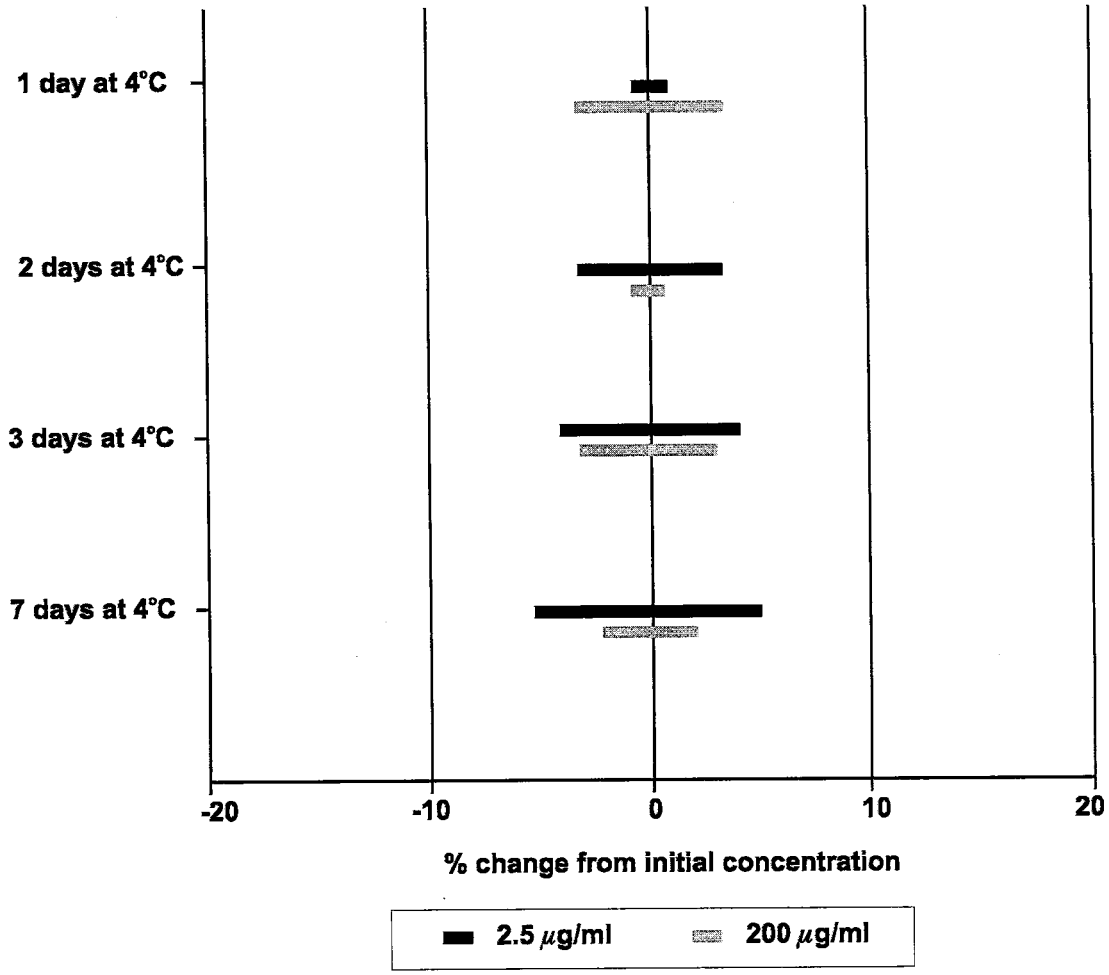

Figure 3.7. Stability of DDI in HPLC water at two different concentrations stored at + 4°C for 1, 2, 3, 7 days.

3.3.6 Stability in in-process sample

The stability of DDI was also evaluated in 25 mM KH_2PO4 (pH 7.4), which was to be used as dilution medium during the evaluation of EE and LC for SLN and/or NLC for DDI or as a washing medium during differential adsorption studies (Chapter 6, *vide infra*). These studies were also conducted at two concentration levels of DDI as described in Section 3.3.5.2. The samples were stored at room temperature (22°C) and on each day of analysis stored and freshly prepared samples (n = 5) spiked with 35 µl of a freshly prepared ACV were analysed.

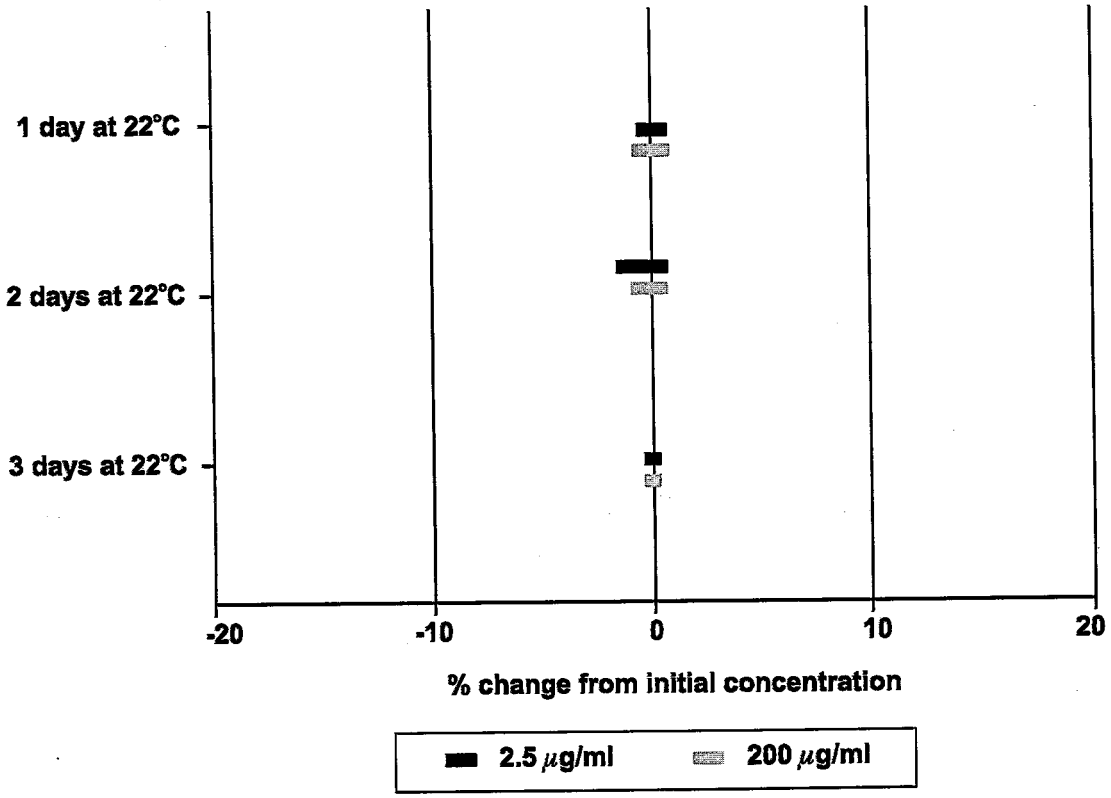

Figure 3.8. Stability of DDI in 25 mM KH_2PO4 (pH 7.4) stored at + 22°C for 1, 2 and 3 days

The percentage response differences between these samples were calculated and used to construct a 90% CI as described by Timm *et al.*, [236] and the data are depicted in Figure 3.8. The change of response for DDI at the lower and upper concentrations prepared in phosphate buffer and stored at room temperature (22°C) for three (3) consecutive days was not significant and not relevant, indicating that DDI was stable in phosphate buffer solution

during the three days of storage. Consequently, DDI samples prepared in KH_2PO_4 pH 7.4 may be kept at 22°C and must be analyzed within a three day period.

3.4 METHOD RE-VALIDATION

A mini re-validation of the fully validated RP-HPLC was undertaken after changes were made to the modular HPLC system as described in Section 3.2.2. These re-validation studies were intended to ensure that the previously validated method maintained the appropriate performance characteristics as specified previously. The revalidation of this analytical method was necessary since a change was made to the solvent delivery system, the autosampler and the detector as outlined in Section 3.2.2 and the method was re-validated in terms of linearity, precision and accuracy.

3.4.1 Linearity

The linearity of the method was established by constructing a calibration curve within the concentration range 2.5-200 µg/ml of DDI prepared as described in Section 3.3.1 and performing least squares linear regression analysis on the calibration curve that was subsequently generated. The calibration curve generated in these studies is shown in Figure 3.9 and revealed that the calibration curve was linear with an R^2 value = 0.9999, a slope of 0.024 and a y-intercept of 0.0122 yielding a curve of $y = 0.024x + 0.0122$.

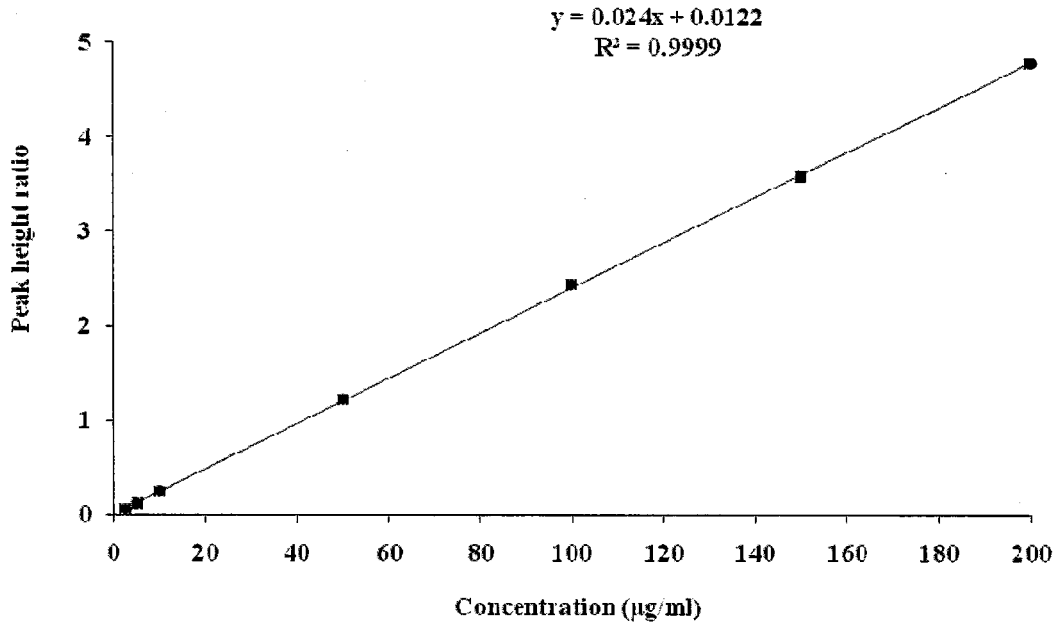

Figure 3.9. Calibration curve constructed for DDI following least squares linear regression analysis of peak height ratios of DDI and ACV versus concentration.

3.4.2 Precision

3.4.2.1 Repeatability

The repeatability was determined as described in Section 3.3.2.1 and a summary of the data generated is listed in Table 3.6. These results indicate that the method for the analysis of DDI was precise in terms of the repeatability criteria established in Section 3.3.2.1.

Table 3.6. Repeatability data for RP-HPLC analysis of DDI (n = 3)

Conc. (µg/ml)	MPHR*	SD	% RSD
2.50	0.0599	0.00230	3.83
100.0	2.40	0.0729	3.03
200.0	4.86	0.0120	0.247

* Mean peak height ratio of DDI/ACV

3.4.2.2 Intermediate precision

The intermediate precision was evaluated as described in Section 3.3.2.2 and the results generated are summarised in and Table 3.7. These data also indicate that the RP-HPLC method for the analysis of DDI conformed to the requirements for the established intermediate precision criterion described in Section 3.3.2.2.

Table 3.7. Intermediate precision data for RP-HPLC analysis of DDI (n = 3)

Day	Conc. (µg/ml)	MPHR*	SD	% RSD
1	2.50	0.0599	0.00230	3.83
	100.0	2.40	0.0729	3.03
	200.0	4.86	0.0120	0.247
2	2.50	0.0618	0.000867	1.40
	100.0	2.44	0.0108	0.441
	200.0	4.80	0.0165	0.344
3	2.50	0.0663	0.00122	1.83
	100.0	2.67	0.0120	0.450
	200.0	5.35	0.0434	0.810

* Mean peak height ratio of DDI/ACV

3.4.3 Accuracy

Accuracy was assessed at three concentrations and reported as described in Section 3.3.3. The data summarized in Table 3.8 reveal that the analytical method was accurate for the analysis of DDI in accordance with the criteria for accuracy established in Section 3.3.3.

Table 3.8. Accuracy data for RP-HPLC analysis of DDI (n = 3)

Theoretical conc. (µg/ml)	Actual conc. (µg/ml)	SD	% RSD	% Bias	% Recovery
7.500	7.260	0.01291	0.1778	-3.20	96.80
75.50	75.47	2.728	3.614	0.632	99.96
175.0	172.9	3.401	2.025	-1.20	98.80

3.5 CONCLUSIONS

An accurate and precise RP-HPLC 1 method with UV detection set at 248 nm has been developed, optimized and validated for the quantitative *in vitro* analysis of didanosine (DDI). Method development studies included evaluation and selection of a suitable analytical column, internal standard (I.S.) and mobile phase composition. Based on the physicochemical

properties of DDI, a Beckman® 60 Å, 4 µm (4.0 i.d. x 150 mm) analytical column packed with dimethyl octylsilyl (C_8) bonded amorphous silica stationary phase was selected as the column of choice for the analysis of DDI. Acyclovir (ACV) was selected as the internal standard (I.S.) as the physicochemical and analytical properties of the molecule are similar to those of DDI.

The separation of ACV and DDI was achieved using an optimized mobile phase composition of a binary mixture of MeOH and 25 mM potassium dihydrogen phosphate (KH_2PO_4) buffer (pH 6.0) (8:92) and a flow rate of 1 ml/min. The use of these chromatographic conditions resulted in retention times of 4.20 min and 11.32 min for ACV and DDI, respectively and a total run time for sample analysis of 13 min. The molarity and pH of the buffer used in the mobile phase had no effect on the retention times of either ACV or DDI. However, an increase in the concentration of methanol used in the mobile phase resulted in a decrease in the retention times of both compounds.

The RP-HPLC analytical method was validated in terms of linearity and range, precision, limits of quantitation and detection. In addition, the stability of DDI in stock solutions and in KH_2PO_4 pH 7.4 was also investigated. The data revealed that the analytical method that had been developed was linear, precise, accurate and sensitive. In addition, DDI was found to be stable in HPLC gradewater (stock solutions) and in 25 mM KH_2PO_4 buffer (pH 6.0) (in-process samples) following storage at 4°C and 22°C, for a maximum of seven (7) days and three (3) days, respectively.

A mini-revalidation of the analytical method was undertaken following changes to the modular HPLC system that had been used to develop, optimize and validate the method. The objective of the mini-revalidation was to ensure that the method maintained its performance characteristics as reported prior to the implementation of the equipment changes. The data from revalidation studies revealed that the analytical method was linear, accurate, and precise for the quantitative *in vitro* analysis of DDI from SLN and NLC. Therefore, the method was applied to the *in vitro* evaluation of EE and LC of SLN and/or NLC of DDI during formulation development and optimization studies.

CHAPTER 4

EVALUATION OF THE THERMAL STABILITY OF DIDANOSINE AND THE SELECTION AND CHARACTERIZATION OF LIPID EXCIPIENTS FOR THE MANUFACTURE OF NANO-PARTICULATE DELIVERY SYSTEMS

4.1 BACKGROUND

Hot high pressure homogenization (HPH) was first described by Müller *et al.,* [27] and was selected as the method of manufacture for the production of DDI-loaded SLN and NLC. This method requires subjecting an active pharmaceutical ingredient (API) to temperatures approximately 5-10°C higher than the melting point of the solid lipid or solid lipid/liquid lipid blends used to manufacture the particles [27, 145]. Production temperatures may reach as high as 90°C depending on the melting point of the solid lipid or solid lipid/liquid lipid mixtures and/or the homogenization pressure selected for the manufacturing process [29]. The use of high production temperatures may lead to the degradation of a thermolabile API and/or lead to changes to the physicochemical properties of the API [133, 204, 237]. Therefore, the first phase of these studies was to establish the thermal stability of DDI in addition to its crystalline and polymorphic behaviour prior to and after exposing the drug to temperatures that the compound would be exposed to during the production of DDI-loaded SLN and/or NLC.

There is dearth of information describing the thermal stability of DDI and/or the potential for the molecule to undergo crystalline and/or polymorphic changes when the drug is exposed to relatively high temperatures. TGA has been used and is recommended as a simple and rapid method for the determination of the thermal stability of an API [133, 237, 238]. Therefore, TGA was used to investigate the thermal stability of DDI and to assess the feasibility of using hot HPH to manufacture DDI-loaded SLN and/or NLC. Similarly, DSC has been used in conjunction with WAXS to assess the crystalline and polymorphic nature of API [133, 237, 238]. Therefore DSC and WAXS were used to evaluate the crystalline and polymorphic behaviour of DDI prior to and after exposing the drug to high temperatures in order to determine whether changes to the crystal structure of DDI occurred following exposure to heat.

The second aspect of these studies was to assess the solubilising-potential of a variety of solid and liquid lipids for DDI in order to select a suitable solid and liquid lipid for use in formulation development and optimization studies. The determination of the solubility of an API in lipid matrices is essential prior to attempting to incorporate the drug into solid lipid carriers [27, 28, 145] as the solubility of a compound in lipid media will influence the drug LC, EE in addition to the usefulness of any solid lipid drug carriers that may be produced [27, 28, 145]. DDI is a hydrophilic compound with an aqueous solubility of 27 mg/ml at a pH 6 [29]. Therefore, the incorporation of DDI into SLN and NLC with a suitable drug loading and EE was expected to pose formidable formulation challenges. Initial solubility studies were designed to identify a solid and liquid lipid with the best solubilising-potential for DDI which would be used as a platform for further formulation development and optimization studies.

It is a pre-requisite for the development of NLC that the solid and liquid lipids used to form technology are miscible at the specific concentrations to be used [30-32]. In addition the solid lipid matrix formed using two lipid components should possess an onset melting point higher than 40°C in order to ensure that NLC remain in the solid state at both room and body temperatures [30-32]. Consequently, the third focus point of these studies was to investigate the miscibility, at different concentrations, of the solid and liquid lipid determined in the solubility studies to have the best solubilising-potential for DDI. DSC was used to determine the melting behaviour and the miscibility of the different solid and liquid lipid blends. The results were used to determine the best binary blend of a solid and liquid lipid for use in the manufacture of the DDI-loaded NLC. It has also been established that the methods used in the manufacture of SLN and/or NLC may change the polymorphic and crystalline state of the lipid nanoparticles in relation to those of the bulk lipid materials from which the nanoparticles were produced [202, 205]. Consequently, studies were conducted to establish the polymorphic and crystalline state of the bulk lipid materials in addition to their state and interaction potential with DDI prior to and following exposure to heat.

4.2 MATERIALS AND METHODS

4.2.1 MATERIALS

4.2.1.1 Overview

The following sections list all materials that were evaluated in solubility studies, in addition to using information supplied by the manufacturers. A full and detailed description of the excipients that were selected from these studies and considered suitable for use for formulation development is summarised in Section 5.2.1 of Chapter 5, *vide infra*. All solid and liquid lipid materials used have a Generally Regarded as Safe (GRAS) status or are approved for oral and/or IV use in humans by one or more international regulatory authorities. The description, physicochemical characteristics, clinical pharmacology and pharmacokinetic aspects of DDI have been reported and described in Chapter 1 of this dissertation. All materials were used as received from the supplier without further testing and were at least of analytical reagent grade.

4.2.1.2 Solid lipid excipients

Precirol® ATO 5 (glyceryl palmitostearate), Compritol® 888 ATO (glyceryl behenate), Labrafil® M 2130 CS (Lauroyl macrogolglycerides (polyoxylglycerides), Gelucire® 50/13 (Lauroyl macrogolglycerides (polyoxylglycerides)) and Gelucire® 44/14 (Lauroyl macrogolglycerides (polyoxylglycerides)) were donated by Gattefossé SAS (Gattefossé SAS, Saint-Priest Cedex, France). Dynasan®116 (triacylglycerol of palmitic acid) and Dynasan® 118 (triacylglycerol of stearic acid) were received from Condea Chemie GmbH (Condea Chemie GmbH, Witten, Germany). Cutina® CP (cetyl palmitate) was purchased from Cognis Deutschland GmbH (Cognis Deutschland GmbH, Düsseldorf, Germany). Imwitor® 312 (glyceryl monolaurate), Imwitor® 900 (glyceryl stearate) and Imwitor® 960 K (glyceryl stearate SE) were kindly donated by Sasol Germany GmbH (Sasol Germany GmbH, Witten, Germany).

4.2.1.3 Liquid lipid excipients

Miglyol® 812 (medium chain triacylglycerols) was received from Caelo GmbH (Caelo GmbH, Hilden, Germany). Transcutol® HP (Diethylene glycol monoethyl ether), Labrafac Lipophile® WL 1349 (Medium chain triglycerides), Labrafac® PG (Propylene glycol dicaprylocaprate), Lauroglycol® FCC (Propylene Glycol Laurate) and Capryol® 90 (Propylene glycol monocaprylate) were donated by Gattefossé SAS (Gattefossé SAS, Saint-Priest Cedex, France).

4.2.1.4 Water

HPLC-grade water was used in all studies. HPLC grade water was prepared using a Milli-RO® 15 water purification system (Millipore Co., Bedford, MA, USA). The Milli-RO® 15 consisted of a Super-C® carbon cartridge, two Ion-X® ion-exchange cartridges and an Organex-Q® cartridge. The water was filtered through a 0.22 µm Millipak® 40 stack filter (Millipore Co., Bedford, MA, USA) prior to use. In addition, for the production and analysis of NLC in Germany, HPLC-grade water was purified using a Milli Q Plus (Millipore GmbH, Schwalbach, Germany).

4.2.2 METHODS

4.2.2.1 Characterization of DDI

4.2.2.1.1 TGA characterization

The thermal stability of DDI was investigated using a Model TG-DTA analyser (Mettler-Toledo GmbH Analytical, Gießen, Germany). A 11.2820 mg sample of DDI, which was between the generally recommended range of 5-20 mg sample size, was weighed directly into an aluminium oxide crucible pan and heated from 30°C to 500°C at a heating rate of 10 K/min. The TGA scan was recorded whilst constantly purging the system with liquid nitrogen at a flow rate of 80 ml/min.

4.2.2.1.2 DSC characterization

The melting point of DDI was determined using a Model DSC 821e Mettler-Toledo DSC (Mettler-Toledo GmbH Analytical, Gießen, Germany). A 1.4890 mg sample of DDI which was between the generally recommended sample size range of between 1-2 mg sample was weighed directly and hermetically sealed into a standard 40 µl aluminium pan. DSC curves for DDI were recorded by heating the sample from 25°C to 225°C and subsequently cooling the sample to 25°C at heating and cooling rates of 10 K/min. An empty pin-holed aluminium pan sealed in a similar manner to the pan containing the sample, was used as the reference. DSC profiles for DDI were generated before and after exposure of the drug to a temperature of 85°C for 1 hour in order to determine the effect of heat on the physicochemical properties of DDI. DSC parameters, such as temperature onset, maximum peak and enthalpy were identified using Mettler-Toledo STAREe software (Mettler-Toledo GmbH Analytical, Gießen, Germany) coupled to the Model DSC 821e Mettler-Toledo DSC.

4.2.2.1.3 WAXS characterization

A WAXS instrument was used to establish the crystalline and polymorphic nature of micronized DDI prior to and following exposure of the drug to a temperature of 85°C for 1 hour. The WAXS patterns for DDI were generated using a Model PW 1830 Philips X-ray generator (Philips Industrial and Electron-Acoustic Systems Division, Amedo, The Netherlands) that was equipped with a copper anode (Cu-Kα radiation, 40 kV, 25 mA λ = 0.15418 nm) and that was coupled to a Model PW18120 Goniometer detector. All measurements were recorded using a step width of 0.04°, a count time of 60 sec, a 2 Theta scanning range and speed set between 0.6-40° and 0.02° per sec, respectively. Samples were mounted onto a glass fibre prior to analysis by WAXS. All samples used for WAXS analysis were the same as those used in DSC studies to ensure ease of data comparison and interpretation.

4.2.2.2 Lipid screening

4.2.2.2.1 Selection of solid lipid material

There are currently no standard methods for the determination of solubility of a drug molecule in a solid lipid excpient. The solubility of DDI was investigated by dissolving increasing amounts of DDI in different molten lipids, followed by visual observation. This approach was continued until no further DDI appeared to dissolve in the molten lipid. DDI is a hydrophilic compound and therefore its solubility in lipid excipients was expected to be limited. Therefore, the use of a 0.005% w/w concentration of DDI in solid lipid was appropriate when commencing these studies. The solubility of DDI in solid lipid was investigated by accurately weighing approximately 10 mg of DDI and 1.995 g of the solid lipid under investigation using a Model ED 124S Sartorius top-loading analytical balance (Sartorius AG, Göettingen, Germany) and transferring both samples to a siliconised glass vial. The glass vial containing the weighed material was exposed to heat using a Model 4230 Innova refrigerated incubator shaker (New Brunswick Scientific, Edison, NJ, U.S.A) with the temperature and speed set at 85°C and 100 rpm, respectively. The solubility of DDI in the molten lipid was assessed visually by observing the disappearance of DDI crystals in the molten lipid dispersion. Following dissolution of the drug, the initial concentration of 0.005% w/w was increased to 0.010% w/w 0.015% w/w, 0.020%.w/w etc., until an end point was reached. The end point was reached when DDI crystals failed to dissolve in the molten lipid after shaking for 24 hours at 85°C.

4.2.2.2.2 Selection of liquid lipid excipients

The saturation solubility of DDI in different liquid lipids was determined using the validated HPLC method described in Chapter 3 *vide infra* after shaking the liquid lipid containing an excess of DDI at 200 rpm for 24 hours at 85°C using a Model 4230 Innova refrigerated incubator shaker (New Brunswick Scientific, Edison, NJ, U.S.A). Approximately 3.20 g of liquid lipid was accurately weighed into a siliconised glass vial using a Model ED 124S Sartorius top-loading analytical balance (Sartorius AG, Göettingen, Germany). Approximately 800 mg of DDI was weighed separately and transferred to the siliconized glass vial containing the liquid lipid. The vial was left to shake for 24 hours after which the oil-DDI mixture was centrifuged using a Model 22 R Heraeus Biofuge centrifuge (Thermo

Electron LED GmbH, Langenselbold, Germany) at 17 000 rpm for 30 min. The supernatant was filtered through a 0.45 μm hydrophilic Sartorius® membrane filter (Sartorius AG, Goettingen, Germany). A100 μl aliquot of the filtrate was diluted and made up to 10 ml with HPLC-grade methanol (Mallinckrodt Baker, Deventer, The Netherlands) and the resultant solution was analysed using HPLC method.

4.2.2.2.3 Selection of a binary mixture of solid and liquid lipid

The solid and liquid lipid that best dissolved DDI as determined from studies described in Sections 4.2.2.3.1 and 4.2.2.3.2 respectively were mixed in different ratios *viz.,* 95:5, 90:10, 85:15, 80:20, 70:30 and 60:40 in order to establish the miscibility of the two lipids. The total amount of lipid selected for use was 1.0 g and each sample was incubated at 85°C for 1 hour using a Model 4230 Innova refrigerated incubator shaker (New Brunswick Scientific, Edison, NJ, U.S.A) with the speed set at 200 rpm. The samples were allowed to cool and were left to stand at room temperature for 24 hours prior to further manipulation. DSC was used to confirm the solid state of the cooled sample and therefore the miscibility of the solid lipid with the liquid lipid. DSC curves were generated by heating samples, weighing between 1-2 mg, from 25°C to 85°C and subsequently cooling to 25°C at heating and cooling rates of 10 K/min. An empty aluminium pan without a pin-hole was used as the reference. In addition, the miscibility between the two components was investigated by smearing a cooled sample of the solid mixture on a hydrophilic filter paper, followed by visual observation to determine the presence of any liquid oil droplets on the filter paper. A binary mixture exhibiting a melting point above 40°C and which did not reveal the presence of oil droplets on the filter paper was selected for use in the development of DDI-loaded NLC.

4.2.2.3 Polymorphism and crystallinity of bulk lipids

In order to determine whether polymorphic modifications to the crystal structure of bulk lipids occurred when the materials were subjected to the temperature conditions that are generally used for the production of SLN and/or NLC, an assessment of the crystallinity of the lipids was undertaken. The production of SLN and/or NLC initially involves melting a solid lipid in the case of SLN or heating a blend of solid and liquid lipids for the manufacture of NLC and then dispersing the molten lipid in a hot aqueous solution of surfactant with the aid of a high speed homogenizer [27, 145]. The second step involves homogenizing the

resultant pre-emulsion with a high-pressure homogenizer to produce a hot o/w nanoemulsion [27, 145]. Subsequent cooling of the nanoemulsion leads to the recrystallization of the lipid molecules to form SLN or NLC depending on the starting material [27, 145]. Therefore the characterization of SLN or NLC using DSC, will involve subjecting the solid lipid matrix to a second melting process [133, 237, 238]. Therefore, DSC analysis of bulk solid lipid or binary mixtures of a solid and liquid lipid would necessitate running DSC scans on the same sample twice. The intention of the first DSC scan is to mimic the process of melting lipid materials prior to subjecting them to a high pressure homogenisation process and the second DSC scan on the same sample emulates DSC analysis of SLN or NLC [205]. However the use of DSC to characterize bulk lipid samples following exposure to heat would require running a single DSC scan only and this would correspond to the analysis of SLN and/or NLC. DSC and WAXS were used to characterise the behaviour of the lipids.

4.2.2.3.1 DSC characterization

The DSC system used in these studies has been described in Section 4.2.2.1.2. The DSC curves for the bulk solid lipid and a binary mixture of solid and liquid lipid were recorded by heating samples from 25°C to 85°C and subsequent cooling to 25°C, at heating and cooling rates of 10 K/min. An empty pin-hole free aluminium pan was used as the reference for the analysis of all bulk lipid samples. The weight of each sample analysed was between 1-2 mg and all the samples were investigated before and after exposure to a temperature of 85°C for one (1) hour.

4.2.2.3.2 WAXS characterization

The WAXS patterns of bulk solid lipid, binary mixtures of solid lipid and DDI and a ternary mixture of solid lipid, liquid lipid and DDI were investigated using WAXS, following the method described in Section 4.2.2.1.3. All samples were investigated prior to and following exposure to 85°C for 1 hour. Furthermore all samples used for WAXS analysis were the same as those subjected to DSC analysis for the ease of data comparison and interpretation. Bragg's equation (Equation 4.1) which relates the wavelength (λ) of an X-ray beam to both the angle of incidence (θ) and the inter-atomic distance (d) was used to transform the data generated to the distance of spacing within a lipid matrix in order to obtain information about lipid modification.

$$d = \frac{\lambda}{sin\,2\theta}$$ Equation 4.1

4.2.2.4 Interaction of bulk lipids with DDI

DSC and WAXS were also used to obtain information relating to any potential interaction between the solid lipid and binary mixtures of solid and/or liquid lipid with DDI. The DSC profiles and WAXS patterns of a binary mixture of the solid lipid and DDI, and a ternary mixture of the solid lipid, liquid lipid and DDI were also investigated using DSC and WAXS methods similar to those described in Sections 4.2.2.1.2 and 4.2.2.1.3, respectively. The concentration of DDI in these mixtures was 5% w/w and the ratio of solid and/or liquid used in these studies was similar to those that were selected for the manufacture of SLN and/or NLC. All samples were evaluated prior to and following exposure to 85°C for one (1) hour, after being allowed to stand at room temperature for 24 hours. Once again samples of between 1-2 mg of material were used for DSC analysis.

4.3 RESULTS AND DISCUSSION

4.3.1 Characterization of DDI

4.3.1.1 TGA characterization

TGA measures the loss in weight of a sample as a function of increasing temperature and the weight loss is then correlated to the thermal stability of a sample, in this case DDI [133, 237, 238]. The TGA profile of DDI is depicted in Figure 4.1 and shows the percent weight loss of DDI as a function of temperature. The percent weight loss of DDI following exposure of the drug to temperatures ranging between 30-500°C at a heating rate of 10 K/min is summarized in Table 4.1.

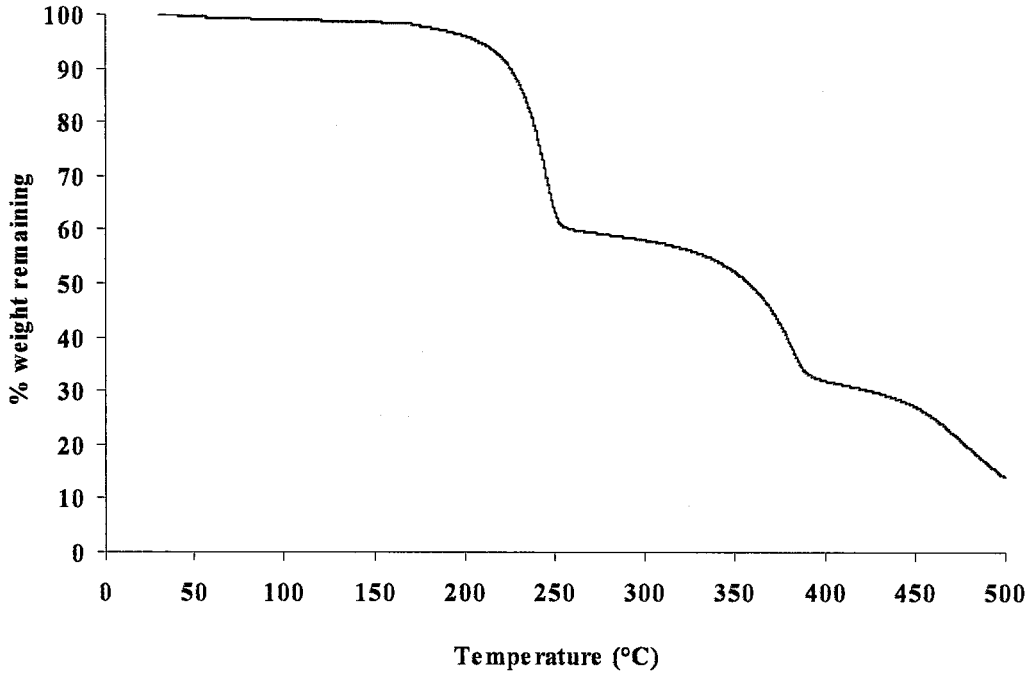

Figure 4.1. TGA profile of bulk DDI showing the percent weight loss of DDI as a function of temperature

Table 4.1. Summary of percent weight loss following TGA analysis of DDI as a function of temperature

Temperature range (°C)	DDI percentage weight loss (%)	Observation
37-163	1.5	Possible water loss
163-278	39.3	1st decomposition phase
298-410	27.0	2nd decomposition phase
420-500	16.3	3rd decomposition phase

The TGA profile of DDI reveals a sample weight loss of 1.5% in the temperature range between 37-163°C, which may be attributed to water loss, since DDI was shown to be slightly hygroscopic when stored at 25°C for eight (8) weeks [3]. DDI appears to decompose in a process involving three stages as the temperature to which the drug sample is exposed exceeds 163°C. In the first instance 39.3 % DDI appears to decompose in the temperature range of 163-278°C. A further 27.0% of DDI decomposes in the second decomposition phase in the temperature range of 298-410°C. The final decomposition phase of DDI occurs in the temperature range 420-499°C with a further additional loss of 16.30% of the weight of DDI.

These studies show that only 1.5% of the initial weight of DDI is lost when the drug is exposed to temperatures ranging between 37-163°C, however a total of 84.1% of the initial weight of DDI is lost when the drug is heated to temperatures ranging between 163-500°C. Consequently, the TGA data reveal that DDI remains stable when heated to temperatures between 37-163°C yet is thermolabile when exposed to temperatures exceeding 163°C. The objective of these studies was to investigate whether DDI was thermolabile when exposed to temperatures between 75-85°C which is the temperature range the molecule would be exposed to when determining the solubility of the molecule in lipid media, as well as during the production of SLN and NLC. These data reveal that DDI is stable under the proposed processing and production as the drug does not exhibit significant weight loss under these conditions. Consequently, the solubility of DDI can be determined in lipid media that are heated to 85°C and DDI-loaded SLN and NLC can be manufactured using a hot HPH technique.

4.3.1.2 DSC characterization

DSC was used to determine the melting behaviour, crystalline and polymorphic nature of DDI prior to and following exposure to heat. The DSC profile of DDI generated before and after exposing the sample to 85°C for one (1) hour is depicted in Figure 4.2. A summary of the melting events of DDI in addition to the calculated width of the melting events (WME) is summarized in Table 4.2. The WME is the calculated difference between the melting and onset temperatures and its magnitude may be used as measure of lattice defects within a crystalline material [202].

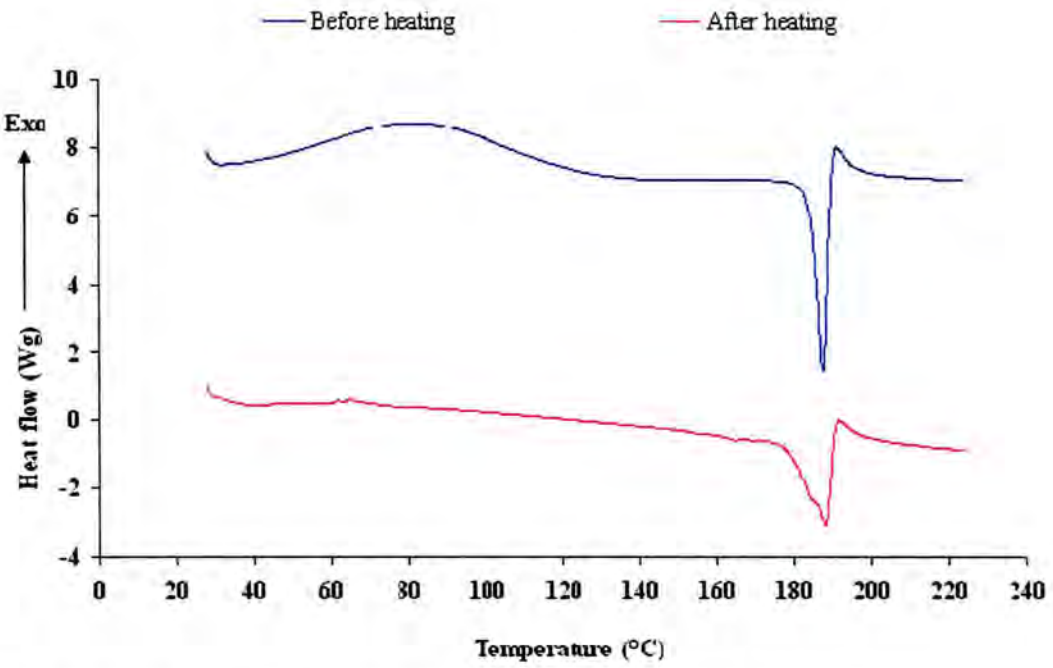

Figure 4.2. DSC profile for DDI prior to and following exposure to 85°C for one (1) hour

Table 4.2. DSC parameters for DDI obtained before and after exposure to 85°C for one (1) hour

Didanosine	Thermal event	Onset (°C)	MP (°C)	Enthalpy (J/g)	WME (°C)
Prior to heating	Exothermic	44.2°	81.1	436.90	-
	Endothermic	184.1	187.3	143.84	3.2
Following heating	Exothermic	179.8	187.5	134.14	7.7

The DSC curve for DDI prior to exposure to heat shows the presence of two thermal events. The first event is an exothermic event with an extrapolated onset temperature and peak maximum temperature occurring at 44.2°C and 81.1°C respectively, with a corresponding enthalpy of 436.90 J/g. This event is indicative of the recrystallization of an unstable polymorphic form of DDI to a more stable polymorphic modification of the compound. The second event is an endothermic event that is indicative of a melting event of a more stable polymorphic form of DDI, with an extrapolated onset temperature and peak maximum at 184.1°C and 187.3°C, respectively and an enthalpy of 143.84 J/g with a relatively narrow width of the melting event of 3.2°C. The endothermic event is clearly strong and sharp, which together with the relatively narrow width of the melting event describes a highly crystalline structure of DDI.

The exposure of DDI to 85°C for one (1) hour resulted in slight changes to the melting behaviour of the molecule. The exothermic event was no longer evident and this may be attributed to the heat to which the drug was exposed to prior to DSC analysis and which possibly results in the unstable polymorphic form of DDI reverting to a more stable modification of the API. Therefore the peak is undetectable when the same sample is exposed to the same temperature range during DSC scanning. The endothermic event exhibits both a decrease in enthalpy and the onset temperature from 143.84 J/g and 184.1°C to 134.14 J/g and 179.8°C, respectively. However the peak maximum remains constant at 187.5°C. In addition, the peak is broader with a WME of 7.7°C and a less intensive response compared to that observed for DDI scanned prior to being exposed to heat.

The decreased onset temperature and enthalpy in addition to the broader WME and less intensive endothermic peak for DDI following heating may be attributed to a decrease in the degree of crystallinity and polymorphic nature of the more stable polymorphic form of DDI that predominates following exposure of the drug to 85°C for one (1) hour. However, adequate interpretation of the DSC data was only achieved using a complementary analytical tool such as X-ray diffraction.

4.3.1.3 WAXS characterization

WAXS was used as a complementary analytical tool to DSC in order to support the DSC data generated in Section 4.3.1.2. The WAXS profile of DDI prior to and following exposure of the drug to 85°C for one (1) hour shown in Figure 4.3.

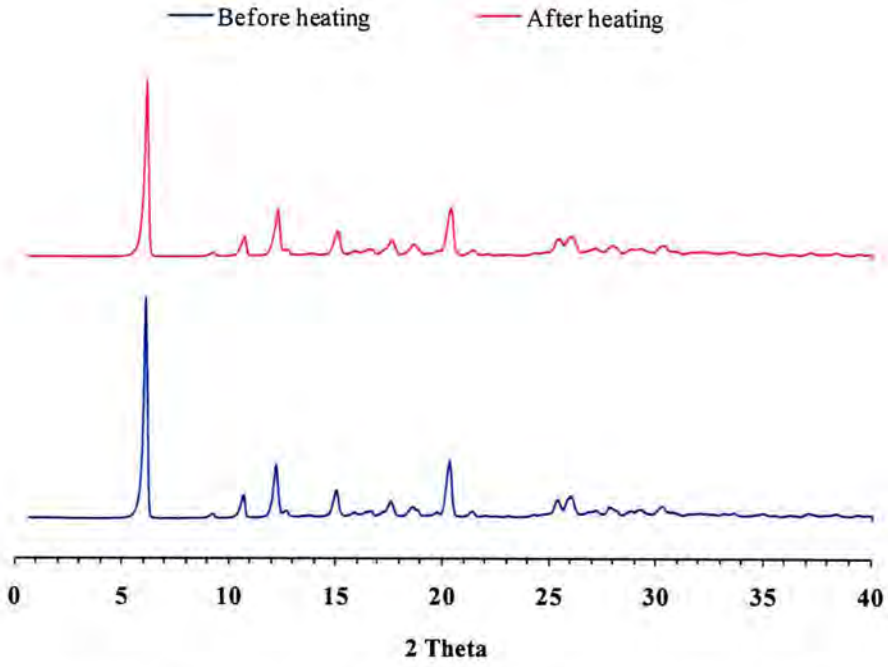

Figure 4.3. WAXS patterns of DDI prior to and following exposure to 85°C for one (1) hour

The WAXS profile generated for DDI prior to and following exposure to heat shows the presence of a number of similar diffraction bands that are characteristic of crystalline substances. Consequently, these data reveal that DDI is a crystalline substance that retains its crystalline state following exposure to heat at 85°C for one (1) hour. However, in general there appears to be a slight decrease in the peak intensity for the DDI sample that was exposed to heat when compared to the peak intensity observed for the DDI sample that was not exposed to heat. The decrease in the intensity of the peaks of the sample exposed to heat may be attributed to a decrease in the degree of crystallinity and possibly a change in the polymorphic nature of DDI following heat exposure. These data support those observed in DSC studies and reveal that exposure of DDI to 85°C for one (1) hour more than likely decreases the degree of crystallinity of the molecule and possibly modifies the polymorphic nature of the compound and this may have an impact on certain physiochemical characteristics e.g. release profile of the drug from NLC formulations.

4.3.2 Lipid screening

4.3.2.1 Selection of solid lipid

Prior to formulation development studies, it was considered essential to assess the solubility of DDI in various solid lipids and the data generated are summarized in Table 4.3.

Table 4.3. The solubility of DDI in various solid lipid excipients

No.	Material	MP (°C)	0.005% w/w DDI	0.010% w/w DDI	0.015% w/w DDI	0.020% w/w DDI
1	Precirol® ATO 5	52-56	soluble	soluble	soluble	insoluble
2	Compritol® 888 ATO	69-74	soluble	soluble	partially soluble	N/A
3	Dynasan® 116	62-64	soluble	soluble	insoluble	N/A
4	Dynasan® 118	70-73	soluble	soluble	insoluble	N/A
5	Softisan® 154	53-58	soluble	soluble	insoluble	N/A
6	Cutina® CP	46-51	soluble	soluble	insoluble	N/A
7	Imwitor® 900 P	54-64	soluble	soluble	insoluble	N/A
8	Geleol®	55-58	soluble	soluble	insoluble	N/A
9	Gelot® 64	55-62	soluble	soluble	insoluble	N/A
10	Emulcire® 61	45-50	soluble	soluble	insoluble	N/A

These data reveal that DDI is practically insoluble in all solid lipids tested. However DDI exhibits a relatively higher degree of solubility in solid lipids consisting of blends of di- and tri-acylglycerols such as Precirol® ATO 5 and Compritol® 888 ATO, but is poorly soluble in solid lipids consisting solely of mono-, di- or tri-acycerides, such as Gelot® 64, Imwitor® 900 P or Dynasan® 116. In addition, the solubility of DDI is better in Precirol® ATO 5 than in Compritol® 888 ATO, since the former consists of a mixture of relatively short chain length acylgycerols of distearate, tripalmitin and tristearin [239]. Compritol® 888 ATO is a blend of mono-, di- and tri-behanate, and the presence of the relatively long-chain behenic acid (C_{22}) backbone appears to increase the lipophilicity of Compritol® 888 ATO and therefore limits the solubility of DDI in this solid lipid. Consequently, Precirol® ATO 5 rather than Compritol® 888 ATO was selected as the solid lipid of choice for use in formulation development and optimization studies of DDI-loaded SLN and NLC.

4.3.2.2 Selection of liquid lipid excipients

The formulation of NLC requires the addition of a liquid lipid to a solid lipid to produce a nano-structured lipid matrix [30, 31]. Therefore, it was essential to select a suitable liquid lipid for use in the formulation of NLC. The selection of a suitable liquid lipid was also based

on the solubilising-potential of the liquid lipid for DDI. Consequently, the solubility of DDI was investigated in various oils and was quantitated using the validated HLPC method described in Chapter 3 and the data generated in these studies are shown in Table 4.4.

Table 4.4. Summary of DSC parameters of DDI obtained prior to and following drug exposure to 85°C for one (1) hour

No.	Material	HLB	Solubility (%)
1	Miglyol®	-	0.013 ± 0.00010
2	Transcutol® HP	-	0.267 ± 0.0160
3	Labrafil Lipofile® WL 1349	2	0.013 ± 0.00029
4	Labrafac® PG	2	0.014 ± 0.00035
5	Lauroglycol® FCC	2	0.022 ± 0.00029
6	Capryol® 90	6	0.079 ± 0.00038

These data reveal that DDI is poorly soluble in all liquid lipids tested. However Transcutol® HP was found to have the best solubilising-potential for DDI and was therefore selected as the liquid lipid for use in the preparation of drug-free and DDI-loaded NLC.

4.3.2.3 Determination of a ratio for solid lipid/liquid lipid blends for NLC production

Following the selection of Precirol® ATO 5 and Transcutol® HP for formulation development studies the two lipids were mixed in different ratios in order to determine the best composition of a binary mixture for the formulation of NLC. Binary mixtures exhibiting melting points higher than 40°C and that are miscible were deemed suitable for use. The miscibility between the two lipids was established using DSC and then by visual assessment. The use of DSC to assess the miscibility of Precirol® ATO 5 and Transcutol® HP was based on the fact that a depression in melting point of Precirol® ATO 5 would be observed following incorporation of Transcutol® HP in the lamellar structure of the solid lipid. In terms of visual assessment, the heated binary mixture was allowed to cool and then left to solidify at room temperature for 24 hours after which a piece of the solid sample was smeared onto a piece of hydrophilic filter paper. The presence or absence of any liquid lipid droplets on the filter paper was indicative of the degree of miscibility of the two lipids. The influence of Transcutol® HP on the melting point and peak onset of Precirol® ATO 5 is depicted in Figure 4.4 and a summary of the melting events observed for the various binary mixtures is listed in Table 4.5.

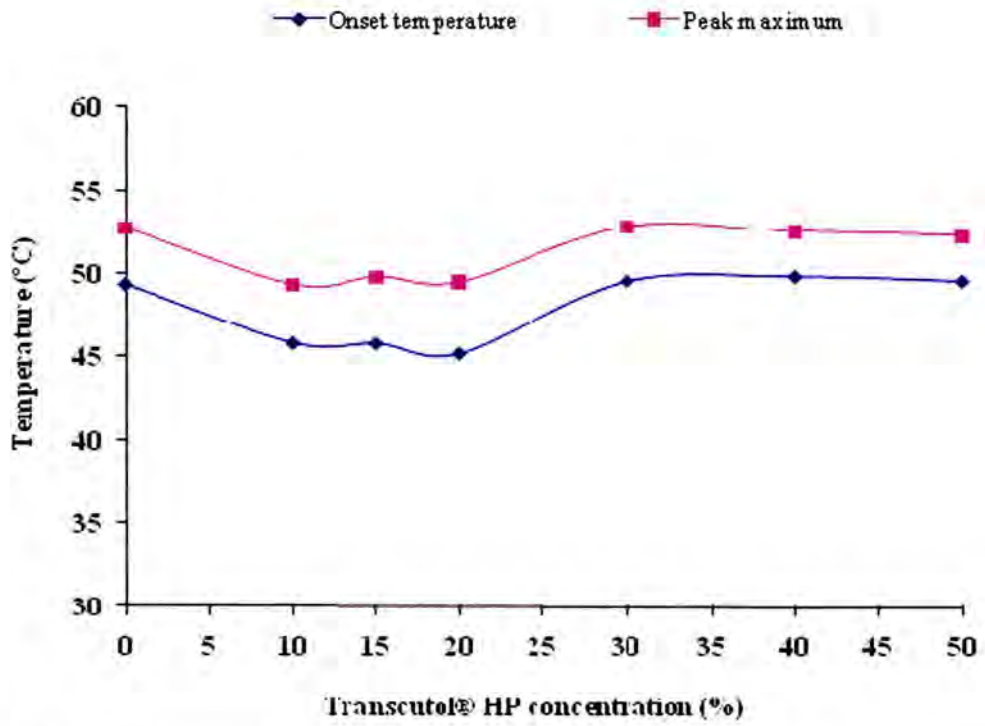

Figure 4.4. Effect of Transcutol® HP on the melting point and peak onset of Precirol® ATO

Table 4.5. DSC parameters for binary mixtures of Precirol® ATO 5 and Transcutol® HP following exposure to heat at 85°C for one (1) hour.

Precirol® ATO 5:Transcutol HP	Thermal event	Onset (°C)	MP (°C)	Enthalpy (J/g)	WME (°C)
100:00	Endothermic	49.33	52.71	125.30	3.38
90:10	Endothermic	45.82	49.33	75.65	3.51
85:15	Endothermic	45.79	49.81	54.61	4.02
80:20	Endothermic	45.20	49.50	35.45	4.30
70:30	Endothermic	49.55	52.85	112.29	3.30
60:40	Endothermic	49.84	52.58	116.60	2.71
50.50	Endothermic	49.56	52.35	115.72	2.79

These results reveal that all binary mixtures studied exhibited melting points above 40°C. However, the onset, peak maximum and enthalpy of Precirol® ATO 5 appears to decrease with an increase in the amount of Transcutol® HP added to the solid lipid up to a concentration of 20% w/w of the liquid lipid. In addition, a gradual increase in the width of the melting event as the amount of Transcutol® HP added to the solid lipid increases to 20% w/w is summarized in Table 4.5. Therefore the WME was also used as an indication of the degree of miscibility of Precirol® ATO 5 and Transcutol® HP. The depression in the onset, peak maximum, enthalpy and WME of Precirol® ATO 5 when up to 20% w/w of Transcutol® HP is added to the solid lipid shows that the two components are miscible when the liquid

lipid is used in this concentration range. These results were further confirmed when using visual observation of samples smeared on filter paper as no droplets of Transcutol® HP were observed on the filter paper.

The addition of ≥ 30% w/w of Transcutol® HP to Precirol® ATO 5 appeared to have no significant effect on the onset, peak maximum and enthalpy of Precirol® ATO 5. In addition, there is a decrease in the value of the WME suggesting that Precirol® ATO 5 has a much more ordered and crystalline structure. When smeared on filter paper these samples also leave behind droplets of the liquid lipid indicating a lower degree of miscibility between Precirol® ATO 5 and Transcutol® HP when ≥ 30% of the liquid lipid is mixed with the solid lipid.

It may well be desirable to have relatively high liquid lipid content in a binary mixture of Precirol® ATO 5 and Transcutol® HP in order to enhance the solubility of DDI in the lipid medium as the drug exhibits a marginally better solubility profile in the liquid lipid than in solid lipids. However, the results suggest that a liquid lipid content of ≤ 20% w/w was optimal and concentrations higher than 20% w/w are likely to result in the production of immiscible mixtures. Consequently, a binary mixture consisting of 20% w/w Transcutol® HP and 80% w/w Precirol® ATO 5 was selected as the most suitable combination of liquid and solid lipid for the formulation of DDI-free and DDI-loaded NLC.

4.3.3 Polymorphic and crystalline nature of bulk lipids

4.3.3.1 Precirol® ATO 5

4.3.3.1.1 DSC characterization

The DSC profile of Precirol® ATO 5 generated before and after exposing the lipid to 85°C for one (1) hour is shown in Figure 4.5 and the DSC data generated in these studies is summarized in Table 4.6.

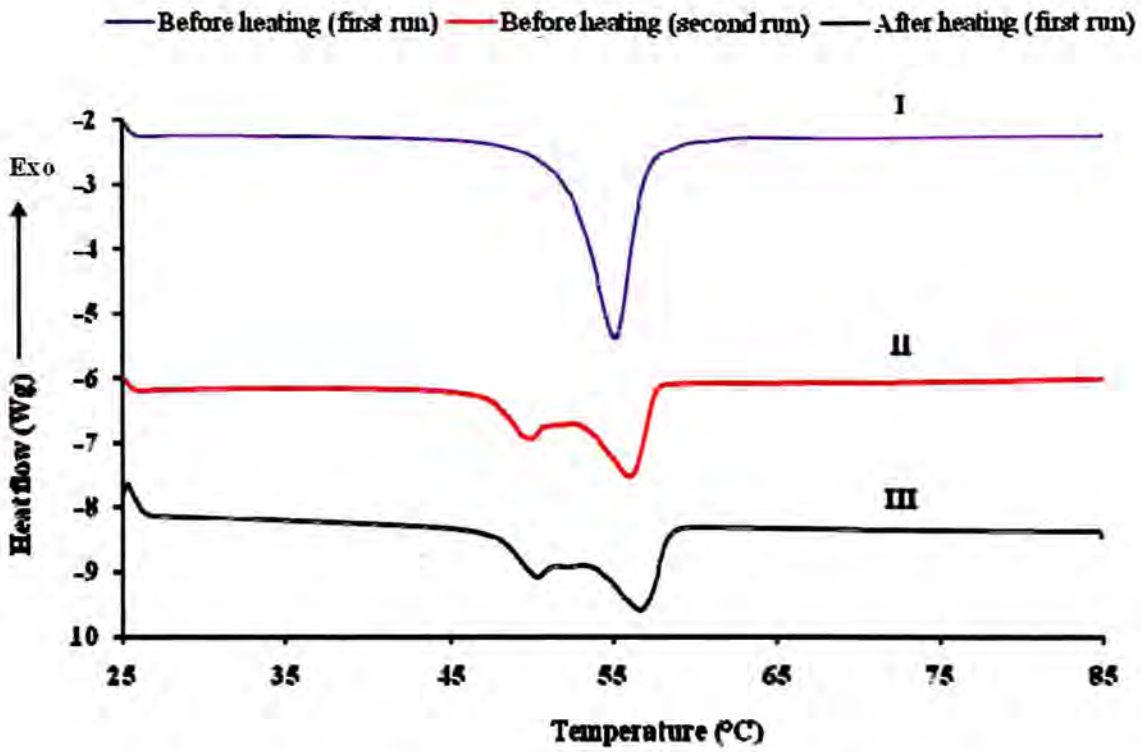

Figure 4.5. DSC profiles of Precirol® ATO 5 generated prior to and following exposure of the lipid to heat at 85°C for one (1) hour

Table 4.6. DSC parameters for Precirol® ATO 5 generated prior to and following exposure of the lipid to heat at 85°C for one (1) hour.

Precirol® ATO 5	Thermal event	Onset (°C)	MP (°C)	Enthalpy (J/g)	WME (°C)
1st run before heating	Endothermic	52.18	55.06	122.04	2.88
2nd run before heating	Endothermic	47.93	56.02	33.76	8.09
1st run after heating	Endothermic	47.98	56.11	39.94	8.13

The first DSC scan of Precirol® ATO 5 generated prior to heating (I) reveals the presence of a single peak with an onset and peak maximum at 52.18°C and 55.06°C respectively, and that corresponds to a single polymorphic form. The WME of the profile is narrow with a value of 2.88°C indicating that prior to heating Precirol® ATO 5 exists as a highly ordered crystalline structure. The second DSC scan of the sample (II) reveals two distinct endothermic events at 49.71°C (minor peak) and 56.02°C (major peak) with an onset temperature at 47.93°C. Similarly, the DSC curve of the sample that was exposed to 85°C prior to running a DSC scan (III) reveals two separate melting events at 49.67°C (minor peak) and 56.11°C (major peak) with an onset temperature at 47.98°C. The values for the WME of DSC profiles II and III are relatively high compared to that observed for the unheated material (I) and are almost

similar, which suggests that exposing Precirol® ATO 5 to heat may create defects within the lipid structure, thereby altering the crystalline nature of Precirol® ATO 5.

The two endothermic events shown in DSC curves II and III are indicative of the presence of two distinct polymorphic forms of Precirol® ATO 5, following exposure to heat. In both cases the minor peak has a lower melting point than the major peak and according to Saupe *et al.,* [166] this peak is indicative of the presence of a metastable α polymorph. Similarly the major peak in both cases has a higher melting point than the minor peak and according to Saupe *et al.,* [166] this peak is indicative of the presence of a stable β polymorphic form of the lipid. It is clearly evident that exposing Precirol® ATO 5 to heat at 85°C modifies the polymorphic nature of the solid lipid. From these data, it can be suggested that Precirol® ATO 5 exists in a single β polymorphic form prior to heat exposure, but that changes into a mixture of α and β polymorphic modifications following exposure of the solid lipid to heat. However, DSC alone cannot be used to draw conclusions concerning the polymorphic and crystalline nature of a solid lipid and therefore WAXS was also used.

4.3.3.1.2 WAXS characterization

WAXS was used to investigate the polymorphic nature of Precirol® ATO 5 prior to and following exposure to heat at 85°C in order to confirm the data generated using DSC. The diffraction patterns of bulk Precirol® ATO 5 prior to and following exposure to heat at 85°C for one (1) hour are depicted in Figure 4.6.

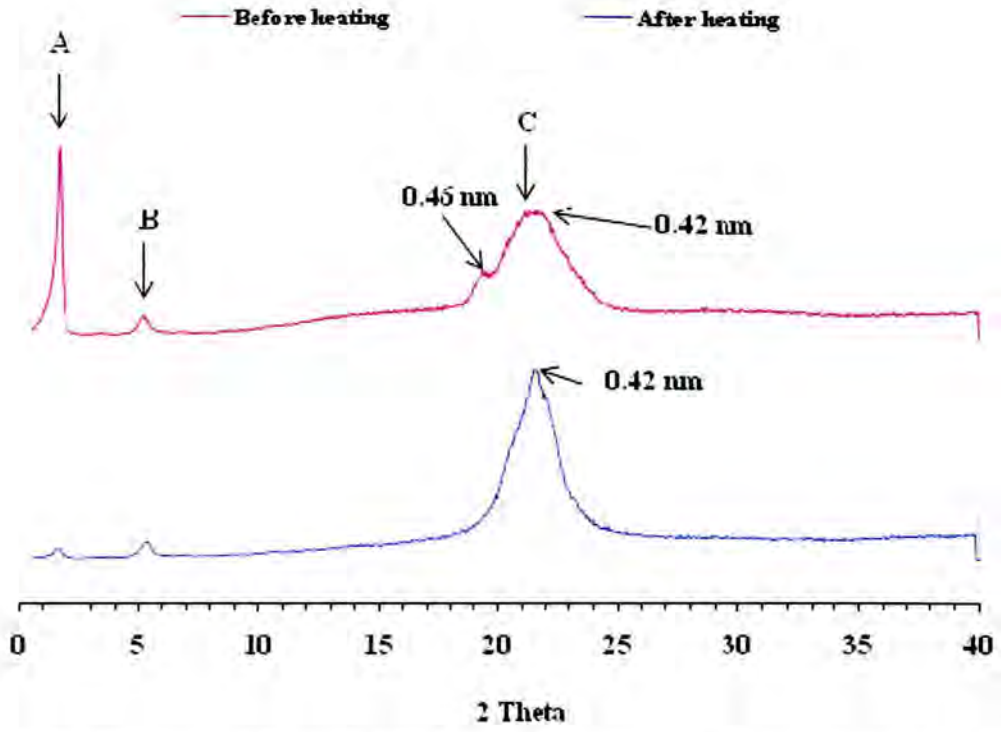

Figure 4.6. WAXS patterns of Precirol® ATO 5 obtained prior to and following exposure of the lipid to heat at 85°C for one (1) hour with associated Bragg spacing values around scattering peak range (point C) used to identify the polymorphic modification of the lipid.

The diffraction patterns of the two samples display equidistant reflections (peaks A and B) in the scattering angle ranging between 0.6-6 (2θ) and these peaks are indicative of a periodic lamellar arrangement within the lipid structure [205]. Exposure of Precirol® ATO 5 to heat appears to decrease the intensity of peaks A and B which suggests that heating the sample creates defects in the lamellar structure of the lipid, and possibly induces polymorphic alterations to that structure. The diffraction patterns shown in Figure 4.6 also reveal that both samples have scattering reflections around point C in the scattering angle ranging between 18-25 (2θ). These are reflections that are used to determine the arrangement of alkyl chains and therefore to identify polymorphic modifications of triacylglycerides [205]. Generally a polymorphic modification of a triacylglyceride can be identified using criteria set for X-ray diffraction patterns when the scattering intensity detected is plotted against the scattering vector (s) [205, 240]. An α-modification has a single scattering reflex with a Bragg's distance ranging between 0.410-0.420 nm, whereas a β′-modification has two reflexes at a Bragg's distance of 0.389 nm and 0.420 nm [205, 240]. Furthermore a β_i-modification reveals three reflexes at a Bragg's distance of 0.389 nm, 0.420 and 0.460 nm [205, 240] and a lipid is said

to exist in a β-modification if all of the criteria listed for other modifications are not met [205]. The Bragg's spacing values calculated for the reflections around point C for both samples and which were used to identify the polymorphic modification of Precirol® ATO 5 prior to and following heating are also shown in Figure 4.6. The Bragg's spacing values were calculated using Equation 4.1, Section 4.2.2.3.2, *vide infra.*

The pattern for Precirol® ATO 5 prior to heating shows two scattering reflections at point C with Bragg spacing values of 0.42 nm and 0.46 nm which is indicative of the presence of a β-modification. These observations are consistent with those made from data generated using DSC and therefore it can be concluded with some degree of certainty that Precirol® ATO 5 exists in the highly crystalline β-modification prior to heating. The WAXS profile for Precirol® ATO 5 following heating reveals a single peak at point C with a Bragg spacing value of 0.42 nm suggesting that a change in the polymorphic form of the lipid from a β- to α-modification has occurred. However DSC data reveal that Precirol® ATO 5 co-exists in the α- and β-modification following heating. This is more than likely still the case, however the use of XRD was unable to detect the presence of the β-modification in the lipid sample exposed to heat. Nevertheless, both DSC and WAXS data reveal that exposing Precirol® ATO 5 to 85°C for one (1) hour alters the degree of crystallinity and therefore the polymorphic nature of the solid lipid. The implication of these observations is that heating Precirol® ATO 5 creates lattice defects within the lipid matrix following recrystallization, which may allow for more efficient incorporation of DDI within the lipid structure formed following manufacture [202, 205].

4.3.3.2 Precirol® ATO 5 and Transcutol® HP

DSC and WAXS were also used to establish the influence of incorporating Transcutol® HP into Precirol® ATO 5 on the polymorphic and crystalline nature of the resultant solid lipid. The binary mixture investigated in these studies consisted of 80% w/w Precirol® ATO 5 and 20% w/w Transcutol® HP. The binary mixture was exposed to heat of 85°C for one (1) hour after which the sample was allowed to cool and then kept at room temperature for 24 hours prior to analysis. The DSC and WAXS profiles for Precirol® ATO 5 after heating at 85°C for one (1) hour was used as a reference. It was deemed unnecessary to run a DSC or WAXS scan of the binary mixture before heating as data obtained from such studies would reflect the melting behaviour and diffraction patterns of Precirol® ATO 5 only.

4.3.3.2.1 DSC characterization

The DSC profile of Precirol® ATO 5 after heating in addition to the DSC profile of a binary mixture of Precirol® ATO 5 and Transcutol® HP (80:20) developed after exposing the lipid mixture to heat at 85°C for one (1) hour is depicted in Figure 4.7. A summary of the DSC data generated in these studies in addition to the calculated WME are listed in Table 4.7.

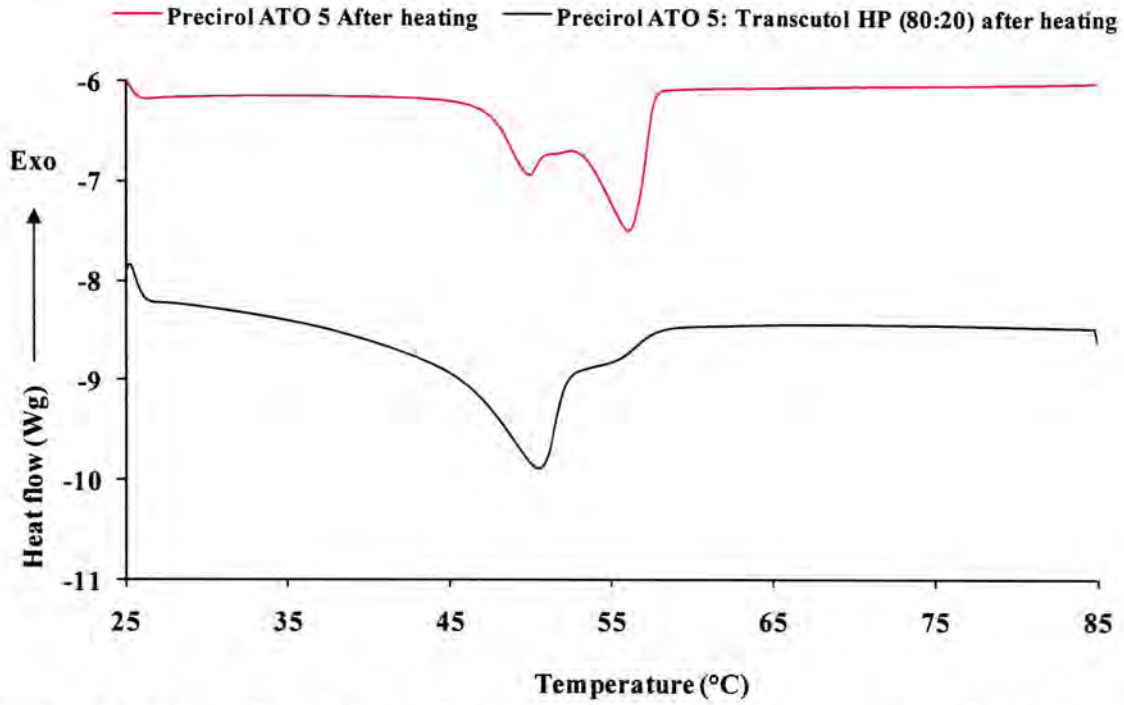

Figure 4.7. DSC profiles of Precirol® ATO 5 and a binary mixture of Precirol® ATO 5 and Transcutol® HP (80:20) generated prior to and following exposure of the lipid to heat at 85°C for one (1) hour.

Table 4.7. DSC parameters of Precirol® ATO 5 and a binary mixture of Precirol® ATO 5 and Transcutol® HP (80:20) generated prior to and following exposure of the lipid to heat at 85°C for one (1) hour.

Material	Thermal event	Onset (°C)	MP (°C)	Enthalpy (J/g)	WME (°C)
Precirol® ATO 5 following heating	Endothermic	47.98	56.11	39.94	8.13
Precirol® ATO 5 and Transcutol® HP (80:20) following heating	Endothermic	43.66	50.33	35.45	6.67

Precirol® ATO 5 exists in a single highly crystalline β-modification prior to heating and the exposure of the solid lipid to heat changes the polymorphic nature of Precirol® ATO 5 from β- to a metastable α-polymorph (Section 4.3.3.1). The DSC curve of the binary mixture of Precirol® ATO 5 and Transcutol® HP (THP) (80:20) shows the presence of two distinct

corresponding lower enthalpy than that observed for Precirol® ATO 5. The major peak corresponds to the presence of the less crystalline α-modification and the small peak to a more stable β-polymorphic modification.

It appears that the inclusion of Transcutol® HP into Precirol® ATO 5 creates defects within the structure of the solid lipid, which favour the transformation of Precirol® ATO 5 from a β- to α-polymorphic modification. However, the detection of a minor peak suggests that the solid lipid formed from the binary mixture of Transcutol® HP and Precirol® ATO 5 co-exists in both the α- and β-modifications and in which the amount of the β-modification present is relatively lower than that of α-modification as suggested by the intensities of the two separate peaks.

4.3.3.2.2 WAXS characterization

The WAXS patterns of the binary mixture of Precirol® ATO 5 and Transcutol® HP (80:20) observed following exposure of the lipid mixture to heat at 85°C for one (1) hour is shown in Figure 4.8. The WAXS profile for Precirol® ATO 5 generated before heating was used as a reference. In addition Figure 4.8 depicts the Bragg spacing values used to identify the presence of the polymorphic modifications of the lipids.

Precirol® ATO 5 shows two reflections at Bragg spacing values of 0.42 nm and 0.46 prior to heating which is indicative of the presence of a β-polymorphic modification. However the binary mixture of Precirol® ATO 5 and Transcutol® HP (80:20) following heating reveals the presence of various reflections at different Bragg distance values. This suggests that the binary mixture of Precirol® ATO 5 and Transcutol® HP (80:20) produces a solid lipid matrix that probably exists in a β-polymorphic modification. However, DSC data revealed a co-existence of α- and β-modifications which again is more than likely the case but WAXS was not able to detect the presence of an α-modification in this mixture. Once again this observation shows the importance of using DSC and WAXS as complementary analytical tools to predict the presence of polymorphism in solid lipid matrices.

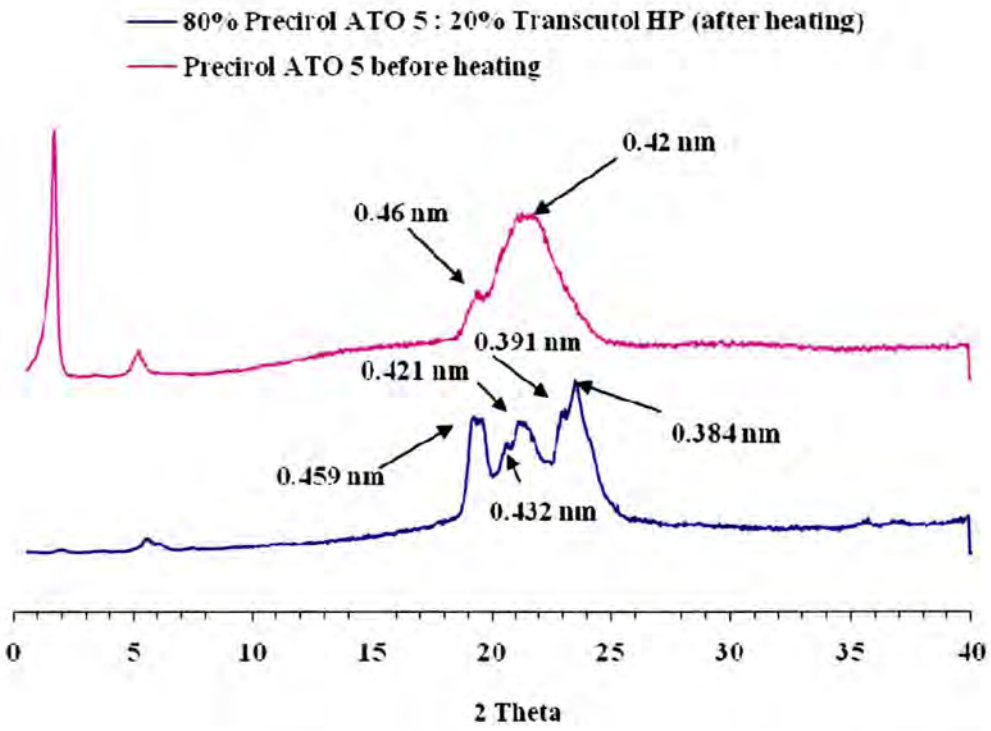

Figure 4.8. WAXS patterns of Precirol® ATO 5 and a binary mixture of Precirol® ATO 5 and Transcutol® HP (80:20) prior to and following exposure of the lipid to heat at 85°C for one (1) hour with associated Bragg spacing values.

4.3.4 Interaction of bulk lipids with DDI

DSC and WAXS were also used to generate information relating to interactions between DDI and Precirol® ATO 5 and a binary mixture of Precirol® ATO 5 and Transcutol® HP (80:20).

4.3.4.1 Binary mixture of Precirol® ATO 5 and DDI

4.3.4.1.1 DSC characterization

The DSC profiles generated following analysis of a binary mixture of Precirol® ATO 5 and DDI following heating to 85°C for one (1) hour is depicted in Figure 4.9, and the DSC parameters are summarized in Table 4.8.

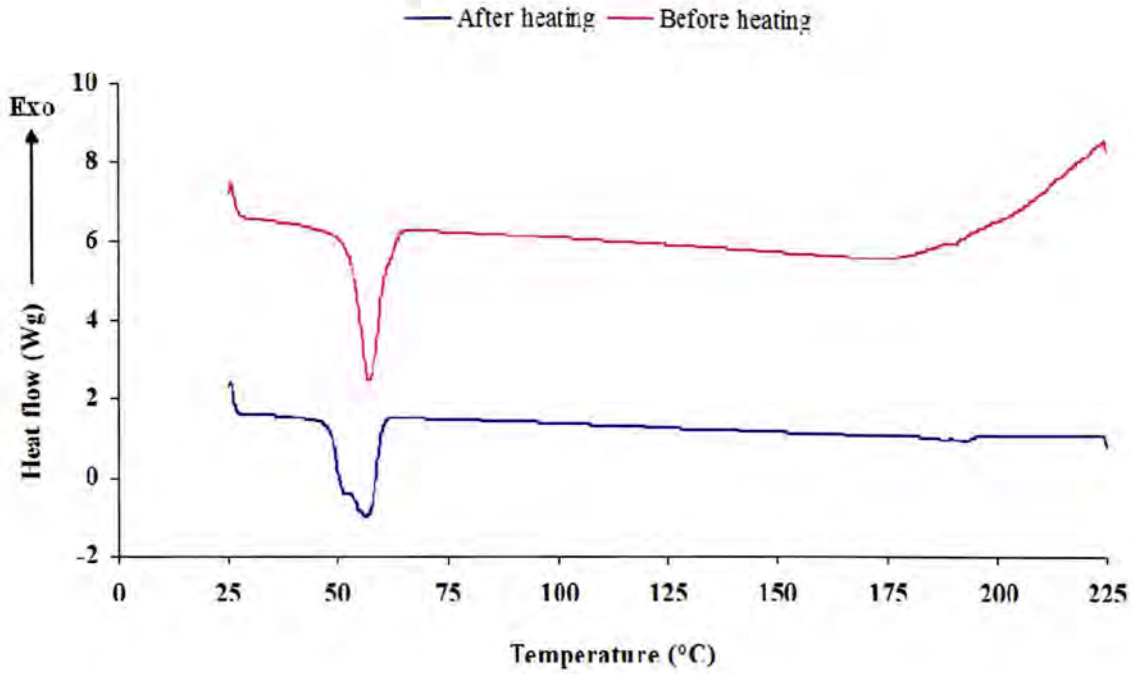

Figure 4.9. DSC profile of a binary mixture of Precirol® ATO 5 and DDI generated prior to and following exposure of the lipid to heat at 85°C for one (1) hour

Table 4.8. DSC parameters of a binary mixture of Precirol® ATO 5 and DDI generated prior to and following exposure of the lipid to heat at 85°C for one (1) hour

Precirol® ATO 5 and DDI	Thermal event	Onset (°C)	MP (°C)	Enthalpy (J/g)
Before heating	Endothermic	52.35	55.82	123.77
	Endothermic	186.33	187.80	0.62
After heating	Endothermic	48.04	56.17	146.24
	Endothermic	188.50	192.73	4.42

The DSC profiles of the binary mixture of Precirol® ATO 5 and DDI prior to and following exposure to heat reveals the presence of peaks that are due to both Precirol® ATO 5 and DDI and that are present at their typical melting points as shown in Sections 4.3.3.1 and 4.3.1.2 respectively. There is clearly no interaction between DDI and the solid lipid. In addition, the presence of a peak due to DDI both prior to and following heating with the binary mixture indicates that DDI was not completely dissolved in the Precirol® ATO 5 and therefore remained in a crystalline state in the solid lipid. Once again this is indicative of the relatively poor solubility of DDI in Precirol® ATO 5.

4.3.4.1.2 WAXS characterization

The WAXS patterns of a binary mixture of Precirol® ATO 5 and DDI obtained prior to and following exposure to heat at 85°C for one (1) hour are shown in Figure 4.10. In addition, the WAXS patterns of DDI after heating and which was used as a reference in these studies to distinguish the diffraction bands of DDI from those of the solid lipid matrix are depicted in Figure 4.10. The diffraction patterns of the binary mixture both before and after heating show a number of reflections (1-4) that are consistent with reflections observed for DDI. This is again indicative of the lack of complete dissolution of DDI in Precirol® ATO 5. DDI was therefore not molecularly dispersed in the lipid matrix at the concentrations used in these studies but remained in crystalline state, even following exposure to heat at 85°C for one (1) hour. These observations are consistent with the data generated from the DSC analysis of the same samples.

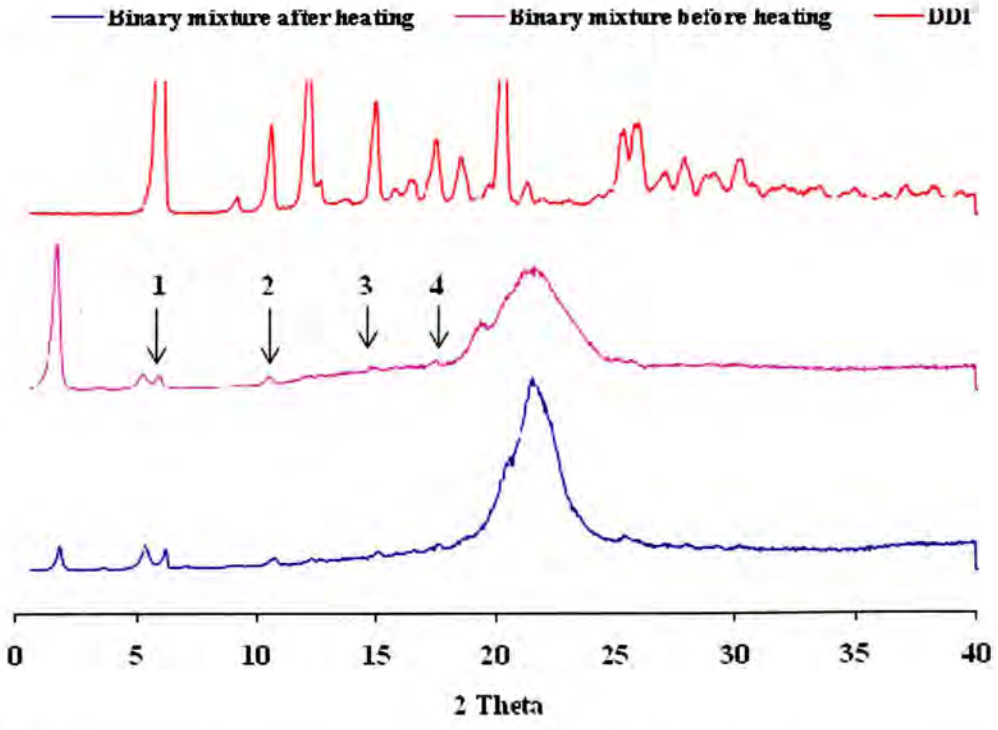

Figure 4.10. WAXS patterns of a binary mixture of Precirol® ATO 5 and DDI obtained prior to and following exposure of the mixture to 85°C for one (1) hour

4.3.4.2 *Ternary mixture of Precirol® ATO 5, Transcutol® HP and DDI*

4.3.4.2.1 *DSC characterization*

The DSC profiles of a ternary mixture of Precirol® ATO 5, Transcutol® HP and DDI obtained before and after exposing the mixture to heat at 85°C for one (1) hour are shown in Figure 4.11 and a summary of DSC parameters generated in these studies is listed in Table 4.9. The DSC profiles of the sample before and after heating clearly reveals the presence of separate endothermic events consistent with those of Precirol® ATO 5/Transcutol® HP solid lipid matrix and DDI. However, the melting peak of DDI in the sample analyzed following heating is smaller than that of DDI in the binary mixture (Section 4.3.4.1.1) and that observed in this ternary mixture before heating. This indicates that DDI has a relatively higher solubility in a mixture of Precirol® ATO 5 and Transcutol® HP than in Precirol® ATO 5 alone, but that it still exists in a crystalline form in the solid lipid or a mixture of solid and liquid lipid.

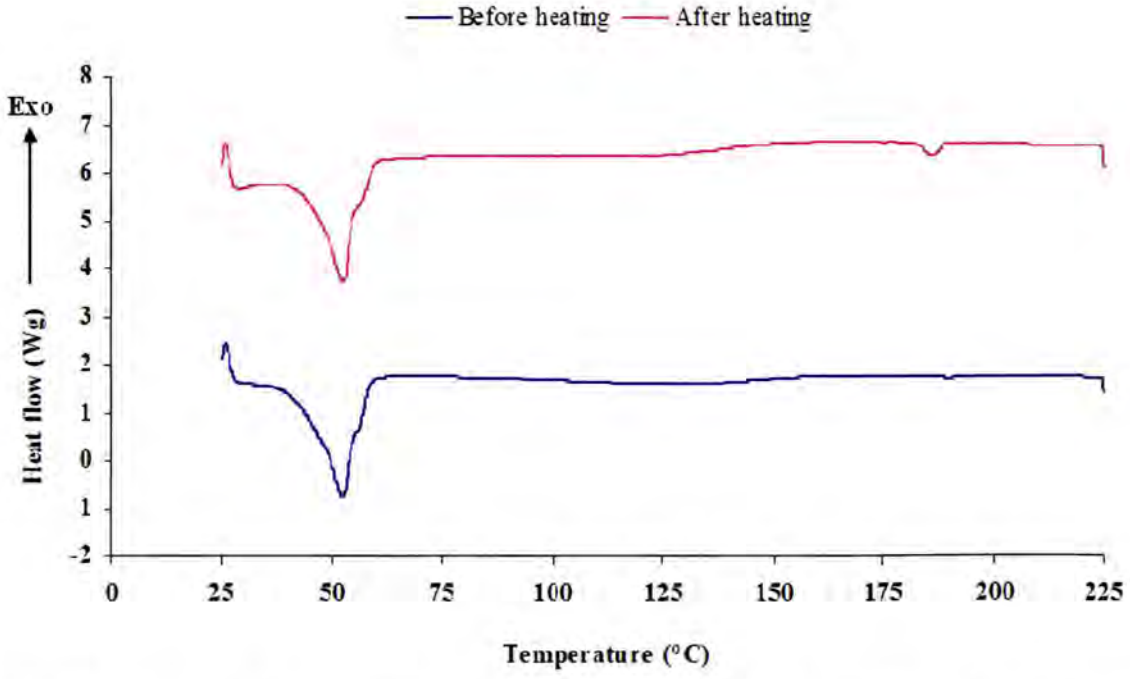

Figure 4.11. DSC profile of a ternary mixture of Precirol® ATO 5, Transcutol® HP and DDI generated prior to and following exposure of the mixture to 85°C for one (1) hour.

Table 4.9. DSC parameters of a ternary mixture of Precirol® ATO 5, Transcutol® HP and DDI obtained prior to and following exposure of mixture to 85°C for one (1) hour.

Precirol® ATO 5 and DDI	Thermal event	Onset (°C)	MP (°C)	Enthalpy (J/g)
Before heating	Endothermic	52.35	55.82	123.77
	Endothermic	186.33	187.80	0.62
After heating	Endothermic	43.86	50.53	158.69
	Endothermic	184.30	187.17	4.02

4.3.4.2.2 WAXS characterization

The WAXS patterns of a ternary mixture of Precirol® ATO 5, Transcutol® HP and DDI generated before and after exposing the mixture to heat at 85°C for one (1) hour and the WAXS diffractions of DDI are shown in Figure 4.12.

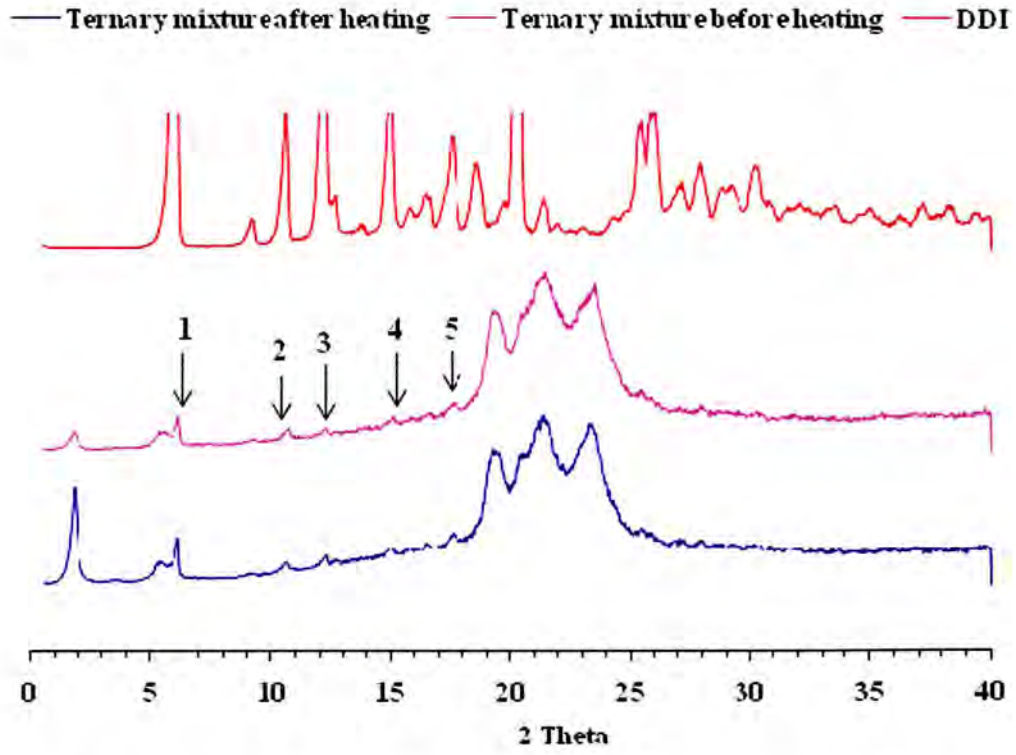

Figure 4.12. WAXS patterns of a ternary mixture of Precirol® ATO 5, Transcutol® HP and DDI generated prior to and following exposure of the mixture to 85°C for one (1) hour

The diffraction patterns of the binary mixture before and following heat exposure show diffraction patterns (1-5) that match the diffraction peaks observed for DDI alone. These results are consistent with those observed using DSC and consequently it can be deduced that DDI is not completely dissolved in a ternary mixture that is comprised of Precirol® ATO 5

and Transcutol® HP at the concentrations used in these studies, but that it coexists in a crystalline state.

4.4 CONCLUSIONS

These studies have shown that DDI is thermostable and consequently a hot high pressure homogenization technique may be used to manufacture DDI-loaded SLN and NLC. However, exposing the drug to temperatures of approximately 85°C may decrease the crystalline nature of the API and change the polymorphic form of the drug. It is evident that DDI is poorly soluble in both solid and liquid lipids however a combination of Precirol® ATO 5 and Transcutol® HP had the best solubilising-potential for DDI of all the lipids investigated. Precirol® ATO 5 appears to exist in a stable β-modification prior to exposure to heat however a mixture of both α- and β-modifications was detected following heating at 85°C for an hour.

The optimum ratio of Precirol® ATO 5 and Transcutol® HP that is suitable for the manufacture of DDI-loaded NLC is 80:20 (Precirol® ATO 5: Transcutol® HP). This is because the two lipids are miscible at this ratio and furthermore the resultant solid lipid matrix had a melting point higher than 40°C. The inclusion of Transcutol® HP into Precirol® ATO 5 changes the polymorphic form of the solid lipid from a stable β-modification to a form that exhibits the co-existence between α- and β-polymorphic forms also indicating that NLC produced using this solid/liquid lipid combination could exist in the α- and/or β-modifications. These studies have also shown that DDI exists in a crystalline state when dispersed at a high drug concentration of 5% w/w in Precirol® ATO 5 or in a binary mixture of Precirol® ATO 5 and Transcutol® HP.

The relatively high solubility of DDI in Transcutol® HP compared to Precirol® ATO 5 indicates that a solid lipid matrix prepared from a binary mixture of Precirol® ATO 5 and Transcutol® HP is likely to have a higher LC and EE for DDI than a matrix consisting of Precirol® ATO 5 alone. In addition, the potential for the solid lipid matrix to exist in the α- and/or β-modifications when Transcutol® HP is added to Precirol® ATO 5 suggests that the expulsion of DDI from a solid lipid matrix during prolonged storage periods is likely to be minimized. Consequently it was considered logical to investigate the feasibility of

incorporating DDI into NLC and not in SLN, as the production of the latter carrier might not readily produce a delivery system with suitable EE and LC of DDI.

CHAPTER 5

FORMULATION AND CHARACTERIZATION OF DDI-LOADED NANOSTRUCTURED LIPID CARRIERS (NLC)

5.1 BACKGROUND

The feasibility of incorporating DDI into NLC was investigated by developing and manufacturing aqueous nanoparticulate dispersions consisting of 20% w/w lipid using a hot high pressure homogenization (HPH) technique. The solid lipid matrix of NLC was comprised of a binary mixture of Precirol® ATO 5 and Transcutol® HP, which were selected as described in Chapter 4. NLC formulations are usually formulated with one or more emulsifying agents that can stabilize the lipid nanoparticles in an aqueous environment. Consequently, the initial stages of the formulation development studies were designed to select a surfactant or combination of surfactants that would ensure the production of stable NLC formulations that contained the water soluble drug, DDI. Once a suitable surfactant or combination of surfactants had been identified, the next stage of the formulation development studies was to identify and select an appropriate pressure and number of homogenization cycles to ensure the production of NLC of an appropriate PS and PSD.

The formulation of DDI-loaded NLC was started using small quantities of DDI due to the limited solubility of DDI in lipids. The concentration of DDI in the formulations was then increased during formulation development and optimization studies in order to evaluate the effects of increasing the amount of DDI used in the formulation, on the drug LC and EE of the nanoparticles. Process and/or formulations variables were identified and used in an attempt to enhance the LC and EE of the nanoparticles for DDI. The NLC were characterized at every stage of formulation development and optimization studies, particularly in terms of PS, PI, ZP and EE and LC. In addition, the degree of crystallinity and lipid modification, shape and surface morphology of the drug-containing NLC were investigated in order to ensure that quality DDI-loaded SLN and/or NLC product were produced.

5.2 MATERIALS AND METHODS

5.2.1 MATERIALS

5.2.1.1 Lipid materials

5.2.1.1.1 Precirol® ATO 5

Precirol® ATO 5 (Gattefossé SAS, Saint-Priest Cedex, France) is a synonym for glyceryl palmitostearate [239, 241], which is a solid lipid consisting of a mixture of mono-, di-, and triglycerides of palmitic (C_{16}) and stearic (C_{18}) acids [239]. The lipid occurs as a fine white powder with a faint odour and is manufactured by direct esterification of palmitic and stearic acids with glycerol, without the use of a catalyst [239]. Precirol® ATO 5 has GRAS status and is generally regarded as a non-toxic and non-irritant material and as a consequence can be used for the production of pharmaceutical formulations for oral administration [239]. Glyceryl palmitostearate has a melting point ranging between 52-55°C, a hydroxyl value of 90-110 mg KOH/g, a saponification of value 175-195 mg KOH/g and a peroxide value of less than 3.0 meq O_2/kg [239].

Precirol® ATO 5 has a hydrophilic-lipophilic balance (HLB) value of 2 [239, 241] and is freely soluble in chloroform and dichloromethane but is practically insoluble in ethanol, mineral oil and water [239]. Glyceryl palmitostearate should be stored at temperatures below 35°C, but for storage periods exceeding one month, the material should be stored at temperatures between 5-15°C in an airtight container and protected from light and moisture [239]. Precirol® ATO 5 is used as a lubricant in solid-oral dosage forms or as a lipophilic matrix for sustained-release tablets and capsules [239]. Furthermore, the lipid can be used to produce microspheres, which can be filled into capsules or compressed into tablets, pellets, coated beads and/or made into biodegradable gels [239].

5.2.1.1.2 Transcutol® HP

Transcutol® HP (Gattefossé SAS, Saint-Priest Cedex, France) is the proprietary name for diethylene glycol monoethyl [241] and is a highly purified liquid lipid with a purity of > 99.9% [241]. Transcutol® HP is a grade of diethylene glycol monoethyl that is suitable for use in oral dosage forms and is currently regulated by a number of international regulatory

authorities [241]. Transcutol® HP is soluble in both water and oil and is regarded as an excellent solvent and/or solubilizer for a number of hydrophobic compounds [241].

5.2.1.2 Emulsifying agents

5.2.1.2.1 Lutrol® F68

Lutrol® F68 (BASF AG, Ludwigshafen, Germany) is the proprietary name for poloxamer 188 and is a non-ionic surface active agent consisting of a block copolymer of polyoxyethylene-polyoxypropylene with a molecular weight ranging between 7680-9510 [242]. The polyoxyethylene portion of the molecule is hydrophilic while the polyoxypropylene portion is lipophilic and consequently Lutrol® F68 is used mainly as an emulsifying or solubilizing agent in oral, parenteral and topical formulations [242]. Poloxamer 188 occurs as white, waxy and free-flowing prilled granules or as cast solid and is practically odourless, tasteless and generally regarded as a non-toxic and non-irritant material [242].

Lutrol® F68 has a melting point ranging between 52-57°C and a dynamic viscosity of 1000 cP when tested at 77°C [242]. Poloxamer 188 has an HLB value of 29 and is freely soluble in water and 95% ethanol [242] and is included in the Inactive Ingredients Database of the Food and Drug Administration (FDA) as an excipient suitable for use in IV injections, inhalations, ophthalmic, oral powders, solutions, suspensions, syrups and topical formulations [242]. Lutrol® F68 is stable in acidic and alkaline solution and in the presence of metallic ions however aqueous solutions of the molecule may support the growth of moulds when prepared without a preservative [242].

5.2.1.2.2 Solutol® HS 15

Solutol® HS 15 (BASF AG, Ludwigshafen, Germany) is the proprietary name for macrogol 15 hydroxystearate and consists of a mixture of mainly monoesters and diesters of 12-hydroxystearic acid and macrogols prepared by the ethoxylation of 12-hydroxystearic acid [243]. Solutol® HS 15 is a yellowish-white, almost odourless waxy mass or paste at room temperature that becomes liquid at approximately 308°C [243]. Macrogol 15 hydroxystearate is regarded as a relatively non-toxic and non-irritant material and is used as a non-ionic emulsifying agent, dissolution enhancer, solubilizing agent and/or as a stabilizing agent in

oral and parenteral pharmaceutical formulations, up to a concentration of 50% w/w [243]. Solutol® HS 15 is very soluble in water, soluble in 95% ethanol and in propan-2-ol and is insoluble in liquid paraffin, however the aqueous solubility of Solutol® HS 15 is inversely proportional to the temperature of the medium in which it is dissolved [243].

Solutol® HS 15 has a solidification temperature ranging between 25-30°C, an HLB value ranging between 14-16, a density of 1.03 g/cm^3 and a hydroxyl value of between 90-110 mg KOH/g [243]. Furthermore, macrogol 15 hydroxystearate has a saponification value ranging between 53-63 mg KOH/g, a peroxide value of less than 5.0 meq O_2/k and a percentage of free macrogols ranging between 27-39% [243]. The chemical stability of macrogol 15 hydroxystearate is high, albeit prolonged exposure of the substance to heat may induce physical separation of the molecule into a liquid and solid phase following cooling, which is reversible by subsequent homogenization [243]. Solutol® HS 15 is stable for at least 24 months if stored in unopened airtight containers at room temperature (25°C) [243].

5.2.1.2.3 Tween® 80

Tween® 80 (Sigma Aldrich Chemie GmbH, Steinheim, Germany) is polyoxyethylene 20 sorbitan monooleate or polysorbate 80, which is a yellow oily liquid with a characteristic odour and a warm, somewhat bitter taste. [244]. Tween® 80 has GRAS status and is a non-toxic and non-irritant material that can be used as a non-ionic emulsifying agent, solubilizing agent and/or as a wetting agent in oral, parenteral, food, topical and cosmetic products [244]. Polysorbate 80 has a molecular weight of approximately 1310, an HLB value of 15 and is soluble in water and ethanol, but insoluble in mineral and vegetable oils [244]. In addition, Tween® 80 has a specific gravity of 1.08 at 25°C, a dynamic viscosity of 425 cP and a hydroxyl value of between 65-60 mg KOH/g [244]. Furthermore, polysorbate 80 has a saponification value ranging between 45-55 mg KOH/g, an acid value of 2.0% and a surface tension of 42.5 mN/m at 20°C [244]. Tween® 80 is stable in the presence of electrolytes, weak acids and bases, however saponification of the material occurs in the presence of strong acids and bases. In addition, polysorbate 80 is sensitive to oxidation and is hygroscopic and consequently, should be stored in a well-sealed container, protected from light, in a cool and dry environment [244]. However, prolonged storage of Tween® 80 can lead to the formation of peroxides [244].

5.2.1.3 Water

HPLC-grade water was used in these studies and was produced as described in Chapter 4 (Section 4.2.1.4).

5.2.2 Methods

5.2.2.1 Production of NLC formulations

All formulation compositions developed and tested during the development and optimization of DDI-containing NLC formulations are listed in Tables 5.1, 5.2 and 5.3. The composition of the NLC formulations e.g. batches DDI-NLC 01 to DDI-NLC 04 that were designed to select and optimize a surfactant or a combination of surfactants aimed at developing stable aqueous dispersions of DDI-loaded NLC formulations is summarized in Table 5.1. The formulation compositions listed in Table 5.2 are for batches DDI-free to DDI-NLC 09 that were used to assess the influence of increasing amounts of DDI on the physicochemical properties of the optimized NLC formulation. A summary of the composition of batch DDI-NLC 10 is shown in Table 5.3 and was used to investigate a novel strategy designed and investigated in an attempt to enhance the LC and EE of the NLC for DDI.

Table 5.1. Composition (% w/w) for formulations developed and tested in optimization studies

MATERIAL	DDI-NLC 01	DDI-NLC 02	DDI-NLC 03	DDI-NLC 04
DDI	0.015	0.015	0.015	0.015
Tween® 80	6.0	-	-	1.0
Lutrol® F68	-	6.0	-	2.0
Solutol® HS 15	-	-	6.0	3.0
Transcutol® HP	5.0	5.0	5.0	5.0
Precirol® ATO 5	15.0	15.0	15.0	15.0
Aqua ad.	100.0	100.0	100.0	100.0

Table 5.2. Composition (% w/w) for formulations tested in drug loading studies

MATERIAL	DDI-FREE NLC	DDI-NLC 05	DDI-NLC 06	DDI-NLC 07	DDI-NLC 08	DDI-NLC 09
DDI	-	0.0150	0.0200	0.0500	0.125	0.250
Tween® 80	1.00	1.00	1.00	1.00	1.00	1.00
Lutrol® F68	2.00	2.00	2.00	2.00	2.00	2.00
Solutol® HS 15	3.00	3.00	3.00	3.00	3.00	3.00
Transcutol® HP	5.00	5.00	5.00	5.00	5.00	5.00
Precirol® ATO 5	15.0	15.0	15.0	15.0	15.0	15.0
Aqua ad.	100	100	100	100	100	100

Table 5.3. Composition (% w/w) of NLC formulations designed to investigate a novel strategy aimed at enhancing the LC and EE of DDI.

MATERIAL	DDI-NLC 10
FORMULA A	
DDI	20.0
Tween 80	2.0
Transcutol® HP	78.0
FORMULA B	
Formula A	25.0
Precirol ATO 5	75.0
FORMULA C	
Formula B	20.0
Tween® 80	0.90
Lutrol® F68	2.0
Solutol® HS 15	3.0
Transcutol® HP	1.1
Aqua ad.	100

5.2.2.1.1 Formulation development and optimization studies

A discontinuous hot high pressure homogenization process was used to produce aqueous DDI-free and DDI-loaded NLC formulations (batches DDI-NLC 01 – DDI-NLC 07) using a Micron LAB 40 APV high pressure homogenizer (APV Deutschland GmbH, Unna, Germany). DDI was added to a lipid phase consisting of Precirol®ATO 5, Transcutol® HP, Solutol® HS 15 and/or Tween® 80 and heated to 85°C. An aqueous phase containing Lutrol® F68 was heated to the same temperature as the lipid phase and the heated aqueous phase was dispersed in the molten lipid phase using a Model T25 Ultra-Turrax T25 homogenizer (Janke & Kunkel GmbH and Co KG, Staufen, Germany) at a speed of 8 000 rpm for one (1) min, to produce a pre-emulsion. The pre-emulsion formed was then homogenized at 85°C using the high pressure homogenizer using three homogenization cycles at 800 bar. The hot o/w nanoemulsion that was produced was immediately filled and sealed in siliconized glass vials and then allowed to cool to room temperature (25°C) to permit recrystallization of the lipid phase to form NLC *in situ*. All samples were kept at room temperature for 24 hours prior to characterization studies.

5.2.2.1.2 Novel strategy aimed at enhancing the LC and EE for DDI

The relatively low solubility of DDI in lipid media was identified as the major factor that would limit the LC and EE of NLC for DDI. Therefore, formulation and process strategies

were established in an attempt to improve the solubility of DDI in the lipid phase. Attempts were made to formulate DDI-loaded NLC using self-emulsifying solid lipids such as Imwitor® 312 (glyceryl monolaurate) and Imwitor® 960 (glyceryl stearate citrate) (SASOL Germany GmbH, Witten, Germany) as these lipids had a high solubility potential for DDI. However, the use of these solid lipids in the manufacture of DDI-loaded NLC resulted in the formation of semi-solid products, prior to high pressure homogenization. The use of low levels of the lipids and/or high concentrations of surfactants did not make any difference to the behaviour of these formulations. Consequently, a novel processing strategy was devised in an attempt to increase the solubility of DDI in the lipid medium. This process involved the production of a nanosuspension of DDI in a liquid lipid e.g. Transcutol® HP using hot high pressure homogenization. The DDI containing lipid nanosuspension was then incorporated into the lipid phase using cold high pressure homogenization. The motivation behind the production of the initial lipid-based DDI nanosuspension was based on the principle used to increase the intrinsic solubility of hydrophobic API in water and which is achieved by the formulation of nanosuspensions of the API [245, 246].

5.2.2.1.2.1 Production of DDI nanosuspension in Transcutol® HP

A nanosuspension of DDI in Transcutol® HP was produced using a Micron LAB 40 APV high pressure homogenizer (APV Deutschland GmbH, Unna, Germany) at a temperature of 85°C. Briefly, an excess of DDI (8 g) was dispersed in 32 ml of Transcutol® HP containing Tween® 80 (2% w/v) using a Model T25 Ultra-Turrax T25 homogenizer (Janke & Kunkel GmbH and Co KG, Staufen, Germany) at 8 000 rpm for one (1) min to produce a course microsuspension. Initially, the course microsuspension was homogenized using a high pressure homogenizer for three or five cycles at relatively low pressures of 100, 500 and 1000 bar e.g. 3x100, 5x500 and 5x1000 bar in order to reduce the size of large DDI crystals and to prevent the API from blocking the homogenization gap and/or causing erosion of the homogenization valve. Following the initial pre-homogenization procedure, the PS of DDI was further reduced in oil by homogenizing the sample at 1500 bar for a total of 20 homogenization cycles. Samples of the product were taken after 1, 5, 10, 15 and 20 cycles and visualized using a light microscope (Section 5.2.2.2.3.1) in order to monitor the progress of PS reduction experiments. The product obtained following 20 cycles of homogenization at 1500 bar was used for production of batch DDI-NLC 10 using cold high pressure homogenization as described in Section 5.2.2.1.2.2.

5.2.2.1.2.2 Production of batch DDI-NLC 10

Batch DDI-NLC 10 was produced using a cold high pressure homogenization technique (Chapter 2, Section 2.4.2.3). Briefly the Transcutol® HP based DDI nanosuspension was added to Precirol® ATO 5 and the mixture was heated to 85°C. The molten lipid phase was immediately poured into liquid nitrogen to allow for the uniform distribution of DDI within the lipid phase and increase the brittleness of the lipid. Following solidification, the dried lipid materials were ground using a mortar and pestle to produce a fine powder, which was then passed through a 200 µm sieve to produce lipid microparticles of 200 µm and less in size [27, 29, 161]. The powdery lipid microparticles were then dispersed in a cold (5°C) solution containing Tween® 80, Solutol® HS 15 and Lutrol® F68 using a Model T25 Ultra-Turrax T25 homogenizer (Janke & Kunkel GmbH and Co KG, Staufen, Germany) at a speed of 8 000 rpm for one (1) min to produce a coarse pre-emulsion. The pre-emulsion was then homogenized using the high pressure homogenizer (APV Deutschland GmbH, Unna, Germany) at 5°C for three cycles at relatively low pressures of 100, 250, 500 and 1000 bar for the similar reasons described in Section 5.2.2.1.2.1. The pre-emulsion was then homogenized at 1500 bar for five (5) cycles to produce batch DDI-NLC 10. The novel production process of DDI-NLC involves a combination of hot high pressure homogenization for the production of lipid-based DDI nanosuspensions and cold high pressure homogenization for the production of batch DDI-NLC 10.

5.2.2.2 Characterization of SLN and NLC

5.2.2.2.1 Particle size analysis

5.2.2.2.1.1 Photon correlation spectroscopy

Photon correlation spectroscopy (PCS) was used to measure the mean PS (z-ave) and PI of SLN and NLC formulations using a Nano-ZS Zetasizer (Malvern Instruments Ltd, Worcestershire, United Kingdom). Approximately 30 µl of each sample was diluted with a 10 ml of double distilled water in order to obtain a suitable scattering intensity, prior to PCS analysis, and the diluted sample was then placed in a 10 mm diameter cell. Ten (10) PCS measurements were performed on each sample at an angle of 90° at 25°C. PS analysis was

performed using Mie theory with the real and imaginary refractive indices set at 1.456 and 0.01, respectively.

5.2.2.2.1.2 Laser diffractometry

Laser diffractometry (LD) was used to establish whether microparticles were present in the NLC formulations using a Model 2000 Mastersizer laser diffractometer (Malvern Instruments Ltd, Worcestershire, United Kingdom) by applying polarization intensity differential scattering (PIDS). The LD data were evaluated in terms of volume distribution diameters of d50%, d90%, d95%, and d99% and by calculating span values. The span value is a statistical parameter that may be used to evaluate the PSD of LD data and was calculated using Equation 5.1.

$$\text{Span value} = \frac{d90\% - d10\%}{d50\%} \qquad \text{Equation 5.1}$$

5.2.2.2.2 Zeta potential (ZP)

The ZP is a measure of the electrophoretic mobility of particles in disperse systems and was evaluated using a Nano-ZS Zetasizer (Malvern Instruments Ltd, Worcestershire, United Kingdom) after switching the equipment from the PCS to the laser Doppler anemometry (LDA) mode. All measurements were performed following dilution of each sample in double distilled water with the conductivity adjusted to 50 µS/cm using 0.9% w/v sodium chloride solution. Approximately 30 µl of each sample was diluted with 10 ml of double distilled water and then placed in a cell specifically designed to conduct ZP measurements. Three (3) LDA measurements were performed on each sample at applied field strength of 20 V/cm. The Helmholtz–Smoluchowsky equation (Equation 2.3, Section 2.5.3, Chapter 2) was used *in situ* to calculate the ZP value for each sample automatically.

5.2.2.2.4 Imaging analysis

5.2.2.2.4.1 Light microscopy

The reduction in PS of DDI when producing Transcutol® HP based DDI nanosuspensions (Section 5.2.2.1.2.1) was monitored using a Leitz Orthoplan light Microscope (Leitz Orthoplan, Wetzlar, Germany) at magnifications of 400x and 630x. Micrographs were captured using a Model CMEX 3200 Euromex camera (Euromex, Arnhem, The Netherlands) that was coupled to the microscope. The light microscope was also used to visualize the NLC and to detect the presence of aggregates of the nanoparticles that may have formed during formulation development and optimization studies.

5.2.2.2.4.2 Scanning electron microscopy (SEM)

The shape and surface morphology of the nanoparticles in aqueous dispersions were determined using a Model TS 5136LM Vega® Tescan scanning electron microscope (Tescan USA, Cranberry Township PA, USA). A drop of each formulation was deposited on a graphite plate and left to dry at room temperature overnight. Following drying, the sample was coated with gold under vacuum for 20 minutes, after which sample was visualized using SEM at an accelerated voltage of 20 kV.

5.2.2.2.4.3 Transmission electron microscopy (TEM)

The shape and surface morphology of aqueous dispersions of SLN and NLC were investigated using a Model JEOL-1210 transmission electron microscope (JEOL 1210, JEOL Inc., Boston, MA). Briefly, each sample was placed on a copper grid with a carbon film and following the removal of excess liquid using a hydrophilic filter membrane, the sample was allowed to dry at 25°C for 30 seconds. The sample was then stained with 1% w/w phosphotungstic acid and the stain was allowed to dry at 25°C for an additional 30 seconds, after which the sample was viewed under the TEM to obtain two-dimensional images of the nanoparticles.

5.2.2.2.5 Crystallographic and polymorphic analysis

5.2.2.2.5.1 Differential scanning calorimetry (DSC)

The degree of crystallinity and polymorphism of the nanoparticles were investigated using a Model DSC 821^e DSC (Mettler-Toledo GmbH Analytical, Gießen, Germany). Aqueous samples of SLN and NLC weighing between 5–10 mg, corresponding to 1 to 2 mg of lipid phase in formulations were weighed directly and hermetically sealed into 40 µl pin-holed aluminium pans. The DSC curves were recorded by heating the sample from 25°C to 225°C and then cooling down from 225°C to 25°C at a heating and cooling rate of 10 K/min. An empty pin-holed aluminium pan sealed in a similar manner to the pans containing the samples for analysis was used for reference purposes. The DSC parameters, such as temperature onset, maximum peak and enthalpy were generated using STARE^e software (Mettler-Toledo GmbH Analytical, Gießen, Germany). The recrystallization indices (RI) of the formulations under investigation were calculated using Equation 2.4, Chapter 2, *vide infra.*

5.2.2.2.5.2 Wide angle X-ray scattering

In order to interpret DSC data completely, WAXS was used to assess the degree of crystallinity and polymorphism of bulk materials and the formulations that were produced. WAXS patterns were generated using a Model PW 1830 WAXS system (Philips Industrial & Electron-Acoustic Systems Division, Amedo, The Netherlands) equipped with a copper anode (Cu-Kα radiation, 40 kV, 25 mA λ = 0.15418 nm) coupled to a Model PW18120 Goniometer detector. All measurements were recorded using a step width of 0.04°, a count time of 60 sec, a 2 Θ scanning range and speed set between 0.6-40° and 0.02° per sec, respectively. The measurement of aqueous SLN and NLC dispersions were preceded by mixing the samples with locust bean gum powder to produce a paste. All samples used for WAXS analysis were the same as those used in DSC analysis for ease of data comparison and interpretation. Data generated using WAXS analysis were transformed from scattering angle to the distance of spacing within the SLN or NLC lipid matrix using Equation 4.1 (Chapter 4, Section 4.2.2.3.2).

5.2.2.2.6 Drug loading capacity (LC) and encapsulation efficiency (EE)

The drug LC and EE of DDI were determined by ultrafiltration using Centrisart filter tubes (Sartorius AG, Goettingen, Germany) that consist of a filter membrane with a molecular weight cut-off of 300 KDa at the base of the sample recovery chamber. A one (1) millilitre aliquot of undiluted sample of DDI-loaded NLC was placed in the outer chamber and the sample recovery chamber was fitted to the top of the sample. The unit was closed and centrifuged at 17000 rpm for 30 minutes using a Model 22 R Biofuge centrifuge (Heraeus Sepatech GmbH, Osterode/Harz, Germany). The principle behind this process is that DDI containing NLC are separated from an aqueous phase and remain in the outer chamber and the aqueous phase is filtered into the sample recovery chamber through the membrane. The amount of DDI in the aqueous phase was estimated using a RP-HPLC that was developed and validated as described in Chapter 3. The LC and EE of the nanoparticles were calculated using Equations 2.5 and 2.6, respectively (Chapter 2, *vide infra*).

5.3 RESULTS AND DISCUSSION

5.3.1 Selection of surfactants

Three non-ionic surfactants, *viz.*, Tween® 80, Solutol® HS 15 and Lutrol® F60 were investigated to establish their potential to stabilize NLC formulations. However, the need to stabilize DDI-NLC with surface active agents (SAA) that have been shown to have the potential to deliver nanoparticles to the brain e.g. Tween® 80 (Chapter 6, Section 6.1) also play a key role in the selection of these SAA. Nevertheless, the primary criterion for the selection of a suitable SAA from among the three surfactants for use in the formulation and manufacture of DDI-free and DDI-loaded NLC was based on the ability of the SAA to produce aqueous NLC formulations that were physically stable on the day of manufacture and for the following seven (7) days when stored at 22°C. Solid lipid nanocarriers can be produced using non-ionic surfactants at concentrations between 2-10% w/w and the higher the concentration of surfactant in the formulation, the smaller the size of the particles and the narrower the PSD [247]. This is due to the fact that increasing the concentration of a SAA decreases the surface or interfacial tension, thereby facilitating the separation of particles during homogenization [29].

DDI-free and loaded NLC were formulated using a surfactant concentration of 6 % w/w as a high concentration of lipid (20% w/w) was used to manufacture these formulations. The limited solubility of DDI in lipids necessitated the use of a relatively high concentration of the lipid phase in order to incorporate as much DDI as possible in the solid lipid nanocarriers. The physical stability of the NLC formulations was evaluated by determining the PS, PI and span value and formulations were only considered physically stable if the PS values were in the nanorange with low PI e.g. less than 0.2. The PS determined using PCS and LD as well as PI, span values of NLC containing Tween® 80 (DDI-NLC 1), Lutrol® F68 (DDI-NLC 2) and Solutol® HS 15 (DDI-NLC 3) were measured on the day (day 0) of manufacture and after seven days of storage at 25°C and the data are summarized in Table 5.4. The same data were also generated for an NLC formulation that was manufactured to contain a combination of all three SAA (batch DDI-NLC 4) and are also summarized in Table 5.4.

Table 5.4. PCS and LD parameters of NLC formulations manufactured using different SAA

FORMULATION	DDI-NLC 01		DDI-NLC 02	
Parameter	**Day 0**	**Day 7**	**Day 0**	**Day 7**
PCS (nm)	482 ± 53	-	381 ± 26	-
PI	0.281 ± 0.0898	-	0.117 ± 0.0790	-
d50% (µm)	0.938	5.30	0.635	31.2
d90% (µm)	4.353	44.5	2.612	155
d95% (µm)	5.752	60.5	4.659	262
d99% (µm)	8.675	94.9	38.82	385
Span value	4.368	8.071	3.748	4.758
FORMULATION	**DDI-NLC 03**		**DDI-NLC 04**	
Parameter	**Day 0**	**Day 7**	**Day 0**	**Day 7**
PCS (nm)	202 ± 3	203 ± 3	208 ± 4	207 ± 4
PI	0.163 ± .0475	0.170 ± 0.044	0.120 ± 0.044	0.130 ± 0.043
d50% (µm)	0.142	0.142	0.144	0.147
d90% (µm)	0.236	0.248	0.235	0.232
d95% (µm)	0.270	0.289	0.257	0.259
d99% (µm)	0.347	0.427	0.306	0.305
Span value	1.084	1.190	0.9600	0.9660

All NLC formulations were aqueous dispersions with a milky appearance on the day of production. The PCS data measured on the day of production reveal that the mean PS of all formulations were in the nanorange, albeit the PI was higher for batches DDI-NLC 01 (Tween® 80) and DDI-NLC 02 (Lutrol® F68) than that observed for batches DDI-NLC 03 (Solutol® HS 15) and DDI-NLC 04 that contained all three surfactants. The relatively high PI is indicative of a large PS distribution and indicates the possible presence of microparticles in batches DDI-NLC 01 and DDI-NLC 02 and which could not be detected by PCS. LD data confirmed the presence of microparticles in these formulations. No microparticles were detected in batches DDI-NLC 03 and DDI-NLC 04. Following storage at 25°C for one week,

batches DDI-NLC 01 and DDI-NLC 02 were semi-solids and all LD data revealed the presence of microparticles. Based on the fact that the d50% of batches DDI-NLC 01 and DDI-NLC 02 were > 5 μm the PS of these formulations was not measured using PCS since only particles up to 3 μm can be measured. These data suggest that batches DDI-NLC 01 and DDI-NLC 02 were physically unstable.

PCS and LD analysis indicate that the PS and PSD of batches DDI-NLC 03 and DDI-NLC 04 did not change significantly following storage at 25°C for one week, thereby suggesting that the formulations were physically stable for at least a week. Consequently either Solutol® HS 15 alone (batch DDI-NLC 03) or a combination of Solutol® HS 15, Tween® 80 and Lutrol® F68 (batch DDI-NLC 04) may be used as the surfactant system for the formulation and manufacture of NLC containing DDI. However, as one of the objectives of this research was to investigate the potential for DDI-loaded NLC to deliver DDI to the brain, a surfactant system in which all three SAA were present was used. Lutrol® F68- and Tween® 80-stabilized nanoparticles have been shown to prolong the circulation time of nanoparticles *in vivo* and to deliver nanocarriers to the brain, respectively [248]. Consequently, Lutrol® F68 and Tween® 80 in addition to Solutol® SH 15 were used to form an emulgent system in the formulation and optimization of DDI-loaded NLC formulations.

5.3.2 Selection of production parameters

The use of a high pressure homogenization technique to produce solid lipid nanocarriers requires that an appropriate pressure and number of homogenization cycles be used to produce nanoparticles in the desirable PS range [29]. This is because the diminution of lipid droplets in a pre-emulsion leading to the formation of nanoparticles necessitates a sufficiently high energy input into the system [249]. Aqueous DDI-free and DDI-NLC dispersions were produced at a relatively high pressure of 800 bars due to the high concentration (20% w/w) of lipid used. The number of homogenization cycles was varied, and Figure 5.1 depicts the effect of increasing the number of homogenization cycles on the PS and PI of DDI-free and batch DDI- NLC 04. These data reveal that increasing the number of homogenization cycles during the production process leads to a decrease in the mean PS and narrowing of the polydispersity indices for the formulations tested.

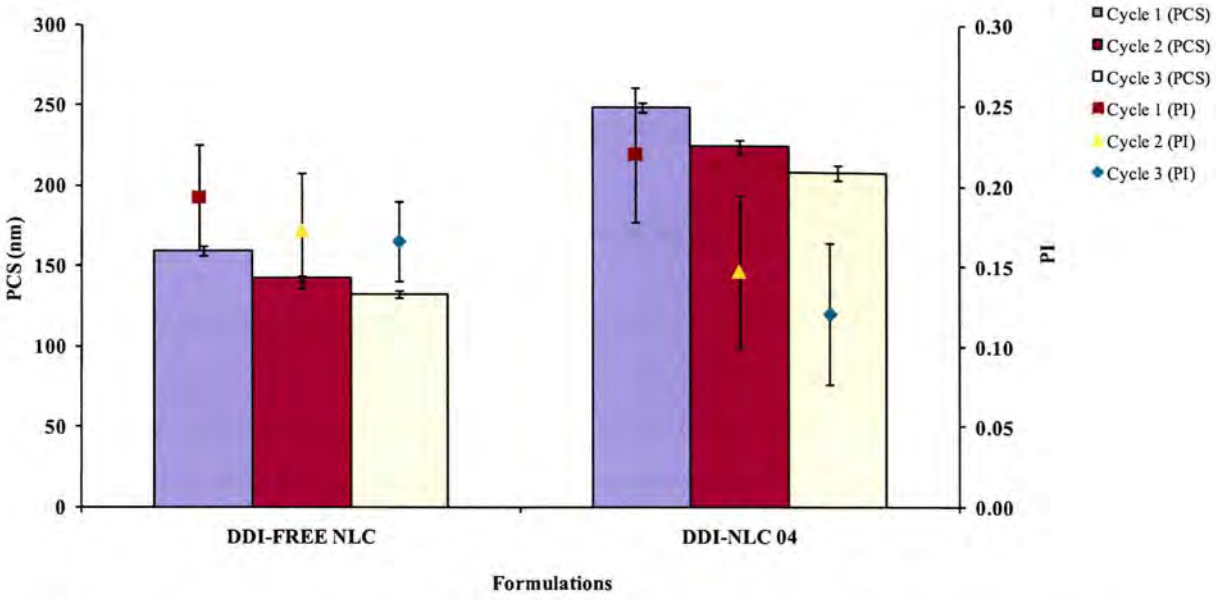

Figure 5.1. Effect of homogenization cycles on the mean PS and PI of DDI-free and batch DDI-NLC 04.

The PS of these formulations as a function of homogenization cycle was also determined using LD and these data are shown in Figure 5.2.

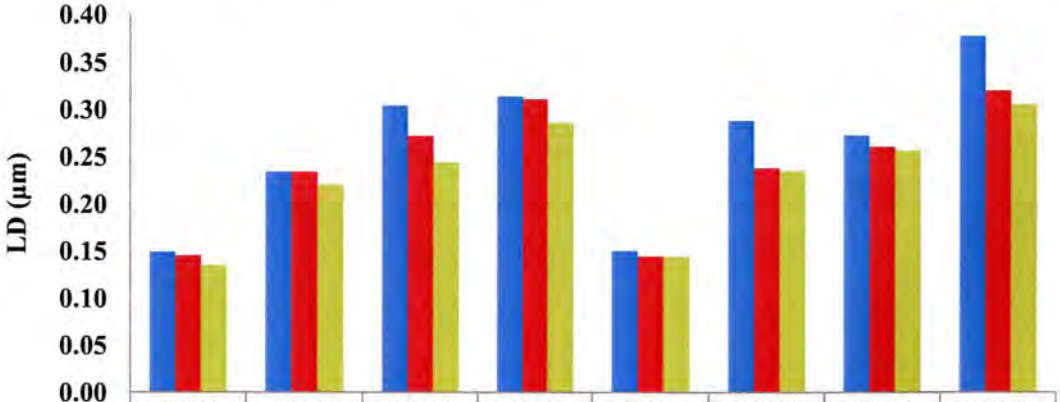

	d50%	d90%	d95%	d99%	d50%	d90%	d95%	d99%
	DDI-FREE NLC				DDI-NLC 04			
Cycle 1	0.149	0.234	0.304	0.314	0.15	0.288	0.273	0.378
Cycle 2	0.145	0.234	0.272	0.311	0.144	0.238	0.261	0.321
Cycle 3	0.135	0.22	0.244	0.286	0.144	0.235	0.257	0.306

Figure 5.2. Effect of number of homogenization cycles on the d50%, d90%, d95% and d99% of DDI-free and batch DDI-NLC 04.

LD data also show a decline in the d50%, d90%, d95% and d99% parameters as the number of homogenization cycles was increased from one to three cycles. It is therefore clear that the

application of 3 homogenization cycles at 800 bar was sufficient to allow for the generation of enough energy to reduce the lipid droplets in the pre-emulsion to nanoparticles. Therefore, all NLC formulations were produced using a hot high pressure homogenization procedure using a pressure of 800 bar and three (3) homogenization cycles, unless otherwise stated.

5.3.3 Influence of DDI loading on NLC formulations

Aqueous DDI-NLC formulations were manufactured using increasing amounts of DDI (Table 5.2) in order to investigate the influence of DDI on the physicochemical properties of the nanoparticles that were produced. The PS and PSD (PI and span value), ZP, and EE for DDI-free and NLC formulations were measured following storage of the formulations for one (1) day and two (2) months at 25°C, and data generated from these studies are summarized in Table 5.5.

Table 5.5. PS (PCS and LD), PSD (PI and span value), ZP and EE data for DDI-free and DDI-loaded NLC following storage at 25°C for one day and two months

BATCH	DDI-free NLC		DDI-NLC 05		DDI-NLC 06	
Parameter	One day	Two months	One day	Two months	One day	Two months
PCS (nm)	132 ± 2	136 ± 7	208 ± 4	197 ± 3	212 ± 5	202 ± 6
PI	0.165 ± 0.025	0.131 ± 0.016	0.120 ± 0.044	0.113 ± 0.057	0.137 ± 0.049	0.113 ± 0.046
d50% (μm)	0.135	0.139	0.150	0.150	0.142	0.149
d90% (μm)	0.234	0.226	0.235	0.234	0.248	0.225
d95% (μm)	0.272	0.254	0.261	0.258	0.287	0.249
d99% (μm)	0.311	0.299	0.306	0.304	0.380	0.292
Span value	1.19	0.825	1.08	0.967	1.25	0.872
ZP (mV)	-12.4 ± 0.9	-12.5 ± 0.4	-17.0 ± 0.9	-15.0 ± 0.1	-18.4 ± 1.0	-17.6 ± 2.1
EE (%)	-	-	78.34 ± 2.44	76.20 ± 1.44	39.37 ± 1.30	38.17 ± 0.90
FORMULATION	**DDI-NLC 07**		**DDI-NLC 08**		**DDI-NLC 09**	
Parameter	**One day**	**Two months**	**One day**	**Two months**	**One day**	**Two months**
PCS (nm)	144 ± 3	143 ± 2	123 ± 1	131 ± 4	148 ± 3	203 ± 7
PI	0.158 ± 0.042	0.0969 ± 0.035	0.141 ± 0.038	0.162 ± 0.048	0.195 ± 0.037	0.321 ± 0.0586
d50% (μm)	0.139	0.139	0.137	0.137	0.149	0.141
d90% (μm)	0.206	0.204	0.202	0.203	0.232	0.230
d95% (μm)	0.228	0.225	0.223	0.223	0.283	0.253
d99% (μm)	0.269	0.262	0.262	0.263	0.308	0.304
Span value	0.840	0.791	0.870	0.825	1.00	1.04
ZP (mV)	-16.6 ± 2.3	-17.6 ± 2.1	-11.4 ± 0.40	-12.2 ± 1.2	-13.3 ± 0.90	-11.7 ± 0.36
EE (%)	37.04 ± 2.56	35.12 ± 1.46	36.52 ± 1.55	34.20 ± 0.55	34.09 ± 2.41	33.02 ± 1.53

5.3.3.1 Particle size and size distribution

The measurement of PS and PSD of NLC dispersions is essential to ensure the production of a stable product of suitable quality. One day following production, the mean PS of DDI-free and loaded NLC was between 123 and 208 nm with a low PI. It is also clear that increasing the amount of DDI into NLC formulations did not have any influence on the PS and PI of the formulations. These findings are in agreement with data that showed loading concentrations of trans retinoic acid had no influence on the PS of solid lipid nanoparticles [250]. The LD data for all formulations are also summarised in Table 5.5 and it is clear that the d99% values are below 350 nm indicating that microparticles are not present in these NLC dispersions. Once again, an increase in the amount of DDI added to the formulation had no effect on the LD data. In addition, the span values for all formulations are relatively low, suggesting a narrow PSD and supporting the PI data that were obtained using PCS. It is also clear that PCS and LD data show that the sizes of the particles in all the formulations remained within the nanometre range following storage for two months at 25°C. Furthermore, the PI and span values remained low during the two month storage periods, indicating that there was little or no aggregation or coalescence of the particles during the storage period. Therefore, these results reveal that all NLC formulations developed in these studies were physically stable in terms of PS and PSD for at least two months.

5.3.3.2 Zeta potential (ZP)

The ZP values for DDI-free and DDI-loaded NLC formulations manufactured with increasing amounts of DDI were generated using water as the dispersion medium and these data are also summarized in Table 5.5. The conductivity of the dispersion medium was adjusted to a standard value of 50 μS/cm in order to avoid any artifacts in the measurement of ZP values as a consequence of day-to-day variability in the conductivity of the water. All formulations produced negative ZP values, which are more than likely a consequence of the functional groups of the surfactants used. Although all three surfactants used in these studies were non-ionic, it is possible that some of the functional groups in one or more of these surfactants became negative when dissolved in water. It is also clear that the ZP values for all formulations were not as negative as those recommended for NLC formulations (ZP values of ≤ -30) to be considered stable and this may be due to a shift in the shear plane of the NLC. However, it is important to note that this rule applies only to colloidal systems that are

stabilized by electrostatic interactions alone. These formulations were developed using a combination of three non-ionic surfactants and as these impart stability to NLC dispersions by steric hindrance, the stability of formulations may be inferred.

It is also clear that the ZP values of all formulations remained constant following storage at 25°C for two months, suggesting that the surface properties of the particles in all formulations were not altered during the two month storage period. The ZP value of DDI-free NLC is higher than those that were obtained for NLC formulations containing relatively small amounts of DDI *viz.*, batches DDI-NLC 05 (6 mg), DDI-NLC 06 (8 mg) and DDI-NLC 07 (20 mg), but are similar to those containing larger amounts of DDI *viz.*, batches DDI-NLC 08 (50 mg) and DDI-NLC 09 (100 mg). DDI is an amphoteric compound that ionizes in water and can have negative and/or a positive charge. Therefore, it is possible that when DDI is used in relatively small quantities, the negative charge predominates and therefore this has an additive effect on the overall charge on the surface of the nanoparticles. However, as additional DDI is added to the formulation, more positively charged DDI become available for interaction with the negative charge of the surfactants on the surface of the particles. Consequently, there is a decrease in the overall charge on the surface of the nanoparticles. Once again, despite the drop in ZP for batches DDI-NLC 08 and DDI-NLC 09, the stability of these formulations can be inferred due to stabilization by steric hindrance provided by the combination of surfactants.

5.3.3.3 Encapsulation efficiency

The drug EE is an important parameter that can influence drug release characteristics and must therefore form an integral part of the formulation development process [112]. It is easier to encapsulate hydrophobic molecules in NLC with high efficiency than hydrophilic drugs such as DDI due to the tendency of hydrophilic molecules to partition out of the lipid phase into the water phase during homogenization. Due to limited solubility of DDI in lipids a small amount of DDI was added incrementally in order to determine the ability of the NLC to entrap DDI. These amounts were considered sufficient for the intended purpose of these studies.

The EE data for DDI determined per unit weight of each NLC formulation are summarized in Table 5.5 and reveal that EE of DDI decreases as the amount of DDI added was increased

from 6 mg for batch DDI-NLC 05 to 100 mg for batch DDI-NLC 09. The data also show that the amount of DDI entrapped in the nanoparticles for each formulation remained constant following storage of the formulations at 25°C for two months, suggesting that despite the relatively low entrapment efficiency of DDI, the formulations were at least chemically stable during the storage period. In spite of low EE values, the NLC were considered suitable for investigation to deliver DDI to the CNS. Nevertheless attempts were made to enhance the EE of DDI-NLC after loading a relatively high amount of DDI to the lipid phase and data obtained in these studies are described in Section 5.3.5.

5.3.3.4 Shape and surface morphology

5.3.3.4.1 Scanning electron microscopy

An attempt was made to visualize the shape and surface morphology nanoparticles in formulations that were developed. However, during the visualization process it became clear that it was not possible to visualize nanoparticles using SEM as the microscope used in these studies was not sensitive enough to detect nanoparticles and only particles > 5 µm could be visualized. Although it was not possible to visualize the particles in all formulations, some microparticles were observed in batches DDI-NLC 06 and DDI-NLC 09 and these are depicted in the SEM micrographs shown in Figure 5.3.

Figure 5.3. SEM micrographs depicting shape and surface morphology of microparticles in batches DDI-NLC 06 and DDI-NLC 09.

The presence of microparticles in these formulations may be due to agglomeration of individual particles during the preparation of the sample prior to SEM. It is clear that the shape and surface of these microparticles is anisometric and smooth and therefore the shape and surface of the nanoparticles in the same formulation may be anisometric by inference. However, in order to determine the actual shape and surface morphology of the nanoparticles TEM was used to allow for the visualization of nanoparticles in NLC formulations and is described in Section 5.3.3.4.2, *vide infra*.

5.3.3.4.2 Transmission electron microscopy

The TEM images obtained for NLC formulations that were examined are depicted in Figure 5.4.

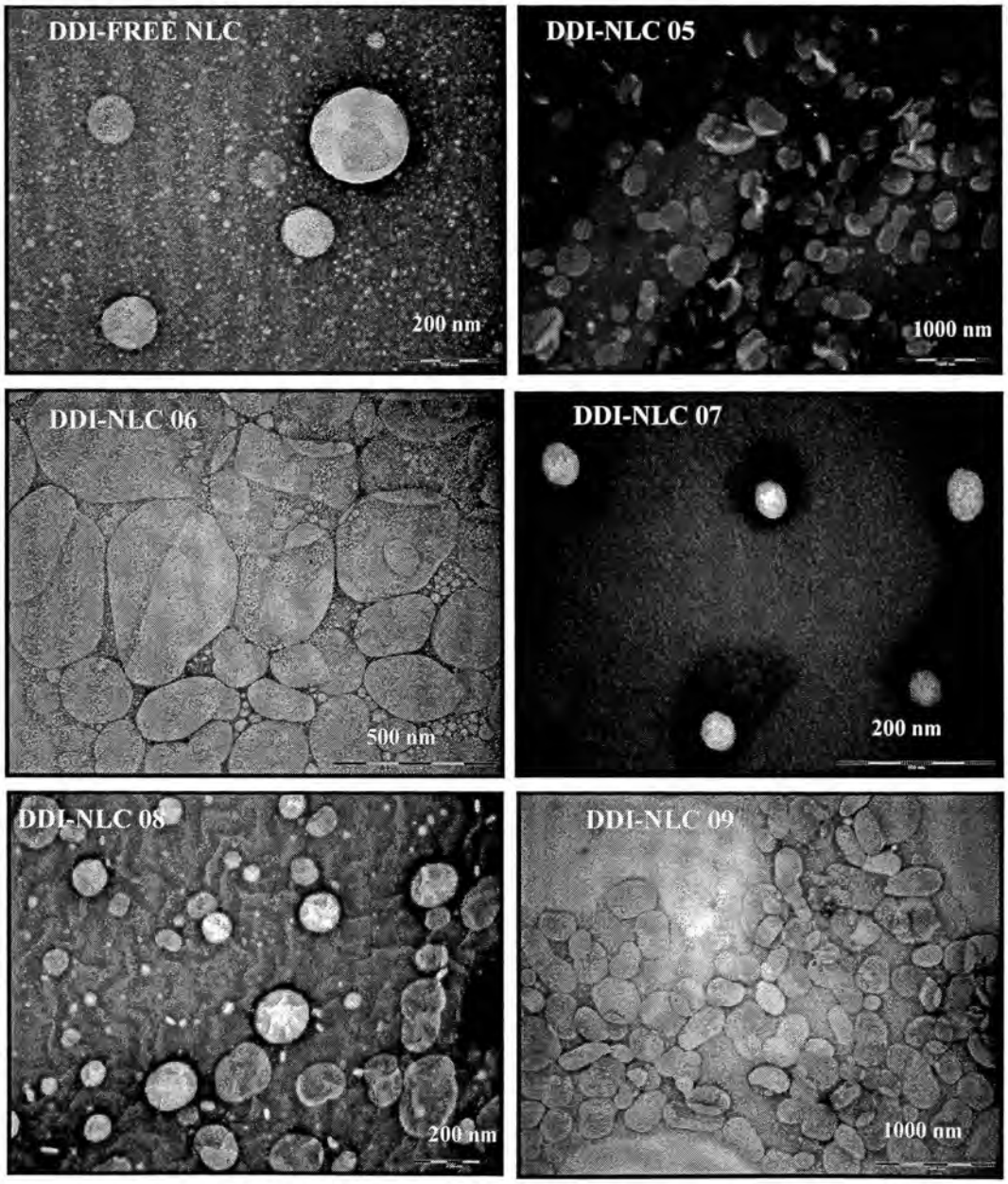

Figure 5.4. TEM micrographs depicting the shape and surface morphology of particles of NLC formulations

The nanoparticles in all formulations except in batches DDI-NLC 06 and DDI-NLC 09 are mainly discrete entities. All particles, irrespective of the formulation investigated are in the nanometre range, however the nanoparticles in batches DDI-NLC 06 and DDI-NLC 09 seemed to have formed agglomerates, which may be due to insufficient drying time of the sample during sample preparation prior to TEM analysis. These agglomerates are more than likely those that were assumed to be microparticles when undertaking SEM analysis. The NLC in DDI-free and batch DDI-NLC 07 were spherical, however, all the other formulations contain a mixture of spherical and non-spherical (anisometric) nanoparticles. The shape of solid lipid nanocarriers is dependent on the purity of the lipid used [204] and particles prepared from highly pure lipids are usually more cuboid in nature [197] whereas those obtained using chemically polydispersed lipids are typically spherical [147]. The lipid matrix used consisted of a mixture of Precirol® ATO 5 and Transcutol® HP, which suggests that the lipid matrix is chemically polydispersed. Consequently, it was expected that only spherical particles would be present in all batches and not only in DDI-free and batch DDI-NLC 07.

The polymorphic nature of the lipid matrices that are used to form solid lipid nanocarriers may determine the shape of the particles, such that particles that exist in the stable β-modification assume anisometric shapes whereas those that exist in the metastable α-polymorphic forms are usually spherical in nature [136, 251]. The shapes of solid lipid nanocarriers established using TEM have been spherical [166] or non-spherical [252-254]. Using TEM, it was found that only DDI-free and batch DDI-NLC 07 produced spherical particles indicating that the nanoparticles in these formulations exist in an α-polymorphic form. However the α-polymorphic modification eventually transforms to the β-polymorphic form on prolonged storage or over time and consequently assumes an anisometric shape. All the other formulations were comprised of spherical and non-spherical particles which indicate that the nanoparticles in these formulations co-exist as the α- and β-polymorphic forms. The polymorphic nature and degree of crystallinity of particles in all formulations that were developed were confirmed using DSC and WAXS (Section 5.3.3.5 *vide infra*).

5.3.3.5 Polymorphism and crystallinity

5.3.3.5.1 DSC characterization

The DSC parameters of aqueous NLC that were measured following storage at 25°C for a period of one day and two months are summarized in Table 5.6. Regardless of the storage period, the onset temperatures, peak maxima (MP) and the melting enthalpies for the NLC formulations were all lower than that of the bulk lipid material, Precirol® ATO 5, which has an onset, MP and calculated enthalpy of 52.18°C, 55.06°C and 122.04, respectively (Section 4.3.3.1.1, Chapter 5, *vide infra*). These parameters remained constant irrespective of the amount of DDI that was added to a formulation again suggesting the low EE for DDI. In addition, all formulations had a melting endotherm, which is indicative that the particles recrystallized and that there were no supercooled melts present in all formulations that were manufactured.

Table 5.6. DSC parameters for DDI-free and DDI-loaded NLC measured following storage at 25°C for one day and two months.

FORMULATION	DDI-FREE NLC		DDI-NLC 05		DDI-NLC 06	
Parameter	One day	Two months	One day	Two months	One day	Two months
Onset (°C)	48.24	48.56	51.43	50.90	50.95	50.87
MP (°C)	53.46	54.87	54.53	54.74	54.01	54.35
Enthalpy (J/g)	15.39	19.25	19.30	21.88	16.45	17.70
RI (%)	63.07	78.63	78.83	89.67	67.42	72.30
FORMULATION	DDI-FREE 07		DDI-NLC 08		DDI-NLC 09	
Parameter	One day	Two months	One day	Two months	One day	Two months
Onset (°C)	49.03	49.12	48.14	48.43	48.95	48.98
MP (°)	53.59	54.30	54.54	53.72	53.90	54.73
Enthalpy (j/g)	16.16	19.29	18.92	19.87	17.04	19.79
RI (%)	45.74	78.80	77.54	81.17	69.84	80.84

It has been established that irrespective of the composition of the lipid matrix used to manufacture solid lipid nanocarriers and/or the type of surfactants used to ensure thermodynamic stability of the system, a major factor affecting the thermal behaviour of solid lipid-based carriers is the PS of the particles [255]. In other words, the onset temperature, MP and melting enthalpy of triacylglycerol-based carriers are directly proportional to the size of the particles [255]. Consequently, the melting parameters of the nanoparticles in all formulations were lower than those of the bulk Precirol® ATO 5. With respect to storage conditions, there is a slight increase in the value of all melting parameters for all formulations when the measurements were derived from samples stored for two (2) months at 25°C

compared to those generated one day after production of the nanoparticles. This is possibly due to the fact that the lipid matrix had not recrystallized fully following storage for one day as confirmed by the relatively low recrystallization index (RI) values obtained for all formulations e.g. RI values less than 100% Therefore, following production and storage for one day, the nanoparticles are likely to exist in the metastable α-polymorphic modification. However, after storage of the formulations for two (2) months, the RI values of the particles increase relatively thereby suggesting that the particles may be reverting to the stable β-modification form the metastable α-polymorphic form. In addition, the melting peak of DDI was not detected in DSC thermograms of all formulations indicating that any DDI that was incorporated into the NLC may be molecularly dispersed in the matrix [204].

5.3.3.5.2 WAXS characterization

The WAXS diffraction patterns of NLC formulations generated following storage at 25°C for one day (A) and two months (B) are shown in Figure 5.5. All NLC formulations showed similar refraction patterns irrespective of the amount of DDI that was added to each formulation and the storage period. The diffraction patterns of all formulations display equidistant reflections (peaks 1 and 2) which are indicative of a periodic lamellar arrangement within the lipid structure and therefore the crystalline nature of the particles in the formulations [205]. The intensities of peaks 1 and 2 following storage of all formulations for two months at 25°C are generally similar to those obtained for the particles following storage under similar conditions for a day. The similarity in the intensity of peaks 1 and 2 for the formulations stored for one day and those stored for two months suggest that there was little difference in the degree of crystallinity of the particles following storage for two months. However, these observations contradict DSC data which reveal a slight increase in the RI of all formulations tested following storage for the same period and that was thought to be indicative of a slight increase in the degree of crystallinity of the particles. Nevertheless, DSC appears to be a more sensitive technique than WAXS and is able to detect small changes in the crystalline nature of the particles.

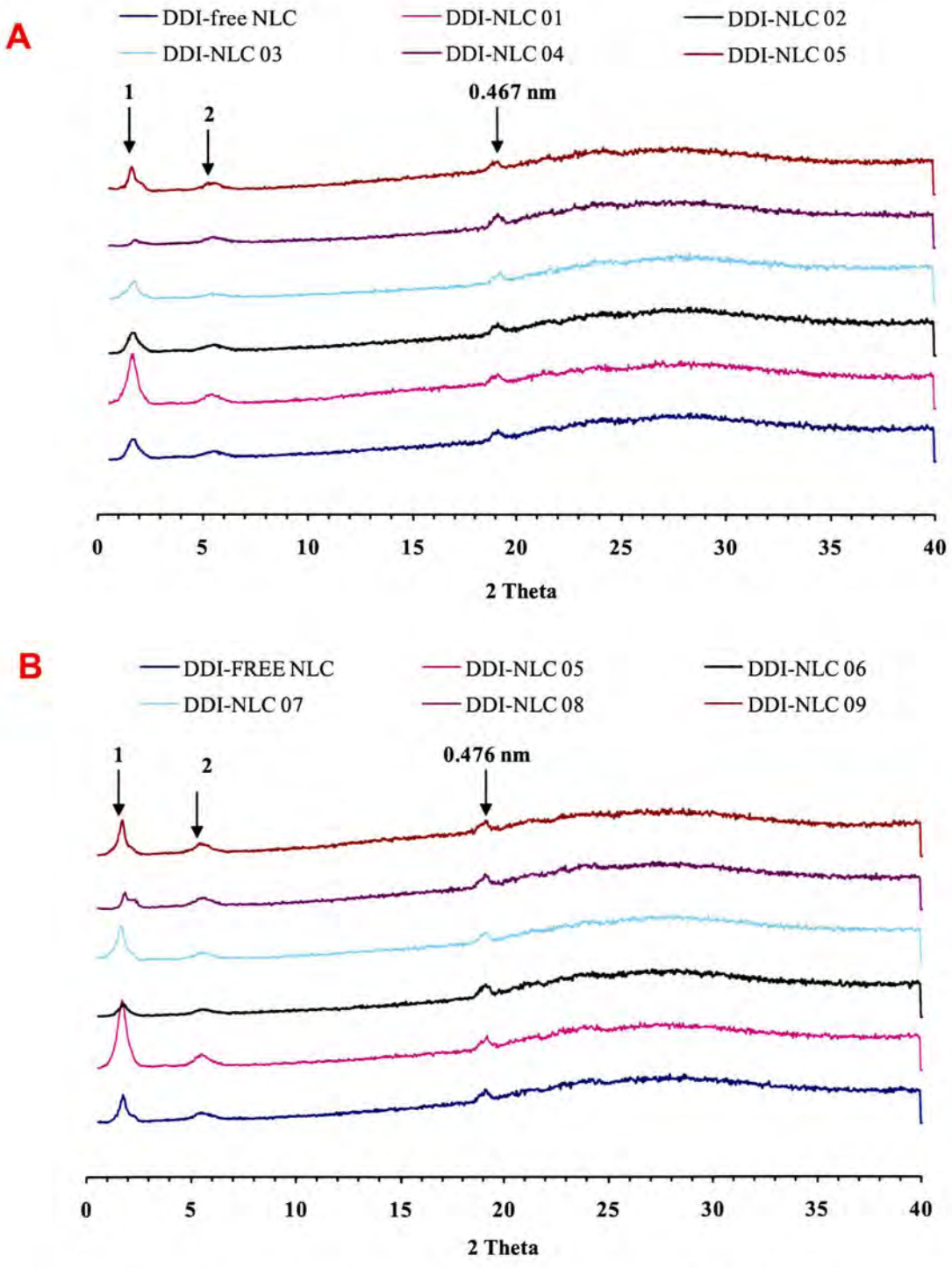

Figure 5.5. WAXS diffraction patterns of NLC formulation generated following storage at 25°C for one day (A) and two months (B).

A Bragg's distance of 0.467 nm for samples stored for 1 day and 0.476 for samples stored for two months under the same conditions, suggests that the particles existed in the β-

polymorphic modification one day after their production and remained similar in form for the two months storage period. However DSC data suggested that the particles existed in the α-modification one day after production and reverted to the stable β-modification over time. A peak was not detected in diffractograms of all formulations for DDI suggesting that any drug that was incorporated in the particles was molecularly dispersed in those matrices.

5.3.4 Enhancement of encapsulation efficiency of DDI

5.3.4.1 Size reduction of DDI in Transcutol® HP

A manufacturing process strategy aimed at improving the EE and LC of NLC for DDI was designed and implemented. A high concentration of DDI (20% w/w) was dispersed in Transcutol® HP and homogenized at high pressure (HPH) in an attempt to reduce the PS of DDI, which could improve the dissolution velocity and therefore the saturation solubility of the DDI in the liquid lipid. The reduction of PS of an API such as in the production of nanosuspensions containing hydrophobic molecules in water using HPH generally requires that the process is monitored by measuring the PS as a function of homogenization pressure or cycle number using PCS and/or LD. However, these analytical techniques require the use of water or liquids of low viscosity as a dispersion medium during analyses. Due to the hydrophilic nature of DDI and the viscous nature of the oil used in these studies, it was not feasible to monitor the size reduction of DDI during production. Rather, polarized light microscopy was used to monitor the process and establish the success or failure of the size reduction process. Samples were taken after applying different numbers of homogenization cycles and visualized under light microscope at magnifications of 400x and 630x and micrographs were recorded using a camera connected to the microscope. The resultant micrographs are shown in Figures 5.6 and 5.7

PARAMETER	MICROSCOPIC MAGNIFICATION	
	400x	630x
DDI powder in Transcutol® HP	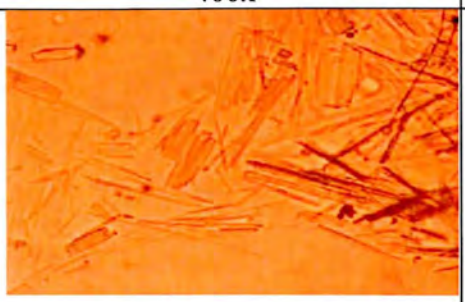	
Ultra-Turrax® 8000 rpm		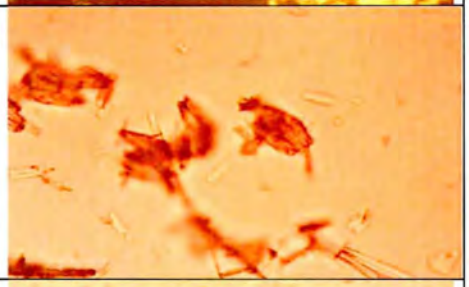
5 x 100 bar	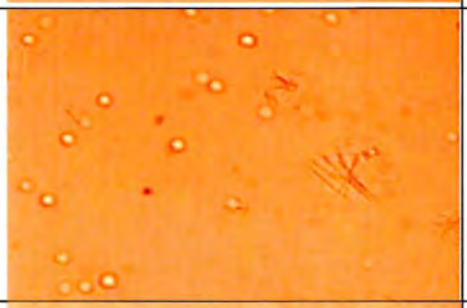	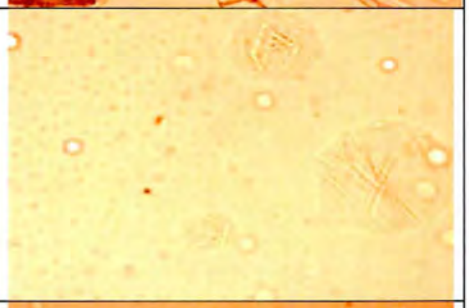
5 x 500 bar		
5 x 1000 bar	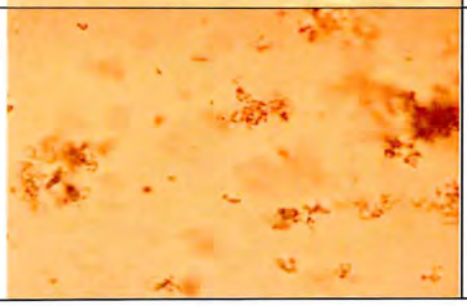	

Figure 5.6. Microscopic images depicting DDI prior to and after application of relatively low homogenization pressures

PARAMETER	MICROSCOPIC MAGNIFICATION	
	400x	630x
1 x 1500 bar	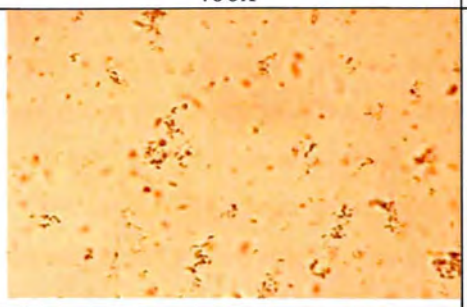	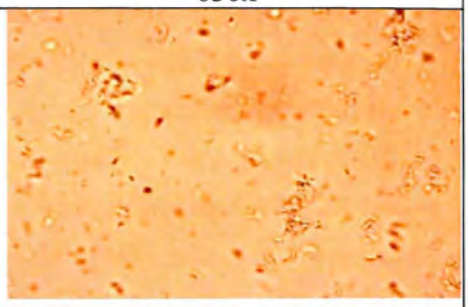
5 x 1500 bar	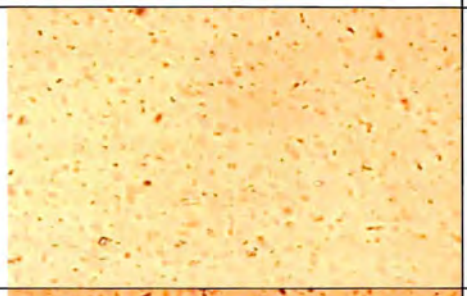	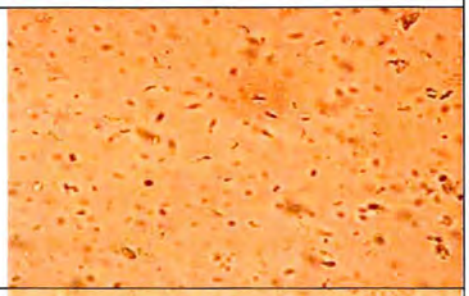
10 x 1500 bar	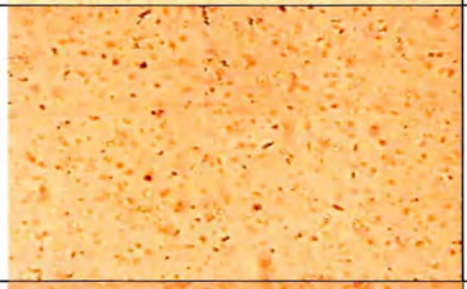	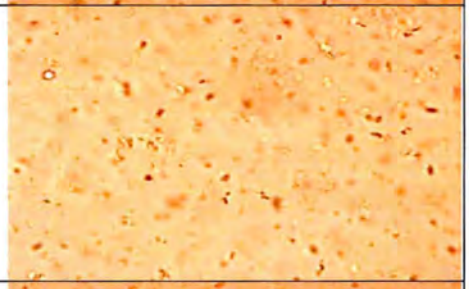
15 x 1500 bar	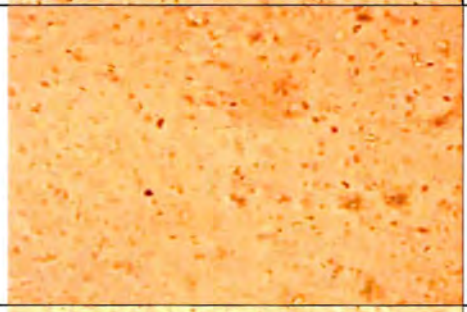	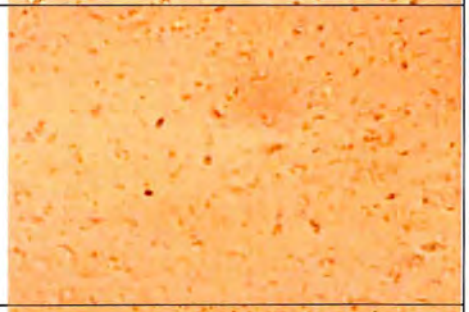
5 x 1000 bar	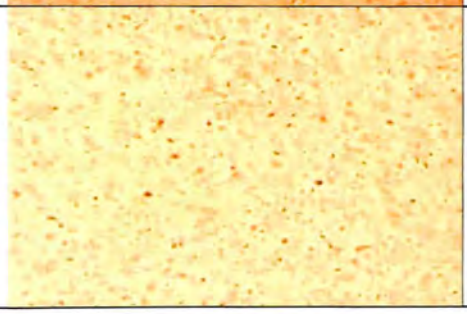	

Figure 5.7. Microscopic images depicting DDI prior to and after application of high homogenization pressures

DDI was dispersed in Transcutol® HP in the presence of Tween® 80 that was used to aid the dispersibility of DDI in the lipid during homogenization and to prevent aggregation of the particles. DDI crystals were clearly needle-shaped and were initially size reduced using an Ultra Turrax® homogenizer at a speed of 8000 rpm. Prior to homogenization at a relatively high pressure of 1500 bar the dispersion was homogenized at relatively low pressures of 100 bar, 500 bar and 1000 bar for five cycles at each pressure level, which resulted in further reduction in the size of the DDI microparticles. This gradual use of high pressure also ensures that large particles in the dispersion are modified in size and shape to prevent them from blocking the homogenization gap and/or causing erosion of the homogenization valve.

Following homogenization at these relatively low pressures, the dispersion was then homogenized at a relatively high pressure of 1500 bar for 20 cycles. It is clear that after homogenization at 1500 bar for one (1) cycle, the particles formed aggregates. However these aggregates were dispersed after the application of 5 and 10 homogenization cycles. The application of 15 cycles appeared to facilitate the agglomeration of particles, however, these agglomerates were again readily disrupted by application of 20 homogenization cycles. Following homogenization for 20 cycles, it was clear that the DDI crystals were sufficiently small and exhibited excellent dispersibility in the liquid lipid. The product obtained from these studies was used to manufacture batch DDI-NLC 10.

5.3.4.2 Production and characterization of DDI-NLC 10

Batch DDI-NLC 10 was produced using cold HPH in order to allow for the retention of DDI in the lipid phase and to minimize the partitioning of DDI from the lipid into the aqueous phase, which occurs when hot high HPH is used. The use of cold HPH was necessary because it was thought that size reduction of DDI would further increase the solubility of the drug in water, therefore partitioning may be more rapid when using hot HPH. However brutal cooling of the lipid phase after melting increases the brittleness of the lipid particles and may ensure that DDI is retained within the lipid matrix. Briefly, 25% w/w Transcutol® HP DDI suspension produced as described in Section 5.3.4.1 was added to the lipid phase to ensure that 5% w/w DDI was loaded to the lipid phase that was later dried using liquid nitrogen. An aliquot (20% w/w) of the resulting powdery material equivalent to 5% w/w DDI was dispersed in cold aqueous surfactant solution to produce batch DDI-NLC 10. The physiochemical properties of the nanoparticles of batch DDI-NLC 10 following storage of the

formulations for one day and two months at at 25°C are summarized in Table 5.7 and these data are compared to those obtained for DDI-free and batch DDI-NLC 09 (100 mg).

Table 5.7. PS (PCS and LD), PI, span value, ZP and EE of DDI-free and batches DDI-NLC 09 and DDI-NLC 10 determined following storage at 25°C for one day and two months.

BATCH	DDI-free NLC		DDI-NLC 09		DDI-NLC 10	
Parameter	**One day**	**Two months**	**One day**	**Two months**	**One day**	**Two months**
PCS (nm)	132 ± 2	136 ± 7	148 ± 3	203 ± 7	201 ± 8	591.1 ± 9
PI	0.165 ± 0.025	0.131 ± 0.016	0.195 ± 0.037	0.321 ± 0.0586	0.440 ± 0.064	0.397 ± 0.236
d50% (μm)	0.135	0.139	0.149	0.141	0.260	0.155
d90% (μm)	0.234	0.226	0.232	0.230	0.406	4.386
d95% (μm)	0.272	0.254	0.283	0.253	1.349	7.604
d99% (μm)	0.311	0.299	0.308	0.304	3.014	19.114
Span value	1.19	0.825	1.00	1.04	4.746	27.72
ZP (mV)	-12.4 ± 0.9	-12.5 ± 0.4	-13.3 ± 0.90	-11.7 ± 0.36	-26.4 ± 0.8	-29.4 ± 0.2
DEE (%)	-	-	34.09 ± 2.41	33.02 ± 1.53	51.58 ± 1.31	49.53 ± 0.19

5.3.4.2.1 Particle size and particle size distribution

The PCS data reveal that the PS of nanoparticles of batch DDI-NLC 10 were in nanometre range with a relatively large PSD following storage for one day and two (2) months at 25°C. In addition, the PI values of the formulation following storage are relatively large also suggesting a wide PSD exists. LD data show that d50% and d90% were in the nanometre range after storage for one day, however only d50% was in the nanometre range following storage for two months. All other LD parameters revealed the presence of microparticles after the two month period with span values showing a wide PSD, suggesting particle growth and therefore a degree of instability of the NLC-formulation in terms of PS following storage. NLC produced using a cold HPH are usually larger in size and show wider PSD compared to those produced using hot HPH techniques and therefore these formulations are inherently unstable [29, 161]. A primary objective of these studies was to establish whether the modified production process could enhance the EE of DDI and therefore instability in respect of PS was only a minor concern.

5.3.4.2.2 Zeta potential

The ZP value for formulation DDI-NLC 10 following storage for two (2) months was relatively higher than that obtained for the same formulation that had been stored for one (1) day. Furthermore, the increase in the negative charge on the surface of the particles did not seem to enhance the stability to the nanoparticles since particle growth was observed. It is

possible that the increased negative potential was unrelated to the presence of the surfactant but rather to an increase in amount of the amphoteric DDI on the surface of the particles.

5.3.4.2.3 Encapsulation efficiency (EE)

An increase in the amount of DDI added to NLC formulations led to a decrease in the EE of DDI. However the inclusion of DDI at a concentration of 5% w/w of the lipid phase and which is equivalent to 1% w/w in the final formulation was added to DDI-containing NLC. This is a large amount of DDI that could have resulted in an extremely low EE. However the EE determined for particles of batch DDI-NLC 10 one day after the production was higher than expected at 51.58 ± 1.31% and a LC equivalent to 3.39 ± 0.63% of the lipid phase was achieved. This suggests a significant improvement in the solubility of DDI in the lipid phase. However, following storage for two months at 25°C, the EE decreased to 49.53 ± 0.19% which was equivalent to a LC of 2.44 ± 0.02, which is indicative that DDI expulsion from the particles during storage has occurred and is evidence of chemical instability of the NLC. However, it is clear that there was an increase in the amount of DDI entrapped in NLC when they are manufactured using this production method.

5.3.4.2.4 Polymorphism and crystallinity

The polymorphism and degree of crystallinity of the particles of batch DDI-NLC 10 was also evaluated to establish whether or not the decrease in the EE of the particles for DDI was related to an increase in the crystallinity of the particles. DSC and WAXS analyses were used in combination to determine these parameters for batch DDI-NLC 10.

5.3.4.2.4.1 DSC characterization

The DSC parameters for formulation DDI-NLC 10 after day one and two months of storage at 25°C are summarized in Table 5.8 and these data are compared to those obtained for DDI-free and batch DDI-NLC 09 (100 mg DDI).

Table 5.8. DSC parameters for batch DDI-NLC 10 measured following storage at 25°C for one day and two months in comparison to data obtained for batches DDI-free NLC and DDI-NLC 09.

BATCH	DDI-free NLC		DDI-NLC 09		DDI-NLC 10	
Parameter	One day	Two months	One day	Two months	One day	Two months
Onset (°C)	48.24	48.56	48.95	48.98	49.21	52.1
MP (°C)	53.46	54.87	53.90	54.73	51.71	56.7
Enthalpy (J/g)	15.39	19.25	17.04	19.79	8.36	23.09
RI (%)	63.07	78.63	69.84	80.84	34.15	63.07

The DSC parameters for batch DDI-NLC 10 measured after one day of storage were lower in value than those obtained when the formulation was assessed after storage for two (2) months. The formulation showed a melting event on each occasion indicating the absence of supercooled melts in the formulation. In addition, the peak for DDI was not detected in the DSC thermograms, suggesting that any DDI that was incorporated in the nanoparticles was molecularly dispersed in the solid lipid matrix. The low RI value for the particles following storage for one day indicates a low degree of crystallinity in the solid lipid matrix and possibly substantial disorder in the crystalline structure therefore confirming the existence of particles in the less stable α-polymorphic form. The disorder in the crystalline structure may be due to the increased solubility of DDI in the lipid phase, leading to a larger amount of DDI being incorporated into the lipid particles. However, the degree of crystallinity of the particles increased rapidly following storage of the particles for two months at 25°C, which may be due to the conversion of the unstable α-modification to the more stable β-polymorphic form. However this conversion also leads to a decrease in the EE of DDI that occurs as a result of the forced expulsion of the DDI from the lipid matrix as the crystalline nature of the nanoparticles increases.

5.3.4.2.4.2 WAXS characterization

The WAXS diffraction patterns for batch DDI-NLC 10 after storage for one day and two (2) months of storage at 25°C are depicted in Figure 5.8.

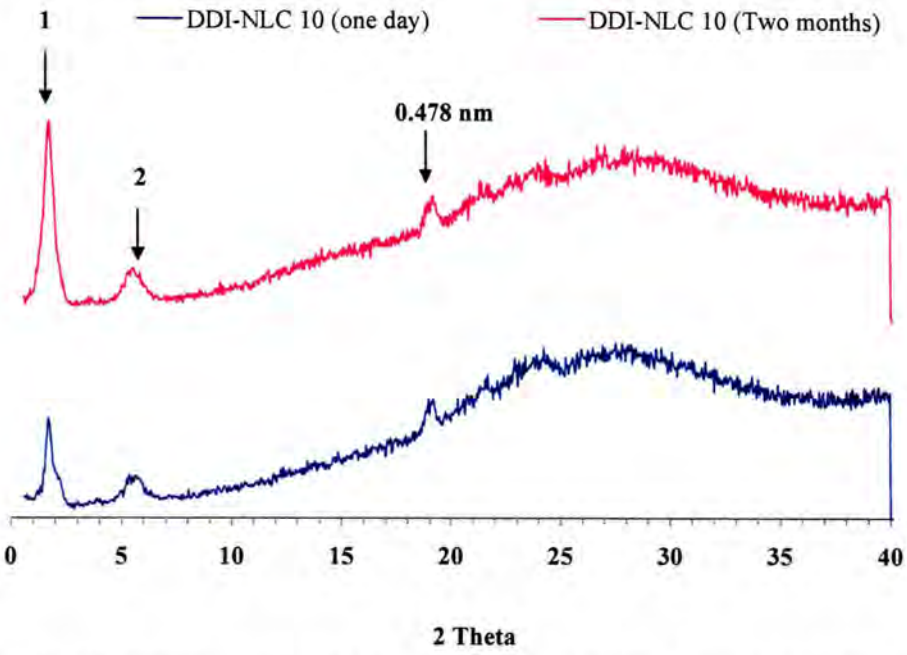

Figure 5.8. WAXS diffraction patterns for batch DDI-NLC 10 following storage of the formulations at 25°C for one day and two months.

The intensity of peaks 1 and 2 which are indicative of the degree of crystallinity in the lipid matrices of the nanoparticles was higher in the sample stored for one day than for the sample stored for two months suggesting that the degree of crystallinity in the formulation stored for two months was greater than that stored for one day. These data support the DSC results observed and consequently, it can be concluded that the decrease in EE of DDI was due to an increase in the degree of crystallinity following storage for two months. In addition, the Bragg's spacing value of 0.478 nm indicates that the particles were in the β-polymorphic modification after one day and following two months storage.

5.4 CONCLUSIONS

Due to the limited solubility of DDI in lipids, initial formulation development studies involved the addition of increasing amounts of DDI to formulations and establishing the impact of DDI on the physicochemical properties of NLC. Initially, it was necessary to determine a surfactant or a combination of surfactants that could be used to stabilize solid lipid nanocarriers in an aqueous environment. Although Solutol® HS was able to stabilize the particles when used alone, the use of a combination of surfactants consisting of Solutol® HS, Tween® 80 and Lutrol® F68 was preferred due to the role of Tween® 80 and Lutrol® F68 in targeted delivery of API to the brain. NLC formulations were manufactured using a hot high pressure homogenization by applying 800 bar for three cycles which were the optimal production parameters.

The addition of increasing amounts of DDI to NLC formulations had no effect on the physicochemical properties such as PS, PI, shape, surface morphology, polymorphic and crystalline nature of the NLC particles. However, the ZP of the particles appeared to be affected by the quantity of DDI used during manufacture. Lower quantities of DDI tend to increase the ZP of the particles whereas larger amounts of the drug seem to decrease the ZP. In addition, the EE of DDI in NLC was relatively low due to the poor solubility of DDI in the lipid medium and the tendency of the drug to partition from the lipid into the water phase. An attempt to increase the solubility of DDI in the lipid phase was necessary in order to achieve a high drug loading in the particles. Attempts to increase the entrapment efficiency of DDI by using self-emulsifying solid lipids were largely unsuccessful as the lipids formed semi-solid products prior to the application of high pressure homogenization. Consequently, a strategy was designed to increase the saturation solubility of DDI in liquid lipid, Transcutol® HP by attempting to increase the dissolution velocity of the drug in this medium. This was achieved by PS reduction of DDI using hot high pressure homogenization.

Microscopic images collected during homogenization in order to monitor the size reduction process revealed that DDI particles gradually decreased in size. The DDI-containing lipid nanosuspension formed in these studies was used to manufacture DDI-loaded NLC using cold high pressure homogenization. This technique proved successful in terms of increasing the amount of hydrophilic drug that was entrapped in the NLC. However the crystallinity of the particles altered during storage and caused some of the drug that had been incorporated to

be expelled from the nanoparticles. In addition, the particles in this formulation showed a tendency to grow in size leading to the formation of microparticles. Therefore, although this manufacturing approach facilitated the production of nanoparticles with higher amounts of encapsulated drug, it was decided to use more stable formulations that contain less drug to investigate the potential use of these particles to deliver DDI to the brain by use of differential protein adsorption. If protein adsorption studies proved to be successful *in vitro*, the particles could be administered intravenously, to establish their fate *in vivo*. Therefore, nanoparticles of a small size and narrow size distribution should be administered as larger particles may precipitate an embolism. The novel method of manufacture of NLC formulations developed in these studies has the potential to produce DDI-loaded NLC with adequate LC and EE for the oral administration of DDI to paediatric patients. However the long-term stability of NLC is likely to be a problem and consequently further investigations are needed to optimize the drug delivery system.

CHAPTER 6

THE USE OF DIFFERENTIAL PROTEIN ADSORPTION TO EVALUATE THE POTENTIAL FOR DELIVERY OF DDI-LOADED NLC TO THE BRAIN

6.1 BACKGROUND

The targeting of an API to a site of action and/or to a specific organ of interest is essential in order to minimize the occurrence of unwanted adverse reactions [256] and/or to enhance the therapeutic effect of an API [257]. This concept may be exploited in an attempt to alleviate conditions such as ADC [17, 18]. The inability of some currently used anti-retroviral compounds to cross the blood brain barrier (BBB) is a major barrier to the adequate management of HIV/AIDS [17]. The HIV actively invades the brain and the microglial cells in the brain serve as the most important reservoirs of the virus [24]. Therefore, targeted delivery of anti-HIV agents to the central nervous system (CNS) by circumventing or facilitating the transportation of these drugs across the BBB may be an ideal opportunity for scientists to address AIDS-related complications such as ADC.

Colloidal drug delivery systems (CDDS) such as polymeric nanoparticles [258, 259], liposomes [260, 261] and solid lipid nanoparticles [140, 258, 262, 263] have been used to target API delivery to the brain. However, the recognition and clearance of intravenously (IV) administered CDDS from the circulatory system by the mononuclear phagocytic system (MPS) are a major hurdle in the use of CDDS for brain and/or any other organ targeting [264, 265]. The action of the MPS on CDDS reduces the circulation time of the delivery system and consequently minimizes or inhibits potential interactions between drug carriers and target organs *via* suitable receptors [264, 265]. It has been acknowledged that the physicochemical properties of the CDDS such as size, charge, surface hydrophobicity and ZP determine the recognition and reuptake of CDDS by the MPS and/or organ distribution of the particles [185, 266, 267]. Consequently, research efforts have been directed towards the modification of the physicochemical properties of CDDS in an attempt to prevent or at least slow down the uptake process of these particles by the MPS [265, 268, 269]. The modification of the surfaces of liposomes [268-270] and polymeric nanoparticles [271] using polyethylene glycol (PEG) chains has been shown to extend the residence time of these carriers in the systemic

circulation. However it has also been shown that particles with similar physicochemical characteristics behave differently *in vivo* [185, 272, 273]. Consequently, knowledge of the physicochemical properties of the CDDS alone is not sufficient to explain the recognition and removal of particles from the systemic circulation by the MPS as well as the organ distribution of the particles *in vivo* [185, 272, 273].

It was later established that a vital factor that determines the fate and/or organ distribution of IV administered CDDS is the preferential adsorption of proteins onto the surface of the particles [274, 275]. In other words, the likelihood that a CDDS is either recognized and removed or remains unnoticed by the MPS in the systemic circulation depends on the nature of plasma proteins that are adsorbed onto the surface of the delivery technology [185, 275]. However the type and amount of protein adsorbed onto the particles are invariably dependent on the same physicochemical properties of the particles that were initially thought to be solely responsible for the fate and/or organ distribution of the delivery system [185, 274]. It is not the total amount, but rather the nature of the adsorbed protein(s) that determines the fate and/or organ distribution of a CDDS [276]. However, it must be noted that for each protein, a minimum amount of the molecule must be adsorbed onto the surface of the particle in order to elicit a response from the MPS or to mediate adherence of the particles to target cells or organs [277].

In this regard, the preferential adsorption of opsonins such as immunoglobulin G (IgG) [278, 279], fibrinogen [280], fibronectin [281], transferrin [282], α2-macroglobulin [283] and complement factors e.g. C4γ [284] onto the surface of CDDS lead to immediate phagocytosis and clearance of the particles from the systemic ciruclation by the MPS [278, 285]. However when the CDDS are not opsonised or when they adsorb dysopsonins such as albumin [286, 287] and immunoglobulin A (IgA) [288] the uptake and removal of the carriers from the circulatory system by the MPS is retarded or inhibited, thereby prolonging the circulation time of the delivery system in the blood [287, 289]. The opsonisation or dysopsonisation of particles depends on the surface properties of CDDS, such that particles coated with certain molecules, for example polyethylene oxide (PEO)-containing non-ionic block co-polymers e.g. poloxamers and poloxamines promote dysopsonisation [272, 290]. CDDS coated with high molecular weight PEG e.g. PEG 6 000 or 20 000 may facilitate opsonisation or dysopsonisation *in vitro* depending on whether plasma or serum are used as the bulk medium [285].

Polymeric nanoparticles stabilized using polysorbate 80 (Tween® 80) are capable of delivering API to the brain [291-293]. Drugs that have been delivered to the brain *in vivo* using polysorbate 80-coated polymeric nanoparticles include dalargin [294, 295], loperamide [296], tubocurarine [297] and doxorubicin [293]. The preferential adsorption of apolipoprotein E (Apo E) onto the surface of the nanoparticles was found to be responsible for the delivery of API to the brain [294, 298-301]. The mechanism of brain targeting phenomena commences with the adsorption of Apo E onto the surface of a particle after which it behaves in a similar manner to conventional low density lipoproteins (LDL) *in vivo* [248]. Consequently, these particles may come into contact and interact with LDL receptors in the BBB leading to their uptake by endothelial cells and delivery across the BBB by endocytosis, followed by subsequent release and diffusion of the API from the nanoparticles into various brain structures [248].

The concept of differential protein adsorption, initially established by Müller and Heinemann [275] has been widely used *in vitro* to predict the *in vivo* fate and/or organ distribution of CDDS [139, 248, 277, 286, 302-304]. Different methods have been used to investigate *in vitro* protein adsorption patterns of CDDS including immunoassay [305, 306], field flow fractionation (FFF) [305, 307], two-dimensional polyacrylamide gel electrophoresis (2-D PAGE) [248, 248, 277, 308, 309], ellipsometry [310, 311] and mass spectroscopy [312]. However, the 2-D PAGE approach is often considered the method of choice for the separation of complex protein mixtures, as the technique not only provides qualitative but also quantitative information for the protein(s) present in a sample of interest [312, 313]. Therefore, an investigation of *in vitro* protein adsorption patterns of DDI-loaded NLC using 2-D PAGE was conducted in order to determine whether delivery of DDI to the brain is possible.

6.2 PRINCIPLE OF 2-D PAGE

6.2.1 Introduction

The 2-D PAGE technique is a sensitive and high-resolution multi-step technology that allows for the separation of proteins from complex mixtures, that may contain hundreds or thousands of components, by use of a combination of isolectric focusing (IEF) and sodium dodecyl sulfate polyacrylamide gel electrophoresis (SDS-PAGE) [314, 315]. Proteins are initially

separated in the first dimension according to their isoelectric point(s) (pI) using IEF and then according to their molecular weight (MW) using SDS-PAGE [315]. 2-D PAGE was initially developed for the separation and identification of proteins from complex mixtures from biological sources e.g. cells, tissues and fluids and was therefore applied only to proteome analysis [314, 315]. The use of 2-D PAGE has been extended to the *in vitro* analysis of protein adsorption patterns of CDDS leading to the publication of a number of protocols for 2-D PAGE [274, 298, 316-318] that have been adapted to make them suitable for these studies. The "standard" protocol for 2-D PAGE that is used to achieve a separation, qualitative and quantitative determination of proteins adsorbed onto CDDS includes five (5) major steps *viz.,* sample preparation, IEF, equilibration and SDS-PAGE, silver staining and analysis of 2-D PAGE gels [274, 298, 316-318].

6.2.2 Sample preparation

The preparation of a sample for 2-D PAGE is a multi-step process that is used to denature, disaggregate, reduce and solubilize the proteins in a sample [319]. The aim of the sample preparation step is to completely disrupt molecular interactions within the polypeptide structure of a protein to ensure that each spot on the 2-D PAGE gel is representative of a single protein [319]. A typical sample preparation process undertaken prior to 2-D PAGE analysis of proteins adsorbed onto CDDS involves four (4) major steps [316]:

i) Incubation of the particles in a relevant medium e.g. plasma or serum,
ii) Separation of the particles from bulk plasma or serum,
iii) Washing of the particles to remove non-adsorbed proteins, and
iv) Desorption of the adsorbed proteins from the surface of the particles.

Care must be taken when performing sample preparation to eliminate chemical modification of the proteins which could lead to the generation of artefacts in the data set [315]. The gel used in 2-D PAGE is sensitive to single charge modifications of a protein and a single protein may produce two or more spots on a 2-D PAGE gel when charge modification takes place during sample preparation [315].

6.2.2.1 Incubation of particles in suitable medium

The initial step in the preparation of a sample for 2-D PAGE analysis involves the incubation of the particles in a suitable medium e.g. plasma or serum for approximately five (5) minutes at 37°C [274, 316, 317, 320]. The medium used in the incubation step can impact on the nature of protein(s) that would be adsorbed onto the surface of the particles present [285, 306, 321]. The selection of the incubation temperature and time is intended to imitate physiological temperature and the time it takes for about 90% of intravenously administered CDDS to be detected and removed by the MPS or to interact with a target organ [272, 320].

6.2.2.2 Separation of particles from the bulk medium

Following the incubation of a CDDS in an appropriate medium, the particles are separated from the bulk medium [316]. The separation is achieved by centrifugation [274, 277, 302, 316, 320, 322-324] or gel filtration [248, 324-326] or magnetic field [324]. Centrifugation is usually the method of choice when there is a relatively large difference in density between the particle carriers and the incubation medium [326]. When the density of a CDDS is much higher than that of the incubation medium, the medium can be readily separated and removed from the particles using a pipette. In instances where the incubation medium has a higher density than that of the particles, these particles are likely to form a coherent, stable and solid layer at the top of the medium, following centrifugation [316]. In such cases, the removal of the bulk incubation medium is achieved by making two holes in the solid layer that has been formed, by the particles at the top of the bulk medium, using a needle and removing the medium by pouring [316]. Where there is little difference between the densities of the CDDS and that of the incubation medium, the two phases cannot be easily separated using simple centrifugation, therefore an alternate method must be used [326]. Gel filtration has been developed and recommended as the method of choice to achieve a separation between CDDS and an incubation medium of similar densities [248, 325, 326]. Gel filtration is essentially a size-exclusion chromatographic technique that separates compounds based on their molecular weight and smaller molecules elute faster than the larger molecules [326]. Since centrifugation is usually less complicated, rapid and less costly than gel filtration, a preliminary centrifugation study may be carried out to determine the feasibility of this approach and if it is not feasible to use centrifugation, gel filtration may used.

6.2.2.3 Removal of non-adsorbed protein materials

Following separation, the particles must be washed to remove residual incubation medium and/or non-adsorbed proteins [316]. This process involves dispersing the particles in water [274, 320, 322] or phosphate buffer pH 7.4 [139, 277, 316] and subjecting the sample to a further centrifugation step. The washing process is repeated up to four (4) times [316, 320]. The influence of the wash medium on protein adsorption patterns of CDDS has been investigated and phosphate buffer is usually preferred as a wash solvent [316]. It is important to note that too few wash cycles may leave residual incubation medium and/or non-adsorbed proteins on the particles [316]. However, too many wash cycles may result in the removal of large quantities of adsorbed proteins from the surface of the particles [316]. Therefore, it may be prudent to consider the use of samples with traces of the incubation medium rather than particles that are devoid of essential proteins as a consequence of excessive washing [316]. In general, particles exposed to three wash cycles can be readily analyzed [316].

6.2.2.4 Desorption of adsorbed proteins

Following the removal of non-adsorbed proteins and the remnants of the incubation medium, adsorbed proteins must be desorbed from the surface of particles, denatured and reduced to disrupt intra- and intermolecular bonds, while maintaining their inherent charge characteristics [315, 316]. The particles are initially dispersed in a solution containing sodium dodecyl sulphate (SDS) and dithioerythritol (DTE) and the resulting mixture is heated to 95°C for five (5) min, followed by cooling at room temperature for two (2) min [327]. The use of a relatively high temperature facilitates denaturing of the proteins and SDS eliminates or minimizes the unfolding of proteins due to aggregation and precipitation by preventing hydrophobic interactions forming between the hydrophobic domains of the protein [328, 329]. After cooling, a lysis buffering solution containing urea, cholamidopropyldimethylhydroxypropanesulfonate (CHAPS), DTE tris(hydroxymethyl)aminomethan (TRIS) and bromophenol blue is added to the sample mixture [315, 316].

Urea disrupts hydrogen bonding that causes proteins to unfold, leading to denaturation of the material [315]. CHAPS is a zwitterion and is a surface active agent that is added to solubilise proteins by interfering with hydrophobic interactions within and/or between proteins.

Furthermore CHAPS is able to displace SDS from the proteins, which if left unchecked may cause horizontal streaks in the resultant 2-D PAGE pattern. Complete unfolding of proteins is achieved using DTE and TRIS buffer which break intra and inter-molecular disulfide links in the protein structure [319, 330]. Consequently the proteins are denatured and their solubility in water increases and subsequent centrifugation of the sample results in the separation of the proteins and particles in solution after which the proteins are collected for use in the IEF procedure [316].

6.2.3 Isoelectric focusing (IEF)

The basic principle of IEF is the separation of charged proteins according to their isoelectric point(s) (pI) on a stationary and stable pH gradient that is oriented in a manner that allows the pH to increase from the anode to the cathode [314, 315]. Separation is achieved as charged proteins move along the pH gradient until they reach a location where the pH of the gradient is the pI of the protein and is therefore the focus point of the protein. In general, the pH gradient is produced using carrier ampholytes (CA) [314, 315] which are molecules that possess different pI and that have net charges that are dependent on the pH of the environment they are in. Following the application of an electrical field to a CA preparation, the molecules re-arrange themselves in a way that allows negatively charged CA or CA with the lowest pI to move towards the anode while those that are positively charged or the CA with the highest pI migrate towards the cathode. Eventually all CA will align themselves between the anode and cathode depending on their pI and the net charge on each molecule will be zero, which creates a pH gradient that is stationary [314, 315].

The diffusion of a CA through an environment is dependent on the electric field across the electrodes. The stability of the pH gradient for the separation of the proteins is determined by the buffering properties of the particular CA used. The major drawback of using CA to produce a pH gradient for IEF is the occurrence of cathodic drift or movement of the pH gradient towards the cathode, which in turn allows the gradient to flatten at the centre and produce a plateau phenomenon [331, 332]. This results in instability of the gradient and a prolonged focusing time that may result in intra- and/or inter-laboratory variations in data [331, 332]. In addition the batch-to-batch variability of CA materials may limit the reproducibility of pH gradient profiles thereby resulting in a lack of reproducibility of the resultant 2-D PAGE data generated within or between laboratories. However, these

disadvantages have been overcome with the introduction of immobilized pH gradients (IPG) for IEF [319, 333].

IPG are generated by co-polymerization of a limited number (< 10) of CA molecules, otherwise known as "immobilines" with acrylamide gel [319, 333]. The use of this technique has eliminated the cathodic shift associated with pH gradients prepared using non-copolymerized CA and therefore enhance the stability of the gradient produced and improve the intra- and inter-laboratory reproducibility of IEF [331, 332]. The pH range of IPG can be ultra-narrow (pH 4.9-5.3), narrow (pH 4-7) or wide (pH 3-12) and the selection of a suitable IPG is dependent on the intended purpose of a study [319, 334-336]. The use of IPG in IEF is considered the method of choice for protein separation and spot identification in 2-D PAGE analysis due to the advantages associated with their use and the fact that a relatively high sample LC can be achieved compared to the use of CA-associated IEF [333, 337]. Individual IPG gel strips are commercially available e.g. Immobiline DryStrips® or IPG-BlueStrips® from Serva Electrophoresis (Heidelberg, Germany) or can be made in a laboratory by an IPG gel casting technique [319, 338].

Commercially available IPG dry strip gels must be rehydrated with a suitable rehydration solution prepared according to specifications, in order to restore their original diameter prior to use for IEF [319] or otherwise an in-gel rehydration technique [339] must be used. An integrated system e.g. IPGphor® [340, 341] that allows in-gel rehydration and IEF to be performed simultaneously overnight can also be used. IPG gel strips are placed into an electrofocusing chamber and the samples are applied onto the surface of the gel strips using cup loading or in-gel rehydration [319, 339]. Following sample application a low power voltage gradient must be applied for the first hour and the voltage is then steadily increased to 3500 V over a number of hours until a steady state with constant focusing is achieved [319].

6.2.4 Equilibration of IPG strips

Prior to SDS-PAGE analysis, IPG strips produced from IEF must be equilibrated twice, with each equilibration step taking approximately 15 minutes. Equilibration is achieved by gentle shaking of the strips in the presence of a solution containing SDS, urea, glycerol, Tris-HCL buffer and traces of bromophenol blue [319, 330, 334]. Dithioerythritol (DTE) and iodoacetamide must be added to the solution used in the first and second equilibration steps,

respectively [319, 330, 334]. The objective of the equilibration process is to permit a full interaction between proteins that have just been separated in the IEF step with SDS prior to SDS-PAGE analysis [319]. Urea and glycerol are required in order to decrease electro-endosmotic effects during analysis and therefore improve the transfer of proteins from IEF to SDS-PAGE [319].

Thiourea, instead of urea, can sometimes be used during equilibration to enhance the transfer of hydrophobic proteins but use of this molecule may cause vertical streaks [342] in the 2-D PAGE gel pattern [343]. DTE is a reducing agent that is used in the first equilibration solution to cleave the sulphide bonds that hold the protein structure together and therefore DTE completes the unfolding of the protein [319, 330]. Iodoacetamine is added to the second equilibration solution in order to alkylate sulfhydryl functional groups and prevent re-oxidation of the molecule [319, 330]. Furthermore, iodoacetamine is used to alkylate any excess DTE that is not used up during the first equilibration step since any unchecked DTE may cause point-streaking in the SDS-PAGE gel after silver staining [319, 330].

Up to 20% of the protein materials undergoing analysis are lost during equilibration and transfer from IEF to SDS-PAGE [344] due to wash-off effects and/or the retention of protein on the IPG strip due to preferential adsorption of materials to the IPG gel matrix and/or insufficient equilibration time [342]. The protein is generally lost in the first few minutes following the first equilibration step and only a minor amount of the material is lost during the second equilibration step and the trend is reproducible for a particular sample [342].

6.2.5 SDS-PAGE analysis

In SDS-PAGE analysis, proteins are separated orthogonally, in the presence of SDS, according to their MW [345]. Therefore following equilibration of IPG strips, SDS-PAGE analysis can be performed using either a horizontal or vertical SDS system [346, 347]. Horizontal systems are suitable for commercially available SDS gels such as ExcelGel® SDS gels (GE Healthcare Lifesciences, Munich, Germany) that are cast on a plastic support [347]. The role of the plastic support is to prevent changes in the size of the SDS gel during the staining procedure, which may arise due to evaporation of organic solvents and expansion when the gels are rehydrated with aqueous-based solvents [342].

The use of a horizontal system permits the SDS gels to be placed onto a cooling plate of a horizontal electrophoresis system [347] and the IPG strips are loaded onto the surface of these SDS gels with the gel-side of the strips facing down, alongside the cathode electrode wick [347]. Vertical systems are usually used for SDS gels that are made in a laboratory and are typically useful for multiple runs, including analysis of up to 20 strips at a time [348]. These systems are particularly useful in large-scale proteome analysis. In general, IPG gel strips are placed on top of vertical SDS-PAGE gels with or without embedding the strips in an agarose gel [347]. Polyacrylamide is usually used for SDS gel casting and the continuous buffering system initially developed by Laemmli [349] is used in SDS-PAGE albeit other buffers e.g. borate buffers may be used [350].

6.2.6 Silver staining

The separation of the proteins in SDS-PAGE is followed by staining of the gels to allow for the subsequent visualization, identification and quantitation of protein spots on the gels [342]. The gels can be stained using silver [351, 352] or Coomassie Brilliant Blue (CBB) [353]. Silver staining methods [351, 352] are generally considered more sensitive than CBB techniques with a detection limit of 0.1 ng of protein per spot [342]. Consequently silver staining is suitable for the detection of trace components within a protein sample as well as for the analysis of protein samples that are only available in limited quantities [342]. However silver staining techniques are laborious and complex and have a limited dynamic range, in addition to poor reproducibility due to subjective end-point determination and the inability to stain certain proteins [342]. Other staining methods include negative reverse staining with metal cations [354], fluorescence staining [355] and labelling with radioactive isotopes [356]. Silver staining was used in these studies due to its sensitivity and ease of analysis of the protein spots. Silver staining is preceded by fixing the proteins in solutions that contain ethanol/acetic acid/water for several hours in order to remove unrelated compounds, such as for example the CA or surface active agents [351, 352] used in the process.

6.2.7 Analysis of 2-D PAGE gels

Following staining, the gels are scanned using a high quality 12- to 16-bit greyscale scanner [345]. This facilitates the production of digital images of the gel for qualitative identification

of the protein spots or quantitative analysis of the polypeptide spots using a computerized image analysis system [345]. The 2-D PAGE images can be captured using a range of devices including modified document scanners, laser densitometers fluorescent and phosphor imagers as well as charge-coupled device (CCD) cameras [345]. The proteins can be qualitatively identified by comparison of protein spots to published reference maps [357]. Reference maps are accessible *via* the internet at www.expasy.org/ch2D/2d-index.html [358].

2D-PAGE digital images can be analyzed using a variety of commercially available software packages such as PDQuest® (Bio-Rad, Hercules, CA, USA), MELANIE® III software (Swiss Institute of Bioinformatics, Geneva, Switzerland), Delta® 2D (Decodon, Greifswald, Germany), Phoretix® 2D and Progenesis® (Nonlinear Dynamics, Newcastle upon Tyne, UK) [345]. Irrespective of the type of software package used, the steps taken during the analysis of digital images of 2-D PAGE gels usually involve the following steps [345]:

i) Pre-processing of gel images e.g. image normalization, cropping and background subtraction,
ii) Spot segmentation (detection) and expression quantification,
iii) Initial user guided pairing of a few spots of the reference and sample gels or landmarking, followed by warping of the sample gel in order to align the landmarks,
iv) Automatic pairing of the balance of the spots,
v) Identification of different proteins,
vi) Data presentation and interpretation, and
vii) Creation of 2-D gel databases.

MELANIE® III software (Swiss Institute of Bioinformatics, Geneva, Switzerland) was used for the analysis of 2-D PAGE gel images.

6.3 MATERIALS AND METHODS

6.3.1 MATERIALS

The materials and chemicals were used as received from the suppliers without further testing and the chemicals were all at least of analytical reagent grade.

6.3.1.1 *Chemical and reagents*

Citrated human plasma was purchased from the German Red Cross (GRK) (Berlin, Germany) and stored at -70°C. HPLC-grade water was produced using a Milli Q® Plus water purification system (Millipore GmbH, Schwalbach, Germany). Glycerol, sodium dodecyl sulphate (SDS), urea, Cholamidopropyldimethylhydroxypropanesulfonate (CHAPS), 1,4-dithioerythritol (DTE), iodoacetamide, tris(hydroxymethyl)aminomethan hydrochloride (Tris-HCL), acrylamide-Bis solution (37.5:1) (30% v/v), agarose, ammonium persulfate, N,N,N'N' tetramethylenediamine (TEMED) and Servalyt® pH 3-10 carrier ampholyte were purchased from Serva Electrophoresis, (Heidelberg, Germany). Acetic acid, liquid paraffin, bromophenol blue, sodium salt, sodium dihydrogen phosphate ($NaH_2PO_4.2H_2O$) and disodium hydrogen phosphate ($Na_2HPO_4.12H_2O$) were purchased from Merck (Merck KgaA, Darmstadt, Germany). Denatured ethanol (96%) was obtained from Branntwein-Monopolstelle (Branntwein-Monopolstelle, Berlin, Germany). Bio-Rad® Silver Stain was purchased from Bio-Rad Laboratories GmbH (Munich, Germany).

6.3.2 METHODS

6.3.2.1 *Selection of NLC formulations*

6.3.2.1.1 *Overview*

Preferential protein adsorption patterns of DDI-loaded NLC formulations were investigated using the formulations listed in Table 6.1. The non-proprietary names and physicochemical properties of the surfactants used are detailed in Section 5.2.1.2, *vide infra*.

Table 6.1. Composition of DDI-loaded NLC formulation investigated in 2-D PAGE studies

MATERIAL	DDI-NLC 1	DDI-NLC 2	DDI-NLC 3	DDI-NLC 4	DDI-NLC 5
DDI	6 mg	100 mg	100 mg	100 mg	100 mg
Tween® 80 (%)	1	6	-	-	1
Lutrol F68 (%)	2	-	6	-	2
Solutol® SH 15 (%)	3	-	-	6	3
Transcutol® HP (%)	5	5	5	5	5
Precirol® ATO 5 (%)	15	15	15	15	15
Aqua ad. (%)	100	100	100	100	100

A combination of three non-ionic surfactants was necessary for the production of NLC formulations (Chapter 5, Section 5.3.1.). Briefly, the rationale for using three surfactants was that Solutol® HS 15 produced the most stable DDI-loaded NLC formulation. However since the objective of these studies was also to assess the potential for the NLC to cross the blood brain barrier and deliver DDI to the brain, the inclusion of Lutrol® F68 and Tween® 80 was considered necessary since CDDS stabilized with Lutrol® F68 and Tween® 80 have the potential to prolong the circulation time of nanoparticles *in vivo* and deliver nanocarriers to the brain, respectively [248]. Therefore the preferential protein adsorption pattern(s) of formulation, DDI-NLC 5 that contained all three surfactants was investigated. The three emulgents were used individually to produce batches DDI-NLC 2, DDI-NLC 3 and DDI-NLC 4, and the protein adsorption patterns of these formulations were compared to that generated for formulation DDI-NLC 5. The total surfactant concentration or combination of surfactants and the loading dose of DDI in each formulation was kept constant.

It has been established (Chapter 5, Section 5.3.3.3) that increasing the amount of DDI in an NLC formulation reduces the EE and LC of the NLC for DDI. Therefore it was assumed that the batch DDI-NLC 1, designed to contain 6 mg of DDI was likely to have fewer drug molecules on the surface of the particles in aqueous formulations than those manufactured to contain 100 mg of DDI, *viz.*, batch DDI-NL 5. Therefore the protein adsorption patterns of batch DDI-NLC 5 was also investigated and compared to that of batch DDI-NLC 1 in order to determine the effects of increased DDI concentration in the aqueous phase of NLC dispersions on the protein adsorption patterns of the particles.

6.3.2.1.2 Characterization of NLC formulations

The NLC formulations were characterized in terms of the physicochemical properties that may have impact on the protein adsorption behaviour of the particles e.g. PS and ZP. The PS was measured using a Nano-ZS Zetasizer® in PCS mode and LD as described in Sections 5.2.2.2.1.1 and 5.2.2.2.1.2, respectively, while the ZP was analyzed using the Zetasizer® in LDA mode as detailed in Section 5.2.2.2.2.

6.3.2.2 Preferential protein adsorption analysis

The 2-D PAGE analysis of DDI-loaded NLC was performed using protocols that have been previously established [274, 298, 316-318].

6.3.2.2.1 Sample preparation

Briefly, 0.3 ml of an aqueous NLC dispersion was added to 0.9 ml of citrated human plasma (GRK, Berlin, Germany) and the mixture was incubated for five (5) minutes at 37°C using a Model NB 22 HAAKE a temperature-controlled circulating water bath (Thermo Fisher Scientific Inc., Waltham, MA, USA). Following incubation, the nanoparticles were separated from the excess plasma by centrifugation at 23 000 g at 20°C for one (1) hour using a Model 22 R Biofuge centrifuge (Heraeus Sepatech GmbH, Osterode/Harz, Germany). The nanoparticles formed a lipid layer overlaying the plasma during centrifugation and the plasma was removed from the tubes by passing a pipette (Eppendorf AG, Hamburg, Germany) through the lipid layer. Following removal of the plasma, the lipid layer was washed three times by adding 0.9 ml of a 0.5 mM sodium phosphate buffer (pH 7.4) followed by centrifugation at 23 000 g for one (1) hour. After completion of the last wash step, the lipid materials were re-suspended in a mixture of 15 µl of HPLC-grade water (Millipore Co, Schwalbach, Germany) and 10 µl of a solubilising solution containing SDS (10% w/v) and DTE (2.32% w/v). The mixture was incubated for five (5) minutes at 95°C and then allowed to cool down for two (2) min at room temperature. The sample was then mixed with 190 µl of a solubilizing solution containing 8 M urea (48% w/v), CHAPS (4% w/v), 0.04 M Tris (0.5% w/v) and 0.065 M DTE (1% w/v). The mixture was stirred using a Model REAX I vortex mixer (Heidolph Elektro GmbH & Co. KG, Kelheim, Germany) and centrifuged for a further 15 minutes at 23 000 g to separate the particles from the solubilizing solution. Once again, the particles formed a layer at the surface of the solubilizing solution. Consequently, the lipid layer was discarded and 215 µl of the solution was retained for use in the first dimension IEF study.

6.3.2.2.2 Isoelectric focusing (IEF)

Isoelectric focusing (IEF) of the adsorbed proteins was performed using Immobiline® DryStrips (18 cm length IPG-BlueStrips) with a nonlinear pH gradient ranging between pH 3-10 (Serva Electrophoresis, Heidelberg, Germany). The IPG strips are usually dry and are

kept frozen at approximately -70°C and consequently must be rehydrated to their original dimensions prior to IEF analysis. The IPG strips were rehydrated using an in-gel rehydration technique [339] Briefly, 340 µl of a rehydration solution, which consisted of 215 µl of the sample and 125 µl of rehydration buffer (8 M urea (48% w/v), CHAPS (2% w/v), DTE (0.2% w/v) and Servalyt® pH 3-10340 (0.5% w/v) was placed into each groove of a rehydration tray (GE Healthcare, Munich, Germany). The protective cover sheets on the IPG strips were removed and the strips were inserted into the grooves of the tray with the gel side face down, while avoiding the incorporation of air bubbles. Care was taken to ensure that the strips were floating in the rehydration solution and that they did not stick to the tray. Following 15 minutes of overlay in rehydration buffer, the strips were covered with 1-2 ml of silicon oil to prevent desiccation of the strips. The rehydration tray was then covered with a lid and the strips were rehydrated overnight at 25°C.

The gels were gently blotted with the filter paper to remove any excess rehydration solution and to prevent urea recrystallization on the surface of the gel during IEF. The temperature of a flat-bed cooling plate (GE Healthcare, Munich, Germany) was adjusted to 20°C and the IPG gel strips were placed side by side approximately 1-2 mm apart with the gel side face up and the acidic or positive end of each gel strip facing the anode. Two paper strips were cut from a 2 mm thick MN 440 filter paper (Macherey-Nagel GmbH & Co.KG, Düren, Germany) to a length corresponding to the width of all IPG strips that were placed on the cooling plate and were soaked in 0.5 ml HPLC grade water. Excess water was removed from the paper strips by blotting with filter paper and the paper strips were used as IEF electrode strips. The IEF strips were placed on top of the aligned IPG gel strips at the cathode and anode ends. The electrodes were then positioned and pressed down on top of the IEF strips gently and the lid of the Multiphor™ II Electrophoresis System (GE Healthcare, München, Germany) was closed. The IEF chamber was equipped with a Consort Model E752 power supply (Turnhout, Belgium). The power supply was then connected to the electrofocussing chamber and a low power voltage gradient of 150 V was applied for the first hour and then increased to 3000 V steadily over a 5 hour period. A summary of the running conditions and the time schedule for IEF studies is listed in Table 6.2.

Table 6.2. Summary of the running conditions for IEF.

PROGRAM STEP	VOLTAGE (V)	TIME (h)	Vh
1	150	1	150
2	300	1	300
3	600	1	600
4	1500	1	1500
5	3000	12.5	37500
Total		16.5	40000

6.3.2.2.3 Equilibration of IPG strips

Prior to SDS analysis the IPG strips were equilibrated for 15 minutes and then 20 minutes in the first and second equilibration solutions, respectively. The IPG strips were transferred from the IEF chamber into a rehydration tray (GE Healthcare, München, Germany) and the strips were initially allowed to equilibrate in 100 ml of a solution containing DTE (2% w/v), SDS (3% w/v), Tris-HCL pH 6.8 (10% w/v), glycerol (87% solution) (34.5% w/v), urea (36% w/v) and traces of bromophenol blue (equilibration solution I). Solution I was removed and replaced with a solution of iodoacetmide (4% w/v), SDS (2% w/v), Tris-HCL pH 6.8 (10% w/v), glycerol (87% solution) (34.5% w/v), urea (36% w/v) and traces of bromophenol blue (equilibration solution II). The IPG strips were placed in a tray with equilibration solutions and gently agitated using a Model KS-10 Buhler shaker (Tübingen, Germany) for both equilibration steps. The second equilibration step was completed 20 minutes after commencement and the solution was then removed. The IPG were then rinsed with SDS-PAGE running buffer prior to the second dimension.

6.3.2.2.4 SDS-PAGE analysis

Vertical SDS slab gels for use in SDS-PAGE analysis were cast using a Protean® II XI multi-gel casting chamber (Bio-Rad Laboratories GmbH, Munich, Germany) with a linear gradient ranging from 8-16% of the total (T) concentration of acrylaminde using bis (N,N-methylene-bis-acrylamide) as a crosslinking agent and a Model 495 gradient former (Bio-Rad Laboratories GmbH, München, Germany). Six gel casting cassettes were made from glass plates (180 x 180 mm x 1.5 mm) (Bio-Rad laboratories GmbH, Munich, Germany). Each cassette consisted of two glass plates stacked together, with two, 1.0 mm thick spacers between them to allow for the formation of the gel slab. A total of 12 glass plates was required for the formation of six (6) gel cassettes in order to ensure that a single SDS-PAGE analysis could be completed. Following casting of the gel, the IPG strips were placed at the

top end of the gel slabs and were fixed with a 0.5% agarose gel solution that contained bromophenol. SDS-PAGE analysis was performed with a total of six (6) gels using a Protean® II XI multi-cell electrophoresis tank (Bio-Rad Laboratories GmbH, München, Germany) connected to a PowerPac® 1000 power supply (Bio-Rad Laboratories GmbH, Munich, Germany) that provided a current of 40 mA per gel strip. The end point of the SDS-PAGE process was reached after the bromophenol blue flow front reached the lower end of the gel strips.

6.3.2.2.5 Silver staining of SDS gel plates

Following the separation of proteins by SDS-PAGE analysis, the SDS gels were stained using Bio-Rad® Silver Stain to permit visualization of the protein spots. A previously established protocol [351, 359] for silver-staining was used and the details for staining procedure are listed in appendix I. The trays containing the gel plates were shaken gently using a Model KS-10 shaker (Buhler, Tübingen, Germany) during the staining procedure according to the time schedule listed in appendix I.

6.3.2.2.6 Analysis of electrophoresis gel plates

The stained gel plates were scanned using a Model UMAX PowerLook® IIII Image Scanner (Amersham Pharmacia Biotech, Uppsala, Sweden) in order to produce digital images of the gel plates for ease of analysis of protein spots. The gels were scanned using LabScan® 5.0 software (Swiss Institute of Bioinformatics, Geneva, Switzerland) in transparent mode with the resolution and colour set at 200 dpi and black filter, respectively. The proteins were qualitatively identified by comparing the location of a spot on a gel to that of a reference map. The amount of protein identified on the digital images of the gel plates were quantitatively determined using MELANIE® III software (Swiss Institute of Bioinformatics, Geneva, Switzerland) and the data for each protein was reduced to determine the percentage (%) of the overall amount of protein pattern detected.

6.4 RESULTS AND DISCUSSION

6.4.1 Characterization of the physical properties of NLC

The physicochemical properties of CDDS, e.g. PS and ZP may influence the protein adsorption pattern of particles that are administered to patients using the IV route. Therefore, prior to investigating protein adsorption patterns, the PS and ZP of DDI-loaded NLC were measured and the data are summarised in Table 6.3.

Table 6.3. PS, PI and ZP of DDI-loaded NLC formulations

PARAMETER	DDI-NLC 1	DDI-NLC 2	DDI-NLC 3	DDI-NLC 4	DDI-NLC 5
PCS (nm)	208 ± 4	764.6 ± 3	977 ± 1	134.1 ± 2	148 ± 3
PI	0.120 ± 0.044	1.0 ± .4	1.0 ± .2	0.44 ± 0.023	0.195 ± 0.037
D50% (μm)	0.150	0.940	0.635	0.142	0.149
D90% (μm)	0.235	4.35	2.59	0.236	0.232
D95% (μm)	0.261	5.75	4.70	0.270	0.283
D99% (μm)	0.306	8.68	37.2	0.347	0.303
ZP (mV)	-17.0 ± 0.5	-17.7 ± 0.6	-24.4 ± 1.0	-16.8 ± 0.6	-13.3 ± 0.9

The PCS data reveal that the mean particles size of NLC that were manufactured using a combination of three non-ionic surfactants *viz.* Tween® 80, Lutrol® F68 and Solutol® HS 15 (batches DDI-NLC 1 and DDI-NLC 5) and that of the formulation containing Solutol® HS alone (DDI-NLC 4) was less than 250 nm and that the polydispersity indices are narrow. In addition the D99% for these formulations was less than 350 nm indicating that almost all the particles in these formulations are within the nano PS range. However, this was not the case for formulations that contained either Tween® 80 (batch DDI-NLC 2) or Lutrol® F68 (batch DDI-NLC 3), only. Although PCS data indicate that the size of the particles in batches DDI-NLC 2 and DDI-NLC 3 lie within the nano range, the LD data reveal the presence of microparticles in these formulations.

The presence of microparticles in batches DDI-NLC 2 and DDI-NLC 3 is an indication that the formulations are less stable than batches DDI-NLC 1, DDI-NLC 4 and DDI-NLC 5. Nevertheless batches DDI-NLC 2 and DDI-NLC 3 were included in these studies to establish whether their respective protein adsorption patterns would be similar to those of formulation batch DDI-NLC 5 due to the surfactant content and not PS. However since the size of the particles in batches DDI-NLC 1, DDI-NLC 4 and DDI-NL 5 are similar, any differences and/or similarities that may be observed for protein adsorption patterns are unlikely to be a

consequence of the size of the particles. On the other hand, the size of the particles may potentially lead to differences in the protein adsorption patterns of particles in batches DDI-NLC 2, DDI-NLC 3 and DDI-NLC 5 that is unrelated to the surfactant content of the particles.

The ZP values for formulation batch DDI-NLC 5 is lower than that for batch DDI-NLC 1, which may be due to the increased amount of DDI in the aqueous phase. It is possible that the presence of DDI in the aqueous phase increases the thickness of adsorption layer thereby shifting the plane of shear to a point that is located further from the surface of the particle, therefore leading to a decrease in the ZP of particles in batch DDI-NLC 5. The ZP value of particles in batch DDI-NLC 5 is also lower than those of batches DDI-NLC 2, DDI-NLC 3 and DDI-NLC 4. This may be due to the fact that using a combination of surfactants (batch DDI-NLC 5) may increase the adsorption layer on the particles leading to a similar situation as previously mentioned. However as the experimental ZP values were negative it was anticipated that similarities would be observed in the protein adsorption patterns for all formulations.

6.4.2 Protein adsorption patterns of NLC

6.4.2.1 Effect of surfactants

The influence of the surfactant on the protein adsorption patterns of the DDI loaded nanoparticles produced is shown, qualitatively, on the 2-D gel images depicted in Figure 6.1.

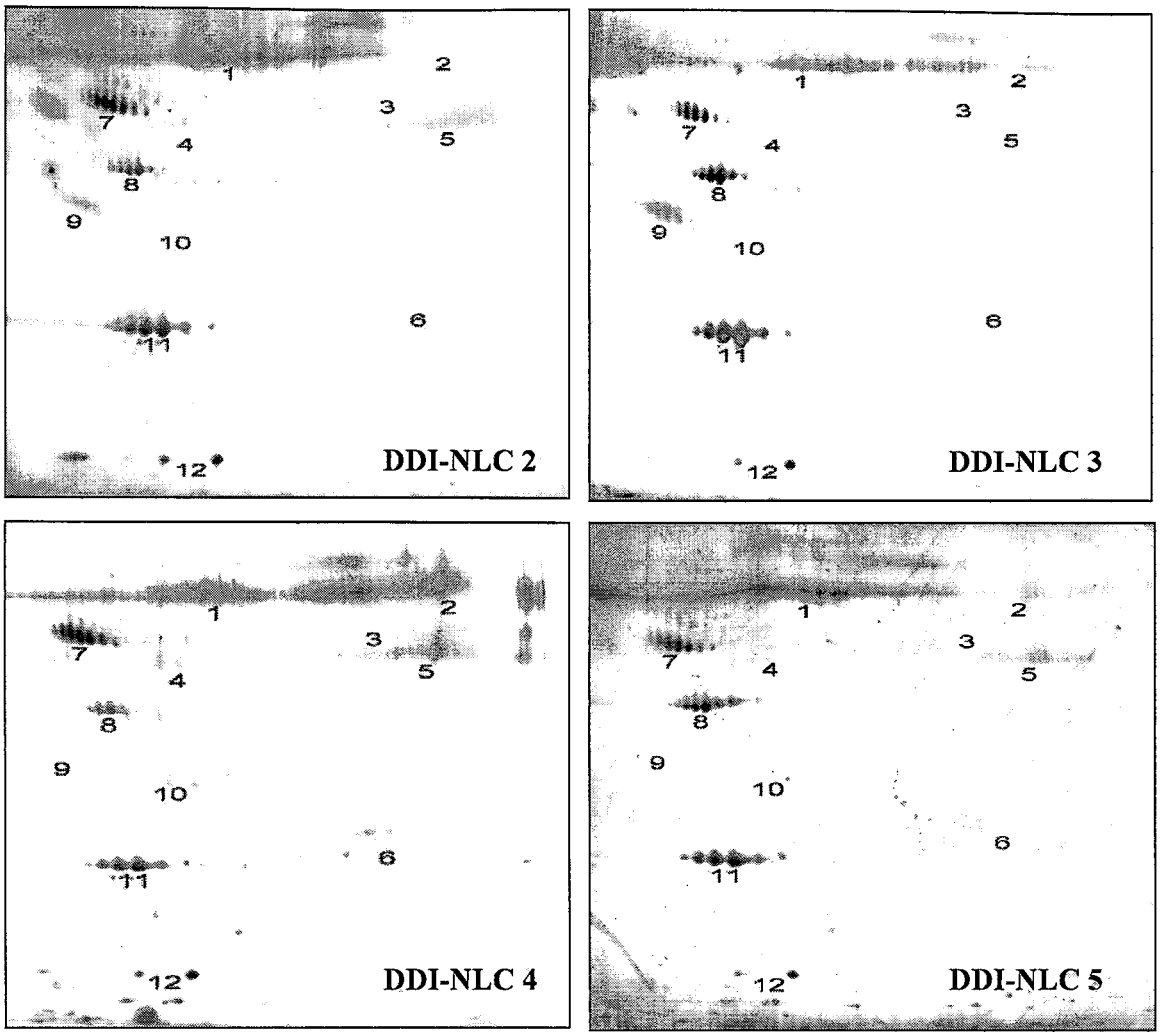

Figure 6.1. 2-D gel images depicting protein adsorption patterns of DDI-loaded NLC: (1) Albumin, (2) Fibrinogen α-chain, (3) Fibrinogen β-chain, (4) Fibrinogen γ-chain (5) Immunoglobulin heavy chain gamma, (6) Immunoglobulin light chain, (7) α-1-antitrypsin, (8) Apolipoprotein A-IV, (9) Apolipoprotein J, (10) Apolipoprotein E, (11) Apolipoprotein A-I, (12) Transthryetin.

From a qualitative perspective, these data reveal that there is no significant difference in the types of proteins that were adsorbed onto the surfaces of the particles under investigation. All formulations, irrespective of the surfactant used appear to have adsorbed some opsonic proteins, such as fibrinogen, from plasma. This indicates that these particles are likely to be recognized and removed from the blood stream by the MPS following IV administration of formulations that contain these nanoparticles [278, 285]. However, albumin which is a dysopsonic protein was also found on the surfaces of the particles, in all formulations investigated. Therefore, the particles are expected to have a relatively long circulation time in the blood as they may not be recognized by the MPS. There is also an indication that some of the formulations adsorbed apolipoprotein E (Apo E) which indicates the potential for these

formulations to deliver DDI to the brain [287, 289]. However, these are qualitative data and only give an overview of protein adsorption patterns for the different formulations. Therefore, quantitative data were generated to elucidate the extent of similarities or differences of protein adsorption patterns of the formulations, more comprehensively. The percent volume of each protein reported as a function of the total volume of the protein adsorbed onto the surface of NLC particles is depicted in Figure 6.2.

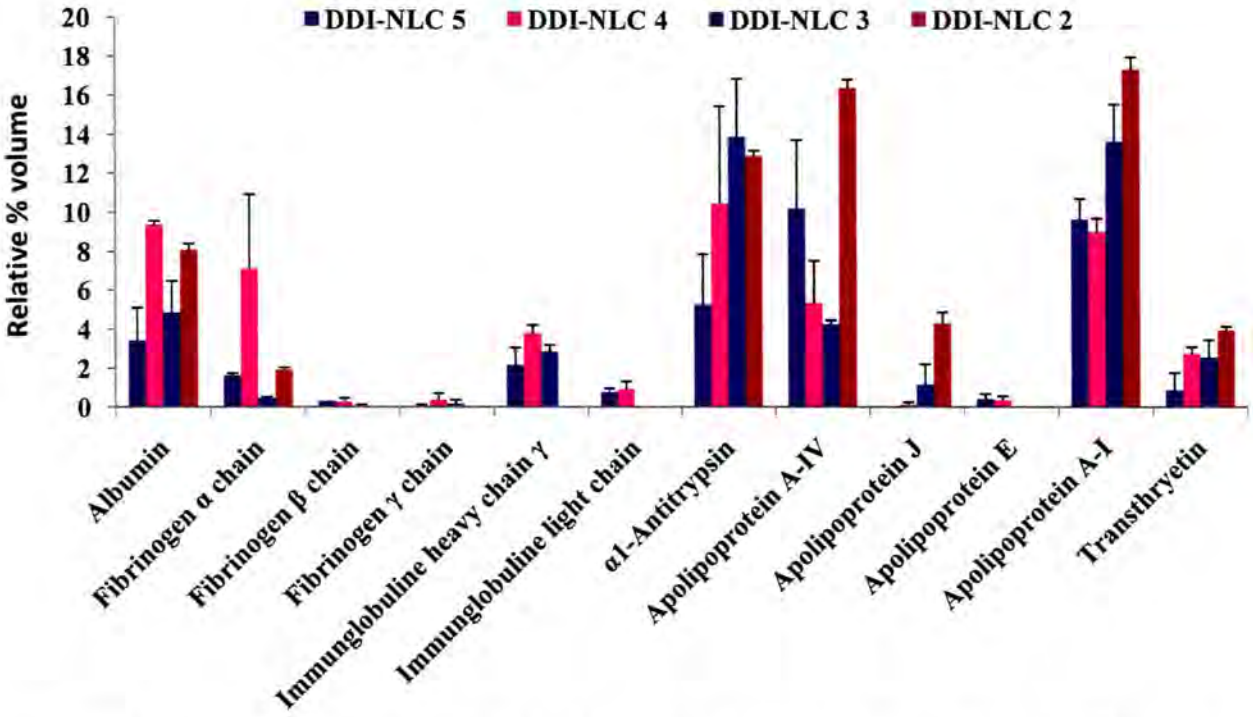

Figure 6.2. Relative percent volume of each protein as a function of the total volume of protein adsorbed onto the surface of NLC particles (n = 2)

The 2-D PAGE studies were performed in duplicate (n = 2) as established in previous studies [139, 302] and the relatively large standard deviation (SD) of some of the adsorbed proteins may be due to variations in the amount of particles collected following centrifugation. The harvesting of particles is dependent on the clarity of separation between the lipid layer and the plasma and NLC particles may be lost when the plasma is removed. In general, a standard sample size is removed from the particles that have been collected and used in protein desorption so as to ensure that the amount of the protein(s) present in each sample is constant. This is usually the case if the initial amount of nanoparticles in plasma is relatively large e.g. between 0.5-2.0 ml [139, 248, 316]. The design of the Eppendorf® centrifuge tubes (Eppendorf AG, Hamburg, Germany) did not permit the use of large sample sizes and

therefore an aliquot of 0.3 ml of the particles was used with 0.9 ml of plasma in order to keep the ratio of particles to plasma (1:3) the same as that used in well-established and published protocols [316].

The sampling and weighing of aliquots of the lipid layer that is formed following centrifugation is usually difficult and will result in the loss of particles. Since a small amount of particles was incubated in the plasma initially and some particles are lost during removal of the plasma, the standard sample size weight approach was not used. Rather the whole lipid layer was collected and used instead after the washing step. Therefore due to the loss of particles whilst removing the plasma and during sample washing steps the amount of the lipid layer and hence the amount of protein used invariably differs, the consequence of which is that a relatively large variation in the amount of adsorbed proteins may be observed.

The preferential adsorption of apolipoprotein E (Apo E) onto the surface of CDDS *in vivo*, following IV administration is essential if the delivery of API, encapsulated into such carriers, to the brain is to be successful [294, 298-301]. The potential for NLC to deliver DDI to the brain is based on whether or not Apo E is preferentially adsorbed onto the surface of the particles, *in vitro*. Batch DDI-NLC 5 was optimized and appeared to have preferentially adsorbed approximately 0.40 ± 0.28% of Apo E in relation to the amount of the other proteins adsorbed. However, the amount of Apo E adsorbed onto the surface of particles in batch DDI-NLC 5 is only marginally higher than the amount of Apo E (0.35 ± 0.21%) adsorbed onto the surface of particles of the formulation containing Solutol® HS 15 only (batch DDI-NLC 4).

Apo E is required for the binding of β-very low density lipoproteins (β-VLDL) to low density lipoprotein (LDL) receptors. [360]. Binding however, is inhibited by the presence of other apolipoproteins such as apolipoprotein C-I (Apo C-I) and apolipoprotein C-II (Apo C-II). Consequently the presence of these apolipoproteins may inhibit the binding of Apo E adsorbed onto the surface of nanoparticles to LDL receptors in the BBB. Therefore, it may be beneficial to have a high ratio of Apo E to Apo C-I or Apo C-II adsorbed onto the surface of the particles in order to achieve targeting of the nanoparticles to the brain [277]. As there was no preferential adsorption of Apo C-I or Apo C-II onto the particles of all batches investigated in these studies, the interaction of the particles that were associated with Apo E

(batches DDI-NLC 4 and DDI-NLC 5) with the LDL receptors in the brain is unlikely to be inhibited by the presence of Apo C-I or Apo C-II.

Another interesting observation is that Apo E receptors are not specific to the brain, but are also present in the liver [286]. Consequently, nanocarriers that have adsorbed Apo E may be directed to the liver rather than targeting the brain. However, apolipoproteins such as apolipoprotein A-I (Apo A-I) and apolipoprotein A-IV (Apo A-IV) are known to suppress the activity of Apo E receptors in the liver [286]. All formulations under investigation also preferentially adsorbed relatively high amounts of Apo A-I and Apo A-IV (Figure 6.2). Therefore, the presence of these apolipoproteins on the surface of the particles is likely to promote brain targeting of the nanocarriers [361]. However this is only likely to be of benefit for batches DDI-NLC 4 and DDL-NLC 5. The amount of Apo A-I and Apo A-IV adsorbed onto particles in batch DDI-NLC 4 was 9.0 ± 0.7% and 5.35 ± 2.2% respectively, while batch DDI-NLC 5 was observed to preferentially adsorb 9.65 ± 1.1% and 10.2 ± 3.5% of Apo A-I and Apo A-IV respectively. The presence of these apoliproproteins at these levels is likely to enhance the potential delivery of particles in batches DDI-NLC 4 and DDI-NLC 5 to the brain *via* an LDL receptor mediated delivery mechanism in the BBB.

While batches DDI-NLC 4 and DDI-NLC 5 show the potential for brain targeting based on protein adsorption patterns, the particles in the formulations that contained Tween® 80 and Lutrol® F68 (Poloxamer 188) (batch DDI-NLC 3) did not adsorb Apo E. This is interesting since Apo E has been observed to adsorb onto the surfaces of CDDS stabilised using Poloxamer 188 [277] or Tween® 80 [248]. However, the results observed for Apo E adsorption onto particles in batch DDI-NLC 3 are not unique and the absence of Apo E on the surface of Poloxamer 188-stabilized nanoparticles has been reported [248]. Tween® 80 has always been associated with a potential for brain targeting of CDDS due to the fact that Tween® 80-coated CDDS invariably adsorb Apo E. A possible explanation for the lack of Apo E adsorption onto the surfaces of particles in batches DDI-NLC 2 (Poloxamer 188) and DDI-NLC 3 (Tween® 80) may be related to the size of the surface area of these particles, which is relatively small as a result of their large PS (Table 6.1).

It is possible that Apo E will be preferentially adsorbed onto the surface of particles that have a relatively large surface area. The surface area of particles in batches DDI-NLC 4 and DDI-NLC 5 is larger due to the small PS of the NLC compared to that of particles in batches DDI-

NLC 2 and DDI-NLC 3. Consequently the preferential adsorption of Apo E onto the surface of the particles may be unrelated to the presence of surfactants in the formulations, but is rather dependent on the surface area of the particles. The relative amount of Apo E adsorbed onto particles in batches DDI-NLC 4 and DDI-NLC 5 in comparison to other proteins, is likely to decrease the percent fraction of the other proteins that can be adsorbed [277]. However, these data predict that DDI can be delivered to the brain *in vivo,* through a BBB LDL mediated mechanism, from the optimized batches DDI-NLC 4 or DDI-NLC 5.

6.4.2.2 Influence of DDI loading

DDI is a hydrophilic drug and as a consequence is likely to partition into the aqueous phase of dispersion from the lipid phase when the amount of API added to the lipid phase is relatively high. As described in Chapter 5 (Section 5.3.3.3) increasing the amount of DDI in NLC formulations from 6 mg to 100 mg led to a decrease in the EE of NLC. Consequently, the drug may be located on the surface of the nanoparticles and interfere with the surface properties e.g. ZP of the particles. Increasing the loading dose of DDI in NLC formulations and the effect on protein adsorption patterns were therefore investigated. The protein adsorption patterns of NLC formulations that contained 6 mg (batch DDI-NLC 1) and 100 mg (batch DDI-NLC 5) are shown on the 2-D gel images depicted in Figure 6.3. The relatively high EE of NLC for DDI of 78.34 ± 2.44% was observed for batch DDI-NLC 1 compared to a low 34.09 ± 2.41% observed for batch DDI-NLC 5.

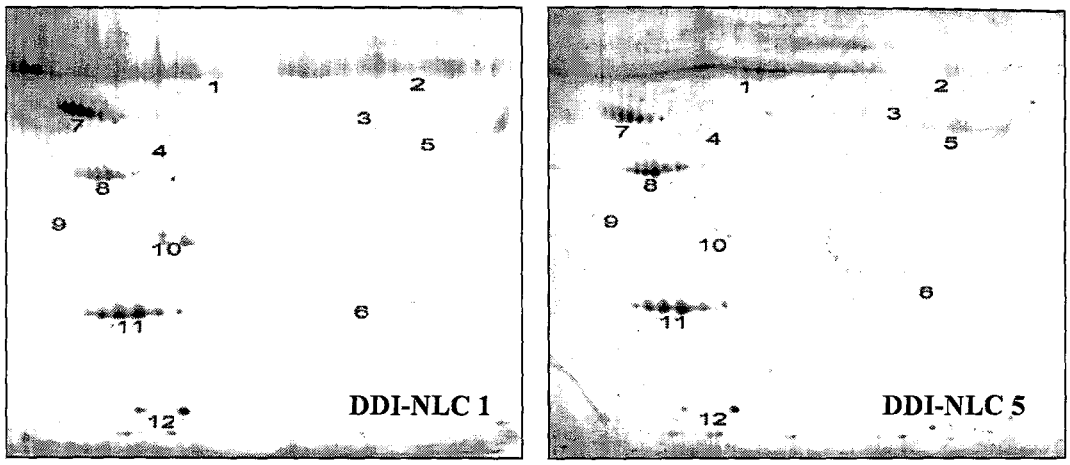

Figure 6.3. 2-D gel images depicting the influence of amout of DDI added to NLC formulations on the protein adsorption patterns of the nanoparticles: (1) Albumin, (2) Fibrinogen alpha chain, (3) Fibrinogen beta chain, (4) Fibrinogen gamma chain, (5) Immunoglobulin heavy chain gamma, (6) Immunoglobulin light chain, (7) alpha-1-antitrypsin, (8) Apolipoprotein A-IV, (9) Apolipoprotein J, (10) Apolipoprotein E, (11) Apolipoprotein A-I, (12) Transthryetin.

From a qualitative perspective there appears to be a similarity in the protein adsorption patterns for formulations DDI-NLC 1 and DDI-NLC 5. In other words, the nature of the proteins adsorbed on the surface of the particles for both formulations is similar. However, quantitative evaluation of the protein adsorption patterns for these formulations reveals something different. The relative percent volume of each protein as a function of the total amount of protein adsorbed onto the particles is shown in Figure 6.4.

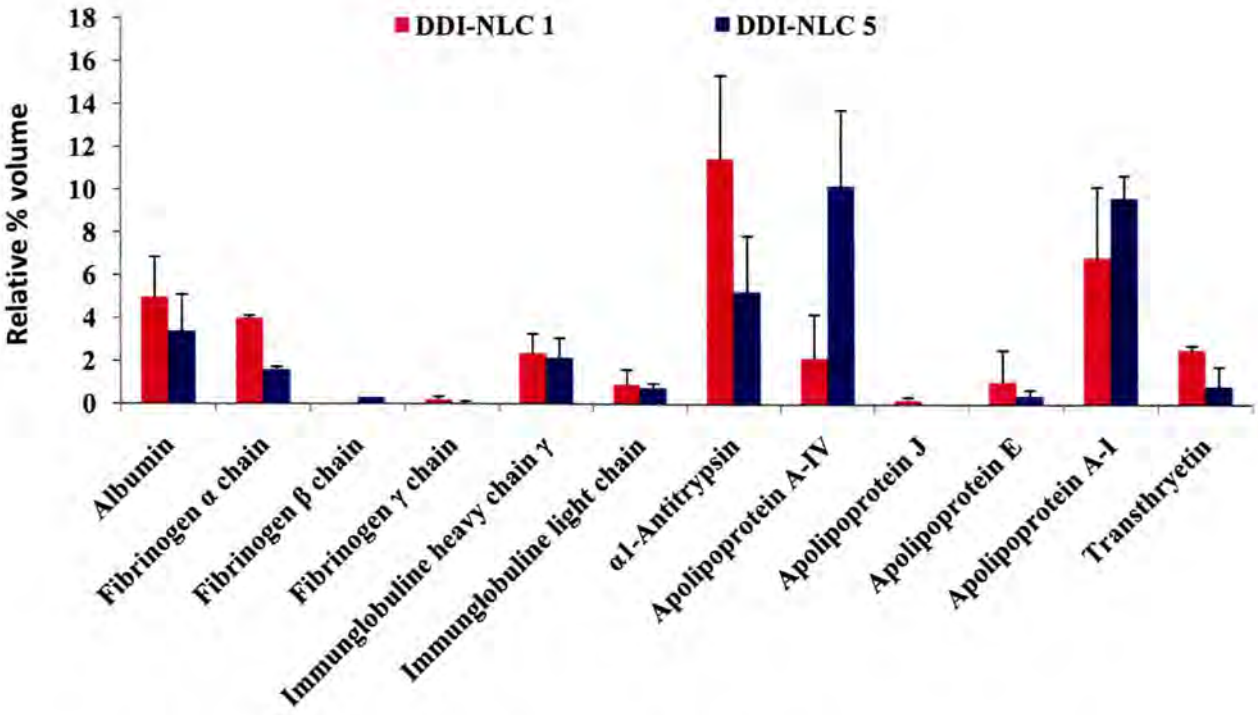

Figure 6.4. Relative percent volume of each protein adsorbed onto the surface of the NLC of batches DDI-NLC 1 and DDI-NLC 5 (n = 2)

On one hand, it is clear that the amount of Apo E adsorbed onto particles of batch DDI-NLC 1 is relatively great compared the amount of the same protein adsorbed onto particles of batch DDI-NLC 5. Therefore, it is possible that the presence of large amounts of DDI in the aqueous phase of the NLC formulation may have a negative impact on the potential to deliver DDI to the brain. The surface charge on the NLC particles in formulations may play a major role in the interaction between nanaparticles and Apo E proteins that are distributed in plasma. However, DDI is an amphoteric molecule and in solution, the positively charged functional groups of the molecule may interact and neutralize negative charges on the surfaces of nanoparticles, thereby decreasing the ability of additional Apo E proteins to interact with the surface of the particles. It is therefore vital that a drug that is added to a formulation is entrapped in particles to facilitate targeting of DDI-loaded NLC to the brain.

On the other hand, it should also be realized that the amounts of Apo A-I and Apo A-IV adsorbed onto particles of batch DDI-NLC 05 are higher than those adsorbed on particles of DDI-NLC 01. Therefore, although the amount of Apo E adsorbed onto the particles of DDI-NLC 05 is less, the presence of relatively large amount of Apo A-I and Apo A-IV may enhance the brain targeting of the small number of particles of DDI-NLC 05 that have

adsorbed Apo E. Consequently, the relatively small amount of DDI that has been encapsulated in DDI-NLC 05 is more than likely to be delivered to the CNS as efficiently as the relatively large amount of DDI that was encapsulated in DDI-NLC 01.

6.5 CONCLUSIONS

The protein adsorption patterns of DDI-loaded NLC reveal that the most stable NLC that was formulated contained three surfactants viz., Tween® 80, Lutrol® F68 and Solutol® HS15 (batch DDI-NLC 5) and has the potential to target the brain, *in vivo*. A formulation that was manufactured using Solutol® HS15 (batch DDI-NLC 4) may also have potential for brain targeting. However, batches DDI-NLC 2 and DDI-NLC 3, which are the formulations that were stabilized using Tween® 80 and Lutrol® F68, separately, failed to adsorb Apo E and therefore may not be suitable for the targeted delivery of DDI to the brain. In addition, these particles were relatively unstable and exhibited a large PS and PSD. Consequently, the failure of these formulations to adsorb Apo E may be unrelated to the surfactant content of the formulation, but is rather a consequence of the relatively small surface area that is associated with these particles. These studies also show that in addition to Tween® 80 that has already been shown to have the potential to target CDDS to the brain, Solutol® HS15 has the potential to achieve a similar objective.

It may be possible that Apo E only preferentially adsorbs to particles with a relatively large surface area, such as those manufactured in batches DDI-NLC 2 and DDI-NLC 5. The results also indicate that an increase in the amount of DDI in the aqueous phase of an NLC formulation will reduce the amount of Apo E proteins that are essential for targeted delivery and that can be adsorbed onto the surface of particles. Therefore although *in vitro* studies show that there is potential for the delivery of DDI to the brain using NLC, it is important to optimize the formulations further to achieve a higher payload capacity for DDI in the nanoparticles prior to determining the fate of DDI loaded nanoparticles *in vivo* and the universal use of NLC to deliver DDI to the brain.

These studies have revealed that DDI-loaded NLC that have been developed and optimized preferentially adsorb proteins, albeit *in vitro,* that are responsible for specific brain targeting *in vivo*. It is therefore clear that based on *in vitro* studies, DDI-loaded NLC have the potential to deliver DDI to the central nervous system. These are important results that may be used as

a platform for conducting *in vivo* studies to establish whether NLC could actually deliver DDI to the CNS. Once *in vivo* studies confirm the presence of DDI in the CNS, NLC could be used as a vehicle for the IV administration of DDI and other ARV agents, which could lead to the adequate management of HIV in the CNS and alleviate ADC in patients with HIV/AIDS and consequently, improve their quality of life.

CHAPTER 7

CONCLUSIONS

The lack of availability of antiretroviral (ARV) medicines in appropriate formulations for paediatric use is one of four obstacles that has been identified as a major hindrance to access of ARV therapy in paediatric patients, particularly in developing countries. Most of the paediatric ARV formulations currently available require children to take frequent doses of unpalatable syrups and/or solutions, many of which require strict adherence to cold chain maintenance and storage. Furthermore, many products have a limited shelf-life or a poor stability profile after opening that is exacerbated due to the harsh climatic conditions that prevail in many developing countries. In reality, the few children that are on ARV treatment in developing countries are reliant on the use of modified adult formulations in order to achieve appropriate therapy. The use of adult formulations requires manipulation of the dosage form by breaking or crushing by parents or care-givers which may lead to under or over-dosing if parents and providers are not supported and guided accordingly.

This practice can lead to resistance, the consequence of which is an impaired quality of life for the patient and a barrier in the fight against HIV/AIDS in paediatric patients. It is therefore imperative that research and development of new drug delivery systems for the oral administration of ARV agents to paediatric patients is conducted as a matter of urgency. Solid lipid nanoparticles (SLN) and nanostructured lipid carriers (NLC) are promising drug delivery systems that may be exploited as potential carriers of ARV drugs for oral administration to paediatric patients. SLN and NLC are colloidal drug carrier systems that are an alternate to polymeric nanoparticles and offer a number of advantages over other colloidal drug carriers, including the enhancement of stability and bioavailability of an API. The first objective of these studies was to investigate the feasibility of developing SLN and/or NLC as a carrier system for the oral administration of didanosine (DDI) to paediatric patients. DDI or 2′, 3′-dideoxyinosine is a dideoxy synthetic analogue of the purine nucleoside inosine that inhibits the replication of the human immunodeficiency virus (HIV). DDI acts as a competitive inhibitor of HIV reverse transcriptase or as a DNA chain terminator following intracellular phosphorylation to the active triphosphate *viz.,* 2′, 3′-dideoxyadenosine-5′-triphosphate. Consequently, DDI is indicated for the treatment of adult and paediatric patients

older than six (6) months who present with advanced HIV infections and who are intolerant to zidovudine (AZT) therapy or who have demonstrated significant clinical or immunologic deterioration whilst on AZT therapy. Didanosine is highly acid labile, one of the consequences of which is a reduction in bioavailability. In order to improve the acid stability and hence bioavailability of DDI the drug is formulated as chewable buffered tablets and powder for oral solution. However, DDI formulations have been reported to cause frequent diarrhoea and other gastrointestinal disturbances, which can be attributed to the use of buffer salts in the formulations. Therefore, there is a need to undertake research into the development of novel formulations that could enhance the acid stability and oral bioavailability of DDI and subsequently avoid the need for the use of buffered products.

Another major obstacle to the successful and/or adequate management of HIV in paediatric and adult patients with ARV agents such as DDI is the inability of the API to cross through the blood brain barrier (BBB) and maintain sufficient therapeutic concentrations in affected brain structures. The virus actively invades the central nervous system (CNS) and the microglial cells in the brain serve as reservoirs of the virus. The failure of ARV agents such as DDI to penetrate the CNS leads to the multiplication and accumulation of the virus, which has resulted in the emergence of HIV/AIDS-related complications such as AIDS dementia complex (ADC). Therefore there is a need for the formulation and development of drug delivery systems that have the ability to deliver anti-HIV agents to the CNS by circumventing the BBB in order to adequately manage HIV infection and inhibition of viral replication within the CNS. Consequently a second objective of this research was to use differential protein adsorption to determine the potential for DDI-loaded SLN and/or NLC to target the brain.

SLN and NLC consist of lipid matrices that are manufactured using physiologically well-tolerated lipids, such as triglycerides and have a mean PS ranging between 50-1000 nm. SLN and NLC are usually suspended in an aqueous medium and stabilized by use of one or more surface active agents. SLN and NLC exhibit advantages over other CDDS such as polymeric nanoparticles and fat emulsions, including their high tolerability *in vivo* [39], excellent oral bioavailability and the opportunity for site specific targeted drug delivery. In addition, the solid nature of SLN and NLC allows for the protection of API against chemical and/or photo degradation. Furthermore, drug release from these systems may be controlled and/or extended over a long period of time. The incorporation of an API into SLN or NLC depends

on factors such as the solubility of the API in the lipid, the physicochemical properties of the API, the lipids and surfactants used in addition to the production method used to manufacture the nanoparticles. Although there are different methods of producing SLN and/or NLC the inclusion of DDI into SLN and/or NLC was achieved using hot and/or cold high pressure homogenization techniques.

A number of different techniques may be used to fully elucidate the physical and chemical nature of SLN and/or NLC. Photon correlation spectroscopy (PCS) and laser diffractometry (LD) were used to measure the particle size (PS) and polydispersity indices (PI) of the nanoparticles. The zeta potential (ZP) of the nanoparticles, which is a parameter that can be used to predict and control the physical stability of aqueous dispersions of SLN and NLC on long-term storage, was evaluated using laser Doppler anemometry (LDA). Furthermore, data relating to the topographical profile of the nanoparticles were generated using scanning electron microscopy (SEM) and/or transmission electron microscopy (TEM). Diffential scanning calorimetry (DSC) and wide-angle X-ray scattering (WAXS) techniques were used to generate information relating to the crystalline nature and polymorphic modification, if any, of the SLN and/or NLC that were manufactured. The drug loading capacity (LC) and encapsulation efficiency (EE) of SLN and/or NLC were established using a validated HPLC method.

Prior to initiating pre-formulation and formulation development studies of DDI-loaded SLN and/or NLC, a reversed phase high performance liquid chromatography (RP-HPLC) method was developed and validated for the analysis of DDI and specifically to determine LC and EE of the nanoparticles for DDI. A major difficulty often encountered in the analysis API in lipid-based samples such as SLN and/or NLC is interference of formulation adjuvants, which are present in these somewhat complex formulations. RP-HPLC is a powerful and reliable analytical tool that can be used for the *in vitro* analysis of formulations of a complex nature. RP-HPLC has the ability to separate a compound of interest and allow for quantitative analysis but also can eliminate almost all interference challenges. A suitable RP-HPLC method was developed and validated for the quantitative analysis of DDI in formulations and for use in *in vitro* dissolution or release testing. Separation of DDI and acyclovir (ACV), the internal standard, was achieved using a Beckman® 60 Å, 4 µm (4.0 i.d. x 150 mm) analytical column packed with a dimethyl octylsilyl (C_8) bonded amorphous silica stationary phase. The mobile phase consisted of a binary mixture of MeOH and 25 mM potassium dihydrogen

phosphate (KH_2PO_4) buffer (pH 6.0) in a ratio of 8:92 and the separation was conducted at a flow rate of 1 ml/min. The samples were monitored with UV detection at a wavelength of 248 nm and the retention time of ACV and DDI were 4.20 and 11.32 minutes, respectively. The total run time for the analysis was approximately 10 minutes. The RP-HPLC analytical method was validated according to international guidelines and was found to be linear, precise, accurate, selective and sensitive and suitable for the quantitation of DDI quantitation. In addition, DDI was found to be stable in HPLC grade water (stock solutions) and in 25 mM KH_2PO_4 buffer (pH 6.0) (in-process samples) following storage for a maximum of seven (7) days and three (3) days at 4°C and 22°C respectively.

Formulation development of DDI-loaded SLN and/or NLC was preceded by formulation studies that were designed to investigate the thermal stability of DDI and to characterize excipients to facilitate the selection of suitable lipids for use in the manufacture of DDI-loaded SLN and/or NLC. The preferred method of manufacture of DDI-loaded SLN and/or NLC was hot high pressure homogenization (HPH). The use of this technique would necessitate exposure of DDI to a temperature of 85°C and which could lead to the degradation and/or alter the physicochemical properties of the compound. There are no published data that described the thermal stability of DDI and/or the potential for the molecule to undergo crystalline and/or polymorphic changes when it is exposed to relatively high temperatures. Therefore, TGA was used to establish the thermal stability of the drug and DSC and WAXS techniques were used to determine the crystalline and polymorphic nature of the drug prior to and following exposure to a temperature of 85°C for one hour. TGA data revealed that DDI was thermostable at temperatures not exceeding 163°C suggesting that DDI-loaded SLN and NLC could be manufactured using a hot high pressure homogenization technique. However, DSC and WAXS data showed that exposure of DDI to a temperature of 85°C may decrease the crystalline nature and alter the polymorphic nature of the drug. The noticeable polymorphic modification of DDI following exposure to a temperature of 85°C must be taken into consideration when evaluating DDI properties as dissolution rates.

Following the establishment of the thermostability of DDI, the selection of lipid excipients for use in the manufacture of DDI-loaded SLN and/or NLC was performed by evaluating the solubility of DDI in different solid and liquid lipids at 85°C. The determination of the solubility of DDI in lipid matrices was essential prior to attempting to incorporate the drug into solid lipid carriers, as the solubility of the API in lipid media would impact the drug LC

and EE of any solid lipid drug carriers that may be manufactured. DDI is a hydrophilic compound with an aqueous solubility of 27 mg/ml at a pH 6 and therefore as expected the drug was poorly soluble in the lipid media that were selected for evaluation. Nevertheless of all the lipids investigated, a combination of Precirol® ATO 5 and Transcutol® HP were shown to have best solubilising-potential for DDI. Consequently, Precirol® ATO 5 and Transcutol® HP were selected for use in the formulation of DDI-loaded SLN and/or NLC. However, the incorporation of DDI into SLN and/or NLC with suitable drug loading and EE posed formidable formulation challenges.

The methods used to manufacture SLN and/or NLC may change the polymorphic and crystalline state of the lipid nanoparticles in relation to those of the bulk lipid materials from which the nanoparticles are produced. Therefore the polymorphic and crystalline state of the bulk lipid materials, in addition to their state and interaction potential with DDI prior to and following exposure to heat were established prior to the production of DDI-loaded SLN and/or NLC. DSC and WAXS techniques were used to characterize the polymorphic nature and degree of crystallinity of Precirol® ATO 5 and eutectic mixtures of Precirol® ATO 5, Transcutol® HP and DDI prior to and following exposure to temperatures that were to be used in the production of SLN and/or NLC. The data generated reveal that Precirol® ATO 5 appeared to exist in the stable β-modification form prior to exposure to heat, however a mixture of both the α- and β-modification forms was detected following heating at 85°C for one hour. Consequently it is likely that SLN dispersed in an aqueous formulation manufactured using Precirol® ATO 5 would exist as a mixture of both the α- and β-polymorphic forms. The DSC and WAXS profiles of a binary mixture of Precirol® ATO 5 and DDI obtained prior to and following exposure to heat at 85°C for one hour showed no interaction between DDI and the solid lipid. In addition, the presence of a peak due to DDI both prior to and following heating with the binary mixture reveal that DDI is not completely dissolved in the Precirol® ATO 5 and remained in a crystalline state whilst dispersed in the solid lipid.

A pre-requisite for the development of NLC formulation is that the solid and liquid lipids used to manufacture the lipid matrix should be miscible at the specific concentrations to be used in the production of the delivery technology. Furthermore, the solid lipid matrix formed using two lipid components should possess an onset melting point that is higher than 40°C in order to ensure that the NLC remain in a solid state at both room and body temperatures.

Therefore, the miscibility of Precirol® ATO 5 and Transcutol® HP was investigated using different proportions of the solid and liquid materials. DSC was used to determine the melting behaviour and the miscibility of the different solid and liquid lipid blends. The results were used to establish the appropriate binary blend to use in the manufacture of the DDI-loaded NLC.

The optimum ratio that was deemed suitable for the manufacture of DDI-loaded NLC was found to be 80:20 (Precirol® ATO 5: Transcutol® HP). The two lipids were miscible and the resultant solid lipid matrix had a melting point higher than 40°C. The inclusion of Transcutol® HP with Precirol® ATO 5 changed the polymorphic form of the solid lipid from the stable β-modification to a form that exhibits the co-existence between the α- and β-polymorphic forms, thereby suggesting that NLC produced using this combination may exist in a combination of the α- and β polymorphic forms. These studies also show that that DDI existed in a crystalline state when dispersed at a drug concentrations of 5% w/w in this binary mixture of Precirol® ATO 5 and Transcutol® HP and that there was little or no interaction between DDI and the lipids.

The solubility of DDI in Transcutol® HP is relatively high compared to that in Precirol® ATO 5 and indicates that a solid lipid matrix prepared from a binary mixture of Precirol® ATO 5 and Transcutol® HP is likely to have a higher LC and EE than a matrix consisting of Precirol® ATO 5 alone. In addition, the potential for the solid lipid matrix to exist in the α- and/or β-modification forms when Transcutol® HP is added to Precirol® ATO 5 suggests that the expulsion of DDI from a solid lipid matrix during prolonged storage periods could be minimal. Consequently, the incorporation of DDI into NLC and not SLN was attempted. The incorporation of DDI into NLC was investigated by developing and manufacturing an aqueous nanoparticulate dispersion consisting of a 20% w/w lipid phase using hot high pressure homogenization and by applying a pressure of 800 bar for three homogenization cycles. Initial formulation development studies were designed to select a surfactant or combination of surfactants that would ensure the production of stable NLC formulations and that would entrap the hydrophilic DDI molecule. The selection of a surfactant system was based on the ability of the emulsifying agent to stabilize DDI-loaded NLC dispersions on the day of manufacture and following storage of the formulation for at least one week at 25°C. The results showed that NLC formulations in which Solutol® HS 15 alone (6% w/w) or where a surfactant system consisting of Tween® 80 (1% w/w), Lutrol® F68 (2% w/w) and

Solutol® HS 15 (3% w/w) were used were stable in terms of PS and PI. Nevertheless, the use of the ternary surfactant system was preferred to using Solutol® HS alone as Lutrol® F68 and Tween® 80 have been used to prolong the circulation time and to target delivery of nanocarriers to the brain successfully.

Following selection of a suitable surfactant system, aqueous DDI-free and DDI-loaded NLC were manufactured. DDI-loaded NLC formulations containing increasing amounts of the drug were produced, however due to the limited solubility of the compound in the lipid phase, only small amounts of API was used in the initial experiments. The impact of the amount of DDI added on the physicochemical properties of the nanoparticles, such as PS, PI, ZP, EE, polymorphism and degree of crystallinity was investigated following storage at 25°C for one day and two months. In addition, the shape and surface morphology of the particles were monitored in order to generate information on the topographical characteristics of the nanoparticles. The mean size of the particles was within the nanometre range with PCS values < 250 nm and d99% values < 400 nm for all NLC formulations. Furthermore, all NLC formulations had a narrow particle size distribution (PSD) irrespective of the amount of DDI that was added during manufacture. There was no direct or inverse relationship between the PS and PI on one hand and the amount of DDI added during manufacture of the nanoparticles on the other. Imaging analysis using TEM also confirmed that the size of the nanoparticles was within the nanometre range and that particles in these formulations were spherical and/or non-spherical (anisometric).

The ZP of NLC formulations was measured in water with the conductivity adjusted to 50 µS/cm and ranged from -18.4 and -11.4 mV when measured one day after manufacture and following storage for two months at 25°C. The addition of small amounts of DDI, *viz.* up 20 mg to the formulations appeared to increase the ZP values of the nanoparticles, however further increases in the amount of drug added, *viz.* 50-100 mg appeared to cause a decrease the ZP of the particles. This phenomenon was related to the amphoteric nature of DDI which seemed to affect the ZP value of the particles depending on the concentration of API used in the formulation. Nevertheless, these ZP values are not as negative as those used as a specification to indicate that NLC formulations are stable (ZP values of ≤ -30 mV). However, these formulations were stabilized using a combination of three non-ionic surfactants that stabilize emulsions by steric hindrance, therefore the stability of formulations may be inferred.

The results of DSC studies revealed that all formulations had a melting endotherm suggesting that the particles had recrystallized and that there were no supercooled melts present in all formulations that were manufactured. In addition, the melting peak of DDI was not detected in DSC thermograms of all formulations indicating that any drug that had been incorporated into the NLC was likely to be molecularly dispersed in that matrix. Furthermore, DSC studies showed that regardless of the storage period and the amount of DDI that was added to each NLC formulation, the onset temperatures, peak maxima (MP) and the melting enthalpies for the NLC formulations were all lower than that of the bulk lipid material, Precirol® ATO 5. These results were related to small PS of the nanocarriers produced in the formulations in comparison to the size of the particles present in the bulk lipid material. DSC analysis also revealed that the recrystalization index (RI) of the particles in all formulations was less than 100% following storage for one day, suggesting that the nanoparticles exist in the metastable α-polymorphic modification. However following storage for two months, the RI values for particles in all formulations increased slightly, suggesting that that the particles may be reverting to the stable β-modification form from the metastable α-polymorphic form.

WAXS analysis revealed that NLC formulations had similar refraction patterns irrespective of the amount of DDI added and the storage period of each formulation. However, the Bragg's distance of 0.467 nm for samples stored for one day and 0.476 for samples stored for two months under the same conditions suggest that the particles existed in the β-polymorphic modification one day after manufacture and remained similar in form for the two month period of storage. In contrast to the DSC data, WAXS analysis did not indicate the existence of the α-polymorphic modification one day after production or two months following storage of the formulations. WAXS technique seems to be a less sensitive analytical tool compared to DSC in detecting the presence of α-polymorphic modifications.

The EE decreased with an increase in the amount of DDI loaded in NLC formulations. Furthermore the amount of DDI entrapped in the nanoparticles of all formaulations remained constant following storage at 25°C for two months. This may be due to the slow recrystallization of nanoparticles and hence the slow conversions of the particles from the α-polymorphic to β-polymorphic form thereby minimizing the expulsion of the drug from the lipid matrix. Consequently, despite the relatively low entrapment efficiency of DDI, the formulations appear to be chemically stable during storage. The limited solubility of DDI in

the lipid phase is the primary reason for the low EE observed. Therefore, in order to increase the saturation solubility of DDI in the lipid phase a novel approach was used to increase the dissolution velocity of the drug in the lipid. The increase in solubility was achieved by PS reduction of DDI using hot high pressure homogenization.

The DDI was dispersed in hot Transcutol® HP and the PS of DDI was reduced gradually using high pressure homogenization at 85°C *in situ*. The PS reduction process was monitored by microscopic visualization of samples taken at different homogenization pressures and number of cycles. The microscopic images collected during these studies revealed that DDI particles gradually decreased in size as had been expected. The DDI-containing lipid nanosuspension produced was then used to manufacture DDI-loaded NLC using cold high pressure homogenization. This technique proved to be partially successful in that an increased amount of DDI was entrapped in the NLC. The major drawback was that a rapid alteration in the crystallinity of the particles occurred during storage resulting in the expulsion of DDI from the nanoparticles. In addition, the nanoparticles produced using this approach were larger than those produced previously and the formulations appeared unstable following storage at 25°C for two months as the particles had increased in size and had formed microparticles. This phenomenon may be a consequence of Ostwald ripening due to a relatively large PS distribution of the particles in the formulation.

Following the manufacture and optimization of DDI-loaded NLC, *in vitro* differential protein adsorption patterns of the formulation were investigated using two-dimensional polyacrylamide gel electrophoresis (2-D PAGE) in order to establish the potential for NLC to deliver DDI to the brain. These studies were carried out using NLC that were loaded with small amounts of DDI as they are more stable, have a small PS and low PI. The 2-D PAGE analysis revealed that the nanoparticles in NLC formulations stabilized using Solutol® HS alone or the optimized ternary surfactant system consisting of Solutol® HS, Tween® 80 and Lutrol® F68 preferentially adsorbed proteins such as Apo E that are responsible for the specific targeting of nanocarriers to the brain. Particles stabilized with Tween® 80 and Lutrol® F68, which have been shown to preferentially adsorb Apo E previously, did not do so in these studies. The lack of adsorption of Apo E may be related to the PS and hence surface area of the particles rather than the nature of the surfactant used to stabilize the nanoparticles. However, these findings have revealed that in addition to Tween® 80 that has already been

shown to have the potential to target CDDS to the brain, Solutol® HS15 has the potential to achieve a similar objective.

This research has shown that it is feasible to incorporate DDI into NLC using hot high pressure homogenization when small amounts of DDI are included in NLC formulations. Furthermore it is possible to load a relatively large amount of DDI to the formulations when the PS of DDI is reduced using hot high pressure homogenization following dispersion of the compound in Transcutol® HP. The resulting product was then transformed into NLC using cold high pressure homogenization with the result that a relatively high EE and LC of NLC was achieved. However the short-term and long-term stability of this formulation must be established and improved and this may be achieved by narrowing the PS distribution which would in turn minimize particle growth through Ostwald ripening. The reduction of the PI may be achieved by milling the powdery lipid materials using ball or mortar milling, prior to high pressure homogenization in a cold surfactant solution. In addition, the *in vitro* release rate of DDI from NLC must be evaluated using conventional or novel methods prior to wide spread use of NLC as a carrier for DDI.

The stability of the formulations may be enhanced by increasing the concentration of the surfactant(s) used although the palatability of the product for paediatric patients may be adversely affected. The LC and EE of NLC may be further enhanced by increasing the amount of DDI that is added to Transcutol® HP prior to size reduction. In this manner, an increase in the saturation solubility of DDI in the liquid lipid may be achieved. An increase in the amount of DDI incorporated into NLC and improvement of the stability of the vehicle are necessary prior to investigating *in vitro* stability of DDI in acidic media. Following optimization of stability and loading capacities, further investigation into the use of NLC for the delivery of DDI to paediatric patients can be undertaken. This innovative solid lipid carrier system has the potential for use as an aqueous-based lipid nanosuspension for the oral administration of DDI to paediatric patients.

The preferential adsorption of proteins such as Apo E onto the surface of DDI-loaded NLC *in vitro* is an indication that these NLC can be used to target the brain to deliver the drug to the CNS. Although it is clear that the amount of DDI loaded to the system must be increased, the *in vitro* data may be used as a platform for conducting *in vivo* studies to establish whether NLC can actually deliver the hydrophilic ARV to the CNS. Should *in vivo* studies confirm

the presence of DDI in the CNS, the use of NLC in parenteral formulations for the administration of ARV agents may be possible. This approach may be a major breakthrough and is likely to improve the management of HIV substantially. In particular the ability to deliver ARV drugs to the CNS would permit the treatment of ADC in patients with HIV/AIDS and consequently, improve their quality of life.

APPENDIX I

SILVER STAIN PROTOCOL

Step no	Reagent	Volume [ml]	Duration [min]
1	Fixative A: 40% ethanol/10% acetic acid (v/v)	400	60
2	Fixative B: 10% ethanol/5% acetic acid (v/v)	400	30
3	Fixative B: 10% ethanol/5% acetic acid (v/v)	400	30
4	Oxidizer	200	10
5	Deionised water	400	10
6	Deionised water	400	10
7	Deionised water	400	10
		repeat steps 5-7 until all the yellow colour is removed from the gels	
8	Silver reagent	200	30
9	Deionised water	400	2
10	Developer	200	~ 30 sec
		develop until solution turns yellow or until brown "smoky" precipitate appears	
11	Developer	200	~5
12	Developer	200	~5
13	Stop 5% acetic acid (v/v)	400	~5

APPENDIX II

BATCH PRODUCTION RECORDS

Note that only the production records for Batches DDI-NLC 09 and DDI-NLC 10 are included here. The batch production records for all other formulations manufactured and assessed during formulation development and optimization studies are available on request.

RHODES UNIVERSITY, Faculty of Pharmacy, Grahamstown, South Africa

Manufactured at FREE UNIVERSITY BERLIN, Department of Pharmaceutics, Biopharmaceutics and NutriCosmetics, Berlin, Germany

BATCH PRODUCTION RECORD

Product name: DDI-loaded NLC **Page 1 of 5**

Batch ID: DDI-NLC 05 **Batch size:** 40 g

MANUFACTURING APPROVALS

Batch record issued by_____ **Date**_____

Master record issued by_____ **Date**_____

RHODES UNIVERSITY, Faculty of Pharmacy, Grahamstown, South Africa

Manufactured at FREE UNIVERSITY BERLIN, Department of Pharmaceutics, Biopharmaceutics and NutriCosmetics, Berlin, Germany

BATCH PRODUCTION RECORD

Product name: DDI-loaded NLC **Page 2 of 5**

Batch ID: DDI-NLC 09 **Batch size:** 40 g

Item	Material	Quantity (% w/w)	Amount/ Batch (g)	Amount dispensed (g)	Dispensed by	Checked by
1	DDI	0.250	0.100	0.10078		
2	Tween® 80	1.00	2.00	2.086		
3	Lutrol® F68	2.00	0.400	0.401		
4	Solutol® HS 15	3.00	1.20	1.208		
5	Transcutol® HP	5.00	2.00	2.086		
6	Precirol® ATO 5	14.75	5.90	5.902		
7	Aqua	74.0	29.6	29.60		

RHODES UNIVERSITY, Faculty of Pharmacy, Grahamstown, South Africa

Manufactured at FREE UNIVERSITY BERLIN, Department of Pharmaceutics, Biopharmaceutics and NutriCosmetics, Berlin, Germany

BATCH PRODUCTION RECORD

Product name: DDI-loaded NLC

Batch ID: DDI-NLC 09

Batch size: 40 g

EQUIPMENT VERIFICATION			
Description	**Type**	**Verified by**	**Confirmed by**
High speed homogenizer	Model T25 Ultra-Turrax T25		
High pressure homogenizer	Micron LAB 40 APV		

RHODES UNIVERSITY, Faculty of Pharmacy, Grahamstown, South Africa

Manufactured at FREE UNIVERSITY BERLIN, Department of Pharmaceutics, Biopharmaceutics and NutriCosmetics, Berlin, Germany

BATCH PRODUCTION RECORD

Product name: DDI-loaded NLC **Page 4 of 5**

Batch ID: DDI-NLC 09 **Batch size:** 40 g

	MANUFACTURING PROCEDURE			
Step	**Procedure**	**Time**	**Done by**	**Checked by**
1	Weigh all the materials			
2	Heat water (item 7) to 85°C in a beaker and disperse Lutrol® F68 (Item 3) into the hot water until a clear solution is obtained. Maintain the temperature of the resultant aqueous phase at 85°C.			
3	Heat lipid phase components together: Precirol® ATO 5 (item 6), Transcutol® HP 5 (item 5), Tween® 80 (item 2) and Solutol® HS 15 (item 4) to 75°C until a clear melt is obtained. Disperse DDI (item 1) in the lipid melt and maintain the temperature at 85°C.			
4	Disperse the heated aqueous phase in the molten lipid phase using high speed stirring at 8000 rpm to form a pre-emulsion.			
5	Homogenize the pre-emulsion at 85°C using the high pressure homogenizer by applying three homogenization cycles at 800 bar			
6	Fill and seal the hot o/w nanoemulsion immediately in siliconized glass vials and allow the product to cool to room temperature (25°C).			
7	Store all samples at room temperature for at least 24 hours prior to characterization.			

RHODES UNIVERSITY, Faculty of Pharmacy, Grahamstown, South Africa

Manufactured at FREE UNIVERSITY BERLIN, Department of Pharmaceutics, Biopharmaceutics and NutriCosmetics, Berlin, Germany

BATCH PRODUCTION RECORD

Product name: DDI-loaded NLC

Batch ID: DDI-NLC 09

Batch size: 40 g

SIGNATURE AND INITIAL REFERENCE			
Full Name (Print)	**Signature**	**Initials**	**Date**

RHODES UNIVERSITY, Faculty of Pharmacy, Grahamstown, South Africa

Manufactured at FREE UNIVERSITY BERLIN, Department of Pharmaceutics, Biopharmaceutics and NutriCosmetics, Berlin, Germany

BATCH PRODUCTION RECORD

Product name: DDI-loaded NLC **Page 1 of 5**

Batch ID: DDI-NLC 10 **Batch size:** 40 g

MANUFACTURING APPROVALS

Batch record issued by_____ **Date**_____

Master record issued by_____ **Date**_____

RHODES UNIVERSITY, Faculty of Pharmacy, Grahamstown, South Africa

Manufactured at FREE UNIVERSITY BERLIN, Department of Pharmaceutics, Biopharmaceutics and NutriCosmetics, Berlin, Germany

BATCH PRODUCTION RECORD

Product name: DDI-loaded NLC **Page 2 of 5**

Batch ID: DDI-NLC 10 **Batch size:** 40 g

Item	Material	Quantity (% w/w)	Amount/ Batch (g)	Amount dispensed (g)	Dispensed by	Checked by
	PRODUCT A	-	-	-		
1	DDI	20.0	8.00	8.013		
2	Tween 80	2.00	0.80	0.808		
3	Transcutol® HP	78.0	31.20	31.19		
	PRODUCT B	-	-	-		
4	Product A	25.0	12.5	12.631		
5	Precirol ATO 5	75.0	37.5	37.571		
	PRODUCT C					
6	Product B	20.0	8.00	8.014		
7	Tween® 80	0.90	0.36	0.3602		
8	Lutrol® F68	2.00	0.80	0.8060		
9	Solutol® HS 15	3.00	1.20	1.206		
10	Transcutol® HP	1.10	0.44	0.4412		
11	Aqua.	73.00	29.20	29.402		

RHODES UNIVERSITY, Faculty of Pharmacy, Grahamstown, South Africa

Manufactured at FREE UNIVERSITY BERLIN, Department of Pharmaceutics, Biopharmaceutics and NutriCosmetics, Berlin, Germany

BATCH PRODUCTION RECORD

Product name: DDI-loaded NLC **Page 3 of 5**

Batch ID: DDI-NLC 10 **Batch size:** 40

g

EQUIPMENT VERIFICATION			
Description	**Type**	**Verified by**	**Confirmed by**
High speed homogenizer	Model T25 Ultra-Turrax® T25		
High pressure homogenizer	Micron LAB® 40 APV		

RHODES UNIVERSITY, Faculty of Pharmacy, Grahamstown, South Africa

Manufactured at FREE UNIVERSITY BERLIN, Department of Pharmaceutics, Biopharmaceutics and NutriCosmetics, Berlin, Germany

BATCH PRODUCTION RECORD

Product name: DDI-loaded NLC **Page 4 of 5**

Batch ID: DDI-NLC 10 **Batch size:** 40 g

	MANUFACTURING PROCEDURE			
Step	**Procedure**	**Time**	**Done by**	**Checked by**
1	Weigh all the materials			
2	Heat Transcutol® HP 5 (item 3) and Tween® 80 (Item 2) to 85°C in a beaker and disperse DDI (Item 1) into the liquid lipid using high speed homogenizer to form a coarse microsuspension (Product A).			
3	Homogenize Product A using a high pressure homogenizer for three or five cycles at relatively low pressures of 100, 500 and 1000 bar e.g. 3x100, 5x500 and 5x1000 bar			
4	Homogenize Product A further using high pressure homogenization at 1500 bar for a total of 20 homogenization cycles to form Formulation B.			
5	Mix Product A (item 4) and Precirol® ATO 5 (Item 5) and heat the mixture to 85°C to form Product B.			
6	Pour the hot product B into liquid nitrogen immediately and crush the dried lipid materials in a mortar using a pestle to produce a fine powder.			
7	Pass the fine powder through a 200 µm sieve to produce lipid microparticles of 200 µm and less in size.			
8	Disperse the powdery lipid microparticles in a cold (5°C) solution containing Tween® 80 (item 7, Solutol® HS 15 (item 9) and Lutrol® F68 (item 8) using high speed stirrer at a speed of 8 000 rpm for 1 min to produce a coarse pre-emulsion.			
9	Homogenize the coarse pre-emulsion using a high pressure homogenizer for three (3) cycles at relatively low pressures of 100, 250, 500 and 1000 bar e.g. 3x100, 3x250, 3x500 and 3x1000 bar.			
10	Homogenize the pre-emulsion further using high pressure homogenization at 1500 bar for a total of five (5) homogenization cycles to form a hot o/w nanoemulsion (Product C)			
11	Fill and seal Product C in siliconized glass vials immediately and allow the product to cool to room temperature (25°C).			
12	Store the product sample at room temperature for at least 24 hours prior to characterization.			

RHODES UNIVERSITY, Faculty of Pharmacy, Grahamstown, South Africa

Manufactured at FREE UNIVERSITY BERLIN, Department of Pharmaceutics, Biopharmaceutics and NutriCosmetics, Berlin, Germany

BATCH PRODUCTION RECORD

Product name: DDI-loaded NLC **Page 5 of 5**

Batch ID: DDI-NLC 10 **Batch size:** 40 g

SIGNATURE AND INITIAL REFERENCE			
Full Name (Print)	**Signature**	**Initials**	**Date**

APPENDIX III

BATCH SUMMARY REPORTS

Note that only the batch summary reports for Batches DDI-NLC 09 and DDI-NLC 10 are included here. The batch summary reports for all other formulations manufactured and assessed during formulation development and optimization studies are available on request.

RHODES UNIVERSITY, Faculty of Pharmacy, Grahamstown, South Africa

Manufactured at FREE UNIVERSITY BERLIN, Department of Pharmaceutics, Biopharmaceutics and NutriCosmetics, Berlin, Germany

BATCH SUMMARY REPORT

Formulator: Kasongo Wa Kasongo
Product: DDI-loaded NLC
Batch ID: DDI-NLC 09
Batch Size: 40 g
Manufacturing Date: 29-08-2009

Item	Material	Quantity (% w/w)	Amount/ Batch (g)	Amount dispensed (g)
1	DDI	0.250	0.100	0.10078
2	Tween® 80	1.00	2.00	2.086
3	Lutrol® F68	2.00	0.400	0.401
4	Solutol® HS 15	3.00	1.20	1.208
5	Transcutol® HP	5.00	2.00	2.086
6	Precirol® ATO 5	14.75	5.90	5.902
7	Aqua	74.0	29.6	29.60

Production equipment used:
High speed homogenization: one (1) minute at 8000 rpm at 85°C
Hot high pressure homogenization: Three (3) homogenization cycles at 800 bar at 85°C.

Summary of some of the parameters evaluated:

FORMULATION	DDI-NLC 09	
Parameter	One day	Two months
PCS (nm)	148 ± 3	203 ± 7
PI	0.195 ± 0.037	0.321 ± 0.0586
d50% (µm)	0.149	0.141
d90% (µm)	0.232	0.230
d95% (µm)	0.283	0.253
d99% (µm)	0.308	0.304
Span value	1.00	1.04
ZP (mV)	-13.3 ± 0.90	-11.7 ± 0.36
EE (%)	34.09 ± 2.41	33.02 ± 1.53

Comments / Observations

RHODES UNIVERSITY, Faculty of Pharmacy, Grahamstown, South Africa

Manufactured at FREE UNIVERSITY BERLIN, Department of Pharmaceutics, Biopharmaceutics and NutriCosmetics, Berlin, Germany

BATCH SUMMARY REPORT

Formulator: Kasongo Wa Kasongo
Product: DDI-loaded NLC
Batch ID: DDI-NLC 10
Batch Size: 40 g
Manufacturing Date: 10-09-2009

Item	Material	Quantity (% w/w)	Amount dispensed (g)
	PRODUCT A	-	-
1	DDI	20.0	8.013
2	Tween 80	2.00	0.808
3	Transcutol® HP	78.0	31.19
	PRODUCT B	-	-
4	Product A	25.0	12.631
5	Precirol ATO 5	75.0	37.571
	PRODUCT C		
6	Product B	20.0	8.014
7	Tween® 80	0.90	0.3602
8	Lutrol® F68	2.00	0.8060
9	Solutol® HS 15	3.00	1.206
10	Transcutol® HP	1.10	0.4412
11	Aqua.	73.00	29.402

Production equipment used:
High speed homogenization: one (1) minute at 8000 rpm at 85°C
Hot high pressure homogenization: 3x100, 5x500, 5x1000 and 20x1500 bar
Hot high pressure homogenization: 3x100, 3x250, 3x50, 5x1000 and 5x1500 bar

Summary of some of the parameters evaluated

BATCH	DDI-NLC 10	
Parameter	**One day**	**Two months**
PCS (nm)	201 ± 8	591.1 ± 9
PI	0.440 ± 0.064	0.397 ± 0.236
d50% (µm)	0.260	0.155
d90% (µm)	0.406	4.386
d95% (µm)	1.349	7.604
d99% (µm)	3.014	19.114
Span value	4.746	27.72
ZP (mV)	-26.4 ± 0.8	-29.4 ± 0.2
EE (%)	51.58 ± 1.31	49.53 ± 0.19

Comments / Observations

REFERENCES

1. UNICEF/WHO technical consultation: improving access to appropriate paediatric ARV formulations. 1-13. 2004. The United Nations Children's Fund (UNICEF) and The World Health Organization (WHO). Last accessed on 3-10-2008.
2. Antivirals: didanosine. In: S. C. Sweetman (editor): *Martindale: the complete drug reference*. London: The Pharmaceutical Press; 2002, pp. 618-619.
3. M. N. Nassar, T. Chen, M. J. Reff and S. N. Agharkar: Didanosine. In: H. G. Brittain (editor): *Analytical Profiles of Drug Substances and Excipients*. New York: Academic Press Inc.; 1993, pp. 185-227.
4. O. Bekers, J. H. Beijnen, M. J. Tank, D.M. Burger, P. L. Meenhorst, A. J. Lombarts and W.J. Underberg: 2'3'-dideoxyinosine (ddI): its chemical stability and cyclodextrin complexation in aqueous media. *Journal of Pharmaceutical and Biomedical Analysis* 1993; **11**(6):489-493.
5. B. D. Damle, S. Kaul, D. Behr and C. Knupp: Bioequivalence of two formulations of didanosine encapsulated enteric-coated beads and buffered tablet, in healthy volunteers and HIV-infected subjects. *Journal of Clinical Pharmacology* 2002; **42**(7):791-797.
6. B. D. Anderson, M. B. Wygant, T. X. Xiang, W. A. Waugh and V. J. Stella: Preformulation solubility and kinetic studies of 2',3'-dideoxypurine nucleosides: potential anti-AIDS agents. *International Journal of Pharmaceutics* 1988; **45**(1-2):27-37.
7. R. T. Dodge, K. W. Shipp and G. D. Miralles: Improved gastrointestinal tolerance and palatability of didanosine in adults by the use of pediatric powder formulation. *Journal of the Association of Nurses in AIDS Care* 1998; **9**(5):27-31.
8. Electronic Package Insert: Videx® (didanosine): chewable/dispersible buffered tablets, buffered powder for oral solution, paediatric powder for oral solution. http://www.fda.gov/cder/foi/label/2001/20155s25lbl.pdf , 1-15. 2007. Bristol-Meyers Squibb Company. Last accessed on 10-02-2009.
9. C. M. Perry and J. A. Balfour: Didanosine: an update on its antiviral activity, pharmacokinetic properties and therapeutic efficacy in the management of HIV disease. *Drugs* 1996; **52**(12):928-962.
10. C. M. Perry and S. Noble: Didanosine: an updated review of its use in HIV infection. *Drugs* 1999; **58**(6):1099-1135.
11. Antivirals for systemic use: didanosine. In: C. J. Gibbon (editor), *SAMF: South African Medicines Formulary*. Cape Town: Health and Medical Publishing Group; 2001, p. 322.
12. B. D. Damle, V. Mummaneni, S. Kaul and C. Knupp: Lack of effect of simultaneously administered didanosine encapsulated enteric coated bead formulation (Videx EC) on oral absorption of indinavir, ketoconazole, or ciprofloxacin. *Antimicroial Agents and Chemotherapy* 2002; **46**(2):385-391.
13. Electronic Package Insert: Videx® EC (didanosine) delayed release capsules, enteric-coated beadlets. http://packageinserts.bms.com/pi/pi_videx_ec.pdf. 2007. Bristol-Meyers Squibb Company. Last accessed on 05-06-2008.

14. Didanosine (ddI, Videx,Videx EC): a simple factsheet from the AIDS Treatment Data Network. http://www.atdn.org/simple/dida.html. 2006. Aids Treatment Data Network. Last accessed on 05-06-2008.

15. U.S. Food and Drug Administration, Center for Drug Evaluation and Reseach: Drugs@FDA: Drug Details, Drug Name (s): Videx EC. htt://www.accessdata.fda.gov/scripts/cder/drugsatfda/index.cfm?fuseaction=search. DrugsDetails . 2008. FDA/Center for Drug Evaluation and Research. Last accessed on 06-06-2008.

16. Electronic Package Insert: Videx® (didanosine): Paediatric powder for oral solution. http://packageinserts.bms.com/pi/pi_videx.pdf. 2007. Bristol-Meyers Squibb Company. Last accessed on 11-02-2009.

17. P. Portegies: AIDS dementia complex: a review, *Journal of Acquired Immune Deficiency Syndromes* 1994; 7(2):S38-S49.

18. M. B. Yatvin, W. Li, M. J. Meredith and M. A. Shenoy: Improved uptake and retention of lipophilic prodrug to improve treatment of HIV. *Advanced Drug Delivery Reviews* 1999; **39**(1-3):165-182.

19. P. Portegies, R. H. Enting, J. de Gans, P. R. Algra, M. M. Derix, J. M. Lange and J. Goudsmit: Presentation of AIDS dementia complex: 10 years of follow-up in Amsterdam, The Netherlands. *AIDS* 1993; 7(5):669-675.

20. J. C. McArthur, O. A. Selnes, J. D. Glass, D. R. Hoover and H. Bacellar: HIV dementia: Incidence and risk factors. In: R. W. Price, S. W. Perry (editors): *HIV, AIDS and The Brain.* New York: Raven Press; 1994, pp. 251-272.

21. M. Perices and D. A. Cooper: Neuropsychological investigation of patients with AIDS and ARC. *Journal of Acquired Immune Deficiency Syndromes* 1990; **36**(2):555-564.

22. R. Price and B. Brew: AIDS commentary: The AIDS dementia complex. *Journal of Infectious Diseases* 1988; **158**(5):1079-1083.

23. B. J. Brew: AIDS dementia complex. *Neurologic Clinics* 1999; **17**(4):861-881.

24. L. K. Schrager and M. P. D'Souza: Cellular and anatomical reservoirs of HIV-1 in patients receiving potent antiretroviral combination therapy. *Journal of American Medical Association* 1998; **280**(1):67-71.

25. C. Schwarz, W. Mehnert, J. S. Lucks and R. H. Müller: Solid lipid nanoparticles (SLN) for controlled drug delivery. I. Production, characterization and sterilization. *Journal of Controlled Release* 1993; **30**:83-96.

26. A. zur Mühlen, C. Schwarz and W. Mehnert: Solid lipid nanoparticles (SLN) for controlled drug delivery-drug release and release mechanism. *European Journal of Pharmaceutics and Biopharmaceutics* 1998; **45**(2):149-155.

27. R. H. Müller, K. Mäder and S. Gohla: Solid lipid nanoparticles (SLN) for controlled drug delivery-a review of the state of the art. *European Journal of Pharmaceutics and Biopharmaceutics* 2000; **50**(1):161-177.

28. R. H. Müller, W. Mehnert, J. S. Lucks, C. Schwarz, A. zur Mühlen, H. Wyhers, C. Freitas and D. Rühl: Solid lipid nanoparticles (SLN): an alternative colloidal carrier system for controlled drug delivery. *European Journal of Pharmaceutics and Biopharmaceutics* 1995; **41**(1):62-69.

29. W. Mehnert and K. Mäder: Solid lipid nanoparticles: production, characterization and applications. *Advanced Drug Delivery Reviews* 2001; **47**(2-3):165-196.

30. R. H. Müller, M. Radtke and S. A. Wissing: Nanostructured lipid matrices for improved microencapsulation of drugs. *International Journal of Pharmaceutics* 2002; **242**(1-2):121-128.

31. M. Radtke, E. B. Souto and R. H. Müller: Nanostructured lipid carriers: A novel generation of solid lipid drug carriers. *Pharmaceutical Technology Europe* 2005; **17**(4):45-50.

32. M. Radtke and R. H. Muller: Nanostructured lipid carriers. *New Drugs* 2001; **2**:48-52.

33. R. H. Müller, M. Radtke and S. A. Wissing: Solid lipid nanoparticles (SLN) and nanostructured lipid carriers (NLC) in cosmetic and dermatological preparations. *Advanced Drug Delivery Reviews* 2002; **54**(1):S131-S155.

34. S. A. Wissing, O. Kayser and R. H. Müller: Solid lipid nanoparticles for parenteral drug delivery. *Advanced Drug Delivery Reviews* 2004; **58**(9):1257-1272.

35. C.O. Olbrich, A. Gessner, O. Kayser and R. H. Müller: Lipid-drug conjugate (LDC) nan oparticles as novel carrier system for the hydrophilic antitrypanosomal drug diminazenediaceturate. *Journal of Drug Targetting* 2002; **10**(5):387-396.

36. J. You, F. Wan, F. de Cui, Y. Sun, Y. Z. Du and F. Q. Hu: Preparation and characterization of vinorelbine bitartrate-loaded solid lipid nanoparticles. *International Journal of Pharmaceutics* 2007; **343**(1-2):270-276.

37. R. Cavalli, O. Caputo, M. Radtke and M. R. Gasco: Solid lipospheres of doxorubicin and idarubicin. *International Journal of Pharmaceutics* 1993; **89**:R9-R12.

38. Didanosine: *The Bristish Pharmacopoeia 2005: incorporating the requirements of the 5th Edition of the European Pharmacopoeia 2004 as amended by Supplements 5.1 and 5.2*. London: The Stationary Office; 2005, pp. 635-637.

39. Didanosine. In: A. C. Moffat, M. D. Osselton and B. Widdop (editors): *Clarke's Analysis of Drugs and Poisons*. London: The Pharmaceutical Press; 2004, pp. 908-909.

40. E. De Clercq: Antiviral drugs in current clinical use. *Journal of Clinical Virology* 2004; **30**(2):115-113.

41. Didanosine. In: M. J. O'Neil, P. E. Heckelman, C. B. Koch and K.J.Roman (editors): *The Merck Index: An Encyclopedia of Chemicals, Drugs, and Biologicals*. Whitehouse Station, NJ, USA: Merck and Co., Inc.; 2006, p. 525.

42. T. L. Lemke. Antiviral agents and protease inhbitors: Didanosine. In: D. A. Williams and T. L. Lemke (editors): *Foye's Principles of Medicinal Chemistry*. Baltimore: Lippincott Williams & Wilkins; 2002, pp. 968-969.

43. C. Sanchez-Lafuente, A. M. Rabasco, J. Alvarez-Fuentes and M. Fernandez-Arevalo: Eudragit® RS-PM and Ethocel® 100 Premium: influence over the behavior of didanosine inert matrix system. *IL Farmaco* 2002; **57**(8):649-656.

44. K. Gallicano: Antiretroviral-drug concentration in semen. *Antimicrob Agents Chemother* 2000; **44**(4):1117-1118.

45. A. D. M. Kashuba, J. R. Dyer, L. M. Kramer, R. H. Raasch, J. J. Eron and M. S. Cohen: Antiretroviral-drug concentrations in semen: implications for sexual transmission of human immunodeficiency virus type 1. *Antimicrob Agents Chemother* 1999; **43**(8):1817-1826.

46. A. P. Cheung and D. Kenney: Partition coefficients and capacity factors of some nucleoside analogues. *Journal of Chromatography A* 1990; **506**:119-131.

47. S. F. Donovan and M. C. Pescatore: Method for measuring the logarithm of the octanol-water partition coefficient by using short octadecyl-poly(vinyl alcohol) high-performance liquid chromatography columns. *Journal of Chromatography A* 2002; **952**(1-2):47-61.

48. J. J. Ellington and T. L. Floyd: Measuring octanol/water partition coefficients by the "slow-stirring" method. Environmental Research Brief, EPA/600/S-96/005, 1-4. 1995. Athens, United States Environmental Protection Agency, Research and Development.

49. S. K. Poole and C. F. Poole: Separation methods for estimating octanol-water partion coefficients. *Journal of Chromatography B* 2003; **797**(1-2):3-19.

50. J. T. Anderson and W. Schrader: A method for measuring 1-octanol-water partition coefficients. *Analytical Chemistry* 1999; **71**(16):3610-3614.

51. Antivirals: didanosine. In: G. W. A. Milne (editor): *Drugs: Synonyms and Properties*. Aldershot: Ashgate Publishing Limited; 2002, p. 487.

52. E. De Clercq: HIV-chemotherapy and -prophylaxis: new drugs, leads and approaches. *International Journal of Biochemistry and Cell Biology* 2004; **36**(9):1800-1822.

53. J. Kahn: New developments in the clinical use of didanosine. *Journal of Acquired Immune Deficiency Syndromes* 1993; **6**(S1):S47-S50.

54. J. Kahn: The clinical use of didanosine. *Advances in Experimental Medicine and Biology* 1996; **394**:245-256.

55. E. De Clercq: Antiviral drugs: current state of the art, *Journal of clinical virology* 2001; **22**:73-89.

56. K. T. Chong and P. J. Pagano: Inhibition of human immunodeficiency virus type 1 infection in vitro by combination of delavirdine, zidovudine and didanosine. *Antiviral Research* 1997; **34**(3):51-63.

57. A. S. Mulato and J. M. Cherrington: Anti-HIV activity of adefovir (PMEA) and PMPA in combination with antiretroviral compounds: *in vitro* analysis. *Antiviral Research* 1997; **36**(11):91-97.

58. M. S. Hirsch, B. Conway, R. T. D'Aquila, V. A. Johnson; F. Brun-Vézinet, B. Clotet, L. M. Demeter, S. M. Hammer, D. M. Jacobsen; D. R. Kuritzkes, C. Loveday, J. W. Mellors, S. Vella, and D. D. Richman: Antiretroviral drug resistance testing in adults with HIV infection: implications for clinical management. *Journal of the American Medical Association* 1998; **279**(24):1984-1991.

59. D. L. Meyers: Prevalence and incidence of resistance to zidovudine and other antiretroviral drugs. *American Journal of Medicine* 1997; **102**(5B):70-75.

60. E. Kojima, T. Shirasaka, B. D. Anderson, S. Chokekijchai, S. M. Steinberg, S. Broder, R. Yarchoan, and H. Mitsuya: Human immunodeficiency virus type 1

(HIV-1) viremia changes and development of drug-related mutations in patients with symptomatic HIV-1 infection receiving alternating or simultaneous zidovudine and didanosinye therapy. *Journal of Infectious Diseases* 1995; **171**(5):1152-1158.

61. M. H St Clair, J. L Martin, G. Tudor-Williams, M. C. Bach, C. L. Vavro, D. M. King, P. Kellam, S. D. Kemp, and B.A. Larder: Resistance to ddI and sensitivity to AZT induced by a mutation in HIV-1 reverse transcriptase. *Science* 1991; **253**(5027):1557-1559.

62. B. G. Gazzard and G. J. Moyle: The role of didanosine in the management of HIV-1 infection. *Antiviral Therapy* 1997; **2**(3):135-147.

63. D. Mayers, J. Bethel, M. A. Wainberg, O. Weislow and S. Schnittman: Human immunodeficiency virus proviral DNA from peripheral blood and lymph nodes demonstrates concordant resistance mutations to zidovudine (codon 215) and didanosine (codon 74). *Journal of Infectious Diseases* 1998; **177**(6):1730-1733.

64. C. Nielsen, L. Bruun, L. R. Mathiesen, C. Pedersen and J. Gerstoft: Development of resistance of zidovudine (ZDV) and didanosine (ddI) in HIV from patients in ZDV, ddI and alternating ZDV/ddI therapy. *AIDS* 1996; **10**(6):625-633.

65. M. A. Winters, R. W. Shafer, R. A. Jellinger, G. Mamtora, T. Gingeras and T. C. Merigan. Human immunodeficiency virus type 1 reverse transcriptase genotype and drug susceptibility changes in infected individuals receiving dideoxyinosine monotherapy for 1 to 2 years. *Antimicrobial Agents and Chemotherapy* 1997; **41**(4):757-762.

66. P. L. Sharma and C. S. Crumpacker: Attenuated replication of human immunodeficiency virus type 1 with a didanosine-selected reverse transcriptase mutation. *Journal of Virology* 1997; **171**(11):8846-8851.

67. C. D. Pilcher, M. D. Perkins, S. A. Fiscus, D. M. Johnston, , R. Dietze, U. H. Duque, A. M. Zago, F. Assad-Antunes and J. J. Eron: Genotypic resistance and the treatment of HIV-1 infection in Espirito Santo, Brazil. *Journal of Infectious Diseases* 1999; **179**(5):1259-1263.

68. Z. Gu, Q. Gao, H. Fang, H. Salomon, M. A .Parniak, E. Goldberg, J. Cameron and M. A. Wainberg. Identification of a mutation at codon 65 in the IKKK motif of reverse transcriptase that encodes human immunodeficiency virus resistance to 2',3'-dideoxycytidine and 2',3'-dideoxy-3'-thiacytidine. *Antimicrobial Agents and Chemotherapy* 1994; **38**(2):275-281.

69. B. A. Larder, A. Kohli, S. Bloor, S. D. Kemp, P. R. Harrigan, R. T .Schooley, J. M. Lange, K. N. Pennington and M. H. St Clair: Human immunodeficiency virus type 1 drug susceptibility during zidovudine (AZT) monotherapy compared with AZT plus 2',3'-dideoxyinosine or AZT plus 2',3'-dideoxycytidine combination therapy. *Journal of Virology* 1996; **70**(9):5922-5929.

70. M. Holodniy, D. Atzenstein, L. Mole, M. Winters and T. Merigant: Human immunodeficiency virus reverse transcriptase codon 215 mutations diminish virologic response to didanosine-zidovudine therapy in subjects with non-syncytium-inducing phenotype. *Journal of Infectious Diseases* 1996; **174**(4):854-857.

71. South African Electronic Package Inserts: Videx® tablets 25, 50, 100, 150 and Videx® peadiatric powder 2g.

(HIV-1) viremia changes and development of drug-related mutations in patients with symptomatic HIV-1 infection receiving alternating or simultaneous zidovudine and didanosinye therapy. *Journal of Infectious Diseases* 1995; **171**(5):1152-1158.

61. M. H St Clair, J. L Martin, G. Tudor-Williams, M. C. Bach, C. L. Vavro, D. M. King, P. Kellam, S. D. Kemp, and B.A. Larder: Resistance to ddI and sensitivity to AZT induced by a mutation in HIV-1 reverse transcriptase. *Science* 1991; **253**(5027):1557-1559.

62. B. G. Gazzard and G. J. Moyle: The role of didanosine in the management of HIV-1 infection. *Antiviral Therapy* 1997; **2**(3):135-147.

63. D. Mayers, J. Bethel, M. A. Wainberg, O. Weislow and S. Schnittman: Human immunodeficiency virus proviral DNA from peripheral blood and lymph nodes demonstrates concordant resistance mutations to zidovudine (codon 215) and didanosine (codon 74). *Journal of Infectious Diseases* 1998; **177**(6):1730-1733.

64. C. Nielsen, L. Bruun, L. R. Mathiesen, C. Pedersen and J. Gerstoft: Development of resistance of zidovudine (ZDV) and didanosine (ddI) in HIV from patients in ZDV, ddI and alternating ZDV/ddI therapy. *AIDS* 1996; **10**(6):625-633.

65. M. A. Winters, R. W. Shafer, R. A. Jellinger, G. Mamtora, T. Gingeras and T. C. Merigan. Human immunodeficiency virus type 1 reverse transcriptase genotype and drug susceptibility changes in infected individuals receiving dideoxyinosine monotherapy for 1 to 2 years. *Antimicrobial Agents and Chemotherapy* 1997; **41**(4):757-762.

66. P. L. Sharma and C. S. Crumpacker: Attenuated replication of human immunodeficiency virus type 1 with a didanosine-selected reverse transcriptase mutation. *Journal of Virology* 1997; **171**(11):8846-8851.

67. C. D. Pilcher, M. D. Perkins, S. A. Fiscus, D. M. Johnston, , R. Dietze, U. H. Duque, A. M. Zago, F. Assad-Antunes and J. J. Eron: Genotypic resistance and the treatment of HIV-1 infection in Espirito Santo, Brazil. *Journal of Infectious Diseases* 1999; **179**(5):1259-1263.

68. Z. Gu, Q. Gao, H. Fang, H. Salomon, M. A .Parniak, E. Goldberg, J. Cameron and M. A. Wainberg. Identification of a mutation at codon 65 in the IKKK motif of reverse transcriptase that encodes human immunodeficiency virus resistance to 2',3'-dideoxycytidine and 2',3'-dideoxy-3'-thiacytidine. *Antimicrobial Agents and Chemotherapy* 1994; **38**(2):275-281.

69. B. A. Larder, A. Kohli, S. Bloor, S. D. Kemp, P. R. Harrigan, R. T .Schooley, J. M. Lange, K. N. Pennington and M. H. St Clair: Human immunodeficiency virus type 1 drug susceptibility during zidovudine (AZT) monotherapy compared with AZT plus 2',3'-dideoxyinosine or AZT plus 2',3'-dideoxycytidine combination therapy. *Journal of Virology* 1996; **70**(9):5922-5929.

70. M. Holodniy, D. Atzenstein, L. Mole, M. Winters and T. Merigant: Human immunodeficiency virus reverse transcriptase codon 215 mutations diminish virologic response to didanosine-zidovudine therapy in subjects with non-syncytium-inducing phenotype. *Journal of Infectious Diseases* 1996; **174**(4):854-857.

71. South African Electronic Package Inserts: Videx® tablets 25, 50, 100, 150 and Videx® peadiatric powder 2g.

http://home.intekom.com/pharm/bm_squib/videx.html . 2009. Last accessed on 14-1-2009.

72. S. Safrin. Antiviral agents: didanosine. In: B.G.Katzung (editor): *Basic & Clinical Pharmacology: International Edition.* New York: The McGraw-Hill Companies; 2001, pp. 833-834.

73. G. D. Morse, M. A. Fischl, M. J. Shelton, S. R. Cox, M. Driver, M. DeRemer and W. W. Freimuth: Single-dose pharmacokinetics of delavirdine mesylate and didanosine in patients with human immunodeficiency virus infection. *Antimicrobial Agents and Chemotherapy*1997; **41**(1):169-174.

74. J. A. Carlson, H. J. Mann, D. M. Canafax: Effect of pH on disintegration and dissolution of ketoconazole tablets. *American Journal of Health-System Pharmacy* 1983; **40**(8):1334-1336.

75. J. H. Lin, I. W. Chen, K. J. Vastag and D. Ostovic: pH-dependent oral absorption of L-735,524, a potent HIV protease inhibitor, in rats and dogs. *Drug Metabolism and Disposition* 1995; **23**(7):730-735.

76. J. Sahai, K. Gallicano, L. Oliveras, K. Shireen, N. Hawley-Foss, and G. Garber. Cations in the didanosine tablet reduce ciprofloxacin bioavailability. *Clinical Pharmacology and Therapeutics* 1993; **53**(3):292-297.

77. B. D. Damle, J. H. Yan, D. Behr, E. O'Mara, P. Nichola, S. Kaul and C. Knupp. Effect of food on the oral bioavailability of didanosine from encapsulated enteric-coated beads. *Jounal of Clinical Pharmacology* 2002; **42**(4):419-427.

78. J. R. Snyman (editor). Videx, Bristol-Myers Squib (P/S): Didanosine (ddI). *Monthly Index of Medical Specialities (MIMS): Includes Active Ingredient/Trade Name Index* 2008; **48**(11):293-294.

79. P. J. Sinko, N. R. Patel and P. Hu: Site-specific oral absorption of didanosine: *in situ* characterization and correlation with extent of absorption *in vivo*. *International Journal of Pharmaceutics* 1994; **109**(2):125-133.

80. C. A. Knupp, W. C. Shyu, R. Dolin, F. T. Valentine, C. Mclaren, R. R. Martin, K. A. Pittman and R. H. Barbhaiya Pharmacokinetics of didanosine in patients with acquired immunodeficiency syndrome-related complex: *Clinical Pharmacology and Therapeutics* 1991; **49**:523-535.

81. B. Magenheim, M. Y. Levy and S. Benita: A new *in vitro* technique for the evaluation of drug release profile from colloidal carriers- ultrafiltration technique at low pressure. *International Journal of Pharmaceutics* 1993; **94**(1-3):115-123.

82. C. Lherm, R. H. Müller, F. Puisieux and P. Couvreur: Alkylcyanoacrylate Drug Carriers II: cytotoxicity of cyanoacrylate nanoparticles with different alkyl chain length. *International Journal of Pharmaceutics* 1992; **84**(1):13-22.

83. P. Santos, A .C. Watkinson, J. Hadgraft and M. E. Lane: Application of microemulsions in dermal and transdermal drug delivery. *Skin Pharmacology and Physiology* 2008; **21**(5):246-259.

84. R. Alverez-Román, G. Barré, R. H. Guy and H. Fessi: Biodegradable polymer nanocapsules containing a sunscreen agent: preparation and photoprotection. *European Journal of Pharmaceutics and Biopharmaceutics* 2001; **52**(2):191-195.

85. P. Couvreur, C. Dubernet, F. Puisieux: Controlled drug delivery with nanoparticles: current possibilities and future trends. *European Journal of Pharmaceutics and Biopharmaceutics* 1995; **41**(1):2-13.

86. W. Weyenberg, P. Filev, D. Van den Plas, J. Vandervoort, K. De Smet, P. Sollie and A. Ludwig: Cytotoxicity of submicron emulsions and solid lipid nanoparticles for dermal application. *International Journal of Pharmaceutics* 2007; **337**(1-2):291-298.

87. S. Klang and S. Benita: Design and evaluation of submicron emulsions as colloidal drug carriers for intravenous administration. In: S.Benita (editor): *Submicron Emulsions in Drug Targeting and Delivery*. Amsterdam: Harwood Academic Publishers; 1998, pp. 119-152.

88. R. Gurny, N. A. Peppas, D. D. Harrington and G. S. Banker: Development of biodegradable and injectible latices for controlled release of potent drugs. *Drug Development and Industrial Pharmacy* 1981; **7**(1):1-25.

89. E. Allémann, R. Gurny and E. Doelker: Drug-loaded nanoparticles: preparation methods and drug targeting issues. *European Journal of Pharmaceutics and Biopharmaceutics* 1993; **39**(5):173-191.

90. R. M. Mainardes and L. P. Silva: Drug delivery systems: past, present and future. *Current Drug Targets* 2004; **5**(5):449-455.

91. L. Illum, M. A. Khan, E. Mak and S. S. Davis: Evaluation of carrier capacity and release characteristics for poly(butyl 2-cyanoacrylate) nanoparticles. *International Journal of Pharmaceutics* 1986; **30**(1):17-28.

92. A. Smith and I. M. Hunneyball: Evaluation of poly (lactic acid) as a biodegradable drug delivery system for parenteral administration. *International Journal of Pharmaceutics* 1986; **30**(2-3):215-220.

93. G. Puglisi, G. Giammona, M. Fresta, B. Carlisi, N. Micali and A. Villari: Evaluation of polyalkylcyanoacrytale nanoparticles as a potential drug carrier: preparation, morphological characterization and loading capacity. *Journal of Microencapsulation* 1993; **10**(3):353-366.

94. T. Pitaksuteepong, N. M. Davies, I. G. Tucker and T. Rades: Factors influencing the entrapment of hydrophilic compounds in nanocapsules prepared by interfacial polymerization of water-in-oil microemulsions. *European Journal of Pharmaceutics and Biopharmaceutics* 2002; **53**(3):335-342.

95. R. Bodmeier and H. Chen: Indomethacin polymeric nanosuspensions prepared by microfluidization. *Journal of Controlled Release* 1990; **12**(3):223-233.

96. M. M. Elsayed, O. Y. Abdallah, V. F. Naggar and N. M. Khalafallah: Lipid vesicles for skin delivery of drugs: reviewing three decades of research. *International Journal of Pharmaceutics* 2007; **332**(1-2):1-16.

97. R. Janknegt, S. de Marie and I. A. Bakker-Woudenberg, D.J.Crommelin: Liposomal and lipid formulations of amphotericin B. clinical pharmacokinetics. *Clinical Pharmacokinetics* 1992; **23**(4):279-291.

98. A. Samad, Y. Sultana and M. Aqil: Liposomal drug delivery systems: an update review. *Current Drug Delivery* 2007; **4**(4):297-305.

99. D. J. Crommelin and H. Schreier: Liposomes. In: J. Kreuter (editor): *Colloidal Drug Delivery Systems*. New York: Marcel Dekker Inc.; 1994, pp. 73-190.

100. M. J. Choi and H. I. Maibach: Liposomes and niosomes as topical drug delivery systems. *Skin Pharmacology and Physiology* 2005; **18**(5):209-219.

101. E. Touitou, H. E. Junginger, N. D. Weiner, T. Nagai, M. Mezei: Liposomes as carriers for topical and transdermal delivery. *Journal of Pharmaceutical Sciences* 1994; **83**(9):1189-1203.

102. Y. Barenholz, D. J. Crommelin: Liposomes as pharmaceutical dosage forms. In: J. Swarbrick and J. C. Boylan (editors): *Encyclopedia of Pharmaceutical Technology*. New York: Marcel Dekker Inc.;1994, pp. 1-39.

103. G. Gregoriadis, A. T. Florence and H. M. Patel: Liposomes in drug delivery. In: A. T. Florence and G. Gregoriadis (editors): *Drug Targeting and Delivery*. Harwood Academic Publishers GmbH: Chur; 1993.

104. D. D. Verma, S. Verma, G. Blume and A. Fahr. Liposomes increase skin penetration of entrapped and non-entrapped hydrophilic substances into human skin: a skin penetration and conforcal laser scanning microscopy study. *European Journal of Pharmaceutics and Biopharmaceutics* 2003; **55**(3):271-277.

105. R. Cortesi and C. Nastruzzi: Liposomes, micelles and microemulsions as new delivery systems for cytotoxic alkaloids. *Pharmaceutical Science and Technology Today* 1999; **2**(7):288-298.

106. A. D. Bangham: Liposomes: realizing their promise. *Hospital Practice (Office ed)* 1992; **27**(12):51-56.

107. S. Heuschkel, A. Goebel and R. H. Neubert: Microemulsions: modern colloidal carrier for dermal and transdermal drug delivery. *Journal of Pharmaceutical Sciences* 2008; **97**(2):603-631.

108. H. Fessi, F. Puisieux, N. Ammoury and S. Benita: Nanocapsule formation by interfacial polymer depostion following solvent displacement. *International Journal of Pharmaceutics* 1989; **55**:R1-R4.

109. C. Mayer: Nanocapsules as drug delivery systems. *International Journal of Artificial Organs* 2005; **28**(11):1163-1171.

110. J. Kreuter: Nanoparticle-based drug delivery systems. *Journal of Controlled Release* 1991; **16**:169-176.

111. J. Kreuter: Nanoparticles. In: J. Kreuter (editor): *Colloidal Drug Delivery Systems*. New York: Marcel Dekker Inc.; 1994, pp. 219-342.

112. M. Joshi and V. Patravale: Nanostructured lipid carrier (NLC) based gel of celecoxib. *International Journal of Pharmaceutics* 2007; **346**:124-132.

113. A. Lamprecht, Y. Bouligand and J.P.Benoît: New lipid nanocapsules exhibit sustained release properties for amiodarone. *Journal of Controlled Release* 2002; **84**(1-2):59-68.

114. A. K. Mehta, K. S. Yadav and K. K. Sawant: Nimodipine loaded PLGA nanoparticles: formulation optimization using factorial design, characterization and in vitro evaluation. *Current Drug Delivery* 2007; **4**(3):185-193.

115. L. C. Collins-Gold, R. T. Lyons and L. C. Bartholow: Parenteral emulsions for drug delivery. *Advanced Drug Delivery Reviews* 1990; **5**:189-208.

116. J. Kreuter: Peroral administration of nanoparticles. *Advanced Drug Delivery Reviews* 1996; **7**:76-86.

117. F. J. Martin: Pharmaceutical manufacturing of liposomes. In: P. Tyle (editor): *Specialized Drug Delivery Systems: Manufacturing and Production Technology*. New York: Mercel Dekker Inc.; 1990, pp. 267-316.

118. V. Andrieu, H. Fessi, M. Dubrasquet, J. P. Devissaguet, F. Puisieux and S. Benita. Pharmacokinetic evaluation of indomethacin nanocapsules. *Drug Design and Delivery* 1989; **4**(4):295-302.

119. V. Heinemann, D. Bosse, U. Jehn, B. Kähny, K. Wachholz, A. Debus, P. Scholz, H.J. Kolb and Wolfgang: Pharmacokinetics of liposomal of amphotericin B (amBisome) in critically ill patients. *Antimicrobial Agents and Chemotherapy* 1997; **41**(6):1275-1280.

120. S. Benita, D. Friedman and M. Weinstock: Pharmacological evaluation of an injectible prolonged release emulsion of physostigmine in rabbits. *Journal of Pharmacy and Pharmacology* 1986; **38**(9):653-658.

121. M. Aboubakar, F. Puisieux, P. Couvreur and C. Vauthier. Physicochemical characterization of insulin-loaded poly(isobutylcyanoacrylate) nanocapsules obtained by interfacial polymerization. *International Journal of Pharmaceutics* 1999; **183**(1):63-66.

122. S. Benita, D. Friedman and M. Weinstock. Physostigmine emulsion: a new injectible controlled release delivery system. *International Journal of Pharmaceutics* 1986; **30**:47-55.

123. L. Mu and S. S. Feng: PLGA/TPGS nanoparticles for controlled release of paclitaxel: effects of the emulsifier and drug loading ratio. *Pharmaceutical Research* 2003; **20**(11):1864-1872.

124. P. Couvreur and C. Vauthier: Polyalkylcyanoacrylate nanoparticles as drug carriers: present state and perspectives. *Journal of Controlled Release* 1991; **17**:187-198.

125. V. Bhardwaj and M. N. V. R. Kumar: Polymeric nanoparticles for oral drug delivery. In: R.Gupta, U.B.Kompella (editors): *Nanoparticle Technology for Drug Delivery*. New York: Taylor and Francis; 2006, pp. 231-272.

126. M. Vert: Polyvalent polymeric drug carriers. *Critical Reviews in Therapeutic Drug Carrier Systems* 1986; **2**(3):291-327.

127. M. C. Venier-Julienne and J. P. Benoit: Preparation, purification and morphology of polymeric nanoparticles as drug carriers. *Pharmaceutica Acta Helvetiae* 1996; **71**(2):121-128.

128. R. Mauludin, R. H. Müller and C. M. Keck: Kinetic solubility and dissolution velocity of rutin nanocrystals. *European Journal of Pharmaceutical Sciences* 2009; **36**(4-5):S02-S10.

129. J. U. Junghanns and R. H. Müller: Nanocrystal technology, drug delivery and clinical applications. *International Journal of Nanomedicine* 2008; **3**(3):295-310.

130. C. M. Keck and R. H. Müller: Drug nanocrystals (DissoCubes, Nanopure) of poorly soluble drugs produced by high pressure homogenization. *European Journal of Pharmaceutical Sciences* 2006; **62**(1):3-16.

131. R. H. Müller, S. Runge, V. Ravelli, W. Mehnert, A. F. Thünemann and E. B. Souto: Oral bioavailability of cyclosporin: solid lipid nanoparticles (SLN) versus drug nanocrystals. *International Journal of Pharmaceutics* 2006; **317**(1):82-89.

132. V. Teeranachaideekul, R. H. Müller and V. B. Junyaprasert: Encapsulation of ascorbyl palmitate in nanostructured lipid carriers (NLC)- Effects of formulation parameters on physicochemical stability. *International Journal of Pharmaceutics* 2007; **340**(1-2):198-206.

133. E. B. Souto, R. H. Müller: SLN and NLC for topical delivery of ketoconazole. *Journal of Microencapsulation* 2005; **22**(5):501-510.

134. V. Jenning and S. H. Gohla: Encapsulation of retinoids in solid lipid nanoparticles (SLN). *Journal of Microencapsulation* 2001; **18**(2):149-158.

135. M. Üner, S. A. Wissing, G. Yener and R. H. Müller: Solid lipid nanoparticles (SLN) and nanostructured lipid carriers (NLC) for application of ascorbyl palmitate. *Pharmazie* 2005; **60**(8):577-582.

136. E. B. Souto and R. H. Müller: Investigation of the factors influencing the incorporation of clotrimazole in SLN and NLC prepared by hot high-pressure homogenization. *Journal of Microencapsulation* 2006; **23**(4):377-388.

137. L. Brannon-Peppas: Recent advances on the use of biodegradable microparticles and nanoparticles in controlled drug delivery. *International Journal of Pharmaceutics* 1995; **116**(1):1-9.

138. L. E. van Vlerken and M. M. Amiji: Multi-functional polymeric nanoparticles for tumour-targeted drug delivery. *Expert Opinion on Drug Delivery* 2006; **3**(2):205-216.

139. T. M. Göppert and R. H. Müller: Polysorbate-stabilized solid lipid nanoparticles as colloidal carriers for intravenous targeting of drugs to the brain: comparison of plasma protein adsorption patterns. *Journal of Drug Targeting* 2005; **13**(3):179-187.

140. I. Pal Kaur, R. Bhandari, S. Bhandari and V. Kakkar: Potential of solid lipid nanoparticles in brain targeting. *Journal of Controlled Release* 2007; **127**:97-109.

141. R. H. Müller and C. M. Keck: Drug delivery to the brain-realization by novel drug carriers. *Journal of Nanoscience and Nanotechology* 2004; **4**(5):471-483.

142. M. Lalanne, K. Andrieux, A. Paci, M. Besnard, M. Re, C. Bourgaux, M. Ollivon, D. Desmaele and P. Couvreur: Liposomal formulation of a glycerolipidic prodrug for lymphatic delivery of didanosine via oral route. *International Journal of Pharmaceutics* 2007; **344**(1-2):62-70.

143. S. Benita and M. Y. Levy: Submicron emulsions as colloidal drug carriers for intraveous administration: comprehensive physicochemical characterization. *Journal of Pharmaceutical Sciences* 1993; **82**(11):1069-1079.

144. G. M. Barratt: Therapeutic applications of colloidal drug carriers. *Pharmaceutical Science and Technology Today* 2000; **3**(5):163-171.

145. S. Jaspart, G. Piel, L. Delattre and B. Evrard: Solid lipid microparticles: formulation, preparation, characterization, drug release and applications. *Expert Opinion on Drug Delivery* 2005; **2**(1):75-87.

146. R. J. Prankerd and V. J. Stella: The use of oil-in-water emulsions as a vehicle for parenteral drug administration. *Journal of Parenteral Science and Technology* 1990; **44**(3):139-149.

147. A. Dingler, R. P. Blum, H. Niehus, R. H. Müller and S. Gohla: Solid lipid nanoparticles (SLN/Lipopearls): a pharmaceutical and cosmetic carrier for the application of vitamin E in dermal products. *Journal of Microencapsulation* 1999; **16**(6):751-767.

148. A. Fassas and A. Anagnostopoulos: The use of liposomal daunorubicin (DaunoXome) in acute myeloid leukemia. *Leakemia and Lymphoma* 2005; **46**(6):795-802.

149. A. Saez, M. Guzman, J. Molpeceres and M. R. Aberturas: Freeze-drying of polycaprolactone and poly(D,L-lactic-glycolic) nanoparticles induce minor particle size changes affecting the oral pharmacokinetics of loaded drugs. *European Journal of Pharmaceutics and Biopharmaceutics* 2000; **50**(3):379-387.

150. U. Edlund, A. C. Albertsson, S. K. Singh, I. Fogelberg and B. O. Lundgren: Sterilization, storage stability and *in vivo* biocompatibility of poly(trimethylenecarbonate)/poly(adipic anhydride) blends. *Biomaterials* 2000; **21**(9):945-955.

151. M. R. Gasco: Solid lipid nanospheres from warm micro-emulions. *Pharmaceutical Technology Europe* 1997; **9**:52-58.

152. M. R. Gasco. Method for producing solid lipid microspheres having a narrow size distribution. 1993. United States of America Patent, no 5250236.

153. R. H. Müller and J. S. Lucks: Arzneistoffträger aus festen Lipidteilchen, Feste Lipidnanosphären (SLN). 1996. European Patent, no 0605497.

154. B. Siekmann and K. Westesen: Sub-micron sized parenteral carrier systems based on solid lipid. *Pharmaceutical and Pharmacological Letters* 1992; **1**:123-126.

155. R. Cavalli, E. Marengo, L. Rodriguez and M. R. Gasco: Effects of some experimental factors on the production process of solid lipid nanoparticles. *European Journal of Pharmaceutics and Biopharmaceutics* 1996; **43**(2):110-115.

156. S. Siekmann and K. Westesen: Melt-homogenized solid lipid nanoparticles stabilized by the nonionic surfactant tyloxapol. *Pharmaceutical and Pharmacological Letters* 1994; **3**:194-197.

157. K. Westesen, H. Bunjes and M. H. J. Koch: Physicochemical characterization of lipid nanoparticles and evaluation of their drug loading capacity and sustained release potential. *Journal of Controlled Release* 1997; **48**(2-3):223-236.

158. K. Westesen and B. Siekmann: Investigation of the gel formation of phospholipid-stabilized solid lipid nanoparticles. *International Journal of Pharmaceutics* 1997; **151**(1):35-45.

159. V. Jenning, A. F. Thünemann and S. H. Gohla: Characterization of a novel solid lipid nanoparticle carrier system based on binary mixtures of liquid and solid lipids. *International Journal of Pharmaceutics* 2000; **199**(2):167-177.

160. M. Muchow, P. Maincent and R. H. Müller: Lipid nanoparticles with a solid matrix (SLN®, NLC®, LDC®) for oral drug delivery. *Drug Development and Industrial Pharmacy* 2008; **34**(12):1394-1405.

161. E. B. Souto and R. H. Müller: Lipid nanoparticles (SLN and NLC) for drug delivery. In: A. J. Domb, Y. Tobata, M. N. V .R. Kumar and S. Farber (editors): *Nanoparticles for Pharmaceutical Applications*. Stevenson Ranch, California: American Scientific Publishers; 2007, pp. 103-122.

162. R. H. Müller, A. Lippacher and S. Gohla: Solid lipid nanoparticles (SLN) as a carrier systen for the controlled release of drugs. In: D.L.Wise (editor): *Hand of Pharmaceutical Controlled Release Technology*. New York: Mercel Dekker; 2000, pp. 377-389.

163. K. Westesen and H. Bunjes: Do nanoparticles prepared from lipids solid at room temperature always possess a solid lipid matrix. *International Journal of Pharmaceutics* 1995; **115**:62-69.

164. J. Kristil, B. Volk, M. Gasperlin, M. Sentjurc and P. Jurkovic: Effects of colloidal carriers on ascobyl palmitate stability. *European Journal of Pharmaceutical Sciences* 2003; **19**(4):181-189.

165. A. Salgueiro, M. A. Egea, M. Espina, O. Valls and M. L. Garcia: Stability and occular tolerance of cyclophosphamide-loaded nanosphers. *Journal of Microencapsulation* 2004; **21**(2):213-223.

166. A. Saupe, S. A. Wissing, A. Lenk, C. Schmidt and R. H. Müller: Solid lipid nanoparticles (SLN) and nanostructured lipid carriers (NLC)-structural investigations on two different carrier systems. *Bio-Medical Materials and Engineering* 2005; **15**(5):393-402.

167. V. Jenning, M. Schäfer-Korting, S. Gohla: Vitamin A-loaded solid lipid nanoparticles for topical use: drug release properties. *Journal of Controlled Release* 2000; **66**(2-3):115-126.

168. M. Igartua, P. Sualnier, B. Heurtault, B. Pech, J. E. Proust, J. L. Pedraz and J. P. Benoit: Development and characterization of solid lipid nanoparticles loaded with magnetite. *International Journal of Pharmaceutics* 2002; **223**(1-2):149-157.

169. R. Cortesi, E. Esposito, H. Luca and C. Nastruzzi: Production of lipospheres as carriers for bioactive compounds. *Biomaterials* 2002; **23**(11):2283-2294.

170. B. Sjöström and B. Bergenstå: Preparation of submicron drug particles in lecithin-stabilized o/w emulsions I. Model studies of the precipitation of cholesteryl acetate. *International Journal of Pharmaceutics* 1992; **88**(1-3):53-62.

171. F. Q. Hu, H. Yuan, H. H. Zhang and M. Fang: Preparation of solid lipid nanoparticles with clobetasol propionate by a novel solvent diffusion method in aqueous system and physicochemical characterization. *International Journal of Pharmaceutics* 2002; **239**(1-2):121-128.

172. F. Q. Hu, Y. Hong and H. Yuan: Preparation and characterization of solid lipid nanoparticles containing peptide. *International Journal of Pharmaceutics* 2004; **273**(1-2):29-35.

173. M. A. Schubert and C. C. Müller-Goymann: Solvent injection as a new approach for manufacturing lipid nanoparticles- evaluation of the method and process

parameters. *European Journal of Pharmaceutics and Biopharmaceutics* 2003; **55**(1):125-131.

174. D. Quintanar-Guerrero, H. Fessi, E. Allémann and E. Doelker: Pseudolatex preparation using a novel emulsion-diffusion process involving direct displacement of partially water-miscible solvents by distillation. *International Journal of Pharmaceutics* 1999; **188**(2):155-164.

175. M. Trotta, F. Debernardi and O. Caputo: Preparation of solid lipid nanoparticles by a solvent emulsification-diffusion technique. *International Journal of Pharmaceutics* 2003; **257**(1-2):153-160.

176. D. Quintanar-Guerrero, D. amayo-Esquivel, A. Ganem-Quintanar, E. Allémann and E. Doelker: Adaptation and optimization of the emulsification-diffusion technique to prepare lipidic nanospheres. *European Journal of Pharmaceutics and Biopharmaceutics* 2005; **26**(2):211-218.

177. P. Shahgaldian, J. Gualbert, K. Aïssa and A. W. Coleman: A study of freeze-drying conditions of calixarene based solid lipid nanoparticles. *European Journal of Pharmaceutics and Biopharmaceutics* 2003; **55**(2):181-184.

178. B. Heurtault, P. Saulnier, B. Pech, J. E. Proust and J. P. Benoit: A novel phase inversion-based process for the preparation of lipid nanocarriers. *Pharmaceutical Research* 2002; **19**(6):875-880.

179. C. M. Keck and R. H. Müller: Drug nanocrystals of poorly soluble drugs produced by high pressure homogenization. *European Journal of Pharmaceutics and Biopharmaceutics* 2006; **62**(1):3-16.

180. A. Lippacher, R. H. Müller and K. Mäder: Investigation on the viscoelastic properties of lipid based colloidal drug carriers. *International Journal of Pharmaceutics* 2009; **196**(2):227-230.

181. R. Lander, W. Manger, M. Scouloudis, A. Ku, C. Davis and A. Lee: Gaulin homogenization: a mechanistic study. *Biotechnology Progress* 2000; **16**(1):80-85.

182. S. Jahnke: The theory of high pressure homogenization. In: R.H.Müller, S.Benita, B.Böhm (editors): *Emulsions and nanosuspensions for the formulation of poorly soluble drugs*. Stuttgart: MedPharm Scientific Publishers; 1998, pp. 177-200.

183. B. Heurtault, P. Saulnier, B. Pech, J. E. Proust and J. P. Benoit: Physico-chemical stability of colloidal lipid particles. *Biomaterials* 2003; **24**(23):4283-4300.

184. K. Jores, W. Mehnert, M. Drechsler, H. Bunjes, C. Johann and K. Mäder: Investigations on the structure of solid lipid nanoparticles (SLN) and oil-loaded solid lipid nanoparticles by photon correlation spectroscopy, field-flow fractionation and transmission electron microscopy. *Journal of Controlled Release* 2004; **95**(2):217-227.

185. R. H. Müller: *Colloidal Carriers for Controlled Drug Delivery and Targeting: Modification, Characterization and In Vivo Distribution.* Stuttgart: Wissenschaftliche Verlagsgesellschaft GmbH, 1991.

186. E. M. B. Souto: SLN and NLC for topical delivery of antifungals 66: 2005, PhD Thesis, Free University Berlin, Berlin, Germany.

187. A. Radomska-Soukharev: Stability of lipid excipients in solid lipid nanoparticles. *Advanced Drug Delivery Reviews* 2007; **59**(6):411-418.

188. J. Pardeike: Nanosuspensions and nanostructured lipid carriers for dermal application, 65-66: 2008, PhD Thesis, Free University Berlin, Berlin, Germany.

189. C. M. Keck and R. H. Müller: Size analysis of submicron particles by laser diffractometry-90% of the published measurements are false. *International Journal of Pharmaceutics* 2008; **355**(1-2):150-163.

190. I. Zimmermann: Possibilities and limitations of laser light scattering techniques for particle size analysis. In: R. H. Müller and W. Mehnert (editors): *Particle and Surface Characterization Methods*. Stuttgart: Medpharm; 1997, pp. 19-26.

191. M. Wedd: Particle size in the sub-micron range by laser diffraction. In: R. H. Müller, and W. Mehnert (editors): *Particle and Surface Characterization Methods*. Stuttgart: Medpharm; 1997, pp. 57-68.

192. R. Xu: Improvements in particle size analysis using light scattering. In: R. H. Müller, and W. Mehnert (editors): *Particle and Surface Characterization Methods*. Stuttgart: Medpharm; 1997, pp. 27-56.

193. Y. C. Kuo and T. W. Lin: Electrophoretic mobility, zeta potential and fixed charge density of bovine knee chondrocytes, methyl methacrylate-sulphonyl methacryalte, polybutylcyanocrylate and solid lipid nanoparticles. *Journal of Physical Chemistry B* 2006; **110**(5):2202-2208.

194. A. Dubes, H. Parrot-Lopez, W. Abdelwahed, G. Degobert, H. Fessi, P.Shahgaldian and A. W. Coleman: Scanning electron microscopy and atomic force microscopy imaging of solid lipid nanoparticles derived from amphiphilic cyclodextrins. *European Journal of Pharmaceutics and Biopharmaceutics* 2003; **55**(3):279-282.

195. D. Hou, C. Xie, K. Huang and C. Zhu: The production and characteristics of solid lipid nanoparticles (SLNs). *Biomaterials* 2003; **24**(10):1781-1785.

196. H. Bunjes, K. Westesen and M. H. J. Koch: Crystallization tendency and polymorphic transitions in triglyceride nanoparticles. *International Journal of Pharmaceutics* 1996; **129**(1-2):159-173.

197. K. Westesen, B. Siekmann and M. H. J. Koch: Investigations on the physical state of solid lipid nanoparticles by synchrom radiation X-ray diffraction. *International Journal of Pharmaceutics* 1993; **93**:189-199.

198. N. J. Coleman and D. Q. M. Craig: Modulated temperature differential scanning calorimetry: a novel approach to pharmaceutical thermal analysis. *International Journal of Pharmaceutics* 1996; **136**:13-29.

199. D. Q. M. Craig: A review of thermal methods for the analysis of the crystal form, solution thermodynamics and glass transition behaviour of polyethylene glycols. *Thermochemica Acta* 1993; **248**:189-203.

200. J. H. Flynn: Analysis of DSC results by integration. *Thermochemica Acta* 1993; **217**:129-149.

201. S. D. Clas, C. R. Dalton and B. C. Hancock. Differential scanning calorimetry: applications in drug development. *PSIT* 1999; **2**(8):311-320.

202. E. B. Souto, W. Mehnert, R. H. Müller. Polymorphic behaviour of compritol 888 ATO as bulk lipid and as SLN and NLC: *Journal of Microencapsulation* 2006; **23**(4):417-433.

203. C. Freitas and R. H. Müller: Correlation between long-term stability of solid lipid nanoparticles (SLN^{TM}) and crystallinity of the lipid phase: *European Journal of Pharmaceutics and Biopharmaceutics* 1999; **47**:125-132.

204. V. Teeranachaideekul, E. B. Souto, V. B. Junyaprasert and R. H. Müller: Cetyl palmitate-based NLC for topical delivery of Coenzyme Q10 - Development, physicochemical characterization and *in vitro* release studies. *European Journal of Pharmaceutics and Biopharmaceutics* 2007; **67**(1):141-148.

205. R. H. Müller, S. A. Runge, V. Ravelli, A. F. Thünemann, W. Mehnert and E. B. Souto: Cyclosporine-loaded solid lipid nanoparticles (SLN): Drug-lipid physicochemical interactions and characterization of drug incorporation. *European Journal of Pharmaceutics and Biopharmaceutics* 2008; **68**(3):535-544.

206. G. Lukowski, J. Kasbohm, P. Pflegel, A. Illing and H. Wulff: Crystallographic investigation of cetylpalmitate solid lipid nanoparticles. *International Journal of Pharmaceutics* 2000; **196**(2):201-205.

207. C. V. Garcia, A. R. Breier, M. Steppe, E. E. S. Schapoval and T. P. Oppe: Determination of dexamethasone acetate in cream by HPLC: *Journal of Pharmaceutical and Biomedical Analysis* 2003; **31**(3):597-600.

208. R. J. Hamilton, P. A. Sewell: Introduction to high performance liquid chromatography. In: R. J. Hamilton, P. A. Sewell (editors): *Introduction to High Performance Liquid Chromatography*. New York: Chapman and Hall; 1981, pp. 1-12.

209. C. P. W. G. Verweij-van Wissen, R. E. Aarnoutse and D. M. Burger: Simultaneous determination of the HIV nucleoside analogue reverse transcriptase inhibitors lamivudine, didanosine, stavudine, zidovudine and abacavir in human plasma by reversed phase high performance liquid chromatography. *Journal of Chromatography B* 2005; **816**(1-2):121-129.

210. Y. Huang, E. Zurlinden, E. Lin, X. Li, J. Toumoto, J. Golden, A. Murr, J. Engstrom and J. R. J. Conte: Liquid chromatographic-tandem mass spectrometric assay for the simultaneous determination of didanosine and stavudine in human plasma, bronchoalveolar lavage fluid, alveolar cells, peripheral blood mononuclear cells, seminal plasma, cerebrospinal fluid and tonsil tissue. *Journal of Chromatography B* 2004; **799**(1):51-61.

211. M. L. Rosell-Rovira, L. Pou-Clavé, R. Lopez-Galera and C. Pascual-Mostaza: Determination of free serum didanosine by ultrafiltration and high-performance liquid chromatography. *Journal of Chromatography B: Biomedical Sciences and Applications* 1996; **675**(1):89-92.

212. S. Notari, A. Bocedi, G. Ippolito, P. Narciso, L. P. Pucillo, G. Tossini, R. P. Donnorso, F. Gasparrini and P. Ascenzi: Simultaneous determination of 16 anti-HIV drugs in human plasma by high-performance liquid chromatography. *Journal of Chromatography B* 2006; **831**(1-2):258-266.

213. H. Rebiere, B. Mazel, C. Civade and P. A. Bonnet: Determination of 19 antiretroviral agents in pharmaceuticals or suspected products with two methods using high-performance liquid chromatography. *Journal of Chromatography B* 2007; **850**(1-2):376-383.

214. *The United States Pharmacopoeia incorporating "The National Formulary"*. Rockville: The United States Pharmacopoeial Convention Inc.; 2006.

215. Didanosine: *The British Pharmacopoeia 2007, incorporating the requirements of the 5th edition of the European Pharmacopoeia 2004 as amended by Supplements 5.1 and 5.2.* London: The Stationary Office; 2007.

216. C. Sanchez-Lafuene, S. Furlanetto, M. Fernandez-Arevalo, J. Alvarez-Fuentes, A. M. Rabasco and M. T. Faucci: Didanosine extended-release matrix tablets: optimization of formulation variables using statistical experimental design. *International Journal of Pharmaceutics* 2002; **237**(1-2):107-118.

217. C. Sánchez-Lafuene, F. M. Teresa, M. Fernández-Arévalo, J. Alvarez-Fuentes, A. M. Rabasco and P. Mura: Development of sustained release matrix tablets of didanosine containing methacrylic and ethylcellulose polymers. *International Journal of Pharmaceutics* 2002; **234**(1):213-221.

218. A. M. C. de Oliveira, T. C. R. Löwen, L. M. Cabral, E. M. dos Santos, C. R. Rodrigues, H. C. Castro and T. C. dos Santos: Development and validation of a HPLC-UV method for the determination in didanosine tablets. *Journal of Pharmaceutical and Biomedical Analysis* 2005; **38**(4):751-756.

219. K. Hammarstrand: Internal standard in gas chromatography. *Varian Instrument Applications* 1976; **10**:10-11.

220. J. Lindholm, M. Johansson and T. Fornstedt: Guidelines for analytical method development and validation of biotechnological synthesis of drugs: production of a hydroxyprogesterone as model. *Journal of Chromatography B* 2003; **791**(1-2):323-336.

221. C. M. Riley: Statistical parameters. In: C. M. Riley and T. W. Rosanske (editors): *Development and Validation of Analytical Methods*. New York: Elsevier Science Inc.; 1996, pp. 44-45.

222. L. R. Snyder, J. J. Kirkland, J. L. Glajch: Solvents. In: L. R. Snyder, J. J. Kirkland, J. L. Glajch (editors): *Introduction to Modern Liquid Chromatography*. New York: John Wiley and Sons Inc.; 1979, pp. 246-268.

223. C. Taninaka, H. Ohtani, E. Hanada, H. Kotaki, H. Sato and T. Iga: Determination of erythromycin, clarithromycin, roxithromycina and azithromycin in plasma by high-performance liquid chromatography with amperometric detection. *Journal of Chromatography B* 2000; **738**(2):405-411.

224. A. Martin: Physical Pharmacy. In: A. Martin (editor). Philadelphia: Lea and Febiger; 1993, p. 169 (370)-189 (372).

225. I. W. Wainer (editor): *Liquid Chromatography in Pharmaceutical Development: an Introduction*. Springfield: Aster Publishing Co.; 1985, pp. 149-179.

226. D. C. Harries (editor): *Quantitative Chemical Analysis*. New York: W.H. Freeman and Company; 1999, pp. 713-753.

227. A. Kristl, A. Mrhar and F. Kozjek: The ionization properties of acyclovir and deoxyacyclovir. *International Journal of Pharmaceutics* 1993; **99**(1):79-82.

228. L .R. Snyder, J. J. Kirkland and J. L. Glajch: Non-ionic sample: reverse and normal-phase HPLC. In: L. R. Snyder, J. J. Kirkland and J. L. Glajch (editors): *Practical*

HPLC Method Development. New York: John Wiley and Sons Inc.; 1997, pp. 223-291.

229. H. Rosing, W. Y. Man, E. Doyle, A. Bult and J. H. Beijnen: Bioanalytical liquid chromatographic method validation: a review of current practices and procedures. *Journal of Liquid Chromatography* 2000; **23**(3):329-354.

230. Guidance for industry: Bioanalytical methods validation. Rockville, U.S. Department of Health and Human Services, Food and Drug Administration, Center for Drug Evaluation and Research and Center for Veterinary Medicine, 2001, pp1-22..

231. Reviewer Guidance: Validation of chromatograhic methods: Rockville, U.S. Department of Health and Human Services, Food and Drug Administration, Center for Drug Evaluation and Research and Center for Veterinary Medicine1994, pp1-20.

232. G. A. Shabir: Validation of high-performance liquid chromatography methods for pharmaceutical analysis: understanding the differences and similarities between validation requirements of the US Food and Drug Administration, The US Pharmacopeia and the International Conference on Harmonization. *Journal of Chromatography A* 2003; **987**(1-2):57-66.

233. ICH Harmonised Tripartite Guidelines: validation of analytical procedures: methodology. ICH Topic Q 2 B, London, International Conference on Harmonization, 1996.

234. ICH Harmonised Tripartite Guidelines: validation of analytical methods: definitions and terminology. ICH Topic Q 2 A. London, International Conference on Harmonization, 1995, pp1-5.

235. T. C. Paino and A. D. Moore: Determination of the LOD and LOQ of an HPLC method using four different techniques. *Pharmaceutical Technology* 1999; **23**(10):82-90.

236. U. Timm, M. Wall and D. Dell: A new approach for dealing with the stability of drugs in biological fluids. *Journal of Pharmaceutical Sciences* 1985; **74**(9):972-977.

237. E. B. Souto, C. Anselmi, M. Centini and R. H. Müller: Preparation and characterization of n-dodecyl-ferulate-loaded solid lipid nanoparticles (SLN®). *International Journal of Pharmaceutics* 2005; **295**(1-2):261-268.

238. T. Veerawat, E. B. Souto and R. H. Müller: Physicochemical characterization and in vitro release studies of ascorbyl palmitate-loaded semi-solid nanostructured lipid carriers (NLC gels). *Journal of Microencapsulation* 2008; **25**(2):111-120.

239. N. A. Armstrong: Glyceryl Palmitostearate. In: R. C. Rowe, P. J. Sheskey and M. E. Quinn (editors): *Handbook of Pharmaceutical Excipients.* London: The Pharmaceutical Press; 2009, pp. 293-294.

240. L. Hernqvist: Crystal structures of fats and fatty acids. In: N. Garti and K. Sato (editors): *Crystallization and Polymorphism of Fats and Fatty Acids.* New York: Marcel Dekker Inc.; 1988, pp. 97-137.

241. Gattefossé Canada: pharmaceutical products catalogue. http://www.gattefossecanada.ca/en/products/pharmaceutical/gattefosse_oral.shtml. 2007. Gattefossé Canada Inc. Accessed on: 12-1-2010.

242. J. H. Collett: Poloxamer. In: R. C. Rowe, P. J. Sheskey and M. E. Quinn (editors): *Handbook of Pharmaceutical Excipients*. London: The Pharmaceutical Press; 2009, pp. 506-509.

243. K. K. Singh: Macrogol 15 hydroxystearate. In: R. C. Rowe, P. J. Sheskey and M. E. Quinn (editors): *Handbook of Pharmaceutical Excipients*. London: The Pharmaceutical Press; 2009, pp. 391-393.

244. D. Zhang: Polyoxyetylene sorbitan fatty acid esters. In: R. C. Rowe, P. J. Sheskey and M. E. Quinn (editors): *Handbook of Pharmaceutical Excipients*. London: The Pharmaceutical Press; 2009, pp. 549-553.

245. P. R. Mishra, L. Al Shaal, R. H. Müller and C. M. Keck: Production and characterization of hesperitin nanosuspensions for dermal delivery. *International Journal of Pharmaceutics* 2009; **371**(1-2):182-189.

246. O. Kayser, C. Olbrich, A. F. Kiderlen and S. L. Croft: Formulation of amphotericin B as nanosuspension for oral administration. *International Journal of Pharmaceutics* 2003; **254**(1):73-75.

247. B. Siekmann and K. Westesen: Melt-homogenized solid lipid nanoparticles stabilized by the nonionic surfactant tyloxapol. I. preparation and particle size determination. *Pharmaceutical and Pharmacological Letters* 1994; **3**:194-197.

248. T. M. Göppert and R. H. Müller: Plasma protein adsorption of tween 80 and poloxamer 188-stabilized solid lipid nanoparticles. *Journal of Drug Targetting* 2003; **11**(4):225-231.

249. C. Schwarz, W. Mehnert and R. H. Müller: Influence of production parameters of solid lipid nanoparticles (SLN) on the suitability for intravenous injection. *European Journal of Pharmaceutics and Biopharmaceutics* 1994; **40**:248-256.

250. S. J. Lim and C. K. Kim: Formulation parameters determining the physicochemical characteristics of solid lipid nanoparticles loaded with all-trans retinoic acid. *International Journal of Pharmaceutics* 2002; **243**(1-2):135-146.

251. M. A. Schubert and C. C. Müller-Goymann: Characterization of surface-modified solid lipid nanoparticles (SLN): influence of lecithin and non-ionic emulsifier. *European Journal of Pharmaceutics and Biopharmaceutics* 2005; **61**(1-2):77-86.

252. Y. Luo, D. Chen, L. Ren, X. Zhao and J. Qin: Solid lipid nanoparticles for enhancing vinpocetine's oral bioavailability. *Journal of Controlled Release* 2006; **114**(1):53-59.

253. E. Ugazio, R. Cavalli and M. R. Gasco: Incorporation of cyclosporin A in solid lipid nanoparticles (SLN). *International Journal of Pharmaceutics* 2002; **241**(2):341-344.

254. J. Liu, W. Hu, H. Chen, Q. Ni, H. Xu and X. Yang: Isotretinoin-loaded solid lipid nanoparticles with skin targeting for topical delivery. *International Journal of Pharmaceutics* 2007; **328**(2):191-195.

255. S. A. Wissing, R. H.Müller, L. Manthei and C. Meyer. Structural characterization of Q10-loaded solid lipid nanoparticles by NMR spectroscopy. *Pharmaceutical Research* 2004; **21**:400-405.

256. M. J. D'Souza and P. DeSouza: Site specific microencapsulated drug targeting strategies- liver and gastro-intestinal tract targeting. *Advanced Drug Delivery Reviews* 1995; **17**(3):247-254.

257. T. M. Allen, E. H. Moase: Therapeutic opportunities for targeted liposomal drug delivery. *Advanced Drug Delivery Reviews* 1996; **21**(2):117-133.

258. A. Beduneau, P. Saulnier, J. P. Benoit: Active targeting of brain tumors using nanocarriers. *Biomaterials* 2007; **28**(33):4947-4967.

259. B. Wilson, M. K. Samanta, K. Santhi, K. P. S. Kumar, N. Paramakrishnan and B. Suresh: Poly(n-butylcyanoacrylate) nanoparticles coated with polysorbate 80 for the targeted delivery of rivastigmine into the brain to treat Alzheimer's disease. *Brain Research* 2008; **1200**:159-168.

260. A. Schnyder and J. Huwyler: Drug Transport to Brain with Targeted Liposomes. *NeuroRX* 2005; **2**(1):99-107.

261. X. Ying, H. Wen, W. L. Lu, J. Du, J. Guo, W. Tian, Y. Men, Y. Zhang, R.J. Li, T. Y. Yang, D. W. Shang, J. N. Lou, L. R. Zhang and Q. Zhang. Dual-targeting daunorubicin liposomes improve the therapeutic efficacy of brain glioma in animals. *Journal of Controlled Release* 2010; **141**(2):183-192.

262. P. Blasi, S. Giovagnoli, A. Schoubben, M. Ricci and C. Rossi: Solid lipid nanoparticles for targeted brain drug delivery. *Advanced Drug Delivery Reviews* 2007; **59**(6):454-477.

263. A. M. Brioschi, S. Calderoni, G. P. Zara, L. Priano, M. R. Gasco and A. Mauro: Solid lipid nanoparticles for brain tumors therapy: State of the art and novel challenges. In: Hari SS (editor): *Progress in Brain Research Nanoneuroscience and Nanoneuropharmacology*: Elsevier; 2009, pp. 193-223.

264. G. Storm, S. O. Belliot, T. Daemen and D. D. Lasic: Surface modification of nanoparticles to oppose uptake by the mononuclear phagocyte system. *Advanced Drug Delivery Reviews* 1995; **17**(1):31-48.

265. S. J. Douglas, S. S. Davis and L. Illum: Biodistribution of poly(isobutyl-cyanoacrylate) nanoparticles in rabbits. *International Journal of Pharmaceutics* 1986; **34**:145-152.

266. Y. Tabana and Y. Ikada: Effect of size and surface charge of polymer microspheres on their phagocytosis by macrophages. *Biomaterials* 1988; **9**(4):356-362.

267. S. S. Davis: Colloids as drug-delivery systems. *Pharmaceutical Technology* 1981; **5**:71-88.

268. M. C. Woodle: Controlling liposome blood clearance by surface-grafted polymers. *Advanced Drug Delivery Reviews* 1998; **32**(1-2):139-152.

269. M. C. Woodle: Sterically stabilized liposome therapeutics. *Advanced Drug Delivery Reviews* 1995; **16**(2-3):249-265.

270. S. Zalipsky, E. Brandeis, M. S. Newman, M. C. Woodle: Long circulating, cationic liposomes containing amino-PEG-phosphatidylethanolamine. *FEBS Letters* 1994; **353**(1):71-74.

271. R. Gref, A. Domb, P. Quellec, T. Blunk, R. H. Müller, J. M. Verbavatz and R. Langer: The controlled intravenous delivery of drugs using PEG-coated sterically stabilized nanospheres. *Advanced Drug Delivery Reviews* 1995; **16**(2-3):215-233.

272. L. Illum, S. S. Davis, R. H. Müller, E. Mak and P. West: The organ distribution and circulation time of intravenously injected colloidal carriers sterically stabilized with a block copolymer, poloxamine 908. *Life Science* 1987; **40**(4):367-374.

273. S. M. Moghimi: Re-establishing the long circulatory behaviour of poloxamine-coated particles after repeated intravenous administration: applications in cancer drug delivery and imaging. *Biochimica et Biophysica Acta (BBA) - General Subjects* 1999; **1472**(1-2):399-403.

274. T. Blunk, D. F. Hochstrasser, J. C. Sanchez, B. W. Müller and R. H. Müller: Colloidal carriers for intravenous targeting: plasma protein adsorption patterns on surface-modified latex particles evaluated by two-dimensional polyacrylamide gel electrophoresis. *Electrophoresis* 1993; **14**(12):1382-1387.

275. R. H. Müller and S. Heinemann: Surface modelling of microspheres as paranteral systems with high tissue affinity. In: R. Gurny, H. E. Junginger (editors): *Bioadhesion: Possibilities and Future Trends*. Stuttgart: Wissenschaftliche Verlagsgesellschaft GmbH; 1989, pp. 202-214.

276. A. Chonn, S. C. Semple and P. R. Cullis: Association of blood proteins with large unilamellar liposomes *in vivo*: relation to circulation lifetimes. *Journal of Biological Chemistry* 1992; **267**(26):18759-18765.

277. T. M. Göppert, R. H. Müller. Protein adsorption patterns on poloxamer and poloxamine-stabilized solid lipid nanoparticles: *European Journal of Pharmaceutics and Biopharmaceutics* 2005; **60**:361-372.

278. P. Camner, M. Lundborg, L. Lastbom, P. Gerde, N. Gross and C. Jarstrand: Experimental and calculated parameters on particle phagocytosis by alveolar macrophages. *Journal of Applied Physiology* 2002; **92**(6):2608-2616.

279. M. J. Hsu and R. L. Juliano: Interactions of liposomes with the reticuloendothelial system. II: Nonspecific and receptor-mediated uptake of liposomes by mouse peritoneal macrophages. *Biochimica et Biophysica Acta* 1982; **720**(4):411-419.

280. D. C. Altieri, P. N. Mannucci and A. M. Capitanio: Binding of fibrinogen to human monocytes. *Journal of Clinical Investigation* 1986; **78**(4):968-976.

281. C. G. Pommier, J. O'Shea, T. Chused, T. Takahashi, M. Ochoa, T. B. Nutman, C. Bianco and E. J. Brown: Differentiation stimuli induce receptors for plasma fibronectin on the human myelomonocytic cell line HL-60. *Blood* 1984; **64**(4):858-866.

282. W. Vogel, A. Bomford, S. Young and R. Williams. Heterogeneous distribution of transferrin receptors on parenchymal and nonparenchymal liver cells: biochemical and morphological evidence. *Blood* 1987; **69**(1):264-270.

283. F. Van Leuven, P. Marynen, L. Sottrup-Jensen, J. J. Cassiman and H. Van den Berghe: The receptor-binding domain of human alpha 2-macroglobulin: Isolation after limited proteolysis with a bacterial proteinase. *Journal of Biological Chemistry* 1986; **261**:11369-11373.

284. M. D. Kazatchkine and M. P. Carreno: Activation of the complement system at the interface between blood and artificial surfaces. *Biomaterials* 1988; **9**(1):30-35.

285. J. C. Leroux, F. De Jaeghere, B. Anner, E. Doelker and R. Gurny: An investigation on the role of plasma and serum opsonins on the internalization of biodegradable poly(DL-lactic acid) nanoparticles by human monocytes. *Life Sciences* 1995; **57**(7):695-703.

286. A. Gessner, C. Olbrich, W. Schröder, O. Kayser and R. H. Müller: The role of plasma proteins in brain targeting: species dependent protein adsorption patterns on brain-specific lipid drug conjugate (LDC) nanoparticles. *International Journal of Pharmaceutics* 2001; **214**(1-2):87-91.

287. K. Ogawara, K. Furumoto, S. Nagayama, K. Minato, K. Higaki, T. Kai and T. Kimura: Pre-coating with serum albumin reduces receptor-mediated hepatic disposition of polystyrene nanosphere: implications for rational design of nanoparticles. *Journal of Controlled Release* 2004; **100**(3):451-455.

288. H. M. Patel: Serum opsonins and liposomes: their interaction and opsonophagocytosis. *Critical Reviews in Therapeutic Drug Carrier Systems* 1992; **9**(1):39-90.

289. S. M. Moghimi, I. S. Muir, L. Illum, S. S. Davis and V. Kolb-Bachofen: Coating particles with a block co-polymer (poloxamine 908) suppresses opsonization but permits the activity of dysopsonins in the serum. *Biochimica et Biophysica Acta* 1993; **1179**(2):157-165.

290. L. Illum, I. M. Hunneyball and S. S. Davis: The effect of hydrophilic coatings on the uptake of colloidal particles by the liver and by peritoneal macrophages. *International Journal of Pharmaceutics* 1986; **29**:53-65.

291. J. Kreuter: Nanoparticulate systems for brain delivery of drugs. *Advanced Drug Delivery Reviews* 2001; **47**(1):65-81.

292. J. Kreuter, V. E. Petrov, D. A. Kharkevich and R. N. Alyautdin: Influence of the type of surfactant on the analgesic effects induced by the peptide dalargin after its delivery across the blood-brain barrier using surfactant-coated nanoparticles. *Journal of Controlled Release* 1997; **49**(1):81-87.

293. A. E. Gulyaev, S. E. Gelperina, A. S. Skidan, G. Y. Antropov and J. Kreuter: Significant transport of doxurubicin into the brain with polysorbate 80-coated nanoparticles. *Pharmceutical Research* 1999; **16**(10):1564-1569.

294. J. Kreuter, R. N. Alyautdin, D. A. Kharkevich and A. A. Ivanov: Passage of peptides through the blood-brain barrier with colloidal polymer particles (nanoparticles). *Brain Research* 1995; **674**(1):171-174.

295. J. Kreuter, P. Ramge, V. Petrov, S. Hamm, E. Svetlana, S. E. Gelperina, B. Engelhardt, R. Alyautdin, H. von Briesen and D. J. Begley: Direct evidence that polysorbate-80-coated poly(butylcyanoacrylate) nanoparticles deliver drugs to the CNS via specific mechanisms requiring Prior binding of drug to the nanoparticles. *Pharmaceutical Research* 2003; **20**(3):409-416.

296. R. N. Alyautdin, V. E. Petrov, K. Langer, A. Berthold, D. A. Kharkevich and J. Kreuter: Delivery of loperamide across the blood-brain barrier with polysorbate 80-coated polybutylcyanoacrylate nanoparticles. *Pharmaceutical Research* 1997; **14**(3):325-328.

297. R. N. Alyautdin, E. B. Tezikov, P. Ramge, D. A. Kharkevich, D. J. Begley and J. Kreuter: Significant entry of tubocurarine into the brain of rats by adsorption to polysorbate 80-coated polybutylcyanoacrylate nanoparticles: an in situ brain perfusion study. *Journal of Microencapsulation* 1998; **15**(1):67-74.

298. M. Lück, W. Schröder, T. Blunk and R. H. Müller: Identification of plasma proteins facilitated by enrichment on particulate surfaces: analysis by two-dimensional

electrophoresis and N-terminal microsequencing. *Electrophoresis* 1997; **18**(15):2961-2967.

299. J. Kreuter: Nanoparticulate systems for brain delivery of drugs. *Advanced Drug Delivery Reviews* 2010; **47**(1):65-81.

300. R. N. Alyautdin, D. Gothier, V. Petrov, D. Kharkevich and J. Kreuter: Analgesic activity of the hexapeptide dalargin adsorbed on the surface of polysorbate 80-coated poly(butyl cyanoacrylate) nanoparticles. *European Journal of Pharmaceutics and Biopharmaceutics* 1995; **41**:44-48.

301. J. Kreuter, D. Shamenkov, V. Petrov, P. Ramge, K. Cychutek, C. Koch-Brandt and R. Alyautdin: Apolipoprotein-mediated transport of nanoparticle-bound drugs across the blood-brain barrier: *Journal of Drug Targeting* 2003; **10**(4):317-325.

302. T. M. Göppert and R. H. Müller: Adsorption kinetics of plasma proteins on solid lipid nanoparticles for drug targeting. *International Journal of Pharmaceutics* 2005; **302**(1-2):172-186.

303. M. E. Price, R. M. Cornelius and J. L. Brash. Protein adsorption to polyethylene glycol modified liposomes from fibrinogen solution and from plasma. *Biochimica et Biophysica Acta* 2001; **1512**:191-205.

304. L. Thiele, J. E. Diederichts, R. Reszka, H. P. Merkle and E. Walter: Competitive adsorption of serum proteins at microparticles affects phagocytosis by dendritic cells. *Biomaterials* 2003; **24**:1409-1418.

305. K. Bergström, K. Holmberg, A. Safranj, A. S. Hoffman, M. J. Edgell, A. Kozlowski, B. A. Hovanes and J. M. Harris: Reduction of fibrinogen adsorption on PEG-coated polystyrene surfaces. *Journal of Biomedical Materials Research* 1992; **26**(6):779-790.

306. R. M. Cornelius, J. Sanchez, P. Olsson and J.L.Brash. Interactions of antithrombin and proteins in the plasma contact activation system with immobilized functional heparin. *Journal of Biomedical Materials Research* 2003; **67**(2):475-483.

307. J. T. Li, K. D. Caldwell: Plasma protein interactions with Pluronic™-treated colloids. *Colloids and Surfaces B: Biointerfaces* 1996; **7**(1-2):9-22.

308. M. E. Norman, P. Williams and L. Illum. *In vivo* evaluation of protein adsorption to sterically stabilised colloidal carriers. *Journal of Biomedical Materials Research* 2010; **27**(7):861-866.

309. J. G. Archambault and J. L. Brash: Protein resistant polyurethane surfaces by chemical grafting of PEO: amino-terminated PEO as grafting reagent. *Colloids and Surfaces B: Biointerfaces* 2004; **39**(1-2):9-16.

310. R. Kurrat, K. Wälivaara, A. Marti, M. Textor, P. Tengvall, J. J. Ramsden and N. D. Spencer: Plasma protein adsorption on titanium: comparative *in situ* studies using optical waveguide lightmode spectroscopy and ellipsometry. *Colloids and Surfaces B: Biointerfaces* 1998; **11**(4):187-201.

311. H. Elwing: Protein absorption and ellipsometry in biomaterial research. *Biomaterials* 1998; **19**(4-5):397-406.

312. R. D. Oleschuk, M. E. McComb, A. Chow, W. Ens, K. G. Standing, H. Perreault, Y. Marois and M. King: Characterization of plasma proteins adsorbed onto biomaterials by MALDI-TOFMS. *Biomaterials* 2000; **21**(16):1701-1710.

313. J. E. Celis, S. Trentemolle and P. Gromov: *Gel-based proteomics: high-resolution two-dimensional gel electrophoresis of proteins: isolectric focusing (IEF) and nonequilibrium pH gradient electrophoresis (NEPHGE)*. San Diego: Academic Press; 2006.

314. J. Klose: Protein mapping by combined isoelectric focusing and electrophoresis of mouse tissues. A novel approach to testing for induced point mutations in mammals. *Hummangenetik* 1975; **26**(3):231-243.

315. P. H. O'Farrell: High resolution two-dimensional electrophoresis of proteins. *Journal of Biological Chemistry* 1975; **250**(10):4007-4021.

316. S. Harnisch and R. H. Müller: Plasma protein adsorption patterns on emulsions for parenteral administration: establishment of a protocol for two-dimensional polyacrylamide electrophoresis. *Electrophoresis* 1998; **19**(2):349-354.

317. D. F. Hochstrasser, M. G. Harrington, A. C. Hochstrasser, M. J. Miller and C. R. Merril: Methods for increasing the resolution of two-dimensional protein electrophoresis. *Analytical Biochemistry* 1988; **173**(2):424-435.

318. A. Gessner, R. Waicz, A. Lieske, B. R. Paulke, K. Mäder and R. H. Müller. Nanoparticles with decreasing surface hydrophobicities: influence of plasma protein adsorption. *International Journal of Pharmaceutics* 2000; **196**(2):245-249.

319. A. Görg, W. Postel and S. Günther: The current state of two-dimensional electrophoresis with immobilized pH gradients. *Electrophoresis* 1988; **9**(9):531-546.

320. A. Gessner, B. Paulke and R. H. Müller: Analysis of plasma protein adsorption onto polystyrene particles by two-dimensional electrophoresis: comparison of sample application and isolectric focusing techniques. *Electrophoresis* 2000; **21**(12):2438-2442.

321. L. Vroman and A. L. Adams: Adsorption of proteins out of plasma and solutions in narrow spaces. *Journal of Colloid and Interface Science* 1986; **111**(2):391-402.

322. A. Gessner, A. Lieske, B. R. Paulke and R. H. Müller. Influence of surface charge density on protein adsorption on polymeric nanoparticles: analysis by two-dimensional electrophoresis. *European Journal of Pharmaceutics and Biopharmaceutics* 2002; **54**(2):165-170.

323. S. Harnisch and R. H. Müller: Adsorption kinetics of plasma proteins on oil-in-water emulsions for parenteral nutrition. *European Journal of Pharmaceutics and Biopharmaceutics* 2000; **49**(1):41-46.

324. K. Thode, M. Lück, M. Kresse, W. Semmler and R. H. Müller: Determination of Plasma Protein Adsorption on Magnetic Iron Oxides: Sample Preparation. *Pharmaceutical Research* 1997; **14**(7):905-910.

325. S. Schmidt, S. Wissing, A. Gessner and R. H. Müller. Plasma protein adsorption patterns on solid lipid nanoparticles (SLNTM): novel sample preparation protocol prior to 2-DE. *International Symposium on Controlled Release of Bioactive Materials and Fourth Consumer Products Conference* 1[28], 1771-1779. 2001. San Diego.

326. T. M. Göppert and R. H. Müller: Alternative sample preparation prior to two-dimensional electrophoresis protein analysis on solid lipid nanoparticles. *Electrophoresis* 2004; **25**(1):134-140.

327. B. C. Cook, G. S. Retzinger: Elution of fibrinogen and other plasma proteins from unmodified and from lecithin-coated polystyrene--divinylbenzene beads. *Journal of Colloid and Interface Science* 1992; **153**(1):1-12.

328. H. Boucherie, G. Dujardin, M. Kermorgant, C. Monribot, P. Slonimski and M. Perrot: Two-Dimensional protein map of Saccharomyces cerevisiae: Construction of a gene-protein index. *Yeast* 1995; **11**(7):601-613.

329. A. Harder, R. Wildgruber, A. Nawrocki, S. J. Fey, P. M. Larsen and A. Görg: Comparison of yeast cell protein solubilization procedures for two-dimensional electrophoresis. *Electrophoresis* 1999; **20**(4-5):826-829.

330. A. Görg, W. Postel, J. Wesser, S. Günther, S. R. Strahler, S. M. Hanash and L. Somerlot: Elimination of point streaking on silver stained two-dimensional gels by addition of iodoacetamide to the equilibration buffer. *Electrophoresis* 1987; **8**(2):122-124.

331. J. M. Corbett, M. J. Dunn, A. Posch and A. J. Moës: Positional reproducibility of protein spots in two-dimensional polyacrylamide gel electrophoresis using immobilised pH gradient isoelectric focusing in the first dimension: an interlaboratory comparison. *Electrophoresis* 1994; **15**(8):9.

332. A. Görg, A. Blomberg, L. Blomberg, S. J. Fey, P. M. Larsen, P. Roepstorff, H. Degand, M. Boutry, A. Posch *et al.,* Interlaboratory reproducibility of yeast protein patterns analyzed by immobilized pH gradient two-dimensional gel electrophoresis. *Electrophoresis* 1995; **16**(10):1935-1945.

333. B. Bjellqvist, K. Ek, P. G.Righetti, E. Gianazza, A. Görg, R.Westermeier *et al.*, Isoelectric focusing in immobilized pH gradients: principle, methodology and some applications. *Journal of Biochemical and Biophysical Methods* 1982; **6**(4):317-339.

334. A. Görg: Two-dimensional electrophoresis with immobilized pH gradients: current state. *Biochemical Society Transactions* 1993; **21**:130-132.

335. R. Wildgruber, G. Reil, O. Drews, H. Parlar, and A. Görg: Web-based two-dimensional database of *Saccharomyces cerevisiae* proteins using immobilized pH gradients from pH 6 to pH 12 and matrix-assisted laser desorption/ionization-time of flight mass spectrometry. *Proteomics* 2002; **2**(6):727-732.

336. O. Drews, G. Reil, H. Parlar and A. Görg: Setting up standards and a reference map for the alkaline proteome of the Gram-positive bacterium *Lactococcus lactis*. *Proteomics* 2004; **4**(5):1293-1304.

337. A. Posch, W. Weiss, C. Wheeler, M. J. Dunn and A. Görg: Sequence analysis of wheat grain allergens separated by two-dimensional electrophoresis with immobilized pH gradients. *Electrophoresis* 1995; **16**(1):1115-1119.

338. A. Görg, W. Postel, R. Westermeier, E. Gianazza and P. G.Righetti: Gel gradient electrophoresis, isoelectric focusing, and two-dimensional techniques in horizontal ultrathin polyacrylamide layers. *Journal of Biochemical and Biophysical Methods* 1980; **3**(5):273-284.

339. T. Rabilloud, C. Valette and J. J. Lawrence: Sample application by in-gel rehydration improves the resolution of two-dimensional electrophoresis with immobilized pH-gradients in the first dimension. *Electrophoresis* 1994; **15**(12):1552-1558.

340. R. Islam, C. Ko and T. Landers: A. new approach to rapid immobilised pH gradient IEF for 2-D electrophoresis. *Science Tools* 1998; **3**:14-15.

341. A. Görg, C. Obermaier, G. Boguth and A. Harder: 2-D electrophoresis with immobilized pH gradients using the IPGphor. *Life Science News* 1999; (1):-4.

342. A. Görg, C. Obermaier, G. Boguth, B. Scheibe, R. Wildgrubber and W. Weiss: The current state of two-dimensional electrophoresis with immobilized pH gradients. *Electrophoresis* 2000; **21**(6):1037-1053.

343. C. Pasquali, I. Fialka and L. A. Huber: Preparative two-dimensional gel electrophoresis of membrane proteins. *Electrophoresis* 1997; **18**(14):2573-2581.

344. X. Zuo, D. W. Speicher: Comprehensive analysis of complex proteomes using microscale solution isoelectrofocusing prior to narrow pH range two-dimensional electrophoresis. *Proteomics* 2002; **2**(1):58-68.

345. A. W. Dowsey, M. J. Dunn and G. Z. Yang: The role of bioinformatics in two-dimensional gel electrophoresis. *Proteomics* 2003; **3**(8):1567-1596.

346. A. Görg, G. Boguth, C. Obermaier, A. Posch and W. Weiss: Two-dimensional polyacryl-amide gel electrophoresis with immobilized pH gradients in the first dimension (IPG-Dalt): The state of the art and the controversy of vertical versus horizontal systems. *Electrophoresis* 1995; **16**(1):1079-1086.

347. A. Görg and W. Weiss: Horizontal SDS-PAGE for IPG-Dalt. *Methods in Molecular Biology* 1999; **112**:235-244.

348. N. G. Anderson and N. L. Anderson: Analytical techniques for cell fractions: two-dimensional analysis of serum and tissue proteins. *Analytical Biochemistry* 1978; **85**(2):331-340.

349. U. K. Laemmli: Cleavage of structural proteins during the assembly of the head of bacteriophage T4. *Nature* 1970; **227**:680-685.

350. W. F. Patton, N. Chung-Welch, M. F. Lopez, R. P. Cambria, B. L. Utterback, and W. M. Skea: Tris-tricine and Tris-borate buffer systems provide better estimates of human mesothelial cell intermediate filament protein molecular weights than the standard Tris-glycine. *Analytical Biochemistry* 1991; **197**(1):25-33.

351. C. R. Merril, D. Goldman, S. A. Sedman and M. H. Ebert: Ultrasensitive stain for proteins in polyacrylamide gels shows regional variation in cerebrospinal fluid proteins. *Science* 1981; **211**(4489):1437-1438.

352. B. R. Oakley, D. R. Kirsch, N. R. Morris: A simplified ultrasensitive silver stain for detecting proteins in polyacrylamide gels. *Analytical Biochemistry* 1980; **105**(1):361-363.

353. V. Neuhoff, N. Arold, D. Taube and W. Ehrhardt: Improved staining of proteins in polyacrylamide gels including isoelectric focusing gels with clear background at nanogram sensitivity using Coomassie Brilliant Blue G-250 and R-250. *Electrophoresis* 1988; **9**(6):255-262.

354. L. Castellanos-Serra, W. Proenza, V. Huerta, R. L. Moritz and R. J. Simpson: Proteome analysis of polyacrylamide gel-separated proteins visualized by reversible negative staining using imidazole-zinc salts. *Electrophoresis* 1999; **20**(4-5):732-737.

355. W. F. Patton: A thousand points of light: the application of fluorescence detection technologies to two-dimensional gel electrophoresis and proteomics. *Electrophoresis* 2000; **21**(6):1123-1144.

356. A. J. Link: Autoradiography of 2-D gels. *Methods in Molecular Biology* 1999; (112):285-290.

357. N. L. Anderson, N. G. Anderson: A two-dimensional gel database of human plasma proteins. *Electrophoresis* 1991; **12**(11):883-906.

358. Expasy proteomics server: world-2D PAGE list: index to 2-D PAGE databases and services. http://au.expasy.org/ch2d/2d-index.html . 27-5-2009. Swiss Institute of Bioinformatics. Last accessed on 15/01/2010.

359. Bio-Rad silver staining. http://www.bio-rad.com/webroot/web/pdf/lsr/literature/Bulletin_9057.pdf. 2010. Bio-Rad Laboratories. Last accessed on 15/01/2010

360. K. H. Weisgraber, R. W. Mahley, R. C. Kowal, J. Herz, J. L. Goldstein and M. S. Brown: Apolipoprotein C-I modulates the interaction of apolipoprotein E with beta-migrating very low density lipoproteins (beta-VLDL) and inhibits binding of beta-VLDL to low density lipoprotein receptor-related protein. *Journal of Biological Chemistry* 1990; **265**(36):22453-22459.

361. S. L. Illum and S. S. Davis: Effect of the nonionic surfactant poloxamer 338 on the fate and deposition of polystyrene microspheres following intravenous administration. *Journal of Pharmaceutical Sciences* 1983; **72**(9):1086-1089.